The pleiotropic effects of a *tolC* mutation in *Vibrio furnissii*

Submitted by

Hannah Louise Upton Tape

to the University of Exeter as a thesis for the degree of Doctor of Philosophy in Biological Sciences

(September 2012)

I certify that all material in this thesis which is not my own work has been identified and that no material has previously been submitted and approved for the award of a degree by this or any other University.

Hannah Tape

ABSTRACT

The ability of bacteria to successfully adapt to changing environments allows for increased resistance to antibiotics, an increasing problem in drug development. Efflux via the cellular membrane is one of the major and most significant mechanisms bacteria employ for defense against antimicrobials. The outer membrane protein, TolC, is a nonspecific channel with broad substrate specificity and is a fundamental constituent of a number of multidrug resistance (MDR) efflux systems. TolC, which interacts with membrane bound antiporters to export various substrates, including antimicrobials, has been a focus for antibiotic development. The capacity to expel a wide range of compounds such as toxins, bile, dyes and detergents, further establishes the significance of these systems in aiding bacterial survival. Continued investigation and discovery of compounds secreted via TolC is required to fully understand the role of efflux systems.

In addition to exporting compounds out of cells, TolC has been researched in connection with a number of metabolic processes including virulence, motility and quorum sensing. This work contributes to knowledge of interactions between these pathways by analysing phenotypic changes and alterations in gene expression in the *tolC*$^{-}$ mutant within *Vibrio furnissii. Vibrio* species are strongly associated with a number of reported phenotypic changes induced by mutations in *tolC,* particularly virulence and quorum sensing; the emerging pathogen *V. furnissii* is therefore a model organism for this study. Notably, this bacterium has become significant within the bio-fuel industry due to reports that it is able to synthesise large quantities of hydrocarbons. The potential for bacteria to produce hydrocarbons and fatty acids suitable for use in bio-fuels has considerable industrial applications. This work establishes the quantities of hydrocarbons and lipids present in *V. furnissii* and examines the role of TolC in the secretion of these compounds.

Resistance nodulation division efflux pumps are a class of MDR systems that have been identified as targets for antimicrobial drug development. Understanding the consequence of disrupting the integral outer membrane component TolC, is therefore of significant interest. This work examines the connection between pathways disrupted within *tolC*$^{-}$ mutants, showing that quorum sensing gene regulation is altered within the mutant and subsequently, expression of the virulence factor AphB is increased. Reduced motility is also observed in the *tolC*$^{-}$ mutant, a phenotype that appears to result from disruption of the membrane and mis-assembled flagella. Investigation into cellular stress, recently reported to occur within *tolC*$^{-}$ mutants, was performed by comparing the capability of wild type and mutant cells to metabolise selenite, and cope with the subsequent increase in superoxides generated. Results show that *tolC*$^{-}$ mutants employ mechanisms which cope with the inevitable intracellular build up of substrates, particularly those that may be toxic to the cell.

ACKNOWLEDGMENTS

I would like to thank Prof. John Love and Prof. Clive Butler for all their support and encouragement throughout this PhD and my scientific career to date. Thanks to Prof. Rob Lee and co-workers at Shell Global Solutions for the opportunity and assistance throughout this project. I am very grateful to Prof. Laura Piddock at the University of Birmingham and Prof. Paul Williams at the University of Nottingham for their help and advice during this work.

Further thanks to Dr. Mark Wood for the synthesis of compounds required in this study and Dr. Hannah Florence for assistance with LC-MS. I would also like to thank Dr. David Parker for GC-MS analysis of samples and staff at the Nottingham Arabidopsis Stock Centre for preparation and hybridization of Microarray Chips. Thank you to Dr. Thomas Lux and Dr. Christine Sambles for designing the Affymetrix Genechips and for guidance with bioinformatics and transcriptome analysis. Further thanks to Peter Splatt for preparation of cells for transmission electron microscopy and for assistance with confocal microscopy. I wish to thank Dr. John Dowdle for providing the *tolC*$^{-}$ mutant studied in this work and Richard Tennant for assitance with FACS.

Thanks to Dr. Elizabeth Dridge for her advice and friendship throughout my time studying within the department and colleagues in the Mezzanine office and the Biocatalyis Centre who have always been on hand for a scientific chat or an after work drink. Special thanks to my family, especially my Mum for her ongoing support and to my friends and partner Tom who, as always, have been a huge encouragement.

TABLE OF CONTENTS

LIST OF FIGURES

LIST OF TABLES AND EQUATIONS

LIST OF ABRIEVIATAIONS

ATP	Adenosine 5'-triphosphate
ABC	ATP Binding Cassette superfamily
AI	AutoInducer
CFU	Colony Forming Unit
DAG	Diacylglyceride
EIC	Extracted Ion Chromatogram
FACS	Fluorescence Activated Cell Sorter
FFA	Free Fatty Acid
GC-MS	Gas Chromatography-Mass Spectrometry
HC	Hydrocarbon
HSL	Homoserine Lactone
IC_{50}	Half Maximal Inhibitory Concentrations
IM	Inner Membrane
IPTG	Isopropylthio-β-galactoside
KEGG	Kyoto Encyclopedia of Genes and Genomes
LC-MS	Liquid Chromatography-Mass Spectrometry
LCH	Long Chain Hydrocarbon
MAG	Monoacylglyceride
MATE	Multidrug And Toxic-compound Extrusion family
MDR	MultiDrug Resistance
MFP	Membrane Fusion Protein
MFS	Major Facilitator Superfamily
MIC	Minimal Inhibitory Concentration
MRM	Multiple Reaction Monitoring
OM	Outer Membrane
OMP	Outer Membrane Protein
PCR	Polymerase Chain Reaction
PMF	Proton Motive Force
RND	Resistance Nodulation Division family
RT-qPCR	Real Time Quantitative Polymerase Chain Reaction

SEM	Scanning Electron Microscopy
SIM	Selected Ion Monitoring
SMR	Small Multidrug Resistance family
TAG	Triacylglyceride
TEM	Transmission Electron Microscopy
TIC	Total Ion Chromatogram
Q-TOF	Quadrupole Time Of Flight
QQQ	Triple Quadrupole

CHAPTER 1 – INTRODUCTION

1.1 Secretion systems

1.1.1. Bacteria: adaptation and survival

The ability to adapt to changing environments is essential for bacterial survival. Microorganisms have developed a number of mechanisms to enable successful growth in varying conditions importantly, they control the movement of substrates across cellular membranes. Metabolite export via secretion systems occurs by active transport of substrates across the outer membrane into the extracellular environment. This process includes the expulsion of natural products which aid bacterial pathogenesis, such as the secretion of toxins to facilitate host invasion (Hueck, 1998). Two-component pathways play a significant role in regulating the secretion of virulence factors, allowing for translocation of proteins across both the inner and outer membranes (Sandkvist, 2001). Virulence factor expression and export is also regulated by quorum sensing which requires the secretion of signalling molecules enabling communication between bacterial cells (Sandkvist, 2001, Henke and Bassler, 2004). This allows cells to coordinate swimming, biofilm formation and host invasion (Waters and Bassler, 2005). In addition to protein secretion enabling host invasion, bacteria have mechanisms for drug export (Paulsen *et al.*, 1996). Multidrug resistance is a persistent problem for the treatment of bacterial infections and the clinical relevance of systems required for antimicrobial export has been established (Zgurskaya and Nikaido, 2000). Understanding these mechanisms is critical to combating virulent strains which are able to adapt and confer resistance to an increasing number of antibiotics. In addition to their role in virulence, secretory pathways are involved in exporting environmental toxins and cellular products such as fatty acids, solvents and bile to help maintain cell fitness (Piddock, 2006). Detoxification of cells is a significant process required to enable growth in diverse conditions and Gram-negative bacteria employ an array of response mechanisms to cope with toxins. Fundamental components of these detoxification mechanisms are linked to efflux systems (Rosner and Martin, 2009). More recently, proteins involved in export systems have been associated with other functions by feeding back to gene regulatory pathways (Zgurskaya *et al.*, 2011). Survival of bacteria therefore requires secretion systems, not only for direct transport of substrates across membranes but also as a method of monitoring the extracellular environment and regulating gene expression accordingly.

1.1.2. Secretion pathways in bacteria

Secretion of compounds via cell membranes is a fundamental process throughout all bacterial domains. To date, six types of secretion systems have been acknowledged in Gram-negative bacteria (Type I, II, III, IV, V and VI), which provide varied methods of substrate export from the

cytoplasmic compartment to outside of the cell. Gram-negative bacteria possess two membranes making export a complicated process; substrates are required to cross the inner and outer membrane before extracellular release. Type I secretion systems span both membranes within Gram-negative bacteria, allowing for direct export from the cytoplasm to the outside of the cell. These systems have a wide substrate specificity and are formed by a simple trimeric complex (Fig 1.1). Secretory systems such as Type III and Type IV also span both membranes, introducing toxins, via a syringe like mechanism, into host cells. Type III systems are linked to pathogencity in several Gram-negative bacteria and function by secreting proteins, via a needle like structure, from the bacterial cytoplasm, directly to the host cytoplasm. The less understood Type IV system also plays a role in pathogencitiy with the capability to exchange genetic material with other bacteria. Secrecion systems such as Type II and Tyoe V export proteins by binding those have been transported to the perimplasmic space and translocating the substrate across the outer membrane. In Type II secretion, translocation via Sec (general secretory), Tat (twin-arginine translocation) or SRP (signal-recognition particle) systems are required to transport proteins into the periplasm where, if required, they are able to pass through an outer membrane bound complex (Pallen *et al.*, 2003). By contrast, Gram-positive bacteria only possess one membrane where a Sec system, similar to that in Gram-negative bacteria, is commonly utilised for protein export.

Export via efflux systems can function via ATP (adenosine 5'- triphosphate) hydrolysis, alternatively utilising proton motive force (PMF), which is created by a chemical gradient of hydrogen ions and/or an electrical charge gradient across the inner membrane. Energy released by substrate oxidation conserves energy which pumps ions across the inner membrane creating an electrochemical gradient, ultimately drives substrate export. Oxidative phosphorylation is an example of this, involving the transfer of electrons from donors such as NADH (reduced nicotinamide adenine dinucleotide) and $FADH_2$ (reduced flavin adenine dinucleotide) to oxygen, ultimately driving ATP synthesis. By contrast to ATP driven export, PMF efflux systems have wider substrate specificity and are associated with multidrug resistance as well as export of proteins, host derived substrates and toxins (Paulsen *et al.*, 1996).

1.1.3. Type I multidrug resistance (MDR) efflux systems

In many prokaryotes, Type I efflux systems, which confer resistance to a number of antibiotics and toxic compounds, are widely researched in association with multidrug resistance (MDR) (Andersen *et al.*, 2001). Type I efflux systems are categorised as five families; the ATP binding cassette superfamily (ABC), the major facilitator superfamily (MFS), the multidrug and toxic-compound extrusion family (MATE), the small multidrug resistance family (SMR) and the resistance nodulation

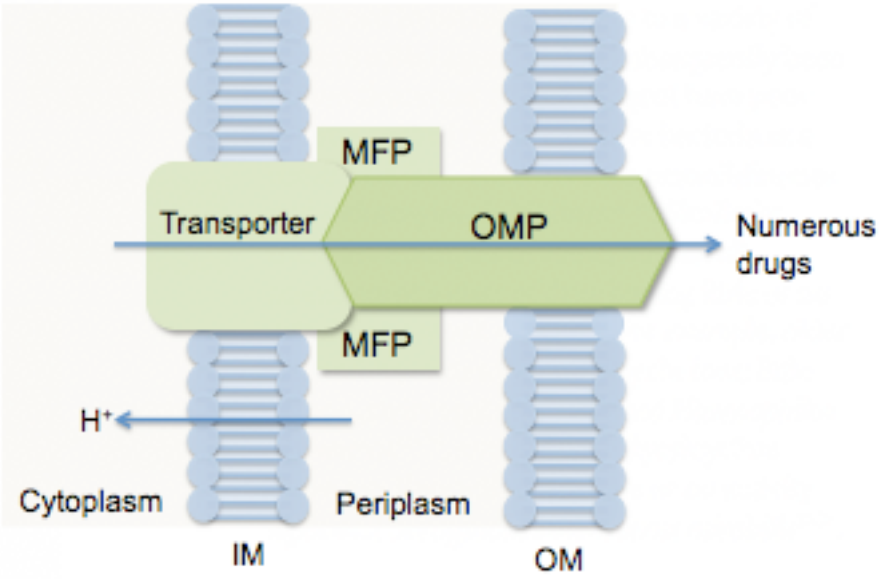

Figure 1.1 The RND efflux system.

Typically comprised of an outer membrane protein (OMP), spanning the outer membrane (OM), a transporter protein spanning the inner membrane (IM) and stablising membrane fusion proteins (MFPs) within the periplasm.

division family (RND) (Piddock, 2006). These families are classified by the number of components in each pump, the number of membrane spanning regions, the energy source used and the type of substrate translocated. ABC and MATE systems are ATP dependant whereas MFS, SMR and RND systems utilise proton motive force as the energy supply (Paulsen *et al.*, 1996). The clinical relevance of the ABC superfamily, the MFS family and RND efflux systems have been widely researched within Gram-negative bacteria. RND systems are emerging targets for antimicrobial drug development and the effect of efflux pump inhibitors (EPIs) are of increasing clinical relevance (Lomovskaya *et al.*, 2001, Blair and Piddock, 2009).

1.1.4. Antibiotic resistance and the resistance nodulation division (RND) family

RND efflux systems have three components: an outer membrane protein (OMP) a membrane fusion protein (MFP) and a membrane bound transporter protein (Fig 1.1) (Fath and Kolter, 1993). This Type I MDR efflux complex is typical of a PMF driven export system, containing an OMP with a number of additional functions and diverse substrate specificity (Paulsen *et al.*, 1996). RND systems increase resistance to a number of antimicrobials such as chloramphenicol, fluoroquniolones, fusidic acid, β-lactams, nalidixic acid, novobiocin and tetracycline (Poole, 2000, Baucheron *et al.*, 2004) and a number of clinically relevant Gram-negative bacteria express this efflux pump including *Pseudomonas aeruginosa*, *Escherichia coli*, *Salmonella Typhimurium* and *Vibrio cholerae* (Fralick, 1996, Piddock *et al.,* 2000, Poole and Srikumar, 2001). Within these organisms the OMP (TolC) is expressed with the MFP (AcrA) and transporter protein (AcrB) forming the AcrAB-TolC efflux system (Zgurskaya and Nikaido, 1999). OMPs, such as TolC in *E. coli* function with a number of other membrane bound transporter proteins in the RND family (Piddock, 2006). TolC is the typical OMP for other MDR systems including those in the MFS and ABC families (Paulsen *et al.*, 1996). Many organisms express RND systems with more than one OMP, additional MFPs and transporter proteins; e.g. *P. aeruginosa* expresses OMPs: OprM, OprJ and OprN (homologues of TolC). These are coupled with a number of MFPs and transporters forming efflux systems MexAB-OprM and MexXY-OprM, MexCD-OprJ and MexEF-OprN (Poole, 2001). The combined mechanisms of these four systems result in resistance to a number of antimicrobials including fluoroquinolones, β-lactams, tetracycline, macrolides, chloramphenicol, novobiocin, trimethoprim and sulphonamides (Köhler *et al.*, 1996, Köhler *et al.*, 1997, Srikumar *et al.*, 1997). *V. cholerae* uses an array of MATE, MFS and RND efflux systems as well as an ABC family, ATP dependent system (Kitaoka *et al.*, 2011). Collectively these export systems confer resistance to a number or antibiotics as well as Triton X-100, SDS, polymyxin B, erythromycin, bile salts and penicillin (RND efflux systems have not only shown resistance to antimicrobials but a

connection to pathogencity and secretion of virulence factors; research has shown TolC is involved in such processes (Bina and Mekalanos 2001, Bina, 2008, Kitaoka *et al.*, 2011).

1.1.5. The role of RND efflux systems in bacterial pathogenicity

RND family efflux systems have displayed association with pathogenicity in a number of (Gram-negative and Gram-positive) bacteria, with a focus on the clinical relevance of this in *V. cholerae* (Piddock, 2006, Bina *et al.*, 2008). AcrAB-TolC in particular is important for *S.* Typhimurium colonization; *acrB* and *tolC* knockout mutants were less able (*acrB*$^{-}$) or unable (*tolC*$^{-}$) to adhere to, invade and survive in mouse macrophage and human embryonic intestinal cells (Buckley *et al.*, 2006). Similarly; in *Campylobacter jejuni*, mutations in the CmeABC efflux system resulted in failure to colonize the host (Lin *et al.*, 2003). The involvement of TolC is relevant to a number of studies, particularly the secretion of virulence factors, such as alpha-haemolysin in *E. coli* and RTX toxins in *V. cholerae* (Bhakdi *et al.*, 1988, Bina and Mekalanos, 2001, Boardman and Satchell, 2004). Mutations within the AcrAB-TolC efflux system result in disruptions to flagella gene expression and reduced motility in *S.* Typhimurium which are fundamental to pathogenicity (Webber *et al.*, 2009). In addition, recent research shows that TolC directly affects the expression of virulence genes such as *toxT* in *V. cholerae* (Minato *et al.*, 2011).

1.2. The AcrAB-TolC efflux system

1.2.1. The outer membrane protein TolC

A 2.1 Å crystal structure of TolC from *E. coli* shows that three TolC protomers form a 140 Å long 'tunnel' which spans the outer membrane and protrudes nearly 100 Å into the periplasmic space (Koronakis *et al.*, 2000) (Fig 1.2A). In following years, the structures of outer membrane proteins in *P. aeruginosa* (OprM) and *V. cholerae* (VceC) were also solved (Akama *et al.*, 2004, Federici *et al.*, 2005). Despite low sequence similarities, the structures of these proteins are very alike; comprising a 12-stranded β-barrel (embedded in the outer membrane), an α-helical domain (which spans into the periplasm) and a mixed α/β equatorial domain (Fig 1.2A). TolC homologues, highly conserved in Gram-negative bacteria, have been identified in over 30 bacterial species (Koronakis *et al.*, 2004) and typically comprise a trimeric efflux system with an MFP and transporter protein (Fig 1.1). The transport mechanism of TolC is triggered by association with the inner membrane complexes and reconstruction of the process has not yet been successful (Koronakis, 2003). Experimental evidence suggests that the inner and outer coiled α-helices realign creating an "open" state of the pore (Zgurskaya *et al.*, 2011).

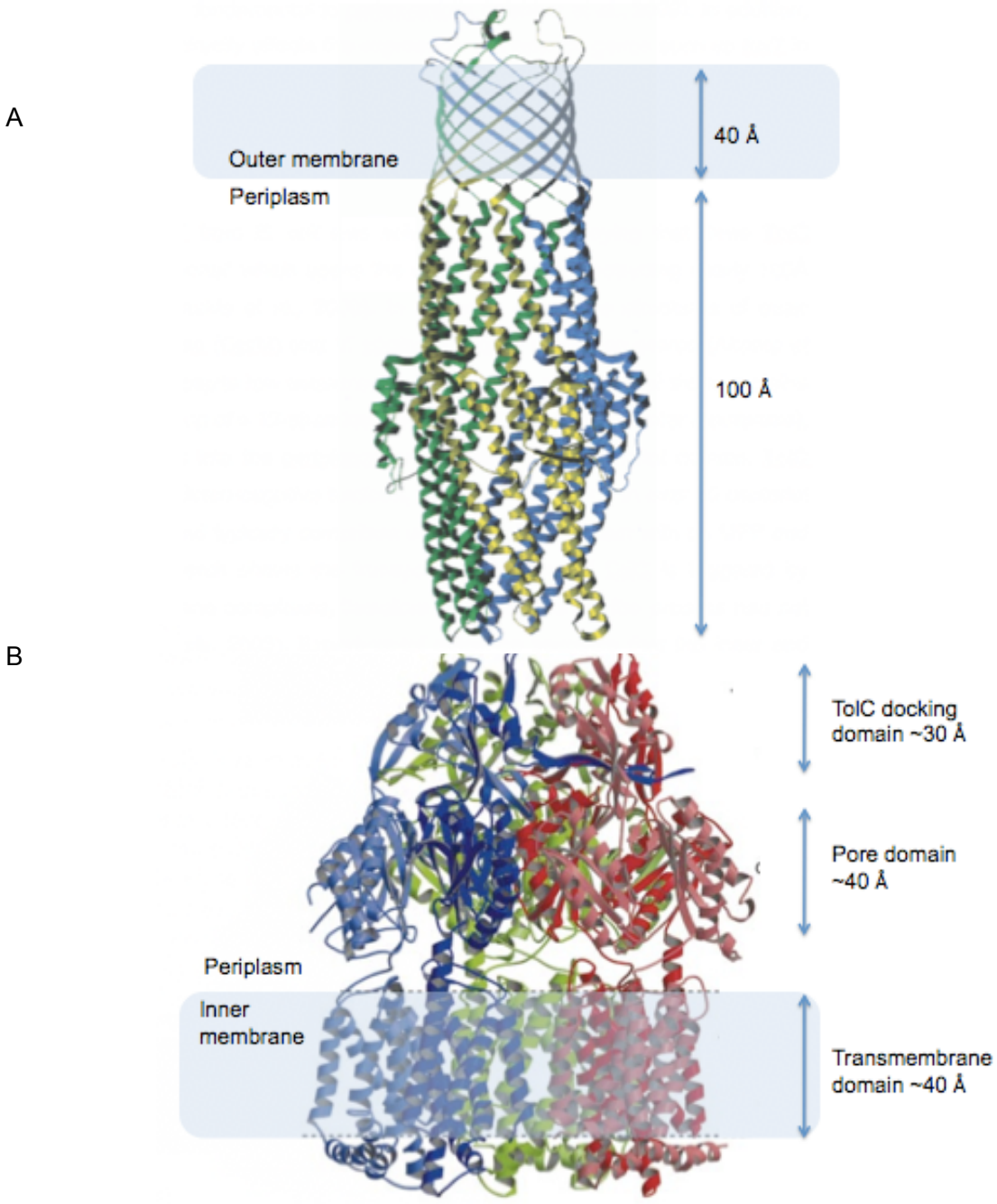

Figure 1.2. Crystal structures of TolC and AcrB.

TolC (A) comprising of three protomers individually coloured. The β-barrel is at the top, embedded in the outer membrane and the α-helical domain spans 100 Å into the periplasm.

The three protomers of AcrB (B) are also individually coloured. The TolC docking domain is at the top, the diameter of the docking domain on AcrB is approximately the same as the bottom of TolC. The pore domains span ~ 40 Å and the transmembrane domains consisting of 12 α-helices span the inner membrane. Adapted from (Murakami *et al.*, 2002).

1.2.2. AcrAB-TolC RND efflux system

One of the most comprehensively studied RND systems is the AcrAB-TolC efflux pump. This complex is formed with the outer membrane spanning protein (TolC), the transporter protein (AcrB, located in the inner membrane) and the stabilising MFP (AcrA, located in the periplasmic space) (Zgurskaya and Nikaido, 2000). Recent data has emphasised the significance of each of these subunits in the functioning of the efflux pump, with evidence of interaction between TolC and AcrB and AcrA independently (Tikhonova et al., *Symmons* et al.*, 2009, Tikhonova* et al.*, 2011). Transporter proteins such as AcrB bind directly to TolC and play a fundamental role in the export of substrates (Tikhonova* et al., *Bavro* et al.*, 2008, Tikhonova* et al.*, 2011). Homologues of AcrB are* widely distributed among Gram-negative and Gram-positive bacteria and are intrinsically linked to drug tolerance.

1.2.3. AcrAB-TolC assembly

Like other OMPs, TolC is synthesised in the cytoplasm and transported across the inner membrane via the Sec pathway. The TolC assembly mechanism within the periplasm is less clear, particularly the insertion of the protein into the membrane (Masi *et al.*, 2009, Zgurskaya *et al.*, 2011). No external factors are apparently required for the folding of the TolC protein, with no interaction with periplamsic chaperones (Werner *et al.*, 2003, Masi *et al.*, 2009). Assembly of the AcrAB-TolC efflux pump appears to involve transient formation of the tripartite complex once AcrAB engages with the substrate. Following this, AcrAB recruits TolC and the trimeric efflux system is formed. AcrB has been crystalised and displays a TolC docking domain, a pore domain and a transmembrane domain with a combined periplasmic length of approximately 170 Å, enough to span the inner membrane (Murakami *et al.*, 2002, Murakami *et al.*, 2004) (Fig 1.2B). AcrB is comprised of 1049 amino acid residues and forms three protomers, each with transmembrane domains. Within the transmembrane domain, the three protomers loosely interact forming a 30 Å wide pore (Fig 1.2B) (Murakami *et al.*, 2002). Three functionally essential charged residues are present within this domain: Asp 407, Asp 408 and Lys 940 (Guan and Nakae, 2001, Murakami *et al.*, 2006). When these sites are protonated a conformational change occurs opening the pore (Murakami *et al.*, 2002).

1.2.4 The membrane fusion protein AcrA

The link between multidrug resistance (MDR) and transporter proteins such as TolC and AcrB is relatively well established but it is recently acknowledged that MFPs, such as AcrA play a significant role in this process (Modali and Zgurskaya, Ge *et al.*, 2009, Modali and Zgurskaya, 2011). Notably, purified TolC and AcrB show no interaction suggesting that AcrA is required for the

stabilisation and function of the efflux pump (Husain *et al.*, 2004, Touzé *et al.*, 2004). AcrD, which behaves in a similar manner to AcrB was initially considered to function without a MFP, however recent data has confirmed dependence on AcrA for drug transport in *S.* Typhimurium (Yamasaki *et al.*, 2011). Genes encoding transporter components of the efflux systems are found in association with MFPs within the genome, particularly those known to interact with TolC, e.g AcrA and AcrB (Paulsen *et al.*, 1996). In addition, bacteria contain cation efflux systems which comprise of gene clusters containing separate membrane spanning proteins that interact exclusively with specific transporters (Zgurskaya *et al.*, 2011).

1.2.5. Substrate binding for export via TolC

Many substrates of AcrAB-TolC show no structural or chemical similarites, which suggests a non-specific process for substrate binding. Substrates are captured from the cytoplasmic and periplasmic compartments by the AcrB transporter protein (Fig 1.3). The structure of this protein implies that substrates are translocated from the cell interior through the transmembrane domain to the central cavity of AcrB. From here, the susbstrate is actively transported through the pore domain into the TolC tunnel (Murakami *et al.*, 2002) (Fig 1.3). Upon substrate binding with AcrB, a conformational change is triggered in TolC, resulting in an opening at the periplasmic entrance of the protein, allowing export of the substrate (Symmons *et al.*, 2009). However, there are disputes about the specificities of this process (Zgurskaya *et al.*, 2011). Two locations of substrate binding have been observed in AcrB, depending on the structure and charge of the molecule. There is a narrow “groove” site and a wider “cave” site that binds simpler molecules (Takatsuka *et al.*, 2010). Novobiocin, tetracycline and erythromycin are examples of “groove binders” and chloramphenicol, carbenicillin and cyclohexane are reported “cave binders”. Nile Red, oxacillin, Triton X-100 are among compounds identified as mixed binders which appear to utilise both binding sites (Takatsuka *et al.*, 2010).

In some bacteria TolC interacts with additional membrane transporters e.g. AcrD within *E. coli,* which although is not within an operon with AcrA, still forms the tripartite system; AcrAD-TolC. AcrB and AcrD show strong sequence similarity, however large periplasmic loops present in both appear to define some differences in substrate specificity resulting in a more restricted range of substrates exported by AcrD (Elkins and Nikaido, 2002). Although not as widely researched as AcrB, AcrD behaves in a similar way, interacting with AcrA and obtaining substrates from the periplasm, evidenced in *E. coli* (C. A. Elkins and H. Nikaido 2002) and *S.* Typhimurium (Yamasaki *et al.,* 2011). The substrates exported via TolC are determined by associated membrane transporters.

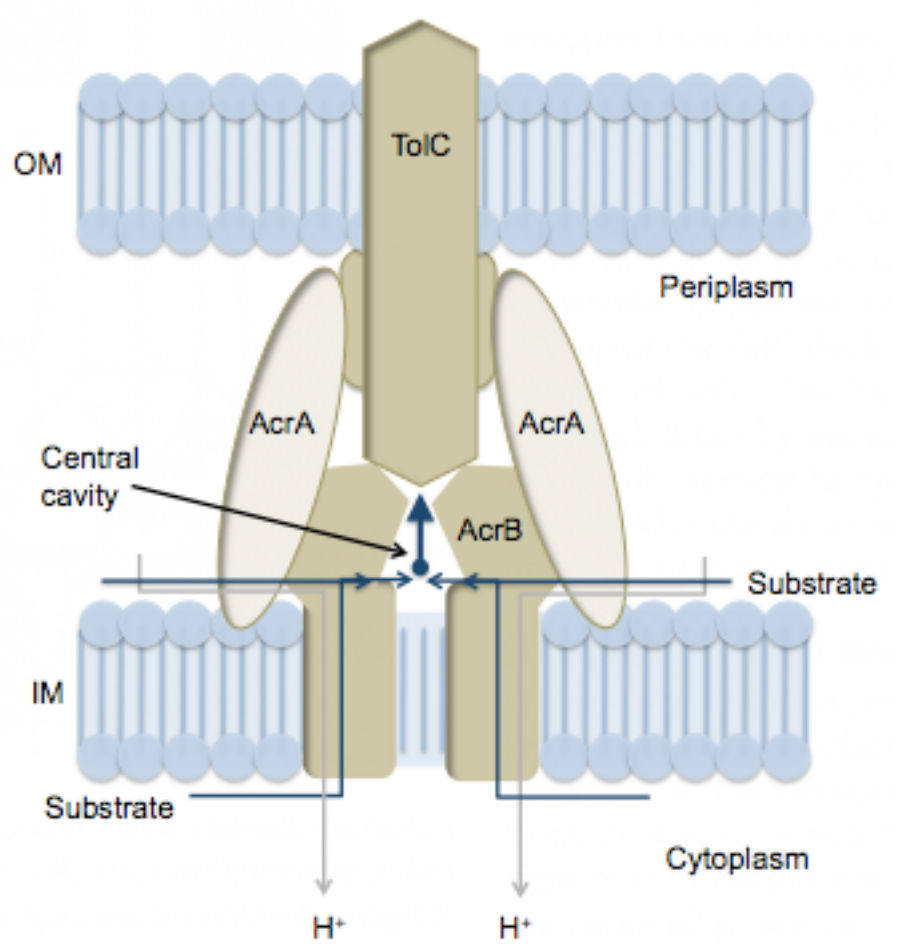

Figure 1.3. The AcrAB-TolC efflux system.

Outer membrane protein, TolC joining AcrB forming a central cavity where substrates are collected from periplasm and cytoplasm before export. Membrane fusion protein, AcrA, stabilises the pump and binds to the inner membrane. Diagram adapted from (Murakami *et al.*, 2002).

Importantly, AcrB and AcrD differ in the antibiotics they are able to secrete making it important to distinguish between these two proteins in order to investigate antibiotic resistance.

1.2.6. Substrates of the resistance nodulation division efflux system

Although antimicrobial resistance has been the focus of RND efflux systems such as AcrAB-TolC, they possess a number of additional functions such as the export of a number of host derived substrates, including bile and fatty acids (Piddock, 2006). The requirement of TolC in bile resistance has been shown in *V. cholerae* (Bina and Mekalanos, 2001), however fatty acid secretion via this system has not been extensively studied. *E. coli* was shown to over express AcrAB when cultured in the presence of a 10 carbon chain fatty acid (Ma *et al.*, 1995, Rosenberg *et al.*, 2003). This evidence supports the ability for the trimeric systems to export a wide range of structures, particularly hydrophobic agents such as fatty acids and solvents (Ramos *et al.*, 2002). In addition there is evidence to support natural efflux of fatty acids and other long carbon chain compounds. *Desulfovibrio desulfuricans*, *Clostridium pasteurianum* and *Vibrio furnissii* have been investigated for their production of extracellular hydrocarbons (Davis, 1968, Bagaeva and Zinurova, 2004, Tornabene *et al.*, 1970, Jones, 1972). The reason for extracellular hydrocarbon production by microbes and how the export mechanism works is not fully understood. Reports have suggested that in sulfate reducing bacteria and *Clostridia*, extracellular hydrocarbons are associated with the formation of cell surface capsules, involved in protection from excreted acids (Bagaeva and Zinurova, 2004). Other reports suggest uses such as cell adhesion to glass surfaces in *Pseudomonas fluorescens* (Nikolaev *et al.*, 2001) and isoprene has been suggested to work as a secondary metabolite in bacterial communication (Hastings and Greenberg, 1999). The capacity for organisms to produce such compounds has a number of applications and needs further study.

1.3. Bacterial fatty acid and hydrocarbon production

1.3.1. Microbial bio-fuels.

Organisms that synthesise long chain hydrocarbons (LCHs) such as alkanes and precursor compounds such as free fatty acids (FFAs) and aldehydes have been extensively studied for use as potential tools for liquid fuel or bio-diesel production (Stone and ZoBell, 1952, Ladygina *et al.*, 2006). Industrial technologies are focused on renewable and sustainable sources of energy and consequently there is now large interest in bio-fuel production. Ethanol, methane and bio-diesel can be used to replace fossil fuels furthermore by utilising sources such as plants and algae, CO_2 can be recycled in the production of bio-fuel (Klass, 1998). Hydrocarbons are essential for fuel and current combustion systems and various groups of microorganisms have been evidenced for

hydrocarbon synthesis. These range from bacteria (Albro and Dittmer, 1969, Tornabene *et al.*, 1970) to fungi (Bird and Lynch, 1974), yeasts and algae. Yeasts such as *Saccharomyces* sp *oviformis* and *Saccharomyces ludwigii* produce intracellular hydrocarbons up to 10.2% of their dry biomass (Merdinger and Frye, 1966, Ladygina *et al.*, 2006). It is established that microalgae produce much higher levels of hydrocarbons, a recent and relevant example is the high hydrocarbon yielding algae (up to 60% of dry biomass) *Botryococcus braunii* (Hillen *et al.*, 1982, Metzger and Largeau, 2005). The interaction of microbes with algae is of further significance where cellulose from algae cell walls can be utilised as a precursor for microbial production of fatty acids and compounds viable for the bio-fuel industry (Hoover *et al.*, 2011).

1.3.2. Bacterial fatty acids

Lipids, commonly found in all organisms, have a number of industrial applications and as precursors for hydrocarbons they are particularly relevant to the bio-fuel industry. Furthermore, these hydrophobic molecules are integral to a number of bacterial processes. Phospholipids and glycolipids are widespread in Gram-negative bacteria and account for a large percentage of cellular fats due to their role as cell membrane constituents. Wax esters, long chain ester fatty acids and alcohols have a number of industrial uses, however compared to glycolipids, these are less common. In some bacteria, such as *Acinetobacter* sp, large amounts of wax esters are produced and accumulate as energy storage compounds, (Ishige *et al.*, 2002). These compounds are produced when the bacterium is grown on long chain alkanes, making it a desirable organism for removal of alkanes from the environment (Makula *et al.*, 1975, Ishige *et al.*, 2003). Glycerides, specifically triacylglycerides (TAGS), diacylglycerides (DAGS) and monoacylglycerides (MAGS) are also, though less commonly, synthesised by bacteria (Alvarez and Steinbüchel, 2002), however TAG accumulation has been reported in *Mycobacterium, Rhodococcus opacus* and more recently *Alcanivorax* species, a marine bacterium relevant in bioremediation (Barksdale and Kim, 1977, Alvarez *et al.*, 1996, Kalscheuer *et al.*, 2007). Free fatty acids (FFAs) account for a relatively high percentage of total fats. In some bacterial species, such as *Corynebacterium diphtheriae* and *S.* Typhimurium*,* these molecules account for more than 20% of cellular fats which are primarily comprised of hexadecanoic (palmitic), octadecanoic (stearic) and octadecenoic (oleic) acids (O'Leary, 1962). Hexadecanoic acid is one of the most common fatty acids serving as a precursor to longer fatty acids and ultimately alkane synthesis. Hexadecanoic acid (C_{16}) and octadecanoic acid (C_{18}) are also converted to unsaturated FFAs; hexadecenoic (palmitoleic) and octadecenoic (oleic) by desaturase enzymes (Stukey *et al.*, 1990). These also contribute a large percentage of FFAs and have additional applications, displaying links to membrane fluidity and transmembrane signalling (Mansilla and de Mendoza, 2005), (Pablo and Mendoza 2006). In addition they are

reported to inhibit *fabI,* a fatty acid synthesis gene targeted for antibacterial drugs (Zheng *et al.*, 2005).

1.3.3 Fatty acid synthesis in bacteria

In bacteria fatty acid synthesis occurs via the FASII pathway and requires a number of enzymes. Enzymes participating in the synthesis of unsaturated and saturated fatty acids and phospholipids (characterised from *E. coli*) are the *fab* enzymes which are collectively known as the fatty acid synthetase complex. Initially, Acetyl-CoA carboxylase converts Acetyl-CoA to Malonyl-CoA, which ultimately acts as a chain extending unit (Davis *et al.*, 2000). Malonyl-CoA is subsequently transferred to an acyl carrier protein (ACP) by FabD, forming Malonyl-ACP, this then combines with Acetyl-CoA enabling fatty acid synthesis (Magnuson *et al.*, 1993, Rock *et al.*, 1996) (Fig 1.4). The cycle involves a condensation reaction by FabH, FabB or FabF, a keto group reduction (FabG), dehydration (FabA, FabZ) and an enoyl reduction (FabI, FabK, FabL). This cycle repeats 7 times to yield hexadecanoyl-ACP which is hydrolysed to give hexadecanoic acid or similarly 8 times to yield octadecanoyl-ACP hydrolysed to form octadecanoic acid (Fig 1.4) (Rock *et al.*, 1996).

1.3.4. Hydrocarbon biosynthesis

Development of analytical techniques led to greater understanding of the composition of hydrocarbons synthesised by microorganisms and subsequently intracellular hydrocarbon biosynthesis (Bird and Lynch, 1974) (Tornabene *et al.*, 1967). Since then, a number of pathways have been suggested for hydrocarbon synthesis from fatty acids but the process is still not fully understood. Most comprehensively studied, is the elongation decarboxylation pathway (Table 1.1) (Ladygina *et al.*, 2006) which involves fatty acid decarboxylation to an aldehyde intermediate and decarbonylation of the aldehyde to produce the hydrocarbon (Table 1.1). This process has been investigated in a number of organisms including *E. coli* (Naccarato *et al.*, 1974), *Pisum sativum* (Cheesbrough and Kolattukudy, 1984, Vioque and Kolattukudy, 1997) and *B. brauniii* (Dennis and Kolattukudy, 1991, Wang and Kolattukudy, 1995). Another widely researched system is the head to head condensation mechanism which also involves decarboxylation of the fatty acid (Albro and Dittmer, 1969). More recently a novel pathway for long chain hydrocarbon synthesis in *V. furnissii* has been suggested via an additional alcohol intermediate (Park, 2005) (Table 1.1).

1.3.5. Advantages of utilising bacteria in bio-fuel production

There are a variety of industrial processes for lipid and hydrocarbon extraction from algal and bacterial strains (Mata *et al.,* 2010). Transesterification of lipids can be carried out to form ester fuels, hydrogenation of algal biomass can yield and improve combustible qualities of hydrocarbons

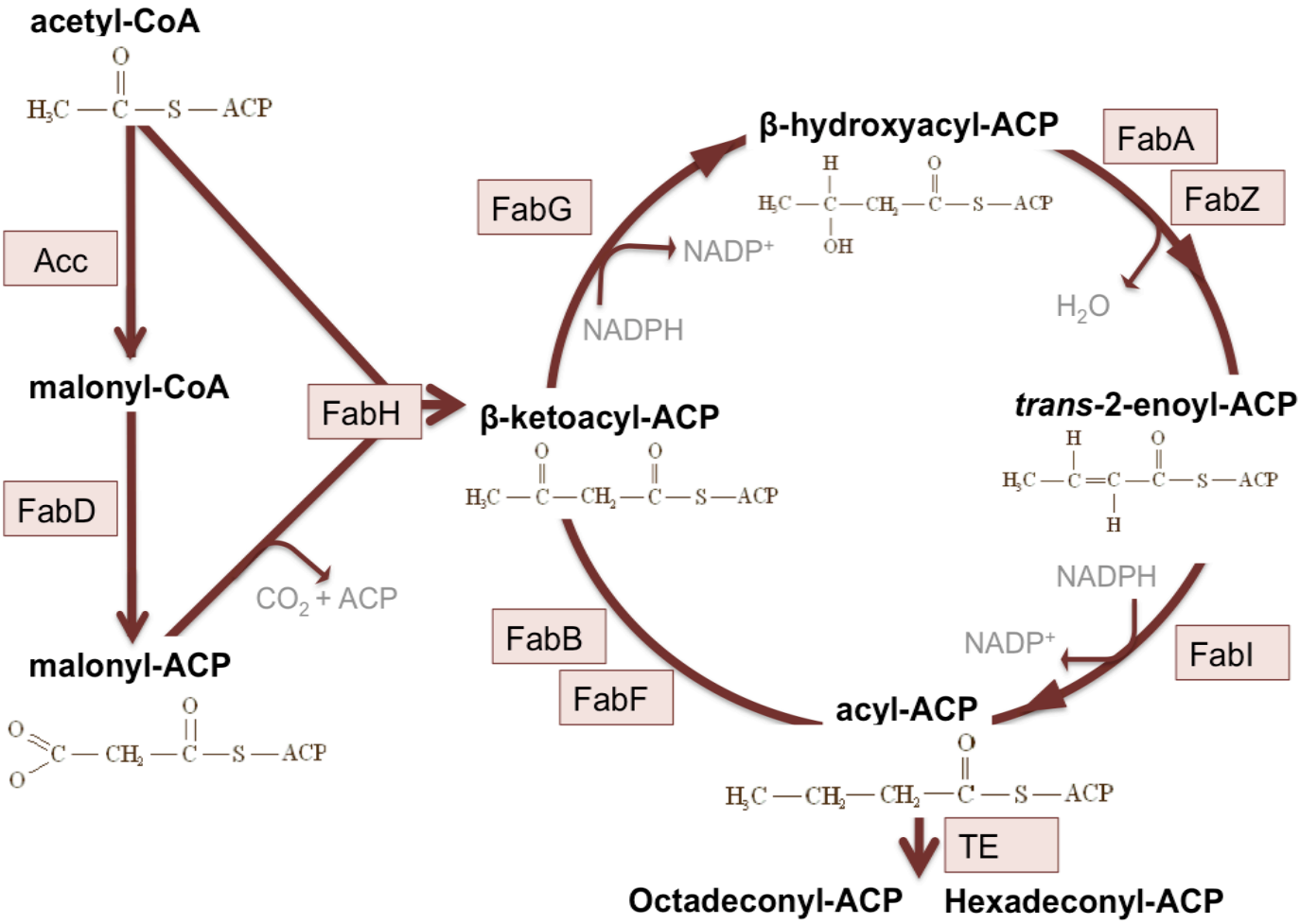

Figure 1.4 Fatty acid synthesis in *E. coli*.

Acetyl-CoA carboxylase (Acc) converts Acetyl-CoA to Malonyl-CoA which is carried to an acyl carrier protein by FabD, forming Malonyl-ACP. Malonyl-ACP and Acetyl-CoA merge to form β-ketoacyl-ACP. Fatty acid synthesis occurs via reactions involving Fab enzymes, following seven cycles, octadeconly-ACP and hexadeconyl-ACP are formed and released by the action of a thioexterase (TE). The products can then undergo elongation via the fatty acid elongation pathway or hydrolysed to form palmitic (C_{16}) and stearic acid (C_{18}).

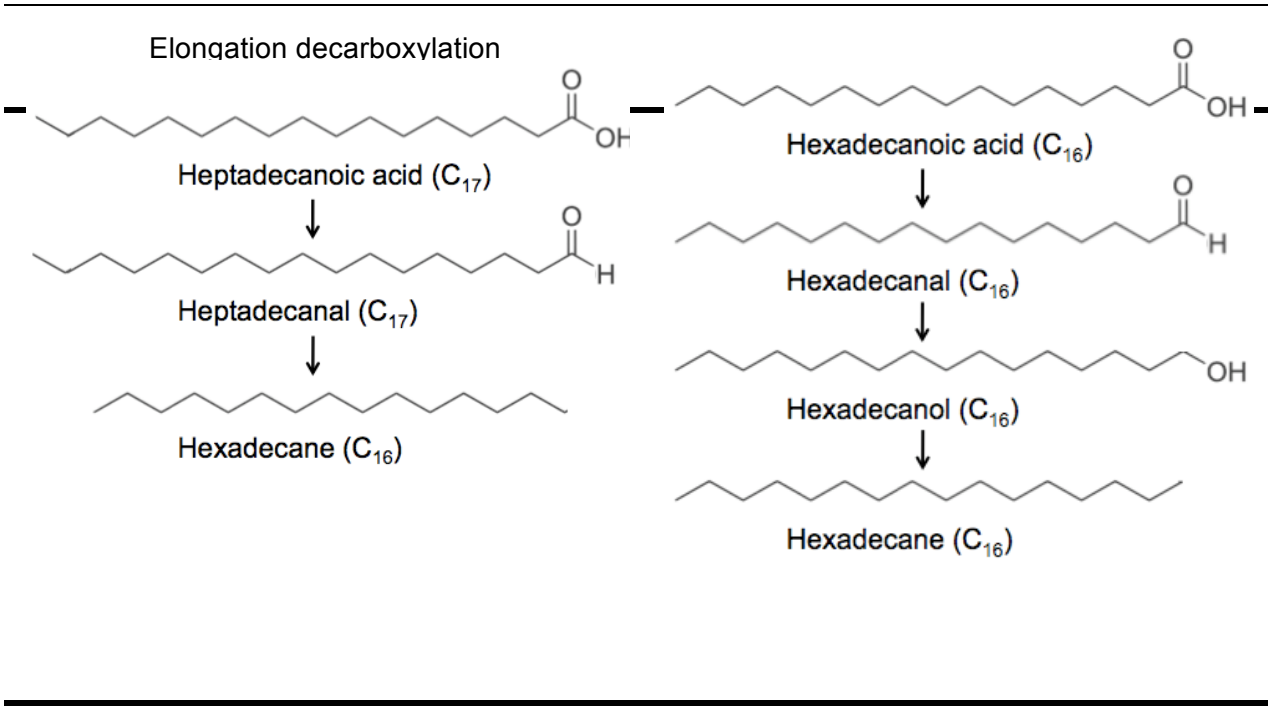

Table 1.1. Hydrocarbon biosynthesis.

Decarboxylation of fatty acid to alkane occurs via aldehyde intermediate, or in proposed pathway in *V. furnissii,* an additional alcohol intermediate (Park, 2005)

(Vitolo and Ghetti, 1994) and liquefaction of microalgal biomass has been used to form oily substances (Sawayama *et al.*, 1999). Another competitor for an economic bio-fuel is bio-ethanol extracted from lignocellulose and microbes have been investigated for use in this process (Zaldivar *et al.*, 2001). Although the focus of bio-fuel production has largely been on hydrocarbon synthesis in photosynthetic algae, there are a number of advantages to utilising bacteria e.g. much faster growth rates and the capacity to culture larger quantities. The ability to manipulate the genes within bacteria is relatively easy and allows analysis of those in the hydrocarbon and fatty acid synthesis pathways; this makes bacteria an appealing target for bio-fuel investigation. All processes for extracting and purifying long chain carbon compounds involve high pressures, high temperatures and consequently high costs. Understanding secretion mechanisms in bacteria and investigating the potential to increase the export of naturally secreted compounds that are industrially viable, is a significant area of interest within the bio-fuel industry.

1.3.5. Engineering the bacterial fatty acid synthesis pathway

The Acyl ACP reductase and aldehyde decarbonylase enzymes in cyanobacteria have recently been identified as targets for engineering alkanes and alkenes from intermediates of fatty acid metabolism (Schirmer *et al.*, 2010). These essential enzymes are responsible for reduction of acyl ACPs to fatty aldehydes and converting the aldehyde to the alkane (Table 1.1). Engineering of the alkane synthesis pathway for increased microbial bio-fuel synthesis has been a focus of recent literature (Nawabi *et al.*, 2011, Li *et al.*, 2012). Generating greater quantities of fatty acids for bio-diesel production by engineering a series of genes within the fatty acid synthesis pathway has proven successful in *E. coli* (Lu *et al.*, 2008). Given the significance of fatty acid synthesis to the bio-fuel industry, reviewing and establishing levels of fatty acids and alkanes naturally synthesised by bacteria is an important area of study. Organisms, other than *E. coli,* that have the natural capacity to synthesise greater concentrations of alkanes and fatty acids may be more suitable targets for industrial applications.

1.3.6. Hydrocarbon producing bacteria

The marine bacteria *Serratia marinorubrum* and *Vibrio ponticus* were among the first organisms to be investigated for hydrocarbon synthesis (Stone and ZoBell, 1952). However the hydrocarbon content in these species is low; for example in *V. ponticus* and *Vibrio marinus* approximately 0.03% of their dry mass corresponds to such compounds (Stone and ZoBell, 1952, Oro *et al.*, 1967). These quantities can be contrasted to *E. coli* which produces 0.0035% of its dry weight in hydrocarbons of length C_{16}-C_{18} (Han and Calvin, 1969, Ladygina *et al.*, 2006). One of the highest hydrocarbon producers is the Gram-negative, anaerobic, sulfate reducing bacteria *D. desulfuricans,*

of which up to 2.25% of its biomass corresponds to intracellular hydrocarbons of length up to C_{35} (Oppenheimer, 1965, Davis, 1968). *Mycobacterium* sp. also produces a similar percentage of its dry mass in hydrocarbons (Jones, 1972). More recently the bacterium *V. furnissii* M1 has been proposed as a high hydrocarbon yielding bacterium, although this has been disputed (Park *et al.*, 2001, Park *et al.*, 2005, Wackett *et al.*, 2007). *V. furnissii* M1 was reported to produce significant levels of alkanes with chain length ranging from C_{18}-C_{24} corresponding to light oil (Park *et al.*, 2005). Optimisation of media was achieved and the highest hydrocarbon yielding media, containing glucose and lactic acid, resulted in a production of up to 26.5 mg of alkanes per 50 ml culture (60% of biomass) (Tornabene *et al.*, 1970, Jones, 1972, Park *et al.*, 2005). A report demonstrating an absence of an alkane producing phenotype in *V. furnissii* M1 (Wackett *et al.*, 2007) suggests that the hydrocarbon levels produced are not significant. Regardless of the claim that *V. furnissii* produces such high quantities of long chain hydrocarbons, other studies show that compared to *E coli,* alkane content in *Vibrio* species is approximately 10 times greater (Ladygina *et al.*, 2006). This places *V. furnissii* as a promising target for the bio-fuel industry.

1.3.7. Vibrio furnissii

V. furnissii is investigated in this study, not only to broaden our understanding of pathogenesis, antibiotic resistance, toxin resistance, and quorum sensing in a less extensively studied *Vibrio* strain, but also to investigate the role of TolC within these mechanisms. These processes are all relevant areas of study within *Vibrio* species and although the connection is not fully understood, they have been researched in association with TolC. (Boardman and Satchell, 2004, Henke and Bassler, 2004, Igbinosa and Okoh, 2008, Kitaoka *et al.*, 2011, Minato *et al.*, 2011). Furthermore, fatty acid and hydrocarbon export is an industrially relevant system to be studied within this bacterium and TolC is a promising target for investigating secretion of these compounds.

V. furnissii, formerly a member of the aerogenic biogroup of *Vibrio fluvialis,* was isolated from patients with acute gastroenteritis (Brenner *et al.*, 1983). *V. fluvialis* was isolated from human faeces and although originally thought to be non-pathogenic, it was later associated with outbreaks of diarrhoea and a fatal case was reported in the early 1980s (Tacket *et al.*, 1982). As a consequence, *V. furnissii*; the free living, Gram-negative marine proteobacterium, was investigated as a potential human pathogen. The importance of this bacteria as an enteric pathogen is yet to be fully established but association with diarrhoea outbreaks have continued (Hickman-Brenner *et al.*, 1984, Lam and Goi, 1985, Magalhães *et al.*, 1993, Dalsgaard *et al.*, 1997) and recent cases of *V. furnissii* bacteremia have been reported (Derber *et al.*, 2011). Of 30 known *Vibrio* species, the lethal pathogen *V. cholerae* is the most intensively studied, although the clinical relevance of other

Vibrios has been determined (Jones and Oliver, 2009, Daniels *et al.,* 2000). *V. furnissii* is one of 13 non-choleric Vibrios that have been implicated in human pathogenicity (Igbinosa and Okoh, 2008, Solomakos *et al.*, 2012), together with *V. parahaemolyticus*; a recently established pathogen associated with gasteroenteritis (Daniels *et al.*, 2000, Ellis *et al.*, 2012, Solomakos *et al.*, 2012). The DNA relatedness of *V. furnissii* to other *Vibrio* species is relatively low (<22%), however sequence similarity is closest to *V. cholerae* and *V parahaemolyticus* (Brenner *et al.*, 1983). The complete genome sequence of *V. furnissii* NCTC 11218 was recently sequenced and like other *Vibrio* species it comprises two circular chromosomes (Lux *et al.*, 2011). Although homologues of a number of *V. cholerae* virulence factors are absent in the *V. furnissii* genome, many are present including *ompU, hlyA, toxS, tcpA/tcpII* (Lux *et al.*, 2011). The association of marine bacterium *V. furnissii* with bio-fuels has stimulated interest over the last decade. *V. furnissii* M1, was isolated from an environmental sample obtained from a sewerage plant in Osaka (Park *et al.,* 2001) and was shown to sythesise vast quantities of alkanes. The sequenced genome of *V. furnissii* NCTC 11218 does not exhibit genes required for hydrocarbon synthesis (Lux *et al.,* 2011, Wackett *et al.,* 2007), which suggests that if hydrocarbons are produced as suggested it is via a novel pathway (Park *et al.,* 2005).

1.4. The secretion of compounds for cell-cell signalling

1.4.1. Quorum derived signalling

Quorum sensing is a growth phase dependant process by which bacteria secrete signalling molecules of varying structure as a method of cell-cell communication (Bassler, 2002). The method by which these signalling compounds are released is not well established although a connection to RND efflux systems and the requirement of active efflux has been determined in *P. aeruginosa* (Evans *et al.*, 1998, Pearson *et al.*, 1999). It is understood that the molecules accumulate extracellularly and are detected by neighbouring cells, this leads to regulatory changes and allows bacteria to coordinate cellular behaviour. As cell density increases, frequently during late exponential phase, so does signal molecule concentration. At a threshold concentration a gene regulatory mechanism is triggered and the activation of these genes allows bacteria to coordinate swimming (Glessner *et al.*, 1999), biofilm formation (Davies *et al.*, 1998), toxin production and regulation of other virulence factors (Storey *et al.*, 1998, Rumbaugh *et al.*, 1999, Zhu *et al.*, 2002, Higgins *et al.*, 2007). Quorum sensing is widely researched among Gram-negative bacteria including *P. aeruginosa* (Williams and Camara, 2009), *S.* Typhimurium and *E. coli* (Surette *et al.*, 1999) as well as a number of *Vibrio* species including *V. fischeri*, *V. harveyi*, *V. vulnificus*, *V. cholerae*, *V. parahaemolyticus* and *V. anguillarum* (Ng *et al.*, 2011). Quorum-derived signalling in

these bacteria plays an important role in a variety of processes combating host defenses.

1.4.2. The quorum regulatory Lux pathway in V. fischeri, V. harveyi *and* V. cholerae

Signalling compounds secreted by bacteria are commonly known as homoserine lactones or autoinducers. In *Vibrio* species, synthesis and detection of these compounds is regulated by the Lux pathway which was first identified in *V. fischeri* (Engebrecht *et al.*, 1983). The comprehensively studied quorum sensing system in *V. fischeri* and *V. harveyi* involves the regulation of luminescence by the *luxCDABE* operon, however the systems in these two bacteria are very different (Lilley and Bassler, 2000, Miller and Bassler, 2001). The regulatory system in *V. fischeri* involves a synthase (LuxI), and a cytoplasmic receptor (LuxR) which, once bound to the homoserine lactone, also acts a transcriptional regulator for the luciferase *luxICDABE* operon (Fig 1.5). The *V. fischeri* quorum sensing system is conserved in other Gram-negative bacteria and plays an essential role in the positive and negative regulation of a number of factors such as biofilm formation, Type III secretion and protease production (McDougald *et al.*, 2000, Hammer and Bassler, 2003, Henke and Bassler, 2004). For example the LasI/LasR system in *P. aeriginosa* regulates virulence gene expression and biofilm formation (Williams and Camara, 2009). Unlike other Gram-negative bacteria, *V. cholerae* and *V. harveyi* posses an alternative two component phospho-regulatory system. Within these systems, for example in *V. harveyi* (Fig 1.6), when cell densitiy and autoinducer concentration is low, phosphate flows from the receptor to LuxU and LuxO. Phospho-LuxO, activates the expression of Qrr (Quorum regulatory RNA) and in turn represses the expression of LuxR which regulates the luciferase operon *luxCDABE* (Lilley and Bassler, 2000, Lenz *et al.*, 2004) (Fig 1.6). During high cell densities dephosphorylation and deactivation of LuxO occurs which results in expression of the *luxCDABE* operon (Bassler, 1999).

V. cholerae and *V. harveyi* contain similar quourum sensing components however they act by different means, hypothetically due to adaptations to evolutionary adaptations to alternative environments (Bassler, 2009). Like *V. furnissii, V. harveyi* is a free living marine bacterium whereas *V. cholerae* utlises humans as a host as well as existing in aquatic environments. Within *V. harveyi* quorum sensing regulates bioluminescence, metalloprotease production and Type III secretion whereas in *V. cholerae* quorum sensing regulates biofilm formationm virulence factor and protease production (Miller *et al.*, 2002). Within *V. cholerae* LuxR negatively regulates virulence factor production meaning at high cell densities expression of virulence factors is repressed.

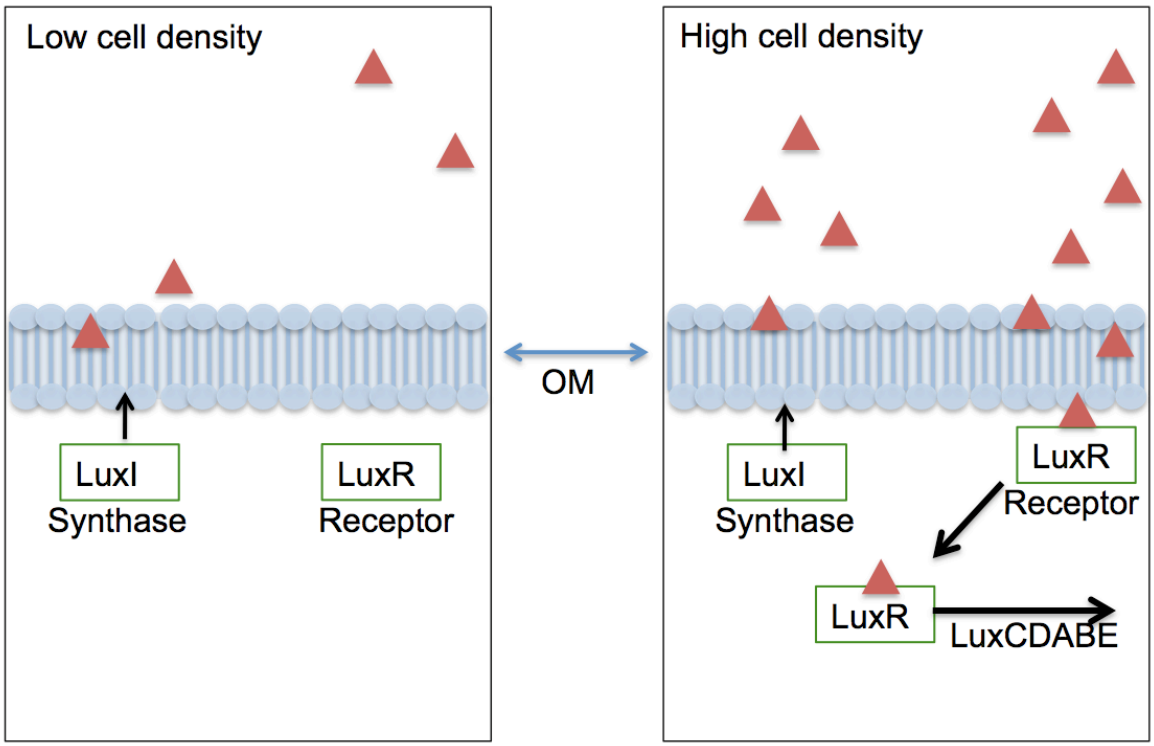

Figure 1.5. The quorum sensing mechanism in *V. fischeri*

A synthase protein LuxI produces signalling compounds and receptor LuxR detects those produced by other bacteria. At high cell densities, a threshold concentration of signalling compounds are detected triggering expression of a pathway which ultimately expresses luciferase operon LuxCDABE, responsible for bioluminescence. Diagram adapted from Bassler (2009).

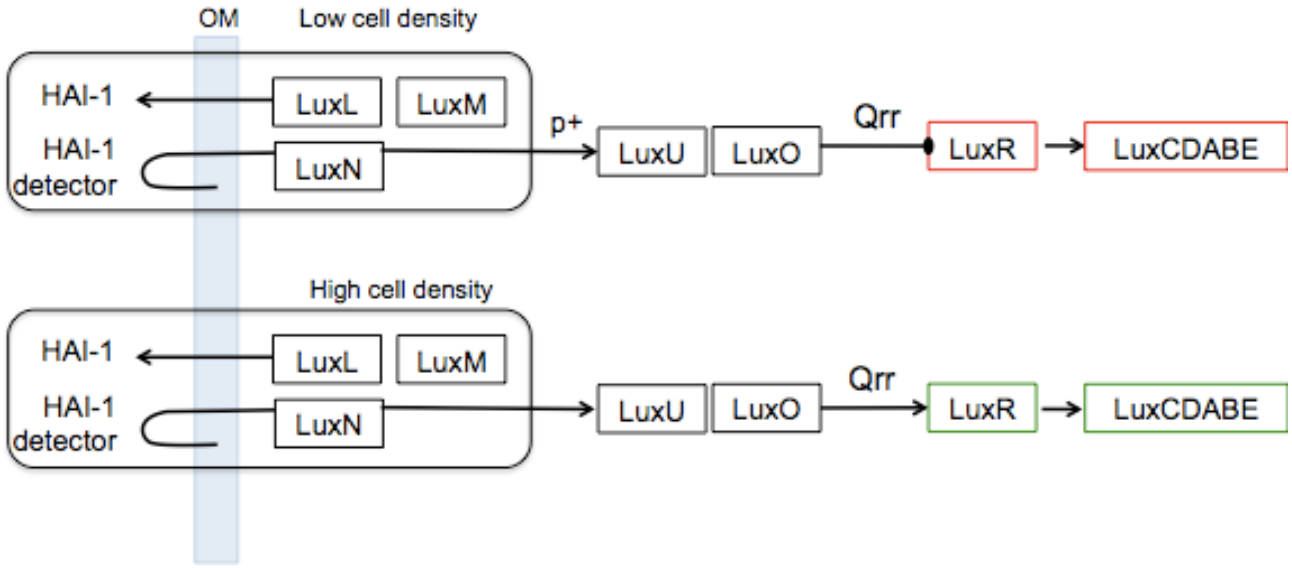

Figure 1.6. The Lux regulatory pathway for HAI-1 secretion and detection in *V. harveyi*

Adapted from the KEGG database. The signalling compound, HAI-1, is synthesised by LuxLM and detected by sensory kinase LuxN in the outer membrane (OM). At low cell density phosphate flows to shared response regulators LuxUO activating expression of quorum regulatory RNA (Qrr) which represses the luxCDABE fluorescence operon. At high cell density dephosphorylation of LuxO means Qrr are not activated and LuxR and LuxCDABE are expressed

1.4.3. Bacterial signalling molecules: Homoserine lactones and autoinducers

Homoserine lactones (HSLs) are the most common signalling compounds implicated in quorum sensing; all containing a homoserine lactone ring but with varying side chains (Fuqua *et al.*, 2001) (Table 1.2). Following the discovery of the homoserine lactones produced by *V. fischeri* and *V. harveyi* a number of additional signalling compounds were identified including 3-oxo-C10-HSL in *V. anguillarum* (Milton *et al.*, 1997) and 3-oxo-C12-HSL in *P. aeruginosa* (Pearson *et al.*, 1994). In addition, structural variations on autoinducer compounds widely researched in *Vibrio* species have been determined (Ng *et al.*, 2011). Of these signalling compounds many are only detected or synthesised by particular organisms but some, like (2*S*,4*S*)-2-methyl-2,3,3,4-tetrahydroxytetrahydrofuran borate (AI-2) (Table 1.2) (Xavier and Bassler, 2003), appear to have a broader specificity among species. Of 25 *Vibrio* species, 23 produce one or more different different types of quorum sensing signalling molecules with *V. harveyi* VIB571, *V. harveyi* VIB645, *V. pomeroyi, V. campbellii, Aliivibrio logei* and *V. furnissii* being the only 6 able to produce three different types of signalling molecule (Yang *et al.,* 2011).

1.4.4. Homoserine lactone and autoinducer synthesis and detection

Unlike *V. fischeri, V. harveyi* has a two component system whereby three chemical signals are synthesised and detected: *N*-(3-hydroxybutanoyl)-homoserine lactone (HAI-1) via the LuxM/N system, AI-2 via the LuxS/PQ system and (*S*)-3-hydroxytridecan-4-one (CAI-1) via the CqsA/S system (Table 1.2) (Cao and Meighen, 1989, Bassler *et al.*, 1994, Bassler, 2009). Within *V. harveyi* there are three biosynthetic pathways for these autoinducers, all of which feed back to the Lux regulatory system, however, the synthases exhibit no similiarity to LuxI in *V. fischeri* (Bassler *et al.*, 1993). *V. cholerae*, more recently studied in relation to quorum sensing, utilises AI-2 and CAI-1 (Table 1.2). The autoinducer CAI-1 contains a long hydrocarbon chain and is synthesised and detected by CqsA and CqsS respectively (Miller *et al.*, 2002, Kelly *et al.*, 2009). Variations on the CAI-1 structure within *Vibrio* species have been recently determined and it is apparent that autoinducer specificity differs between strains. These data have been used to categorise *Vibrio* species based on CAI-1 selectivity (Ng *et al.*, 2011, Wei *et al.*, 2011).

1.4.5. Secretion of autoinducers

It is accepted that secretion of autoinducers and acyl homoserine lactones occurs via membrane diffusion. This was initially demonstrated in *V. fischeri* by introducing autoinducer N-(3-oxohexanoyl) into cultures and observing that the intracellular concentrations of the compound rapidly equilibrate to external concentrations (Kaplan and Greenberg, 1985). A number of additional signalling molecules with varying chemical structures have since been discovered and it cannot be

Homoserine lactones		
Name	Structure	Chemical name and reference
HSL (Homoserine lactone)	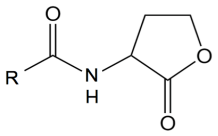	Acyl - homoserine lactone general structure
AI-1 (3-oxo-C6-HSL)	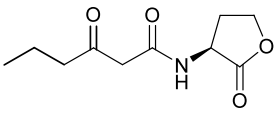	N-(3-oxohexanoyl)-L-homoserine lactone (Eberhard *et al.*, 1981)
HAI-1 (3-OH-C4-HSL)	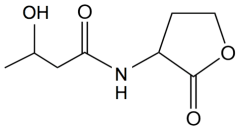	3-hydroxybutanoyl homoserine lactone (Cao and Meighen, 1989)
Autoinducers		
AI-2	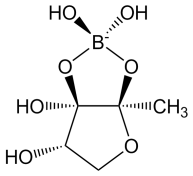	(2*S*, 4*S*)-2-methyl-2,3,3,4-tetrahydroxytetrahydrofuran borate (Chen *et al.,* 2002)
CAI-1	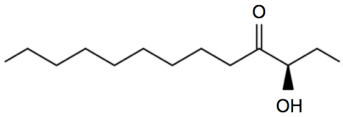	(*S*)-3-hydroxytridecan-4-one (Higgins *et al.*, 2007)

Table 1.2. Quorum sensing signalling compounds.

Including first acyl-homoserine lactone discovered (3-oxo-C6-HSL) in *V. fischeri* and the three known autoinducers in *Vibrio* species; *V. harveyi* autoinducer (HAI-1), autoinducer 2 (AI-2) (interspecies signalling compound) and CAI-1.

assumed that all diffuse across membranes freely. More recent research suggests that transport systems are required for export of some signalling compounds. There is evidence supporting active efflux of the homoserine lactone $3OC_{12}$-HSL in *P aeruginosa* via the MexAB-OprM efflux system (Evans *et al.*, 1998, Pearson *et al.*, 1999) and the more hydrophilic AI-2 compound also requires a transport system (Kamaraju *et al.*, 2011). TolC, in association with membrane bound antiporters, provides a nonspecific membrane spanning channel; a model secretion system for the diverse array of chemical signals that require export.

1.5. Implications of mutating tolC

1.5.1. TolC and associated interactions

TolC spans both cell membranes and is therefore intrinsically linked to membrane integrity. It plays a number of roles other than those implicated in MDR, acting as a cell surface receptor for bacteriophage TLS and the secretion of α-haemolysin in *E. coli* (Wandersman and Delepelaire, 1990, German and Misra, 2001). Mutations in *tolC* produce pleiotropic phenotypes, from altering ultimate cell density during stationary phase (Yang *et al.*, 2006) and decreasing toxin secretion and adhesion to and invasion of host cells in *S.* Typhimurium (Webber *et al.*, 2009). Such phenotypes may be due to decreased expression of various other genes including membrane bound efflux proteins associated with TolC and genes associated with the cell envelope. TolC mutants in *S.* Typhimurium have also displayed phenotypic changes in motility and decreased expression of flagella proteins (Webber *et al.*, 2009). The connection between TolC and these expression changes has not been established although quorum sensing is a system which could potentially link the observed phenotypes.

1.5.2. The role of of TolC in cellular detoxification

Expression changes of TolC alters the regulation of a number of systems required for cell survival including export of metabolites, acid tolerance, membrane integrity, virulence and antibiotic resistance (Zgurskaya *et al.*, 2011). TolC and AcrAB expression are induced by the *soxSR* regulon supporting evidence that this efflux system plays a role in superoxide metabolism (Imlay, 2008, Zgurskaya *et al.*, 2011). The SoxSR system is responsive to stress conditions ultimately promoting acid tolerance and superoxide resistance (Greenberg *et al.*, 1990, Tsaneva and Weiss, 1990, Aono *et al.*, 1998). SoxS detects redox stress and SoxR acts as a transcriptional regulator, inducing expression of *tolC* and *acrAB* among other proteins (Rosner and Martin, 2009, Gu and Imlay, 2011). Superoxides are highly toxic molecules generated by partially reduced oxygen species and are inevitable by-products of aerobic metabolism (Fridovich, 1978). They are also generated when molecular oxygen reacts with electrons produced from environmental redox reactions such as

glutathione oxidation (Ross, 1988, Cheeseman and Slater, 1993) (Fig. 1.7). The O_2^- superoxide radicals generated by this process can also undergo reduction to form the reactive oxygen species: H_2O_2 which can react to form the most reactive and damaging hydroxyl radical, $OH^\bullet$ (Fig. 1.7) (Brawn and Fridovich, 1981, Cheeseman and Slater, 1993). The expression of *soxSR* is induced by the presence of reactive oxygen species, this in turn regulates a series of proteins and enzymes to dispel superoxides (Fridovich, 1983). Superoxide dismutase plays an essential role in degrading superoxides; with increased expression occurring when bacteria experience oxidative stress (Bébien *et al.*, 2002). *E. coli* cells, devoid of superoxide dismutase enzymes, have shown an accumulation of O_2^- leading to reduced growth when cultured aerobically (Carlioz and Touati, 1986). The association of *tolC*, with the *soxRS* system strongly implies the efflux system aids the cell in defense against superoxides however further study is required.

1. $O_2 + e^- \rightarrow O_2^{-\bullet}$	Superoxide formed by reduction of oxygen by transfer of electron
2. $O_2 + 2e^- + 2H^+ \rightarrow H_2O_2$	Hydrogen peroxide (ROS) formed by two electron reduction
3. $2O_2^{-\bullet} + 2H^+ \rightarrow H_2O_2 + O_2$	Hydrogen peroxide (ROS) also formed by reaction of superoxides
4. $2O_2^{-\bullet} + H_2O_2 \rightarrow OH^\bullet + OH^- + O_2$	Hydrogen peroxide (ROS) reacts with superoxides producing hydroxyl radicals.
5. $H_2O_2 + Fe^{2+} \rightarrow OH^\bullet + OH^- + Fe^{3+}$	Reactive hydrogen peroxide breaks down in the presence of transition metal ions also producing hydroxyl radicals

Figure.1.7. Superoxide reactions in bacteria.

Synthesis of superoxides (reaction 1), reactive oxygen species (ROD) hydrogen peroxide (reactions 2 and 3) and hydroxyl radicals (reactions 4 and 5).

AIMS

Prior to the start of this study, random transposon mutagenesis was carried out in *V. funissii* to find mutants yielding higher levels of hydrocarbons. Four *tolC*$^-$ knockout mutants displayed an increase in Nile Red fluorescence, indicating increased levels of cellular hydrophobic molecules (Greenspan and Fowler, 1985). These mutants will be used to establish the difference in hydrocarbon and fatty acid concentration present intracellularly and extracellularly between wild type and *tolC*$^-$ mutant. Thus determining the quantity of these compounds produced by *V. furnissii* and the potential role of TolC in their export.

The *V. furnissii tolC*$^-$ mutants provide a paradigm for the study of quorum sensing and the role of TolC in this cell-cell signalling process. By analysing the supernatant of both wild type and mutant cultures, this work aims to identify signalling compounds utilised by *V. furnissii* and determine whether TolC plays a role in exporting them. Further understanding will be gained by investigating expression changes in the quorum sensing pathway within the *tolC*$^-$ mutant.

TolC is a target for antibiotic development but despite a great deal of research into the role of TolC in antibiotic export, the phenotypic effects of mutating *tolC* need further analysis. This work aims to investigate the global consequence of disrupting the *tolC* gene by analysing the wild type and mutant transcriptomes. This will be used to further understand phenotypic changes that arise from *tolC* mutations and how they are connected. Resistance to various antibiotics will also be determined in *V. furnissii* with a view to giving an indication of the membrane antiporters interacting with TolC in *V. furnissii.*

In order to determine the effects of oxidative stress potentially imposed by altering the function of this fundamental membrane protein, the wild type and *tolC*$^-$ mutant will be exposed to toxic selenium anion, selenite. Glutathione rich bacteria are able to reduce selenite to elemental selenium via reactions which utilise glutathione and generate superoxides in the process. Exposing wild type and mutant cells to selenite and ultimately increased superoxide levels will be carried out to determine how detrimental mutations in *tolC* are to the ability of cells to survive and adapt under oxidative stress.

CHAPTER 2 - MATERIALS AND METHODS.

2.1. Bacterial strains and cultures

All bacterial strains used in this study are outlined in Table 2.1. Bacteria were maintained as glycerol stocks by mixing an actively growing culture with glycerol (60%) and freezing aliquots in liquid nitrogen before storing at -80˚C. Prior to each experiment, glycerol stocks were spread on Luria-Burtani (L.B.) plates (15% w/v agar) using a sterile loop and incubated for 24 h at 37˚C. Individual colonies were selected and cultured in 10 ml L.B. medium (10 g/l tryptone; 10 g/l NaCl; 5 g/l yeast extract) to O.D. $_{600nm}$ 1.6 and used as starter cultures. For the selection of *tolC*$^{-}$ mutants, antibiotics were added to L.B. agar and liquid medium as follows: for the *tolC*$^{-}$ mutant: kanamycin (50 μg/ml), for TolC overexpressor: gentamicin (10 μg/ml) and for the complement strain: gentamicin (10 μg/ml) and kanamycin (50 μg/ml).

For initial Nile Red fluorescence analysis, genomic DNA and RNA extractions, 50 ml L.B. medium was inoculated with starter cultures (1% v/v) in 250 ml conical flasks and grown at 37˚C under aerobic conditions. Cultures were shaken at 180 rpm and contained antibiotic selection as required. For any additional Nile Red fluorescence experimentation and GC-MS analysis, wild type *V. furnissii* and *tolC*$^{-}$ mutant were cultured on nutrient defined medium adapted from Oh *et al.*, (2007); 100 mM Tris-HCl (pH 8.0), 200 mM NaCl, 10 mM NH_4Cl, 1 mM $MgSO_4$, 10 mM sodium succinate, 0.2 mM K_2HPO_4. Bacteria were cultured under the same conditions as for L.B. medium. Prior to inoculation from starter cultures, the defined medium was supplemented with 1 mM micronutrient solution (1 ml L^{-1} of 1 M stock solution) as described by (Park *et al.*, 2001). Micronutrients were filtered using 50 ml syringes through sterile Minisart® 0.2 μm filters. For all experiments, bacteria were cultured in triplicate. Where *E. coli* was used as a control for lipid analysis, the DH5α strain was used. Where minimal media (M9) was used as a growth medium, M9 salts (5X) (Sigma) (56.4 g) were dissolved in dH_20 (1 L). Prior to inoculation, media was supplemented with filtered sterile micronutrients (1 mM), glucose (20 mM) and magnesium sulfate (2 mM).

For bacteria cultured for RNA extractions, wild type *V. furnissii* and *tolC*$^{-}$ mutant were cultured on L.B. media containing antibiotic selection as described above, TolC overexpressor and complement were induced after 1 h growth with 1 mM IPTG. All bacterial strains were cultured to stationary phase (O.D. $_{600nm}$ 2.2). In addition wild type was cultured to early, mid and late exponential phases and stationary phase (O.D. $_{600nm}$ 0.6, O.D. $_{600nm}$ 1.2, O.D. $_{600nm}$ 1.8 and O.D. $_{600nm}$ 2.2 respectively).

For analysis of superoxide resistance, bacteria were cultured in 50 ml falcon tubes on L.B. media (10 ml) supplemented with selenite (2 mM, unless otherwise stated), inoculated from starter cultures with no antibiotic supplement for mutant growth.

Strain	Reference
Vibrio furnissii NCTC 11218	The National Collection of Type Cultures (Health Protection Agency, United Kingdom) (Lux *et al.*, 2011)
E. coli BW20767	Invitrogen
E. coli TOP10	Invitrogen
One Shot *ccd*B Survival Competent *E. coli* cells	Invitrogen
E. coli DH5α	Invitrogen

Table 2.1. Strains of organisms used in this study

2.2. Nile Red assay

To determine the lipid content of the cells, the lipophilic dye Nile Red (*9*- diethylamino-5*H*-benzo(a)phenoxazine-5-one) was used to stain the cells. Three 250 μl volumes of cultures were transferred to a 96 well plate, 20 μl of 40 μM Nile Red stock solution was injected into the selected wells (to a final concentration 3 μM). Samples were left for 5 min and the average fluorescence for each well (from 5 readings per well) was recorded using excitation wavelength of 490 nm and an emission wavelength of 560 nm on an Infinite® 200 PRO microplate reader (TECAN).

For analysis of fluorescence during wild type and *tolC*$^-$ mutant bacterial growth, aliquots were taken as previously described at regular time intervals from growing cultures. Prior to addition of Nile Red to each sample an O.D. $_{600nm}$. measurement was taken using the Infinite® 200 PRO microplate reader (TECAN).

2.3. Genomic DNA extraction

Genomic DNA was extracted from wild type *V. furnissii* and *tolC*$^-$ mutant using the GenElute™ Bacterial Genomic DNA kit following manufacturer's instructions. Extracted DNA was quantified using the NanoDrop 1000 spectrophotometer (Thermoscientific) and used for PCR and sequencing.

2.4. Polymerase Chain Reaction (PCR)

For the amplification of the *tolC* gene from wild type *V. furnissii* forward and reverse primers were designed to span the entire gene (TolC Fwd and TolC Rev, see Table 2.2) and obtained from Cogenics. PCR reactions (20 μl) were prepared with Phusion™ High-Fidelity polymerase (New England Biolabs), following manufacturers instructions. PCR conditions consisted of an initial denaturing phase of 30 s at 98˚C followed by 30 cycles of 10 s at 98˚C (denaturation), 30 s at 58˚C (annealing) and 1 minute at 72˚C (extension), finishing with a final extension period of 10 min at 72˚C.

Primer	Sequence
TolC Rev	5' ATG AAG AAA TAA AGT GCC TGT TCG 3'
TolC Fwd	5' CAA TTT GAG TTA CAC TCT CG 3'
Transposon REV	5' GTT GCG ATA AAA AGC GTC AG 3'
TolC-JAA	5' TGC TGC AAG GCG ATT AAG 3'
TolC JAA 2	5' GCG ATC AAC TCA AGC CGC AGC 3'
*att*B FWD	5' **AAA AAG CAG GCT** TCG AAG GAG ATA GAA CCA TGA AAA AAC TGC TTC CAC TAC TA 3'
*att*B REV	5' **AGA AAG CTG GGT** GTT ATT TCT TCA TGG CTT TCA TGC C 3'

Table 2.2. Polymerase chain reaction primers.

Bold indicates "*att*B*"* sites

2.5. Sequencing

The *tolC*$^{-}$ mutant obtained for investigation in this study contained the TnAraOut transposon (Mekalanos and Judson 2000). To determine location of the transposon within the *tolC* gene, *tolC*$^{-}$ mutant DNA was extracted (section 2.3). Sequencing utilising the "transposon REV" primer (Table 2) was undertaken to provide the 3' to 5' sequence of the beginning of the transposon and the sequence of *tolC* leading to the transposon insertion site (see appendices Fig. 8.1 for sequencing results).

2.6. Agarose gel electrophoresis

Products from PCR were analysed using agarose gel electrophoresis. The 20 μl samples contained 6X blue loading dye (Promega) (3 μl) and were separated on 1% (w/v) agarose gels containing 5% (v/v) ethidium bromide. The gels were made and run in TBE buffer at 100 V, 200 mA for 30 min.

DNA ladders (Bioline Hyperladder 1, 1 kb or Fermentas GeneRuler™ ,1 kb) were used as size markers for the samples and the DNA fragments were visualised on a UV light box.

2.7. Gateway cloning

2.7.1. BP reaction

Initially an *att*B flanked *tolC* PCR product was created using "*att*B FWD and *att*B REV primers" in Table 2.2. A Gateway® entry clone was created using this PCR product and pDONR221 vector (Invitrogen) using the Invitrogen BP clonase II enzyme mix and carried out according to the manufacturers instructions (Invitrogen). The reaction was incubated at 25˚C for 1 h and the reaction terminated using proteinkinase K (1 μl).

2.7.2. BP reaction transformation

The entry clone was transformed into *E. coli* TOP10 cells by mixing 1 μl of BP reaction with 50 μl of *E. coli* TOP10 cells and then incubated on ice for 30 min. Reactions were heated to 42˚C for 30 s then 250 μl of SOC medium (Invitrogen) was added to the mixture and incubated at 37˚C for 1 h, with shaking at 180 rpm. The bacterial suspension (100 μl and 20 μl) were spread on L.B. plates supplemented with antibiotic selection for pDONR221 (100 μg/ml kanamycin). Bacterial colonies were selected and cultured overnight on 10 ml L.B. medium containing 100 μg/ml kanamycin and plasmid DNA was extracted using QIAprep spin miniprep kit (QIAGEN).

2.7.3. LR reaction

The *tolC* gene was transferred from the entry clone to expression vector pSRKGmJAA (constructed by Dr. J. Dowdle, see Fig. 3.3) using the Invitrogen LR reaction kit (LR clonase II enzyme mix) using 150 ng of plasmid DNA extracted from the BP reaction and 150 ng of destination vector pSRKGmJAA following manufacturers protocols. The new plasmid was identified as pSRKJAA-TolC and was transformed into *E. coli* TOP10 cells and plasmid DNA extracted as described for the BP reaction transformation (2.7.2) using 50 μg/ml gentamicin as the antibiotic selection for the pSRKJAA vector. The final product (pSRKJAA-TolC) was transformed into One Shot *ccd*B Survival Competent *E. coli* cells (Invitrogen) by mixing 1 μl of LR reaction with 50 μl of One Shot *ccd*B Survival Competent *E. coli* cells and incubating on ice for 30 min. Reactions were heated to 42˚C for 30 s then 250 μl of SOC medium (Invitrogen) was added to the mixture and incubated at 37˚C for 1 h, with shaking at 180 rpm. The bacterial suspension (100 μl and 20 μl) were spread on L.B. plates supplemented with antibiotic selection for pSRKGmJAA vector (50 μg/ml gentamicin). Plasmid DNA was extracted using QIAprep spin miniprep kit (QIAGEN) with 50 μg/ml gentamicin as selective antibiotic. Gentamicin selects for cells containing the vector and the *ccd*B survival cells

are only able to grow when the pSRKJAA vector contains the *tolC* product. Confirmation of the LR product was confirmed by digest using *Bam*HI fast digest enzyme (Fermentas) with extracted plasmid DNA according to manufacturers instructions. Samples of the plasmid DNA were also sequenced by Cogenics (JAA primers, Table 2).

2.7.4. Conjugation, transfer of expression vector; pSRKJAA-TolC into V. furnissii.

Transformation of extracted pSRKJAA-TolC plasmid DNA into *E. coli* BW20767 conjugating cells was carried out by mixing 50 ng of plasmid DNA with 50 μl of *E. coli* BW20767 cells and heating at 42˚C for 45 s. The cell suspension was placed on ice for 2 min then 1 ml L.B. was added to the mixture and incubated for 1hr at 37˚C. 100 μl of the bacterial suspension was spread on L.B. plates supplemented with 50 μg/ml gentamicin. Four wild type *V. furnissii* colonies, four *tolC*$^-$ mutant colonies and four *E. coli* BW20767 colonies (containing pSRKJAA-TolC), were inoculated in L.B. supplemented with 100 μg/ml kanamycin for the *tolC*$^-$ mutant and 50 μg/ml gentamicin for *E. coli*, and incubated at 25˚C overnight. *V. furnissii* cultures were diluted to OD_{600nm} 0.4 and the OD_{600nm} of *E. coli* BW20767 cultures was 0.3-0.8. 1 ml of each culture was centrifuged at 3,800 x *g* for 5 min, and washed in 1 ml L.B.. Cells were centrifuged at 3,800 x *g* for 5 min and re-suspended in 250 μl L.B. The 250 μl aliquots of wild type *V. furnissii* and *E. coli* BW20767 were combined (n=4) and 100 μl of this mix was applied to the centre of a filter placed on an L.B. agar plate and incubated at 37˚C for 5-6 h. The same procedure was performed for the *tolC*$^-$ mutant and *E. coli* BW20767 (n=4) to create a *V. furnissii* TolC complement. The filter was removed and washed with 1 ml L.B. 200 μl of this suspension was plated onto minimal M9 media plates containing 60% glycerol. *E. coli* BW20767 cells are unable to grow in M9 media, therefore this method selects for only *V. furnissii*. Four colonies were selected, cultured in M9 media containing 25 μg/ml gentamicin for the overexpressor formed by conjugated wild type and BW20767 cells, and 25 μg/ml gentamycin and 50 μg/ml kanamycin for the complement formed by conjugated *tolC*$^-$ mutant and BW20767 cells. Both the TolC overexpressing strain and TolC complement strain were stored as glycerol stocks at -80˚C .

2.8. Total RNA isolation

Bacteria were cultured for total RNA extraction as described in section 2.1, 10 ml of each culture (three biological replicates) was centrifuged (3,800 x *g*, 4˚C , 10 min) in a sterile 50 ml falcon tube and the pellet re suspended in TRI Reagent® (1 ml per 10 x 10^6 cells). The homogenate was incubated at room temperature for 5 min. 1-bromo-3-chloro-propane (100 μl per 1 ml TRI Reagent®) was added, mixed and incubated for a further 10 min at room temperature. Samples were centrifuged (12,000 x *g,* 4˚C*,* 10 min), the aqueous phase transferred to fresh eppendorf and

200 μl propan-2-ol added. Samples were vortexed for 5 s, incubated at room temperature for 10 min then transferred to a spin column for RNA cleanup using RNAeasy mini kit (QIAGEN). RNA was eluted in 50 μl of RNase-free water.

2.9. RNA precipitation

Where extracted RNA was below the required concentration for microarray analysis (<250 ng/μl), RNA precipitation was performed to concentrate the sample. A 1:10 v/v ratio of 3M sodium acetate and 1 ml of 100% ethanol was added to RNA samples. Samples were mixed and placed at -80˚C for 3 h, the reaction was then centrifuged (12,000 x *g*, 4˚C, 15 min) and supernatant removed. The supernatant was subsequently washed with 500 μl of 75% ethanol and centrifugation was repeated (12,000 x *g*, 4˚C , 5 min). The supernatant was removed and pellet dried in air for 10 min prior to re suspension in 15 μl RNAse free water.

2.10. RNA quality control

The concentration of RNA was initially measured using a NanoDrop 1000 spectrophotometer (Thermoscientific). Quality control standards were applied to all RNA samples to ensure A_{260}:A_{280} values were > 1.7. To determine RNA quality, samples were prepared to run on the 2100 Bioanalyser (Agilent), by diluting as necessary to concentrations of approximately 150 ng/μl. For analysis the Agilent RNA 6000 Nano Kit was used, specifically designed to quantify and anlayse mRNA samples of concentrations between 25 and 500 ng/μl. All solutions and samples required for the 2100 Bioanalyser (Agilent), were allowed to warm to room temperature for 30 min prior to analysis. 10 μl of RNA samples and 2 μl of RNA ladder were heated to 70˚C for 2 min, prior to loading onto the microfluidic chips, carried out according to manufacturers protocol.

2.11. Reverse transcription

For RT-qPCR and microarray analysis cDNA was synthesised using the QIAGEN QuantiTect Reverse Transcription Kit following manufacturers instructions. Initially the gDNA elimination reaction was prepared for all wild type and *tolC*$^-$ mutant RNA samples by treating 2 μg of RNA with 4 μl of gDNA Wipeout Buffer and dH_2O to a total volume of 28 μl. The reaction was incubated fro 2 min at 42˚C. The reverse transcription reaction was prepared by mixing 2 μl of reverse transcriptase, 5 μl of 5X RT buffer and 2 μl of RT primer mix. The 28 μl gDNA elimination reaction was then added to the reverse transcription mix on ice and incubated for 25 min at 42 ˚C. A final incubation for 3 min at 95˚C was carried out before storing the synthesised cDNA at -20˚C.

2.12. RT-qPCR Optimisation

Primers and dual fluorescent labeled TaqMan probes were designed specifically for *tolC* and *GAPDH* by Eurofins MWG Operon (Table 2.3) (see appendices Table 8.1 for sequence location in genes). For primer optimisation, amplification of the *tolC* and *GAPDH* products was achieved by performing PCR using cDNA extracted from wild type *V. furnissii* using the primers listed in Table 2.3. The PCR was performed using Phusion™ High-Fidelity polymerase (New England Biolabs), following the manufacturers instructions including 3% (v/v) DMSO. Conditions were optimised for both *tolC* and *GAPDH* and consisted of an initial denaturing phase of 30 s at 98˚C followed by 30 cycles of 10 s at 98˚C, 1 min at 55˚C and 1 min at 72˚C, finishing with a final extension period of 10 min at 72˚C. DNA fragment size was analysed by gel electrophoresis (section 2.6). To determine the performance of the RT-qPCR, a standard curve was generated for both *tolC* and *GAPDH* using a range of six diluted concentrations of total wild type cDNA. These samples were produced by carrying out serial dilutions (1:5) using the CAS1200 robot (Corbett robotics) to achieve concentrations of 1500, 300, 60, 12, 2.4 and 0.48 ng/μl. Accurate measurements of the serial dilutions were performed using the NanoDrop 1000 spectrophotometer (Thermoscientific) and were shown to be 1447, 285, 59.3, 10.8, 2 and 0.4 ng/μl. For acquisition of sample data, particularly concentrated samples wild type and *tolC*$^{-}$ mutant cDNA was diluted to within range of the standard curve (0.1 – 1.5 μg/μl).

Primer	Sequence
FWD TOLC	5’ ACA ACT ACA GCA GCT ACA AC 3’
REV TOLC	5’ TGA GAC GAC ACA TTA CCA CC 3’
FWD GAPDH	5’ TGC TGC TCA AAA CAT CAT CC 3’
REV GAPDH	5’ AGT CAG TTT GCC GTT TAG TTC 3’
PROBE TOLC	5’ CCA CGA AAA TAA CGA CTT CAA CAT TGG TCT 3’
PROBE GAPDH	5’ GCA GCT AAA GCA GTA GGC GTT GTT C 3’

Table 2.3. RT-*q*PCR primer sequences

2.13. RT-qPCR data acquisition

RT-qPCR was performed on wild type cDNA prepared for the standard curve at concentrations of 1447, 285, 59.3, 10.8, 2 and 0.4 ng/μl measured using the NanoDrop 1000 spectrophotometer (Thermoscientific). For comparison of *tolC* expression in samples, cDNA was extracted from wild type *V. furnissii* at varying time points, *tolC*$^{-}$ mutant and overexpressor cDNA at concentrations

between 0.5 and 1.5 μg/μl. Reactions were prepared by mixing cDNA, primers, probe and Taq. Maxima Probe qPCR Master Mix (2X), suitable for dual fluorescence probes, according to manufacturers instructions. All RT-qPCR reactions were mixed using a CAS1200 robot (Corbett robotics), three technical replicates and three biological replicates were run for each sample using the RG600 RT-qPCR machine (Corbett Robotics). The two-step thermocycling protocol was carried out with the following conditions: initial denaturing phase of 10 min at 95˚C followed by 40 cycles of 15 s at 95˚C, 30 s at 55˚C and 30 s at 72˚C.

2.14. RT-qPCR data analysis

All RT-qPCR data analysis was carried out using Rotor Gene 6000 1.7 series software. The standard curve was created by inputting the concentrations of cDNA measured using the NanoDrop 1000 spectrophotometer (Thermoscientific); 1447, 285, 59.3, 10.8, 2 and 0.4 ng/μl. The point at which the signal is detected is determined by the Cycle time (Ct), the Ct corresponding to each concentration was plotted to determine the linearity and reproducibility of the assay. Threshold limits were established as 0.035 for *GAPDH* and 0.025 for *tolC*. The standard curve data was imported to the sample run data and Ct values were read from the interpolation of the threshold level and amplification curve for both *tolC* and *GAPDH*, samples with Ct values > 40 were discarded. The concentration of *tolC* mRNA was in relation to concentration of *GAPDH* mRNA was extrapolated from the standard curve.

2.15.1 Antibiotic resistance determined by half maximal inhibitory concentration (IC_{50})

Half maximal inhibitory concentrations (IC_{50}) were determined by culturing wild type *V. furnissii* in 15 ml falcon tubes containing 5 ml L.B. media supplemented with increasing concentrations of antibiotics (Sigma Aldrich). Growth conditions were as described in section 2.1. Bacteria were cultured in L.B. containing gentamicin, erythromycin and tetracycline at the following concentrations: 0, 2.5, 5.0, 7.5, 10, 12.5 and 15 μg/ml, streptomycin at 0, 5, 10, 15, 20, 25, 30 and 35 μg/ml, kanamycin, novobiocin, paromomycin and ampicillin at 15, 30, 45, 60, 75 and 100 μg/ml. Once 50% growth was calculated for each of the antibiotics, *tolC*$^{-}$, overexpressor and complement were cultured in L.B. media as previously described (section 2.1) supplemented with the empirically determined IC_{50} concentrations: gentamicin (7.5 μg/ml), erythromycin (7.5 μg/ml), tetracycline (5 μg/ml), streptomycin (10 μg/ml), kanamycin (15 μg/ml), novobiocin (20 μg/ml), paromomycin (15 μg/ml) and ampicillin (25 μg/ml).

2.15.2 Antibiotic resistance determined by minimal inhibitory concentrations (MIC)

More accurate antibiotic resistance was determined by establishing the minimum inhibitory concentration for chloramphenicol, tetracycline, ampilcillin, norfloxacin, novobiocin and gentamicin. Stock solutions at a concentration of 256 μg/ml were prepared for each antibiotic and the concentration confirmed using the NanoDrop 1000 spectrophotometer (Thermoscientific). Serial dilutions (1:2) of the six antibiotics were subsequently made and 250 μl of each dilution (256, 128, 64, 32, 16, 8, 4, 2, 1, 0.5, 0.25 and 0.125 μg/ml) was transferred into 96 well plates. Four replicates were allowed for each strain (wild type, *tolC*$^{-}$, overexpressor) (appendices Fig. 8.5). Starter cultures were prepared as described in section 2.1 and 1 ml mixed with 7 ml of L.B. medium, then further diluted with L.B. media by a factor of 1:200. To ensure the initial inoculum was equal for each strain, colony forming units (CFUs) were quantified. 100 μl of each starter culture was spread on L.B. agar plates and colonies counted after 24 h incubation at 37˚C. The 96 well plates, including controls containing L.B. with no antibiotic supplement, were inoculated with starter cultures (1% inoculum) and incubated at 37˚C for 24 h. A microplate reader was used to obtain the $O.D._{600nm}$ values, the minimum inhibitory concentration was established using an average of the four replicates, where $O.D._{600nm}$ was greater than 0.1.

2.16. Confocal microscopy

For visualisation of Nile Red fluorescence samples were treated with the dye as described previously for the Nile Red assay (section 2.2) and 5 μl of culture was immediately transferred to a microscope slide for confocal laser imaging. A 510-Meta laser scanning confocal microscope (Zeiss) was used, fitted with a Plan-apochromat 62x/1.40 oil immersion lens (Zeiss). Cells were imaged at an excitation wavelength of 488 nm and emission wavelength set to 595-615 nm using a 488 nm/595 nm dichroic mirror and a 560 nm/615 nm band pass filter. Laser power, detector gain and offset were kept fixed for the different samples to allow direct comparison. Fluorescence images were obtained using the Carl Zeiss LSM 510 software. To avoid photo bleaching, images were obtained within 5-10 min of slide preparation.

2.17. Fluorescence activated cell sorter (FACS)

To separate fluorescing and non-fluorescing cells, Nile Red was added as described previously (section 2.2) and cultures were sorted using the FACS Aria II (BD Biosciences, USA). The fluorescence of the cells was measured using an excitation wavelength of 488 nm and emission wavelength 616/23 nm. 10,000 fluorescing cells were sorted at a flow rate of 2.0 psi above system pressure (20 psi) and then quantified as a percentage using FACS software. To collect the separated populations, 1 million fluorescing or non fluorescing cells were collected in PBS buffer

(8g of NaCl, 0.2 g of KCl, 1.44 g of Na_2HPO_4 and 0.24 g of KH_2PO_4 in II dH_2O) centrifuged (3,800 x *g*, 4˚C, 10 min) and re suspended in L.B. (500 μl), this suspension was used to inoculate a starter culture for further growth analysis.

2.18. Preparation of cell pellets and supernatants

For lipid extraction, wild type and *tolC*$^-$ mutant were cultured on 50 ml nutrient defined media as described in section 2.1 until O.D. $_{600nm}$ 0.6 – 0.8. Cultures were centrifuged at 3,800 x *g* for 10 min. The supernatant was retained and 20 ml filtered through sterile Minisart® 0.2 μm filters into falcon tubes (50 ml). The pellet was re suspended in 1ml of PBS buffer and transferred to 15 ml falcon tubes. Tubes containing cell pellets were covered with Nescofilm® and pierced. Following freezing in liquid nitrogen, the tubes were placed in a vacuum and freeze dried overnight. For analysis of autoinducers in bacterial supernatants, bacteria were cultured in M9 minimal media (section 2.1) and prepared as described

2.19. Lipid extraction from cell pellets.

To extract lipids from bacterial cells, 40 mg of freeze-dried pellets were homogenised using diatomaceous earth (Dionex) and transferred to a 1 ml stainless steel Dionex accelerated solvent extractor cells. Lipids were extracted into 5 ml dichloromethane (DCM) using a DIONEX ASE150 accelerated solvent extraction system. The protocol involved extraction at 100˚C in two, 5 min cycles, a 100% rinse volume and 60 s purge time. 5 ml DCM containing lipid extracts from wild type and *tolC*$^-$ mutants were transferred to glass vials and the solvent evaporated under a nitrogen stream. The residue was re suspended in 250 μl of DCM containing d8-naphthalene (10 μg/ml) which was used as an internal standard. Each re suspension was filtered using 1 ml glass syringe and 13 mm x 0.2 μM PTFE Iso-Disc filters (Supelco) into 1.5 ml Agilent screw cap autosampler vials fitted with 300 μl inserts. Vials were sealed using bonded PTFE coated caps (Chromacol). Samples were derivitised using N,O-Bis (trimethylsilyl) trifluoroacetamide (BSTFA) to prevent fatty acids sticking to the GC-MS column. BSTFA (10 μl) was added to each sample and heated at 80˚C for 40 min and allowed to cool to room temperature prior to GC-MS analysis.

2.20. Lipid extraction from media and supernatants.

To extract lipids from bacterial supernatants, 20 ml of spent media from wild type and *tolC*$^-$ mutant cultures were filtered through sterile Minisart® 0.2 μm filters prior to lipid extraction. For testing the sensitivity of the method, heptadecanoic acid was added as an internal standard to M9 minimal media at concentrations of 0, 15, 30 and 45 μg to the M9 media. Sample pH was adjusted to pH_3 using HCl and extraction carried out using chloroform and methanol (Bligh and Dyer, 1959). The

supernatants were left overnight shaking in 250 ml conical flasks at 4˚C with chloroform (25 ml) and methanol (50 ml). A further 25 ml of chloroform was added followed by 0.9% NaCl (25 ml). The solvent layer (40 ml) was retrieved, transferred to round bottomed 250 ml flasks and reduced to 2 ml under vacuum using a Buchi rotavapor evaporator. The remaining 2 ml was evaporated under a nitrogen stream and the residue resuspended in DCM and filtered as described for pellet extraction.

2.21. Gas Chromatography-Mass Spectrometry (GC-MS)

Data were acquired using the Trace GC-MS 2000 (ThermoQuest Finnigan) running a Restek Rtx-5MS 15 m x 0.25 mm x 0.25 μm GC column. Samples were injected into the capillary column in the splitless mode and helium was used as a carrier gas at a flow rate of 1.0 ml min^{-1}. The temperature of the oven began at 25˚C (for 2 min), increased to 320˚C at 10˚C min^{-1} and was held for 10 min (injector temperature 250˚C).

For analysis at Shell Global Solutions the samples were run using the cold on-column GC-MS method (for detection of thermally unstable analytes) and also in split mode GC-MS (split ratio 20:1, with the injector at 250˚C), this procedure allows for increased sensitivity and avoids sample overloading. Chemical ionisation using methane was carried out on one of each sample type in order to obtain molecular mass information.

For mass spec analysis at Exeter University, identification of compounds was determined by comparison to the NIST 2.0 mass spectral database using the Xcalibur data system. Search accuracy was expressed as the reverse search matching score (RSI), concentration of compounds with RSI > 800 was subsequently calculated.

2.22. Gas Chromatography-Mass Spectrometry data analysis

Quantitation of compounds was achieved by calculating the peak area ratio of compound of interest to an internal standard; d8-naphthalene (10 μg/ml). Biological replicates used for direct comparison were those with the same internal standard peak areas. For comparative quantification of compounds in sample extracts the concentration (μg/ml) of each compound was calculated using the equations 2.1A and 2.1B. The quantities of free fatty acids and total fats in cell pellet extracts were calculated as a percentage of biomass from GC-MS data obtained at Shell Global Solutions, assuming 100% extraction efficiency. Supernatant quantification was achieved by calculating the concentration of free fatty acids as a percentage of total supernatant volume.

A

$$\text{Target compound } (\mu g) = \frac{\text{target compound peak area}}{\text{standard peak area}} \times \text{conc. of internal standard } (\mu g/ml) \times \text{vol. of extract } (ml)$$

B

$$\text{Biomass } (\%) = \frac{\text{target compound } (\mu g)}{\text{cell extract } (\mu g)} \times 100$$

Equation 2.1. Calculating concentration of compounds detected by GC-MS as Biomass %.

2.23. Pathway analysis using the Kyoto Encyclopedia of Genes and Genomes

Maps of metabolic pathways were obtained from the Kyoto Encyclopedia of Genes and Genomes (KEGG) pathway database (Kanehisa *et al.,* 2002). For pathways established in *V. furnissii*, the *V. furnissii* gene annotations and sequences were obtained *via* this database (fatty acid pathway: vfu 00071, flagella assembly pathway: vfu 02040). Quorum sensing protein sequences were established for *V. harveyi* ATCC BAA-1116 (pathway: vha 02020) and compared directly with the GenBank non-redundant protein database using BLASTp to identify homologous proteins in *V. furnissii* and other *Vibrio* species.

2.24. Phylogenetic analysis

Phylogenetic trees based on amino acid sequences were constructed using Phylogeny.fr. Sequence alignment was carried out using the multiple alignment tool MUSCLE, results were curated using G Blocks to eliminate poorly aligned positions. Phylogentic trees were created using PhyML, a bootstrapping procedure was performed and branches with support values below 50% were collapsed.

2.25. Growth curves

For comparison of wild type and *tolC*$^{-}$ mutant growth bacteria were cultured in M9 minimal media containing glucose, as previously described. At regular time intervals of approximately 1.5 h, 500 μl of culture was removed and O.D. $_{600nm}$ measurement taken using an Eppendorf BioPhotometer. Three biological replicates were cultured for both wild type and *tolC*$^{-}$ mutant.

2.26. Microarray chip hybridisation and transcriptome analysis

Wild type and *tolC*$^-$ mutant RNA was extracted and cDNA synthesised as described in sections 2.8 and 2.11 respectively and sent to NASC for preparation and hybridisation, post-hybridisation washing, staining and scanning of GeneChips. GeneChips were designed by Dr. Thomas Lux for targeted hybridisation of *V. furnissii* using oligonucleotides. cDNA with fluorescent tags were annealed, following cDNA hybridisation. GeneChips were scanned using a GeneChip scanner 3000 (Affymetrix). Normalisation of fluorescent intensity values was performed using Mas 5.0. Manipulation and visualisation of data to determine significantly differentially expressed genes was performed using GeneSpring GX v11.5. Six microarray chip samples were divided into the control group (3 x wild type samples) and the mutant group (3 x *tolC*$^-$ mutant samples) and differential expression of proteins was established between the groups. A two tailed t-test was performed by the GeneSpring GX v11.5 software, allowing statistical parameters to be applied ($p<0.05$). When analysing multiple expression changes throughout the whole transcriptome, the Benjamini-Hochberg FDR multiple testing correction was used.

2.27. Extraction of quorum sensing signalling molecules from bacterial supernatants

Supernatants were prepared as described in section 2.18 and 20 ml underwent acidified ethyl acetate (AEA) extraction following established protocol (Fletcher *et al.,* 2007). Briefly, AEA was prepared and mixed in equal volumes with the supernatant in a separating funnel. After vigorous shaking for 10 min, the supernatant was removed and re-extracted with a further addition of 40 ml AEA. Solvent layers were pooled and evaporated using a Buchi rotavapor evaporator and finally under nitrogen stream as described for fatty acid extraction (section 2.20). The residue was re-suspended in 0.5 ml of MeOH. 300 μl was removed and filtered using 1 ml glass syringe and 13 mm x 0.2 μM PTFE Iso-Disc filters (Supelco) into 1.5 ml agilent screw cap vials for analysis by liquid chromatography mass spectrometry (LC-MS)

2.28. Liquid Chromatography Mass Spectrometry (LC-MS)

Samples were analysed on an Agilent 6500 series quadrupole time of flight (Q-TOF) mass spectrometer and Agilent 6400 series triple quadrupole (QQQ) mass spectrometer. For Q-TOF analysis samples were run in different ionisation modes in order to detect compounds containing OH groups (run in negative ionaisation mode) or NH_2 groups (run in positive ionsation mode). Extracts suspended in 5 μl MeOH were applied to a 2.1 mm by 100 mm, 1.8 μm particle size, stable bond $C1_8$ reverse phase column, a 3.5 kV potential (+ or −) was applied to the capillary, and nitrogen was used as a desolvation and collision gas. For both positive and negative mode, Solvent A was 10mM ammonium acetate in 5% acetonitrile, 95% H_2O and 0.1% formic acid and Solvent B

was 95% acetonitrile, 5% H_2O and 0.1% formic acid. The flow rate was 0.25 ml min^{-1} with the following gradient: *t*=0, 0% B, *t* = 4 min, 100% B, *t* = 6 min, 100% B, *t* = 6.5 min, 0% B, *t* = 11 min, 0% B. With a 1 minute post time. Autosampler temperature was at 4˚C. Column temperature was 35˚C.

Multiple reaction monitoring (MRM) scans were carried out using the triple quadrupole (QQQ). Precursor and product ions were scanned using m/z values, fragmentation (V) and collision energies (V) as laid out in Table 2.4. (Dwell time was 100 ms for each). 5 μl samples were applied to a 2.1 mm by 150 mm, 3.5 μm particle size, eclipse plus C_{18} reverse phase column and parameters were as follows: column temperature 30˚C, gas temperature; 350˚C, gas flow rate 9 l min^{-1}, nebulizer pressure; 35 psi. For runs in positive mode the capillary voltage was 4000 kV and 350 kV for runs in negative mode. Solvent A was 10 mM ammonium acetate in 55% acetonitrile, Solvent B was 5% acetonitrile. The flow rate was 0.3 ml min^{-1} with the following gradient: *t*=0, 0% B, *t* = 6 min, 100% B, *t* = 10 min, 100% B, *t* = 10.5 min, 0% B, with a 5 min post time.

QSSM	Precursor ion (m/z)	Product ion (m/z)	Fragmentator (V)	Collision energy (V)
HSLs	$(M+H)^+$			
C4-HSL	172.1	102.1	85	15
C6-HSL	200.1	102.1	85	15
C8-HSL	228.1	102.1	85	15
C10-HSL	256.1	102.1	85	17
C12-HSL	284.1	102.1	85	17
C14-HSL	312.1	102.1	85	19
3-oxo-C4-HSL	186.1	102.1	85	15
3-oxo-C6-HSL	214.1	102.1	85	15
3-oxo-C8-HSL	242.1	102.1	85	17
3-oxo-C10-HSL	270.1	102.1	85	17
3-oxo-C12-HSL	298.1	102.1	85	19
3-oxo-C14-HSL	326.1	102.1	85	21
3-OH-C4-HSL	188.1	102.1	85	15
3-OH-C6-HSL	216.1	102.1	85	15
3-OH-C8-HSL	244.1	102.1	85	17
3-OH-C10-HSL	272.1	102.1	85	17
3-OH-C12-HSL	300.1	102.1	85	19
3-OH-C14-HSL	328.2	102.1	85	19
	$(M-H)^-$			
CAI-1	213.2	59.1	94	10

Table 2.4. Conditions used for QQQ based detection of HSL and autoinducer compounds

2.29. CAI-1 synthesis

Synthetic CAI-1 synthesis was carried out at University of Exeter by Dr. Mark Wood *et al* according to (Higgins *et al.*, 2007) and (Kelly *et al.*, 2009) appendices. For LC-MS analysis a 1000X stock solution of synthesised CAI-1 was prepared in methanol. 10 μl of a 10 μM sample of CAI-1 was used for LC-MS analysis (section 2.28).

2.30. Re-introduction of supernatants into growing cultures

Wild type and *tolC*$^-$ mutant bacteria were cultured on 50 ml M9 minimal media containing 20 mM glucose to late exponential phase (wild type: O.D. $_{600nm}$ 2.1, *tolC*$^-$ mutant O.D. $_{600nm}$ 1.8) and 50 ml of supernatant collected and filtered as described in section 2.18. The 50 ml of supernatant was frozen in 250 ml conical flasks in liquid nitrogen and dried under vacuum for 48 h. The freeze drying process was performed on 50 ml of minimal M9 media for use as a control. The residue was re-suspended in 5 ml dH_2O and stored in sterile falcon tubes. 2 ml of concentrated spent supernatants were added to growing *tolC*$^-$ mutant cultures (prior to stationary phase at O.D. $_{600nm}$ 1.5) and growth curve data collected (section 2.25). For re-introduction of freeze dried M9 minimal media, 0.5 ml on concentrate was added to growing *tolC*$^-$mutant cultures at O.D. $_{600nm}$ 1.5.

For re-introduction of synthetic CAI-1, stock solution of CAI-1 dissolved in MeOH (and MeOH control (50 μl)) were added to growing wild type and *tolC*$^-$ mutant cultures at O.D. $_{600nm}$1.4 -1.6. Final concentrations 100 nm, 10 nm, 1 μM, 10 μM and 20 μM.

2.31. Pfam protein family analysis

To identify AcrB/D/F proteins in *V. furnissii*, identification of significant Pfam domains was performed by Dr Thomas Lux by comparing sequences to the Pfam protein family database. Genes identified were located on the *V. furnissii* NCTC 11218 genome (Lux *et al.*, 2011) using Artemis Genome Browser (Wellcome Trust Sanger Institute). Amino acid sequences used to compile phylogenetic tree as described in section 2.24.

2.32. Motility of bacteria on L.B. agar plates

M9 minimal plates containing 0.25% and 0.5% agar (w/v) were inoculated from glycerol stocks (wild type and *tolC*$^-$ mutant) by stabbing with a sterile loop and incubated at 37˚C for 5 days. Colony size was determined by imaging and measuring the size manually each day. Data were obtained in triplicate.

2.33. Transmission electron microscopy (TEM).

All transmission electron microscopy was carried out with a Jeol 1400 TEM with images obtained at 80 Kv. Preparation for flagella visualisation via TEM was carried out on wild type and *tolC*$^{-}$ mutant bacteria cultured in M9 minimal media to O.D. $_{600nm}$ 1.5. Samples for TEM were diluted 1:5 in PBS buffer. The samples were negatively stained; 4 μl of cell suspension was added to a formvar coated 300 mesh copper grid add and left for 1 minute. To remove the sample a small strip of filter paper was touched to the edge of the grid. A 4 μl drop of 2% w/v uranyl acetate in water was added and withdrawn with filter paper for visualisation.

For analysis of selenium particles in *V. furnissii* cultures grown on L.B. media containing 2 mM selenite. Samples were fixed and prepared by adding 10 ml of culture to 10 ml of fixative 2% (w/v) paraformaldeyhde, 2.5% (v/v) glutaraldehyde in 0.1 M cacodylate buffer pH 7.2 in a 50 ml falcon and gently mixed for 5 min. Samples were centrifuged (3,800 x *g*, 3 min), supernatant removed and pellet re suspended in fixative (10 ml) and cooled on ice for 3 h. Subsequent sample preparation was carried out by Peter Splatt at the University of Exeter by embedding in 3% (w/v) agarose LM in 0.1 M cacodylate buffer pH 7.2. After cooling on ice, the section of agar was removed and cut into 3x3 mm pieces, washed, stained with 1% (w/v) uranyl acetate for 1 h, washed, and dehydrated. After embedding in TAAB Low Viscosity Resin Hard (TAAB Laboratories Equipment Ltd.), sections of 80 to 90 μm thickness were cut with a diamond knife and applied to carbon-coated Formvar films on 300-mesh copper grids. Sections were stained with uranyl acetate and lead citrate, placed on filter paper and air dried before being imaged.

2.34. Oxidative stress analysis determined by selenium quantification

Selenium was quantified as described by (Biswas *et al.*, 2011) to measure the selenite processed by *V. furnissii* cells. Bacteria were cultured in 10ml L.B. media as described previously and after 24 h, 36 h, 48 h, 55 h and 72 h growth. A 200 μl cell suspension was removed for the selenite depletion assay (section 2.35), the remainder of the culture was centrifuged (3,800 x *g*, 20 min) to pellet the selenium. Pellets were washed twice with 10 ml of 1 M NaCl and finally re suspended in 10 ml of 1 M Na_2S to dissolve the elemental selenium. Absorption of the red-brown solution was measured at 500 nm using a Shimadzu UV-2101 PC UV-VIS Scanning Spectrophotometer.

2.35. Oxidative stress analysis determined by selenite depletion.

Selenite content were determined spectrophotometrically by using a modification of the method described by (Kessi *et al.*, 1999): 10 ml of 0.1 M HCl, 0.5 ml of 0.1 M EDTA, 0.5 ml of 0.1 M NaF and 0.5 ml of 0.1 M disodium oxalate were mixed in a 20 ml glass vial wrapped in foil to eliminate

light. A 200 µl sample from culture grown for 24 h, 36 h, 48 h, 55 h and 72 h was added. 2.5 ml of 0.1% 2,3-diaminonaphthalene in 0.1 M HCl was added. After the contents were mixed, the tubes were incubated at 40˚C for 40 min and then cooled to room temperature. The selenium-2,3-diaminonaphthalene complex was extracted with 3 ml of cyclohexane by shaking the tubes vigorously for 1 min. To obtain a reading within the range of the spectrophotometer the organic phase was diluted 1:5 and the absorbance at 377 nm was determined by using a 1-cm-path-length cuvette and a Shimadzu UV-2101 PC UV-VIS Scanning Spectrophotometer. Calibration curves were obtained by extracting selenite from 10 ml L.B. medium containing known concentrations between 0 and 2 mM (0, 0.2, 0.5, 0.8, 1.0, 1.5, 2.0 mM). A 1:5 dilution of the final extract was made and the absorbance at 377 nm was plotted against concentration confirming a linear relationship between selenite concentration and absorption. All measurements were carried out in triplicate.

2.36. Determining colony forming units

Colony forming unit (CFU) counts were used to monitor growth during selenium production due to elemental selenium interfering with O.D. $_{600nm}$ readings. Wild type and *tolC*$^{-}$ mutant bacteria were cultured on L.B. media containing 2 mM selenite as previously described (section 2.1). After 0 h, 5 h, 11 h, 23 h, 29 h, 34 h, 48 h, 58 h, 72 h and 80 h, 100 µl of the cell suspension was removed and 1:100 serial dilutions made. Dilution factors varied from 10^5 for samples collected for CFU count after 5 h, 10^6 for those collected from 11 h – 34 h and 10^7 for cultures grown for 48 h – 80 h. 10 and 100 µl of the final serial dilutions was plated on L.B. agar plates and colonies were counted after incubation for 24 h at 37˚C. At time points 0 h, 11 h, 23 h, 34 h, 48 h, 58 h and 72 h 200 µl of culture was removed for the selenite depletion assay (section 2.35).

CHAPTER 3 - FATTY ACID PRODUCTION IN *VIBRIO FURNISSII* AND SECRETION VIA TOLC.

3.1 INTRODUCTION

Bacteria that synthesise significant quantities of long chain carbon molecules (alkanes, alkenes, fatty acids and aldehydes) are relevant to the study of bio-fuels. The *Vibrio furnissii* M1 strain has been reported to produce significant levels of hydrocarbons, however the potential to yield high levels of alkanes has been recently disputed (Park *et al.*, 2005, Wackett *et al.*, 2007). The authenticity of the claims of a *V. furnissii* strain yielding hydrocarbons at least 20 times that of other alkane synthesising bacteria needs to be established, however the M1 strain has not been released for further study. The genomes of the four originally isolated *V. furnissii* strains show high homology (Brenner *et al.,* 1983), therefore studies will be undertaken using the *V. furnissii* NCTC 11218 strain. Regardless of the ability of the bacterium to reproduce a hydrocarbon yield of 60% of biomass (as reported), *Vibrio* species are shown to produce markedly higher quantities than *E. coli* (Ladygina *et al.*, 2006). There is also evidence that *V. furnissii* produces extracellular hydrocarbons (Tornabene *et al.*, 1970, Jones, 1972) but secretion of long chain hydrocarbons (LCHs) has not yet been confirmed or quantified.

Microbial production of fatty acids has been a recent focus of the bio-fuel industry (Lu *et al.*, 2008). Lipid biomass varies considerably between bacterial strains (O'Leary, 1962) but research shows that *Vibrio* species commonly yield relatively high levels of saturated fatty acids (Oliver and Colwell, 1973), although this has not been established in *V. furnissii.* Although synthesis of lipids in bacteria is widely researched, possible fatty acid secretion mechanisms have not been established (Manilla-Pérez *et al.*, 2010). There is evidence of extracellular deposits of wax esters in *Acinetobacter* sp. (Makula *et al.*, 1975) and *Fundibacter jadensis* when cultured in the presence of alkanes (Bredemeier *et al.*, 2003). A recent transposon mutant screen in *Alcanivorax* species identified genes potentially responsible for export of triacylglycerides (TAGs) and wax esters, within a multidrug and toxic-compound extrusion family (MATE) efflux system (Manilla-Pérez *et al.*, 2010). Although it is unlikely that *V. furnissii* synthesises these less commonly produced lipids, the evidence suggests fatty acid export could be via a nonspecific export system. Free fatty acids (FFAs) are more commonly synthesised among bacteria and recent research identified extracellular accumulation of these molecules in cultures of *E. coli* with fatty acid synthesis gene mutations, particularly FadD knockout mutants (Li *et al.*, 2012). The long chain fatty acid CoA-ligase (FadD) is

involved in fatty acid degredation and mutations in this gene have displayed a significant increase in extracellular fatty acids.

There is potential to increase fatty acid biosynthesis in bacteria by engineering the fatty acid synthesis pathway, as carried out in *E. coli* (Lu *et al.*, 2008), however due to the fundamental nature of the lipid biosynthetic pathway, overexpression requires significant engineering of cellular metabolism. There are also a number of potential effects of increasing cellular levels of fatty acids, particularly as fatty acid levels are related to membrane fluidity and signalling (Cybulski *et al.,* 2002, Aguilar and De Mendoza, 2006). Greater understanding is required to enable increase of lipid production and export while minimizing disruption to other cellular functions. Secreted fatty acids or alkanes, in particular are more viable for industrial applications, as extraction costs are reduced. Further understanding LCH and fatty acid export is therefore overdue and is a focus of this study.

Preliminary experimentation in this project determined potential high lipid yielding *tolC*$^{-}$ knockout mutants in *V. furnissii* 11218. Prior to this study, knockout mutants were generated by random transposon mutagenesis and screened using the Nile Red assay, the lipophilic dye (Nile Red) fluoresces when in a non-polar environment, giving an indication of the level of cellular lipids (Greenspan and Fowler, 1985, Elsey *et al.*, 2007). 620,000 mutants were screened, 50,000 assayed and ultimately five mutants displayed an increase in fluorescence. Following bioinformatic analysis four mutations were detected within *tolC* and a fifth within an alcohol dehydrogenase. The *tolC*$^{-}$ mutants were provided as a starting point for this study by Dr. John Dowdle. The initial aim was to investigate the mutants for increased levels of lipids and understand further the role of TolC in this phenotypic change. Analysis of the structure and quantity of the compounds giving rise to the increase in fluorescence was therefore performed. In addition, the intracellular or extracellular location of the hydrophobic compounds and the relevance of this to bacterial bio-fuel production will be investigated.

Although not as clinically relevant as some other *Vibrio* species, there is recent evidence that claims *V. furnissii* as an emerging pathogen. To date antibiotic resistance has not been fully investigated in the bacterium (Hickman-Brenner *et al.*, 1984, Dalsgaard *et al.*, 1997, Derber *et al.*, 2011). RND-efflux systems are widely researched in relation to antimicrobial export therefore resistance to a number of antibiotics will be investigated in *V. furnissii* wild type and the *tolC*$^{-}$ mutant.

3.2. RESULTS

3.2.1 Investigating the transposon insertion in tolC$^-$ *mutants.*

Initial screening from the random transposon mutagenesis showed that four *tolC*$^-$ mutants produced a large increase in Nile Red fluorescence compared to the wild type. The Nile Red dye (*9*-diethylamino-5*H*-benzo(a)phenoxazine-5-one), emits a characteristic fluorescence at approximately 575 nm when in a non-polar environment, specifically in the presence of neutral storage lipid droplets. Quantification of this fluorescence was established by culturing wild type and *tolC*$^-$ mutants in Luria-Burtani (L.B.) medium. After 24 h growth, 3 x 250 μl samples from each culture were assayed for Nile Red fluorescence (methods 2.2). Results show that the increased fluorescence within all the *tolC*$^-$ mutants is markedly greater with an approximate increase of 300% (Fig. 3.1A). To confirm the disruption of the *tolC* gene, wild type *V. furnissii* and the *tolC*$^-$ mutant were cultured in L.B. medium and genomic DNA was extracted according to the manufacturers protocol. PCR based detection of the *tolC* gene was carried out using primers spanning the entire gene (methods 2.4, Table 2.2) to give an expected product size of 1.5 kb in the wild type (Fig. 3.1B). PCR carried out on DNA extracted from the *tolC*$^-$ mutants did not amplify the *tolC* gene indicating its absence. The mutant "H10" was chosen as a selective representation for further study. The TnAraOut transposon (Judson and Mekalanos, 2000) was used for the random transposon mutagenesis (by Dr. John Dowdle). To confirm the insertion of this transposon within the *tolC* gene in the H10 mutant and to determine it's location, the *tolC*$^-$ mutant was sequenced using a reverse primer designed to span the start of the transposon (methods 2.4, Table 2.2). Sequencing shows the transposon to be inserted 153 bps into the coding gene sequence (Fig. 3.2) (appendices, Fig. 8.1). Transcriptome analysis carried out in chapter 5 confirmed that none of the surrounding genes (displayed in Fig. 3.2) show significant differential expression in the *tolC*$^-$ mutant.

3.2.2. Overexpression and complementation of TolC.

The TolC complementation and overexpression was carried using the gateway cloning method. Initially an entry clone was created following the Invitrogen BP protocol and transformed in *E. coli* TOP10 cells. Following this the LR reaction was carried out to transfer the *tolC* gene into a broad host range expression vector pSRKGmJAA. The expression vector used was adapted from pSRKGm (Khan *et al.*, 2008) by Dr. John Dowdle to incorporate the toxic *ccdB* gene. During the LR reaction, this *ccdB* suicide gene is replaced by *tolC* enabling a screen for successful transformants into BW20767 competent cells. The vector map of pSRKGmJAA+TolC is displayed in Figure 3.3. showing the designed location of the *tolC* gene once *ccdB* is replaced. Gentamicin selects for cells

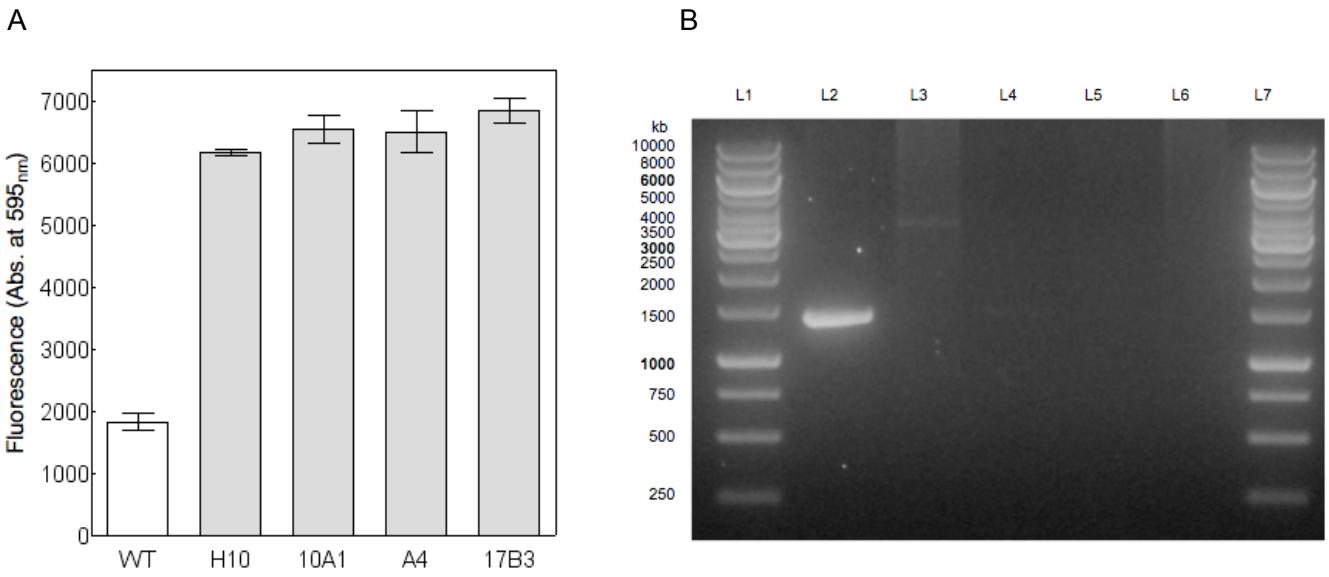

Figure 3.1. Transposon mutant analysis

A. Nile Red fluorescence determined in wild type *V. furnissii* (WT), and *tolC*⁻ mutants: H10, 10A1, A4 and 17B3 cultures after 24 h growth. Error bars represent average of 3 biological replicates, all *tolC*⁻ mutants show increased fluorescence.

B. Agarose gel electrophoresis performed following PCR amplification of *tolC* in wild type *V. furnissii* and four *tolC*⁻ mutants. L1 and L7 – Gene Ruler 1kb DNA ladder, L2 wild type (*tolC* product present ~ 1.5 kb) L3 – H10, L4 – 10A1, L5 – A4, L6 – 17B3. No DNA fragment is present in all four knockout mutants.

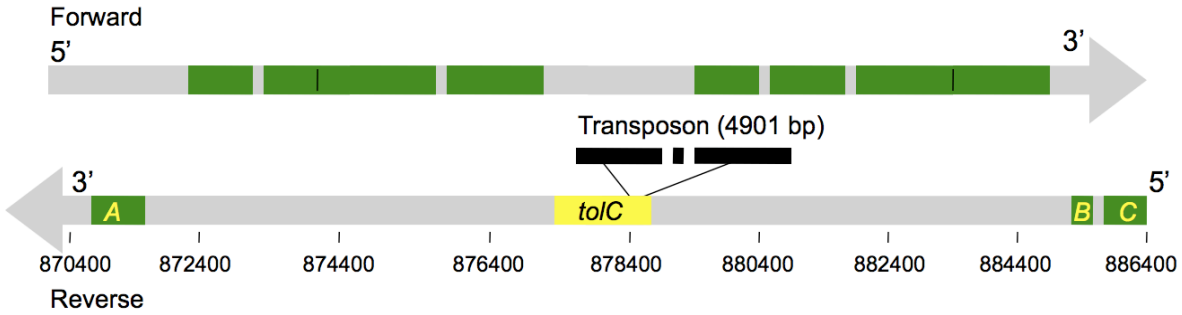

Figure 3.2. Graphical representation of transposon insertion in the *V. furnissii* mutant, H10.

Determined following sequencing of the transposon insertion in the "H10" *tolC* mutant. The grey arrow (from 5'-3') represents the mutated open reading frame (ORF) containing *tolC.* The insertion site of the transposon is indicated, 153 bp into *tolC.* Gene *A* codes for an ion transport protein, genes *B* and *C* code for proteins of unknown function.

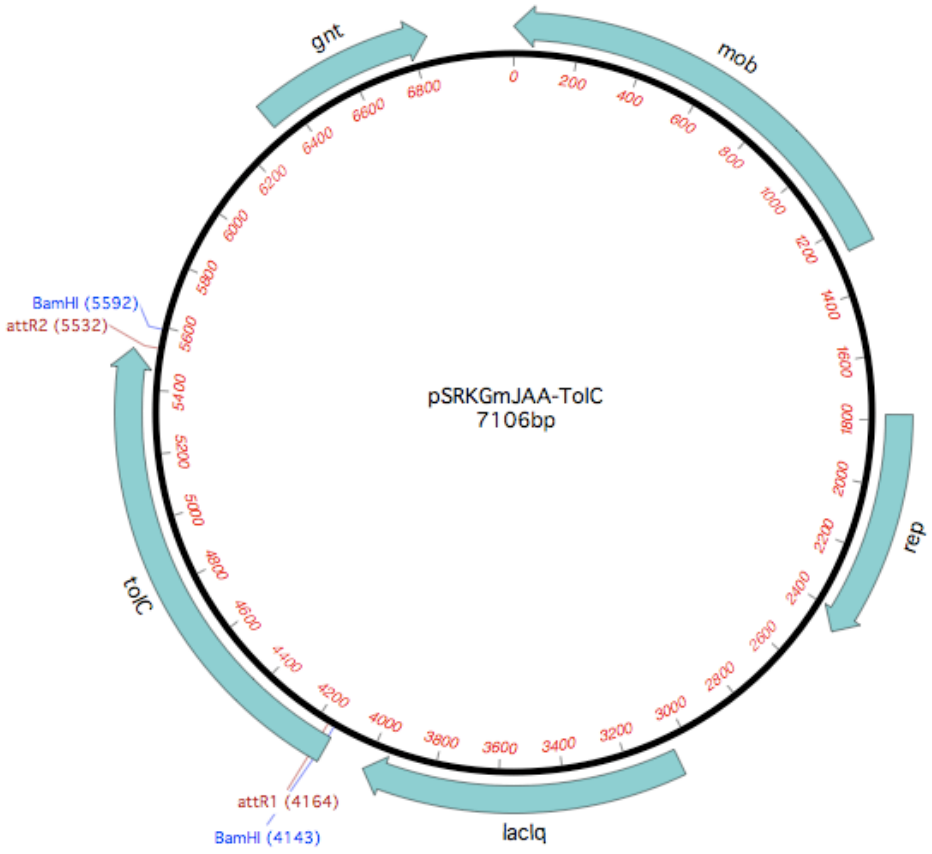

Figure 3.3. Expression vector pSRKGmJAA-TolC

Adapted from pSRKGm (Khan *et al.*, 2008) for transformation of *tolC* into *V. furnissii* containing inserted gene following gateway cloning. Diagram compiled using MacVector 12.6.0 with key genetic determinants displayed: including replication (rep), gentamicin resistance (gnt), mobilisation (mob) and expression cassette (*lacI*q). The *attR* sites are displayed as well as the *Bam*HI restriction sites.

containing the vector and only those where *tolC* has successfully replaced the *ccdB* gene will survive. For additional confirmation of the gene insertion a diagnostic restriction digest was performed using *Bam*HI (restriction sites displayed in Fig. 3.3) following plasmid DNA extraction (appendices Fig. 8.2). The vector was then transferred into *V. furnissii* cells by conjugation; for complementation of the gene, the vector containing *tolC* was conjugated with knockout mutant cells and for overexpression of the gene the same protocol was used with wild type cells. The plasmid DNA was extracted and a digest was carried out with *Bam*HI enzyme (restriction sites either side of *tolC*) for confirmation of gene insertion into vector (appendices, Fig.8.2.). The overexpressor was cultured in L.B. medium, nutrient defined medium and M9 medium containing IPTG (methods 2.1) to determine the effect overexpression had on growth. It was noted that growth in nutrient defined or minimal media was unsuccessful (following 24 h) and growth rate of the overexpressor on L.B medium was markedly slower compared to wild type (appendices Fig. 8.3). Control cultures of the over expresser were grown without IPTG and these showed the same results as those cultured with IPTG (appendices Fig. 8.3) suggesting leaky expression from the plasmid.

3.2.3. Quantitative and qualitative analysis of RNA and cDNA.

Analysis of *tolC* gene expression was achieved by RT-qPCR. Total RNA was extracted from wild type, *tolC*$^{-}$ mutant, complement and overexpressor. RNA sample concentration was determined using a NanoDrop 1000 spectrophotometer (Thermoscientific), and quality was determined using a 2100 Bioanalyser (Agilent) (methods 2.10). Parameters were applied to ensure sample purity: (A_{260}:A_{280}) < 1.7 and 16S and 23S rRNA bands defined on the Bioanalyser gel (Fig. 3.4). The process of gel electrophoresis through a micro-fluidic chip performed by the Bioanalyser involves dyed RNA in the mobile phase passing over a detector. Fluorescence emitted by this dye is then quantified and represented as a gel image. This procedure enables accurate sizing and quantification of RNA fragments in lower sample concentrations (25-250 ng/μl). Extraction of usable RNA was not achieved from the TolC complement, a weak 16S band was detected but degradation of the mRNA was apparent in all repeated extractions (Fig. 3.4). The Bioanalyser histograms are used for visualising sample degradation, the complement strain displays a relatively high abundance of low molecular weight species indicating substantial degradation (Fig. 3.5). RNA precipitation was carried out to concentrate complement samples but RNA suitable for RT-qPCR was ultimately not extracted. Two clear peaks corresponding to 16S and 23S were achieved in the wild type, knockout mutant and overexpressor, confirming high quality RNA (Fig. 3.5A).

3.2.4. Optimisation of RT-qPCR using standardised cDNA concentrations

In order to analyse the expression of TolC; Glyceraldehyde-3-phosphate dehydrogenase (*GAPDH*)

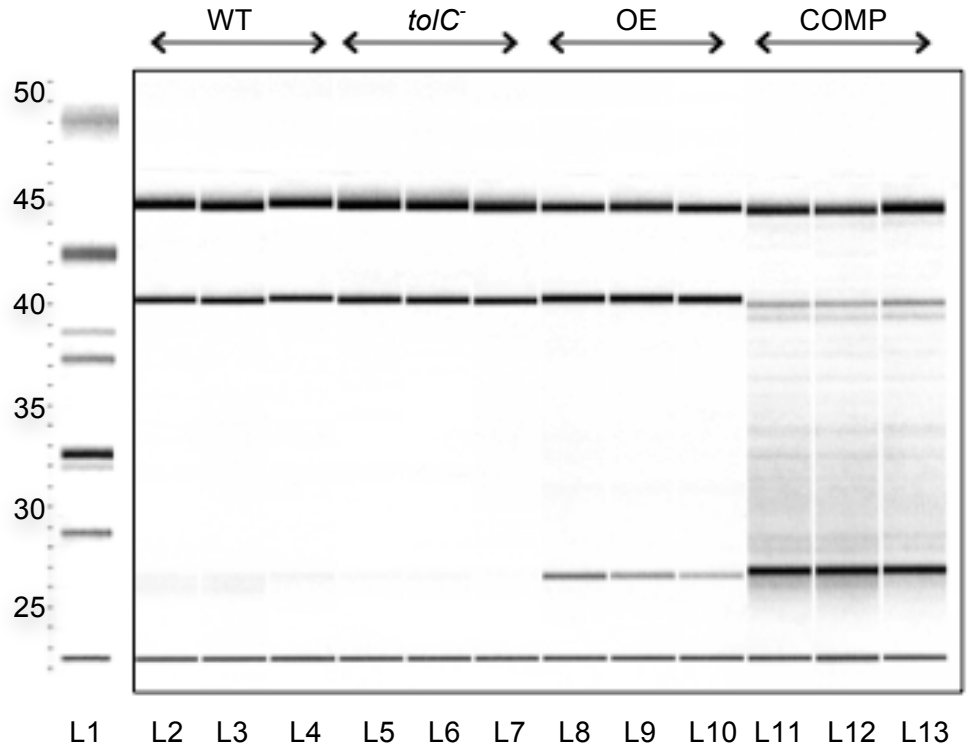

Figure 3.4. Bioanalyser gel image

Displaying quality of extracted RNA. L1: Ladder, L2-4: wild type (WT), 5-7: *tolC*$^{-}$ mutant, 8-10: overexpressor (OE), 11-13: complementation (COMP), n=3 (biological replicates). Sharp bands of 23S and 16S ribosomal RNA can be seen in L2-L10 demonstrating the integrity of total RNA isolated. Degradation is apparent in the complement samples (L11-L13).

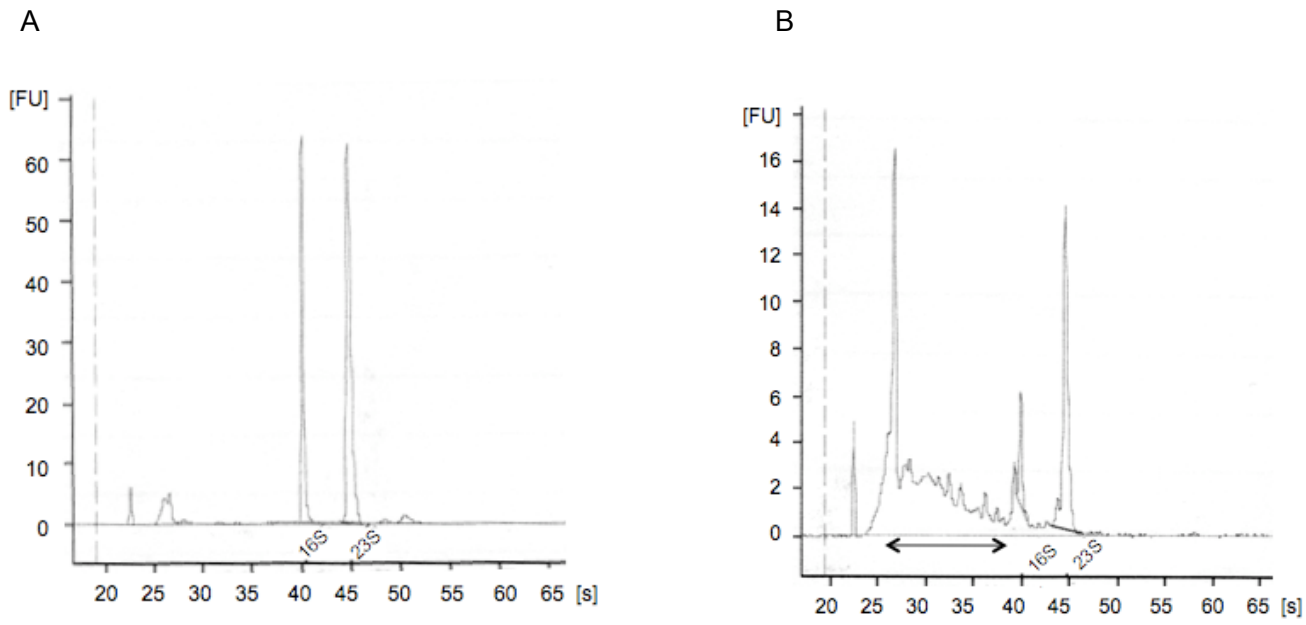

Figure 3.5. Bioanalyser histograms

Representing quality of RNA in A: Wild type and B: Complement. Clear 16S and 23S peaks in wild type samples indicative of quality RNA, representative of *tolC*$^{-}$ mutant and overexpressor samples (n=3). Degradation apparent in complement sample as indicated by arrow.

was chosen as a control housekeeping gene. The expression of GAPDH maintains consistent expression therefore the expression of TolC could be measured in relation to it. Synthesis of wild type, *tolC*$^-$ mutant and overexpressor cDNA was achieved using Qiagen QuantiTect reverse Transcription Kit. *GAPDH* and *tolC* primers with targeted probes were designed and conditions were optimised on cDNA by PCR amplification. PCR products of the correct size were amplified with both *GAPDH* and *tolC* primers using wild type cDNA (appendices Table 8.1, Fig. 8.4). For analysis of mRNA transcription, RT-qPCR was subsequently carried out. Initially a standard curve was derived from serial dilutions (1:5) of wild type RNA, concentrations were calculated as 1447, 285. 59.3, 10.8, 2, 0.4. (ng/μl), which were prepared in triplicate. Amplification plots from the extension phase fluorescent emission data collected during the PCR amplification of *GAPDH* and *tolC* were analysed, all three biological replicates for each serial dilution showed the same levels of fluorescence, the *tolC* data output is displayed as an example (Fig. 3.6A). Cycle time (Ct) values were calculated by determining the point at which the fluorescence exceeds the threshold limit (0.035 *GAPDH*, 0.025 *tolC*). Standard curves were established for both *GAPDH* and *tolC,* the *tolC* standard curve is shown as a representation of both controls which gave very similar results (Fig. 3.6B) (*GAPDH* data are shown in appendices Fig. 8.5). The relationship between Ct and concentration is linear (efficiency: 1.08 for *tolC* standard curve and 1.09 for *GAPDH*).

3.2.5 Determining TolC expression in wild type, tolC$^-$ *mutant and overexpressor.*

RT-qPCR was carried out on wild type, *tolC*$^-$ mutant and overexpressor, following RNA extraction as described previously (section 3.2.4). The expression of both GAPDH and TolC was calculated for each sample by quantifying the mRNA using the Ct values and the standard curve (methods 2.14). The housekeeping gene, *GAPDH* was used to calculate relative expression of *tolC* using Rotor Gene 6000 1.7 series software. All samples analysed were at concentrations within range of the standard curve (0.5 to 1.5 μg/μl) and any samples that displayed a Ct value > 40 were not used. Results show that relative expression of TolC in the mutant is almost zero and there is a significant increase of approximately 100% in the overexpressor (Fig. 3.7).

3.2.6 Use of the Nile Red assay to investigate TolC expression.

The Nile Red assay was used within this study to analyse the lipid present in wild type, *tolC*$^-$ mutant and overexpressor. However, data published by (Bohnert *et al.*, 2010) after this investigation was begun, show Nile Red to be a substrate of TolC. Therefore differences in cellular Nile Red fluorescence can be related to TolC function, the assay is used here for the purpose of analysing TolC expression in the wild type, *tolC*$^-$ mutant, complement and overexpressor (Fig. 3.8). Samples were taken from stationary phase cultures and transferred to a 96 well plate before the Nile Red

A

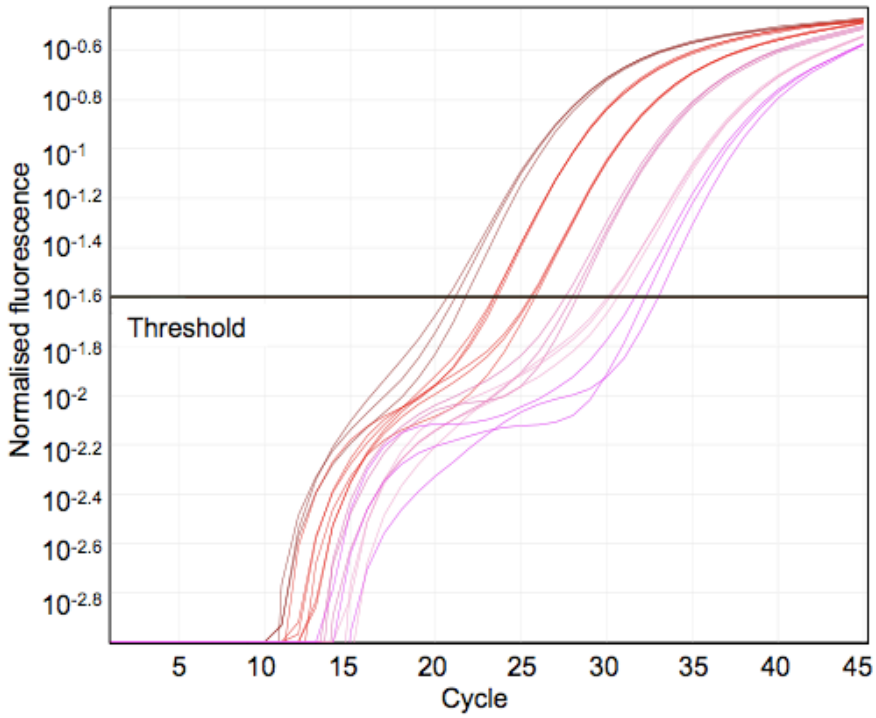

B

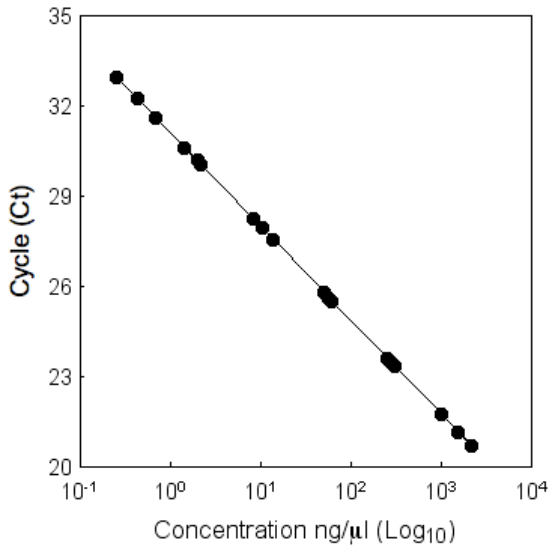

Figure 3.6. RT-qPCR *tolC* standard curve data.

A. Example of extension phase fluorescent emission data collected during the PCR amplification of *tolC*. Serial dilution concentrations (ng/µl): 1447, 285, 59.3, 10.8, 2, 0.4

B: Concentration (Log_{10}) plotted against threshold amplification cycle number (Ct), displaying linear regression. Each concentration was prepared in triplicate with six technical replicates, RT-qPCR for both *tolC* and *GAPDH* were carried out, data show *tolC* standard curve, *GAPDH* standards in appendices Fig. 8.5.

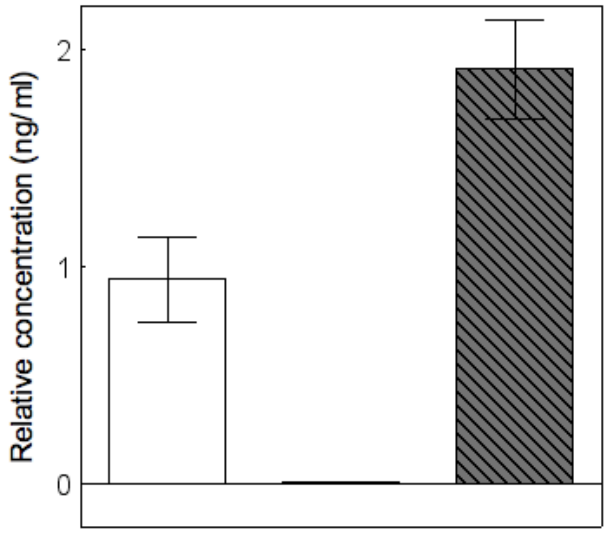

Figure 3.7. Quantification of RT-qPCR

Results display relative concentration of *tolC* mRNA in wild type ▭ knockout mutant ▭ and overexpressor (cultured with IPTG 1mM) ▨. Error bars represent standard deviation (n=3 samples), significant decreased in TolC expression in knockout and increase in the overexpressor compared to wild type (two tailed t-test $p<0.05$).

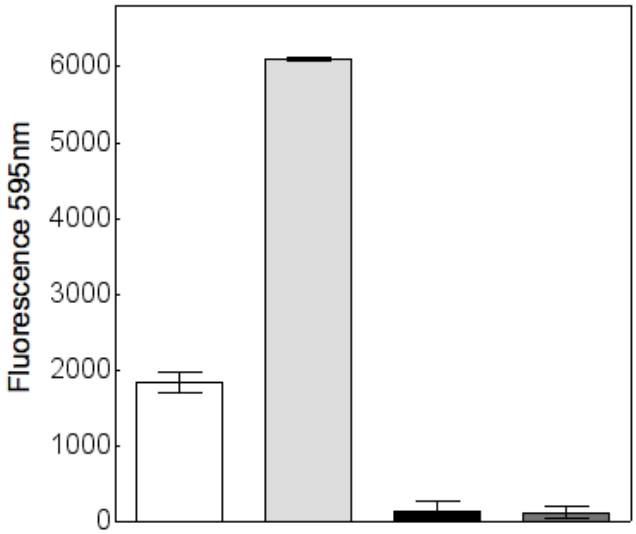

Figure 3.8. Nile Red fluorescence of wild type, *tolC*$^{-}$ mutant, complement and overexpressor.

Absorbance at 595 nm determined after 24 h growth on L.B. media (methods 2.2). All cultures assayed once in stationary phase, 3 technical replicates obtained, standard deviation displayed by error bars. Wild type ▭, *tolC*$^{-}$ mutant ▭ Complement ■, Overexpressor ▨. Over expressor and complement cultured with IPTG (1 mM), experiment also carried out without IPTG, fluorescence levels remained the same.

assay was performed. The knockout mutant displays increased fluorescence as previously shown (Fig. 3.8) and the overexpressor displays a significant reduction in fluorescence, however the complement does not give similar readings to that of the wild type and in fact exhibits similar activity to the overexpressor. Evidence from these data suggests that the complement strain is not successfully expressing TolC at a similar level to the wild type. Control samples of both complement and over expressor grown without IPTG and results were the same suggesting leaky plasmid expression. Growth of the complement is limited and subsequent RNA extraction was unsuccessful, the complement strain was therefore not utilised for further analysis.

3.2.7. TolC confers resistance in V. furnissii*, determined by IC_{50} data*

Determining antibiotic resistance in wild type *V. furnissii* and *tolC*$^{-}$ mutant was undertaken to establish the role of TolC as an antimicrobial exporter in *V. furnissii*. An additional aim of this experiment was to provide phenotypic evidence of the knockout mutation and overexpression of TolC. Initially wild type *V. furnissii* was cultured on L.B. medium containing increasing concentrations of 8 antibiotics, categorised by 5 classes; gentamicin, kanamycin, streptomycin and paramomycin (aminoglycosides), ampicillin (aminopenilicillin), novobiocin (aminocoumatin), tetracycline (tetracycline), erythromycin (macrolide) (Fig 3.9). IC_{50} values were determined as concentration required to inhibit bacterial growth by 50%. Wild type, knockout mutant and overexpressor were subsequently grown on L.B. medium containing antibiotics at the calculated IC_{50} concentrations (Fig. 3.10A and 3.10B). The *tolC*$^{-}$ mutant displays decreased resistance to gentamicin, streptomycin, ampicillin, novobiocin and erythromycin (Fig. 3.10A). The *tolC*$^{-}$ mutant contains a kanamycin resistant gene, and the overexpressor contains a gentamicin resistance gene explaining the increased resistance to the corresponding antibiotics in these strains compared to the wild type. Furthermore, the overexpressing strain exhibits a significant increase in resistance to kanamycin, streptomycin and paramomycin ($p<0.05$) (all aminoglycosides). Data also display a significant decrease in resistance to ampicillin (two tailed t-test $p<0.05$) (Fig. 3.10B). Ultimately the *tolC*$^{-}$ mutant shows decreased resistance to a number of antiobiotics and the over expressor displays increased resistance to aminoglycosides. These data not only confirm expected results from a *tolC*$^{-}$ knockout mutant and over expressor, it gives an indication of the membrane bound antiporter interacting with TolC as aminoglycoside resistance is associated with AcrD.

3.2.8. Determining minimum inhibitory concentrations of antibiotics in V. furnissii.

For further anlysis of antibiotic resistance in the *tolC*$^{-}$ knockout mutant and over expressor, minimum inhibitory concentrations (MICs) of 7 antibiotics were determined in wild type, *tolC*$^{-}$ mutant and overexpressor. Resistance to two further groups of antibiotics: chloramphenicol (phenicol) and

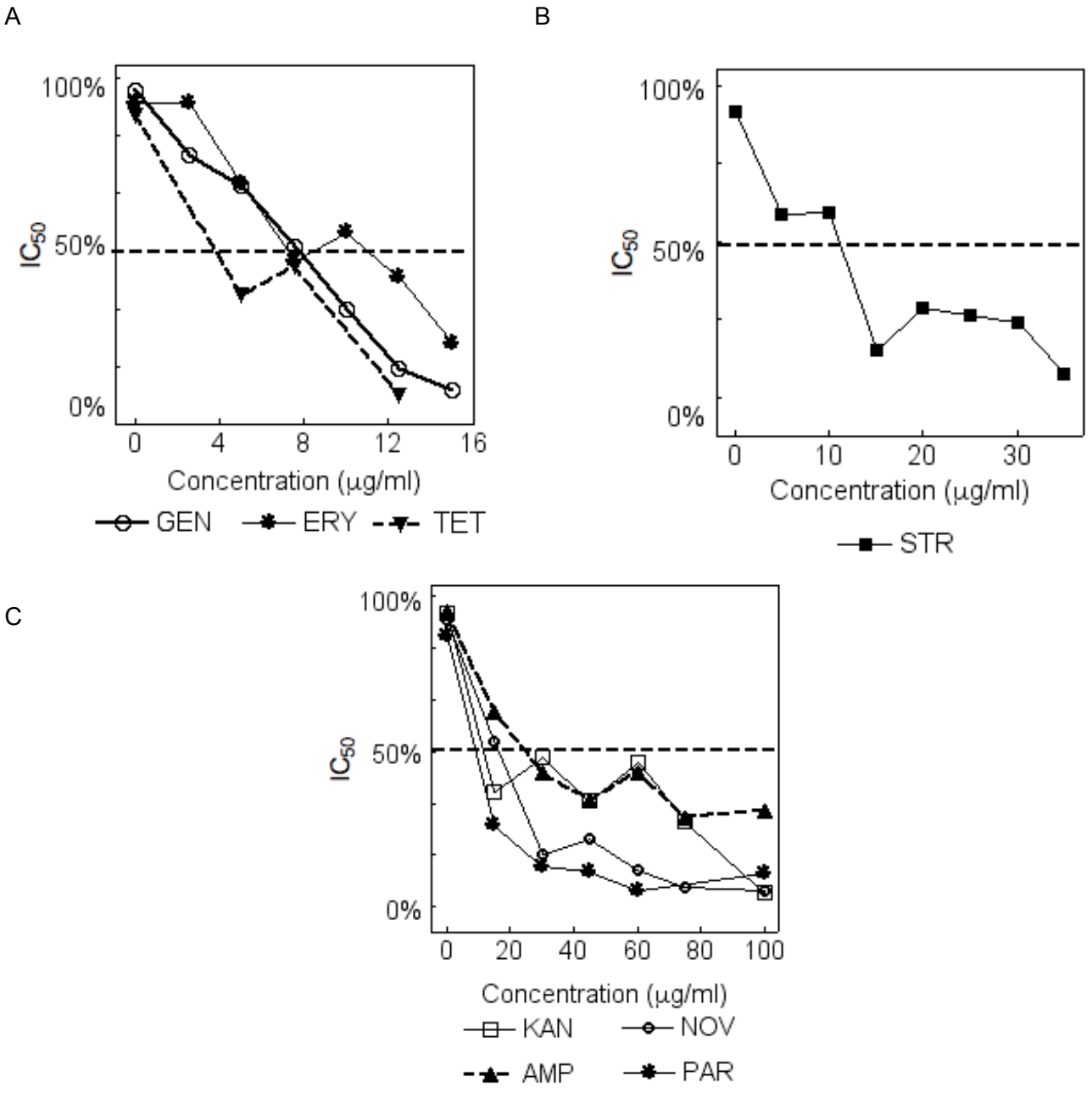

Figure 3.9. Determining IC_{50} values in *V. furnissii.*

Wild type *V. furnissii* were cultured in 5 ml L.B. media containing increasing concentrations of 8 antibiotics for 24 h. IC_{50} (50% growth efficiency) is indicated and corresponds to O.D. $_{600nm}$ 0.5.

A: IC_{50}: Gentamicin (7.5μg/ml), erythromycin (7.5μg/ml), tetracycline (5μg/ml)

B: IC_{50}: Streptomycin (10μg/ml)

C: IC_{50}: Kanamycin (15μg/ml), novobiocin (20μg/ml), paromomycin (15μg/ml) and ampicillin (25μg/ml).

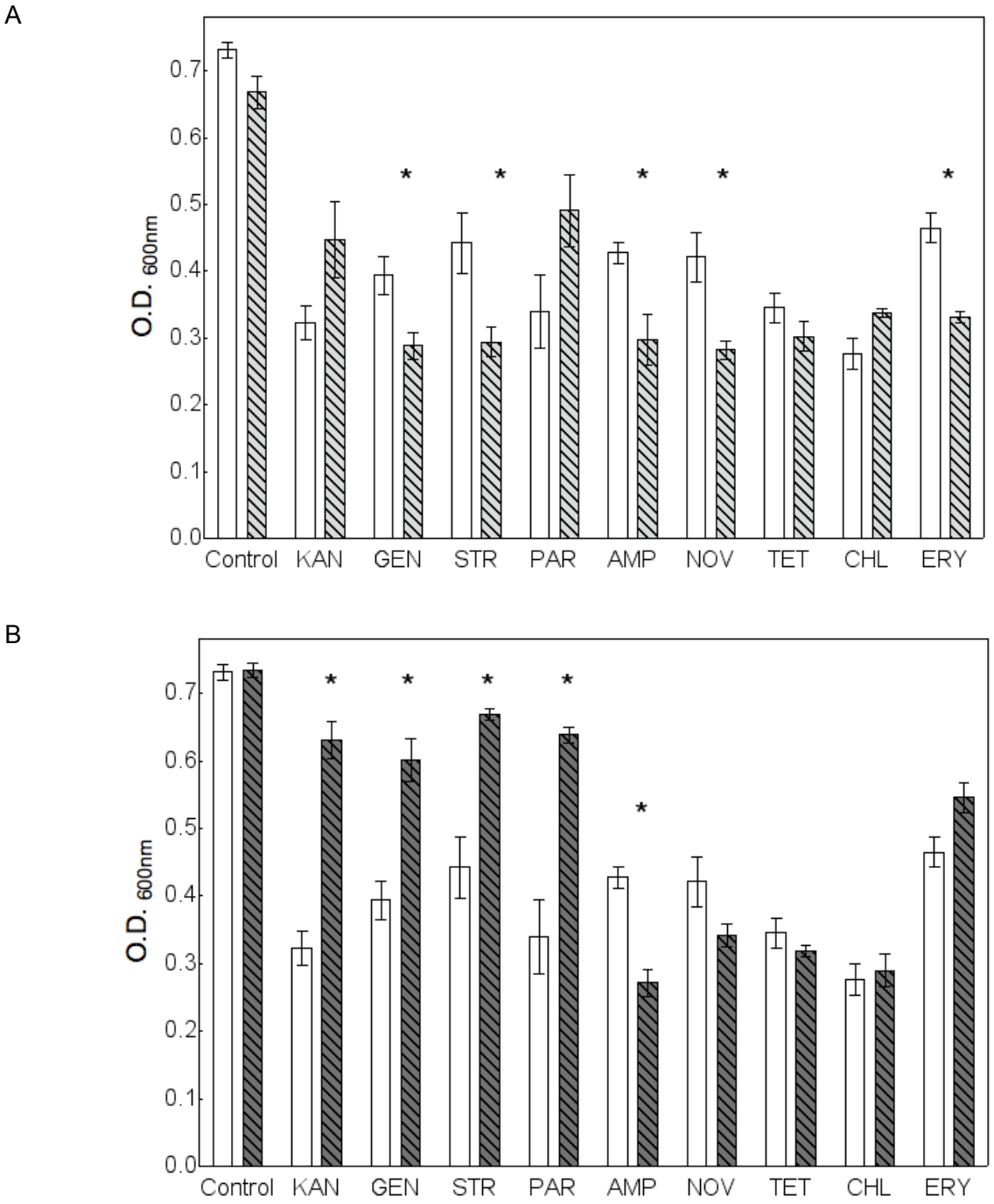

Figure 3.10. Growth of *V. furnissii* wild type, *tolC*⁻ mutant, and overexpressor in media containing antibiotics at IC_{50} concentrations.

Bacteria cultured on L.B. media containing antibiotics at IC_{50} concentrations previously calculated (Fig. 3.9). A: *tolC*⁻ mutant and wild type B: overexpressor and wild type

Wild type ▭, *tolC*⁻ mutant ▨, overexpressor ▩

Significant differences indicated on graph (two tailed t-test $p<0.05$), n=3.

norfloxacin (fluoroquinolone) were also established using MIC analyses. 96 well plates containing L.B. medium and antibiotics at increasing concentrations were inoculated with starter cultures (n=4) (methods 2.15.2, appendices Fig. 8.6), the colony forming units (CFUs) were determined for each starter culture and were consistent for all cultures: Wild type: $2.1x10^8$ and $1.7 x10^8$, *tolC*$^-$ mutant: $2.1 x10^8$ and $2.9 x10^8$, overexpressor: $2.56 x10^8$ and $3.8 x10^8$. The knockout mutant displays a lower MIC in contrast to wild type in all antibiotics initially determined by IC_{50} data (Table 3.1, Table 3.2), further supporting reduced resistance in the mutant to the antibiotics investigated. The IC_{50} and MIC data show consistency (Table 3.2), however, unlike IC_{50}, results of the MIC data suggest resistance to streptomycin is not altered between wild type and mutant (Table 3.2). Further comparison of the IC_{50} and MIC data shows resistance to tetracycline is conferred by TolC in the MIC data set (knockout mutant MIC: 0.125 μg/ml, wild type MIC: 1 μg/ml) (Table 3.1) but not in the IC_{50} results (Fig. 3.10A). An explanation for the difference in these results could be that the calculated IC_{50} concentration was too high. Some growth was recorded in the presence of norfloxacin and novobiocin during MIC analysis (MIC 0.5 μg/ml and 1 μg/ml respectively) (Table 3.1) but not more so than the wild type (MIC 1 μg/ml and 8 μg/ml respectively). Notably there was no growth in the presence of gentamicin which would be expected. The assays were incubated for a further 24 h but there was no further growth suggesting that growth of the overexpressor was not successful in 96 well plates and that IC_{50} data is a more reliable method for determining antibiotic resitance for this strain. The combined IC_{50} and MIC data give a comprehensive analysis of antibiotic resistance in both the *tolC*$^-$ knockout mutant and the overexpressor, confirming the role of TolC in antibiotic resistance in *V. furnissii.* Chapter 5 will provide more in depth analysis of the membrane bound transporters acting with TolC in this organism to export antibiotics.

3.2.9. Monitoring lipid production in wild type V. furnissii *and* tolC$^-$ *mutant.*

To monitor cellular lipid content in wild type and *tolC*$^-$ mutant cells Nile Red fluorescence was analysed in culture extracts throughout bacterial growth. The Nile Red assay is used to detect lipid production but, more recently, Nile Red was established as a TolC substrate (Bohnert *et al.*, 2010). Prior to this finding the Nile Red assay was carried out under conditions optimal for lipid synthesis in a nutrient defined medium (methods 2.1). Within this medium, the overexpressor was unable to grow successfully ($O.D._{600nm}$ after 24 h < 0.25) so the focus for this study was a comparison of wild type and *tolC*$^-$ mutant. Growth curves display an increase in Nile Red fluorescence (abs at 595 nm) in mutant cultures of at least 100% relative to wild type (Fig. 3.11). Fluorescence in both wild type and mutant begins in early exponential phase. During mid exponential phase the levels of Nile Red fluorescence in the mutant increase at a much greater rate. The difference is at its greatest during late exponential phase during which, the difference in mutant fluorescence reaches 5.7 times that

	MIC (μg/ml)						
Strain	Antibiotic						
	CHL	TET	AMP	NOR	NOV	GEN	STR
Wild type	2	1	128	1	8	2	4
tolC⁻ mutant	0.25	0.25	2	<0.125	<0.125	0.5	4
Overexpressor	<0.125	<0.125	<0.125	0.5	1	<0.125	<0.125

Table 3.1. Minimum inhibitory concentrations of wild type *V. furnissii* and *tolC*⁻ mutant.

Determined for chloramphenicol (CHL), tetracycline (TET), ampicillin (AMP), norfloxacin (NOR), novobiocin (NOV), gentamicin (GEN) and streptomycin (STR) determined for wild type, *tolC*⁻ mutant and overexpressor. Knockout mutant displays decreased resistance to all antibiotics after 24 h of incubation, overexpressor shows no increase in resistance after 48 h. Data obtained n=4.

Strain	Method	Antibiotic									
		KAN	GEN	STR	PAR	AMP	NOV	TET	CHL	ERY	NOR
tolC⁻ mutant	IC_{50}	↔	↓	↓	↔	↓	↓	↔	↔	↓	
	MIC		↓	↔		↓	↓	↓	↓		↓
Overexpressor	IC_{50}	↑	↑	↑	↑	↓	↔	↔	↔	↔	
	MIC		↓	↓		↓	↓	↓	↓		↓

Table 3.2. Summary of antibiotic resistance data determined by IC_{50} and MIC.

Kanamycin, gentamicin, and streptomycin (aminoglycosides) indicated in grey. NA: mutant contains resistance gene, ↓:bacteria display decreased resistance to antibiotic, ↑ : indicates increased resistance to antibiotic in contrast to wild type. ↔ no change in sensitivity. Knockout shows decreased resistance to antibiotics from all groups, overexpressor shows increased resistance to aminoglycosides only.

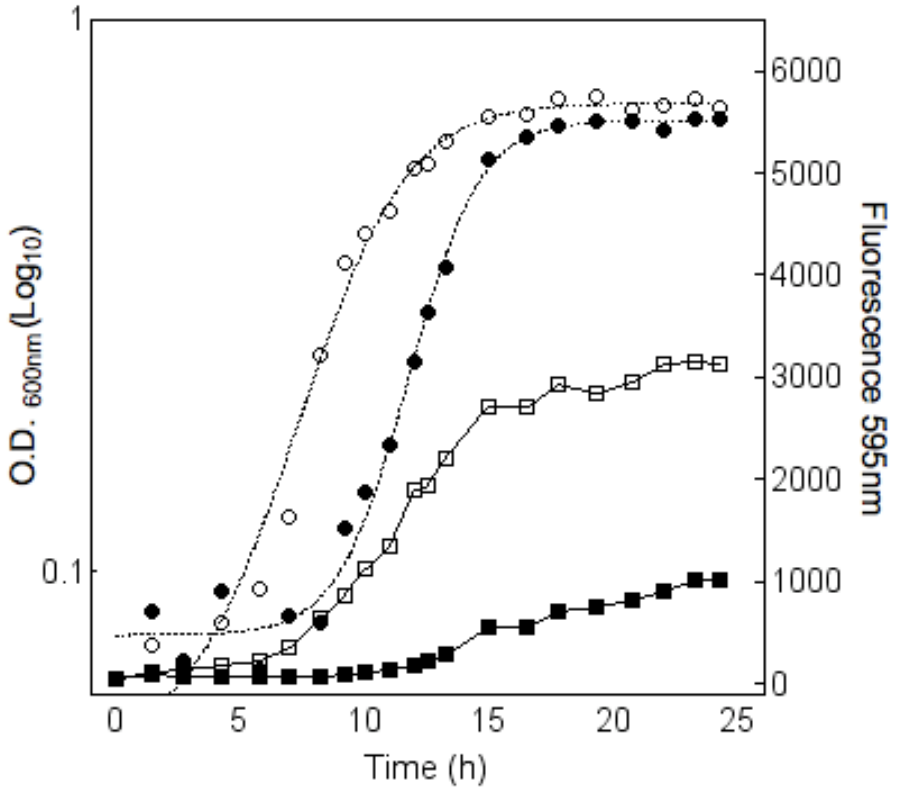

Figure 3.11. Nile Red fluorescence monitored in wild type *V. furnissii* and *tolC*⁻ knockout mutant during bacterial growth.

Bacteria were grown on nutrient defined media, data was carried out in triplicate, results are typical of all data sets. Wild type growth *tolC*⁻ mutant growth Wild type fluorescence *tolC*⁻ mutant fluorescence.

Wild type	*tolC*⁻ mutant	Fluorescence (595nm), Fluorescing cell count (FACS and manual).

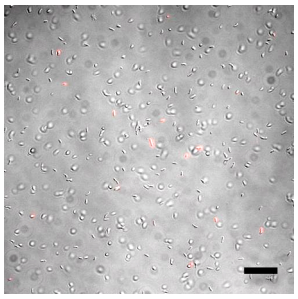
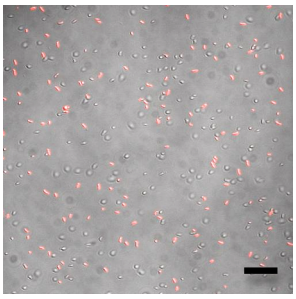

Mid exponential phase

	O.D.	Fl (NR Assay)	Fl cells (Count)	% Fl cells (FACS)
WT	0.484	419	~13	0.30
KO	0.455	1302	~104	72.40

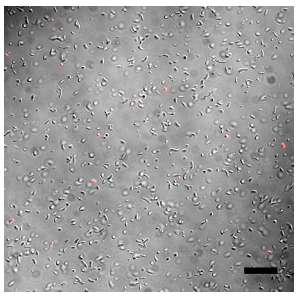
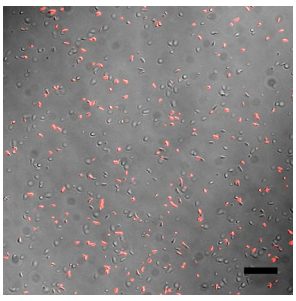

Late exponential phase

	O.D.	Fl (NR Assay)	Fl cells (Count)	% Fl cells (FACS)
WT	0.645	611	~15	5.50
KO	0.634	2007	~138	77.40

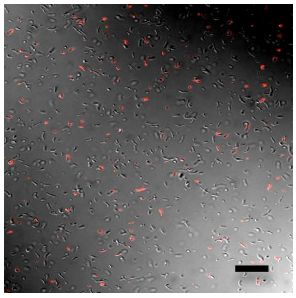
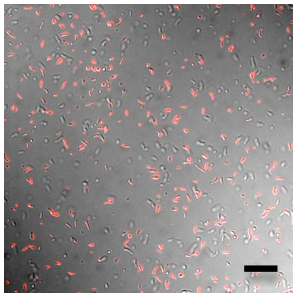

Stationary phase

	O.D.	Fl (NR Assay)	Fl cells (Count)	% Fl cells (FACS)
WT	0.780	1317	~90	20.50
KO	0.794	2645	~205	44.20

Figure 3.12. Confocal microscope images of wild type *V. furnissii* and *tolC*⁻ mutant at three growth stages.

Table insets display corresponding $O.D_{600nm}$ readings (average of 3 technical replicates), the number of fluorescing (Fl) cells counted in the images, fluorescence readings quantified by Nile Red assay and % of fluorescing cells determined by FACS for each growth stage (Fig. 13A and 13B). scale bar (▬) corresponds to 10 μm. Number of fluorescing cells increases throughout growth and overall less are fluorescing in mutant cultures, confirmed by combined methods. Data presented are representative of n=3 samples for each growth stage.

of the wild type (WT fluorescence value = 369 ($O.D._{600nm}$ 0.523) and mutant fluorescence value = 2074 ($O.D._{600nm}$ 0.512). These data provide initial information about the nature of Nile Red fluorescence in relation to *V. furnissii* cell growth and how this differs between the wild type and the *tolC* mutant. Results show that there is a significant increase in fluorescence in the mutant and that this is consistent throughout bacterial growth. Further analysis is required to determine if this increase in fluorescence correlates solely to a higher lipid content in the $tolC^-$ mutant or if TolC expression contributes to this result.

3.2.10. Investigating Nile Red fluorescence within V. furnissii *cells.*

To determine visually the increased Nile Red fluorescence in the $tolC^-$ mutant, wild type and $tolC^-$ mutant cultures were prepared and analysed by fluorescence microscopy at 3 growth phases (Fig. 3.12). After incubation with 3 μM Nile Red, the fluorescence reading was obtained on an Infinite® 200 PRO micro plate reader (TECAN) and the remainder of the sample prepared for laser scanning Confocal microscopy (LSCM). A higher cellular Nile Red fluorescence was observed in the knockout mutant (Fig. 3.12) consistent with previous data (Fig. 3.11). Nile Red assay values are presented with each image that was subsequently obtained, along with an estimated visual count of fluorescing cells (Fig. 3.12). These data are consistent, confirming the increase in Nile Red fluorescence in the mutant and an overall increase throughout bacterial growth. Notably, images show that not all cells in a field of view are fluorescent but that the mutant has a greater number of fluorescing cells compared to wild type. For more accurate quantification, samples (taken from the same cultures used for Confocal microscope imaging) were analysed by a fluorescence activated cell sorter (FACS), which is able to determine the approximate number of fluorescing and non-fluorescing cells. The fluorescing cells were counted in each sample and presented as a percentage (Fig. 3.13). These percentages closely correspond to the number of cells fluorescing in the images (Fig. 3.12). An example of FACS data obtained for wild type and knockout mutant at stationary phase displays the increase in fluorescing cells in the knockout mutant (77.4%) compared to wild type (5.5%) (Fig. 3.13). The increase in fluorescence within the mutant could simply be explained by a Nile Red build up within the cells in the absence of TolC which is interpreted as an increase in lipid content in the mutant. However, there are fluorescing and non-fluorescing populations in both wild type and mutant cultures, suggesting Nile Red fluorescence is growth phase dependant.

A

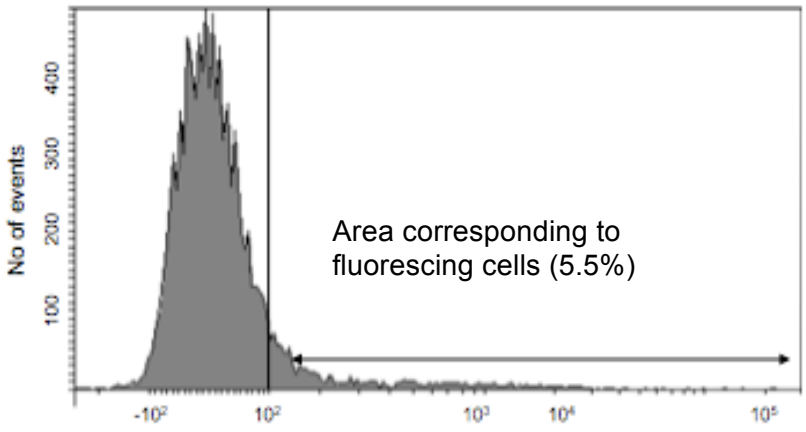

B

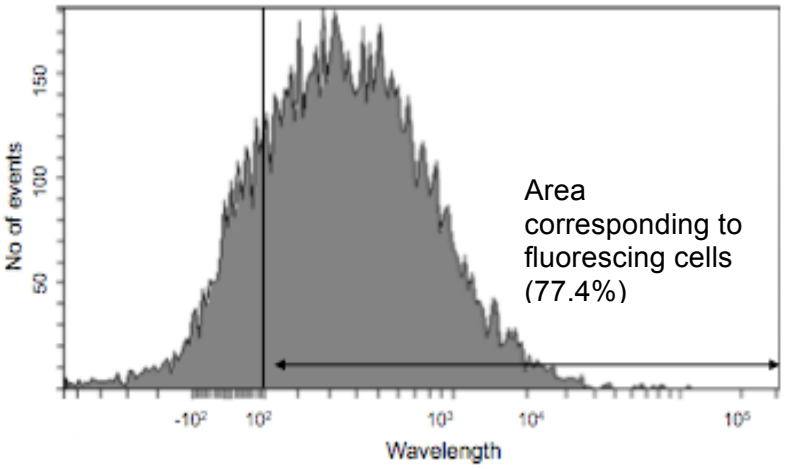

Figure 3.13. FACS analysis of fluorescing (F) and non-fluorescing populations (NF).

Data obtained from wild type and *tolC*$^{-}$ mutant cultures during late exponential phase. A. Wild type, B, *tolC*$^{-}$ mutant. An increased number of fluorescing cells within the knockout mutant culture can be observed in contrast to the wild type, consistent with the microscope images.

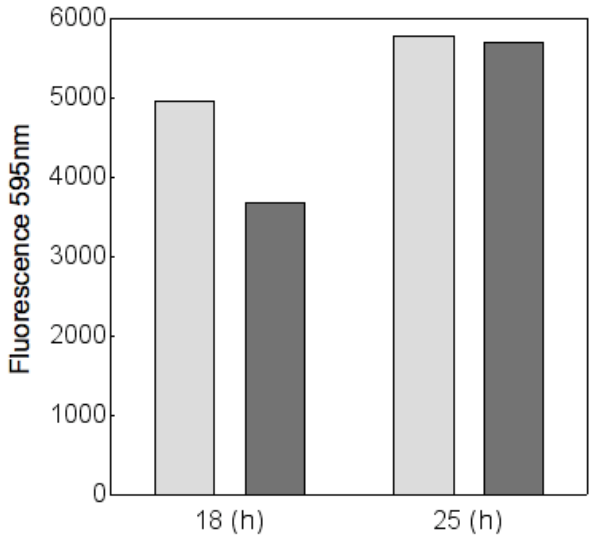

Figure 3.14. Wild type cultures divided into fluorescing (F) and non-fluorescing (NF) populations.

Fluorescence readings were taken at 18 and 25 h, both populations returned to the same fluorescence level. fluorescing: ▭ non-fluorescing: ▬

3.2.11. Investigating the growth phase dependant nature of Nile Red fluorescence.

The separate fluorescing (F) and non-fluorescing (NF) populations observed in wild type and *tolC*$^{-}$ mutant cultures suggest that the Nile Red fluorescence relates to growth phase of individual cells. To examine this hypothesis, the two populations in wild type *V. furnissii* were separated and re-cultured to determine if populations remained solely as F or NF. Isolating F and NF populations was achieved by FACS separation (methods 2.17) where 10 million cells of each population were collected in 2 ml of PBS buffer. Following centrifugation, cells were re-suspended in 500 μl L.B. media and subsequently used to inoculate 5 ml of fresh L.B. media. After 25 h growth, both cultures returned to a mixed population of fluorescing and non-fluorescing cells, as determined by the Nile Red assay (Fig. 3.14), suggesting the fluorescence is growth phase dependant.

3.2.12. Relating Nile Red fluorescence to TolC expression

The hypothesis that Nile Red fluorescence, observed by confocal imaging, is related to TolC expression in wild type bacteria suggests that expression of TolC vaires throughout growth. To determine if the increased fluorescence correlates with TolC expression RNA was extracted from cells cultured in L.B. media at 4 growth points, cDNA was subsequently synthesised and RT-qPCR was performed. Relative expression of TolC increases throughout growth displaying highest expression at late exponential phase (Fig. 3.15). Given this result it would be expected that fluorescence would be lower at this stage due to successful export of Nile Red but this is not supported by the confocal images and other previous data (Fig. 3.12). Although the increase in Nile Red fluorescence in the *tolC*$^{-}$ mutant could be explained by an absence of TolC function as suggested by (Bohnert *et al.*, 2010), these results show Nile Red fluorescence in wild type *V. furnissii is* not directly correlated to TolC expression. This suggests that the uptake of Nile Red is potentially growth phase dependant and that lipid content in the *tolC*$^{-}$ mutant is higher thatn the wild type, however this needs to be determined by further experimentation.

3.2.13. Investigating cellular lipid and hydrocarbon levels

For precise analysis of the lipid compounds present in the wild type and *tolC*$^{-}$ mutant cultures, cell pellets were analysed by Gas Chromatography-Mass Spectrometry (GC-MS) at different stages of growth. Wild type and *tolC*$^{-}$ mutant cells were cultured in nutrient defined media adapted from (Park *et al.*, 2001) and (Oh *et al.*, 2007) and cell pellets were freeze dried following centrifugation. Lipids were then extracted with di-chloromethane using a DIONEX ASE150 accelerated solvent extraction system and analysed by GC-MS for presence of hydrocarbons and long chain fatty acids. *V. furnissii* has been reported to produce hydrocarbons up to 60% of its biomass (Park *et al.*, 2001) but our data show this not to be the case in this strain (Fig. 3.16). In *V. furnissii* 11218 the alkanes .

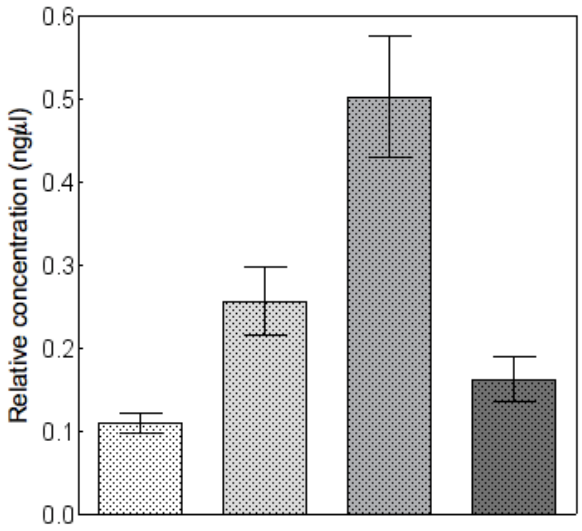

Figure 3.15. Relative expression of TolC during wild type bacterial growth, determined by mRNA concentration. TolC expression is relative to housekeeping gene GAPDH.

Early exponential phase, mid exponential phase, late exponential phase, stationary phase. Error bars represent n=3 samples

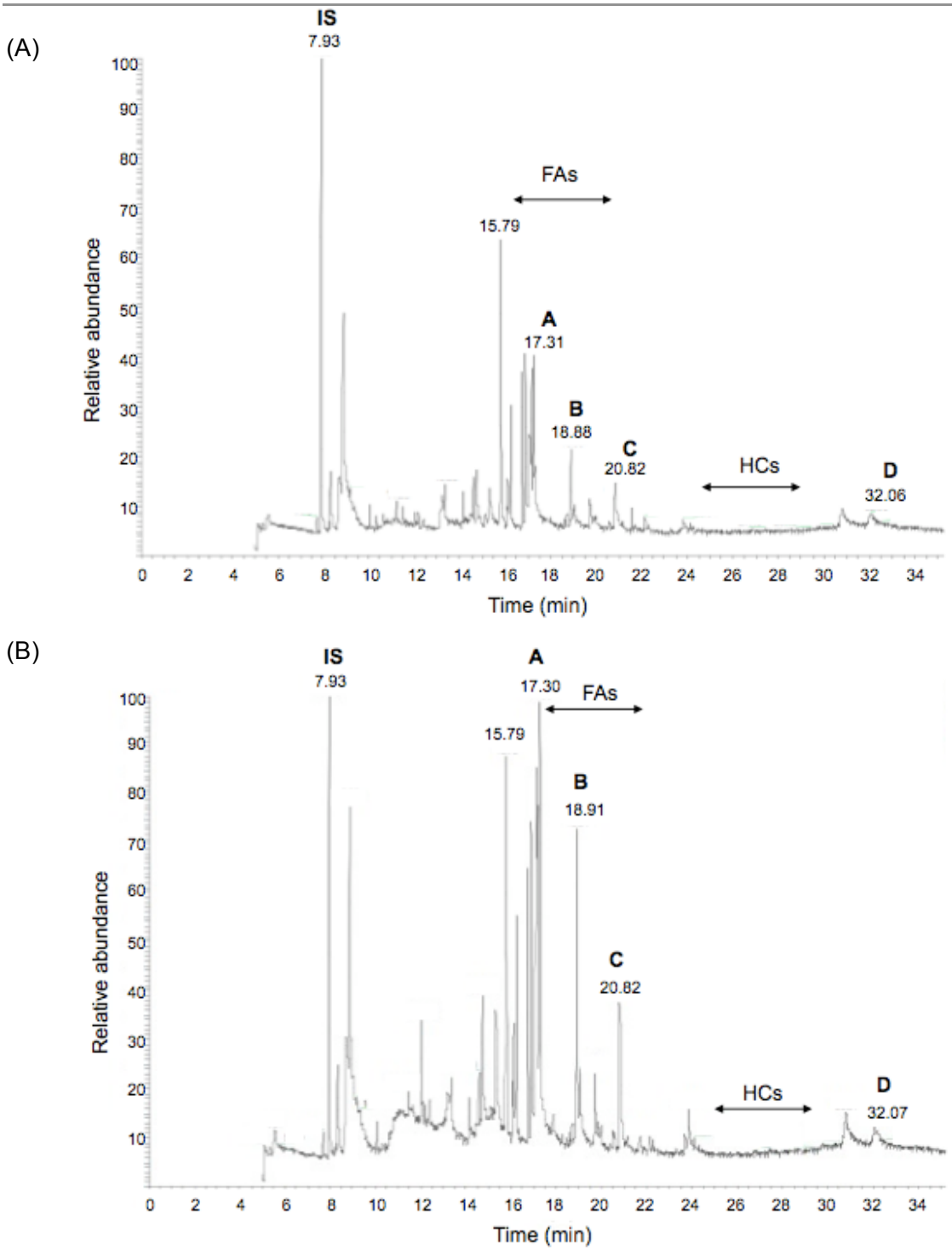

Figure 3.16. GC-MS trace displaying fatty acid (FA) and hydrocarbon (HC) peaks present in wild type (A) and *tolC*$^{-}$ mutant (B) cell extracts.

Three biological samples were analysed and three technical replicates were carried out, data are typical of stationary phase cell pellet profile. IS: internal standard. A (C_{16}): (Z)-9-hexadecenoic acid, B (C_{16}): hexadecanoic acid and C (C_{18}): (9*Z*)-octadecenoic acid.

Structure (Compound A)			
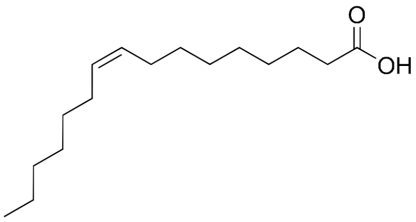			
RT	Name	WT peak area	KO peak area
17.3	(9*Z*)-hexadecenoic acid	7065523	9076788

Structure (Compound B)			
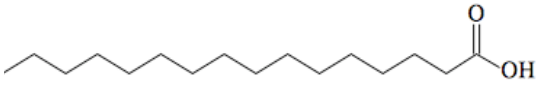			
RT	Name	WT peak area	KO peak area
18.9	hexadecanoic acid	6459903	9271849

Structure (Compound C)			
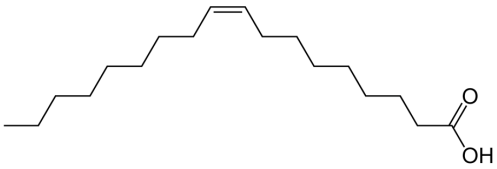			
RT	Name	WT peak area	KO peak area
20.8	(9*Z*)-octadecenoic acid	2762850	4556700

Figure 3.17. Free fatty acids identified in *V. furnissii* wild type (WT) and *tolC*$^{-}$ mutant (KO) cell pellets.

Retention times (RTs): 17.3, 18.9, 20.8 mins. Corresponding relative peak areas are representative of typical result from two biological replicates and two technical replicates, knockout mutant peak areas greater than wild type implying increased cellular concentrations. All compounds satisfy parameters RSI >800 and probability >90.

present are in fact too low in concentration to calculate using GC-MS. The presence of alkanes (C_{16} to C_{28}) would be expected at a retention time of approximately 22 to 32 min, as indicated in Fig 3.16 however no such peaks are detected. No hydrocarbons were detected in bacteria cultured on L.B. media or M9 minimal media. Compounds identified were those with a reverse search matching factor (RSI) > 800 and a probability > 90, allowing accurate matching of the library mass spectrum to that of the target compound. Complying to these parameters were two free fatty acids (FFAs) of carbon length 16 and 18 present in both the wild type and the *tolC*$^-$ mutant (Fig. 3.17): (Z)-9-hexadecenoic acid (palmitoleic acid), hexadecanoic acid (palmitic acid) and (9*Z*)-octadecenoic acid (oleic acid). These are among the most abundant (FFAs) detected in the bacterium (Fig. 3.16). An internal standard (d8–naphthalene, 10 μg/μl) was added to the extracts to allow quantification of compounds and direct comparison between samples. Peak areas corresponding to the C_{16} and C_{18} fatty acids indicate a higher level of these compounds in *tolC*$^-$ mutant cell pellets (Fig. 3.17). Although alkanes are not detected by GC-MS in *V. furnissii* there appears to be a relatively high level of FFAs, considerably more so in the *tolC*$^-$ knockout mutant. It is not clear at this stage if these are the compounds giving rise to increased Nile Red fluorescence but it is possible that FFAs are accumulating in greater quantities due to the lack of functioning TolC.

3.2.14 Quantification of intracellular free fatty acids

For accurate quantification of FFAs, the compounds were quantified as a percentage of the total biomass extracted (20 mg) by calculating the ratio of the target compound peak areas to the internal standard (10μg/ml d8-naphthalene) (methods 2.2). The concentration of these fatty acids is significantly higher in the *tolC*$^-$ mutant cell pellets during late exponential phase ($p<0.05$) (Fig. 3.18B). The combined levels of the three FFAs corresponds to more than 0.02% total biomass in the wild type and 0.04% in the mutant which represents a 250% increase. This increase in FFAs suggests either more FFAs are being produced or more FFAs are retained within the *tolC*$^-$ mutant cells. The levels of these compounds appear to remain consistent in the wild type between mid exponential and late exponential phase (Fig. 3.18A and 3.18B), however in the *tolC*$^-$ mutant cell pellets an increase in FFA levels can be noted.

3.2.15. Determining cellular lipid content of V. furnissii.

FFAs have been quantified using GC-MS but, for analysis of total lipid content and the percentage of lipid that is accounted for by FFAs, extracts were further analysed by GC-MS at Shell Global Solutions. Wild type *V. furnissii* and *tolC*$^-$ mutant cells were cultured in a minimal media (M9) and cells harvested at late exponential phase. Cell pellets were freeze dried, extracted into solvent as

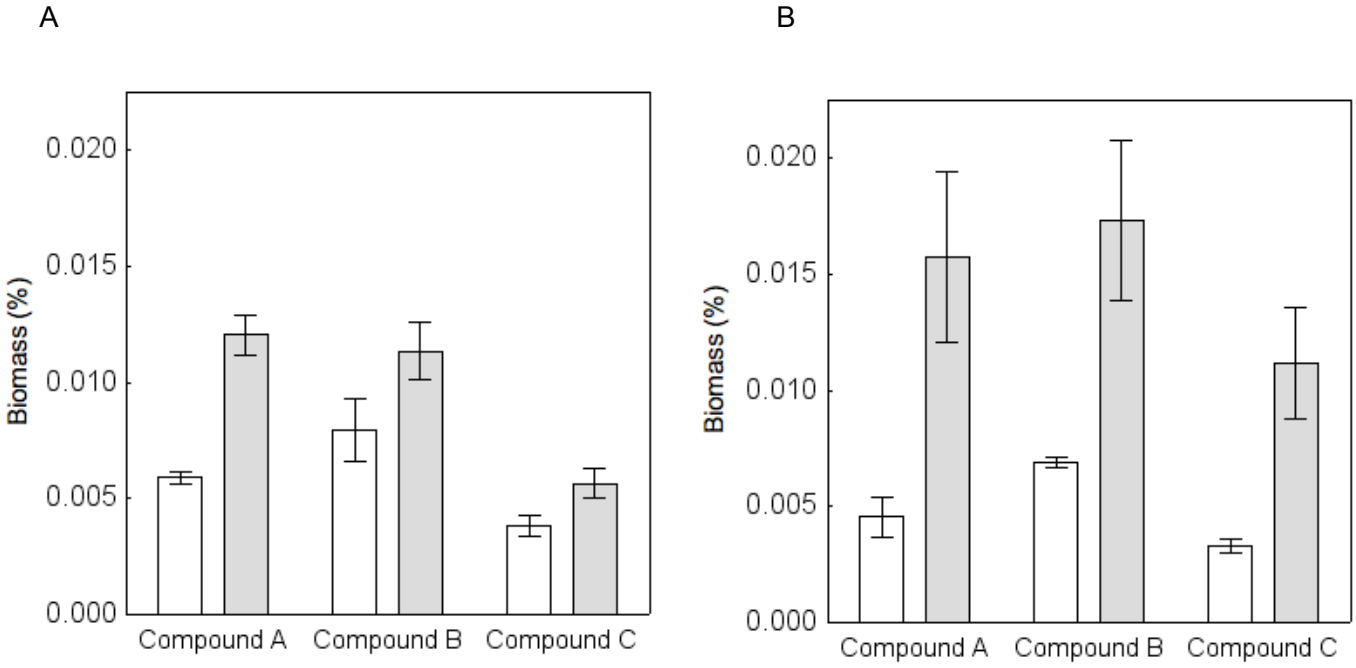

Figure 3.18. Concentration (cellular biomass %) of FFAs present in wild type and *tolC*$^{-}$ mutant cell pellets.

A: During early exponential phase (O.D. $_{600nm}$ 0.43 +/- 0.02) B: During late exponential phase (O.D. $_{600nm}$ 0.77 +/- 0.02) quantified from GC-MS peak areas relative to standard (methods). Wild type ▭, knockout mutant ▭ Compound A: (9Z)-hexadecenoic acid, compound B: hexadecanoic acid, compound C: (9Z)-octadecenoic acid (Fig. 3.17). Statistically significant increase of FFAs in knockout cell pellets during late exponential phase (P=0.0104 - two tailed, paired t-test). Combined biomass of three fatty acids in wild type: ~0.02, in *tolC*$^{-}$ mutant: ~0.05

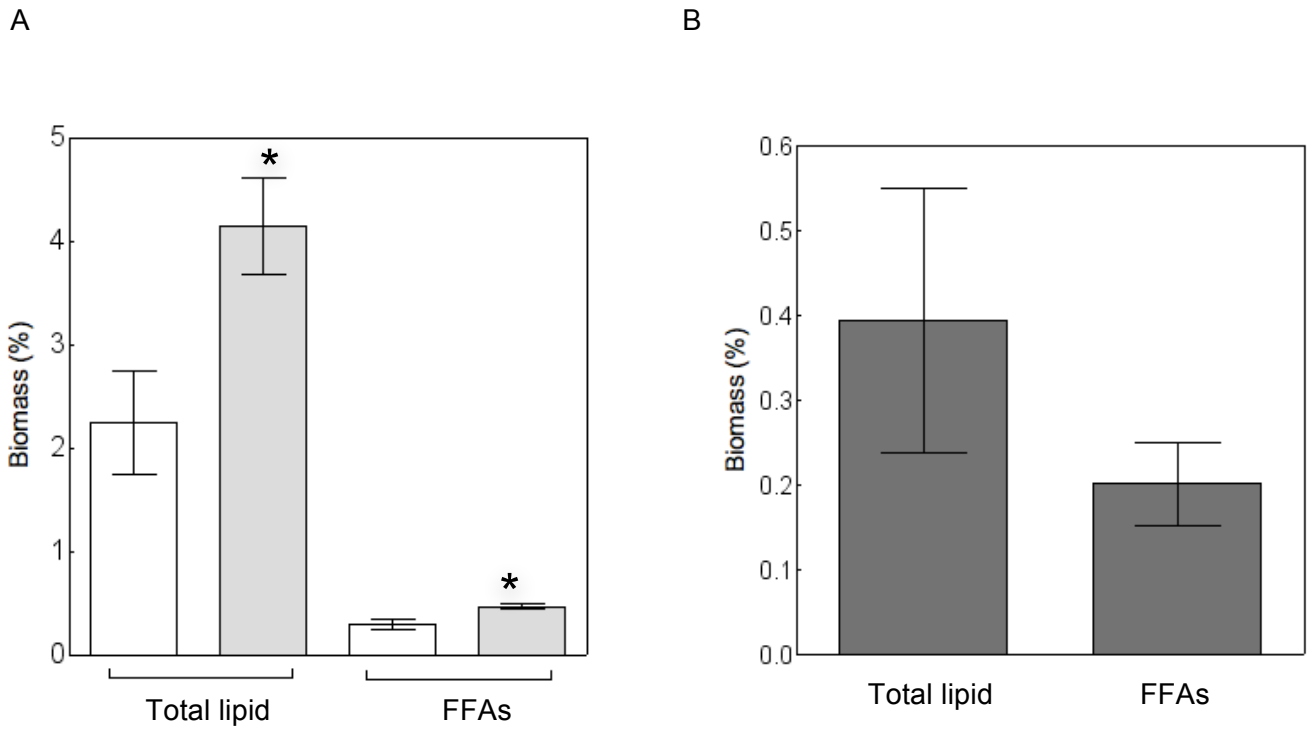

Figure 3.19. Quantification of total lipids and free fatty acids (cellular biomass %).

A: Late exponential phase extracts: Wild type ▭, knockout mutant ▭ Significant increase in total lipids and FFAs in knockout mutant (two tailed t-test, $p<0.05$) indicated by (*) n=3

B. Late exponential phase extracts in *E. coli* ▨.

Total lipids account for approximately ~0.4% in *E. coli* of total biomass, compared to ~ 2% in the wild type and ~4% in the *V. furnissii tolC*$^{-}$ mutant.

previously for analysis in section 3.2.13 and sample extracts analysed for quantification of FFAs, monoacylgycerides (MAGs), diacylglycerides (DAGs), triacylglycerides (TAGs) and sterols, (n=3). Of the total lipid analysed, DAGs accounted for over 85% in all samples and TAGs correspond to less than 1% of the lipid composition (appendices Table 8.2). Data presented quantifies FFAs separately from total lipids (Fig. 3.19A). Extracts from late exponential phase confirm a significant increase in the total lipids present in the mutant cells ($p<0.05$), corresponding to approximately 4% of the biomass, compared to approximately 2% in the wild type. Quantification of FFAs shows there is also a significant increase in cellular levels in the mutant ($p<0.05$), consistent with previous data. FFAs correspond to on average 0.4% of total biomass in the mutant and 0.2% in the wild type. The FFA biomass concentrations are considerably higher than those originally detected (Fig. 3.18B), suggesting this method of detection is more efficient. Notably, the ratios between wild type and *tolC*$^-$ mutant are consistent. These combined data suggest that there are greater quantities of fatty acids produced by the *tolC*$^-$ mutant, or alternatively that more are retained in the cells.

3.2.16. Comparison of lipid content in V. furnissii *and* E. coli *cells*

To determine the accuracy of the methods used and for comparison to *V. furnissii,* an *E. coli* control was also cultured to late exponential phase and cellular lipids were extracted and analysed. Results show that FFAs correspond to approximately 0.25% of cellular mass in the *E. coli* control (compared to 0.3% in *V. furnissii* wild type) (Fig. 3.19A and 3.19B). However, overall, the total of lipids analysed here represent approximately 0.4 % of biomass in *E. coli*, 5 fold less than wild type *V. furnissii* (~2%) (Fig. 3.19A and 3.19B). Total lipids in *E. coli* corresponds to approximately 0.5% of total biomass which is not as high as expected (Steen *et al.*, 2010), however the lipid quantification by Shell Global Solutions does not include membrane phospholipids which contribute a large percentage of cellular fats (Rock *et al.*, 1996). The ratio between FFAs and total lipid content is as expected within *E. coli*, notably *V. furnissii* has a higher lipid content up to 10 fold more in the *tolC*$^-$ mutant compared to *E. coli*.

3.2.17. Optimising a method for free fatty acid detection in spent media.

Previous data show an increase in FFA concentration, specifically C_{16} and C_{18}, in the *tolC*$^-$ mutant cells. It is reasonable to suggest, due to the nature of TolC as an export protein, that this increase may be due to retention of FFAs in the mutant cells. To investigate this hypothesis, a method was developed to extract lipid from filtered supernatants (methods 2.20). By spiking media with increasing concentrations of heptadecanoic acid (C_{17}), the method could be optimised and detectable levels of FFAs were established. Initial investigations were carried out in L.B. media and

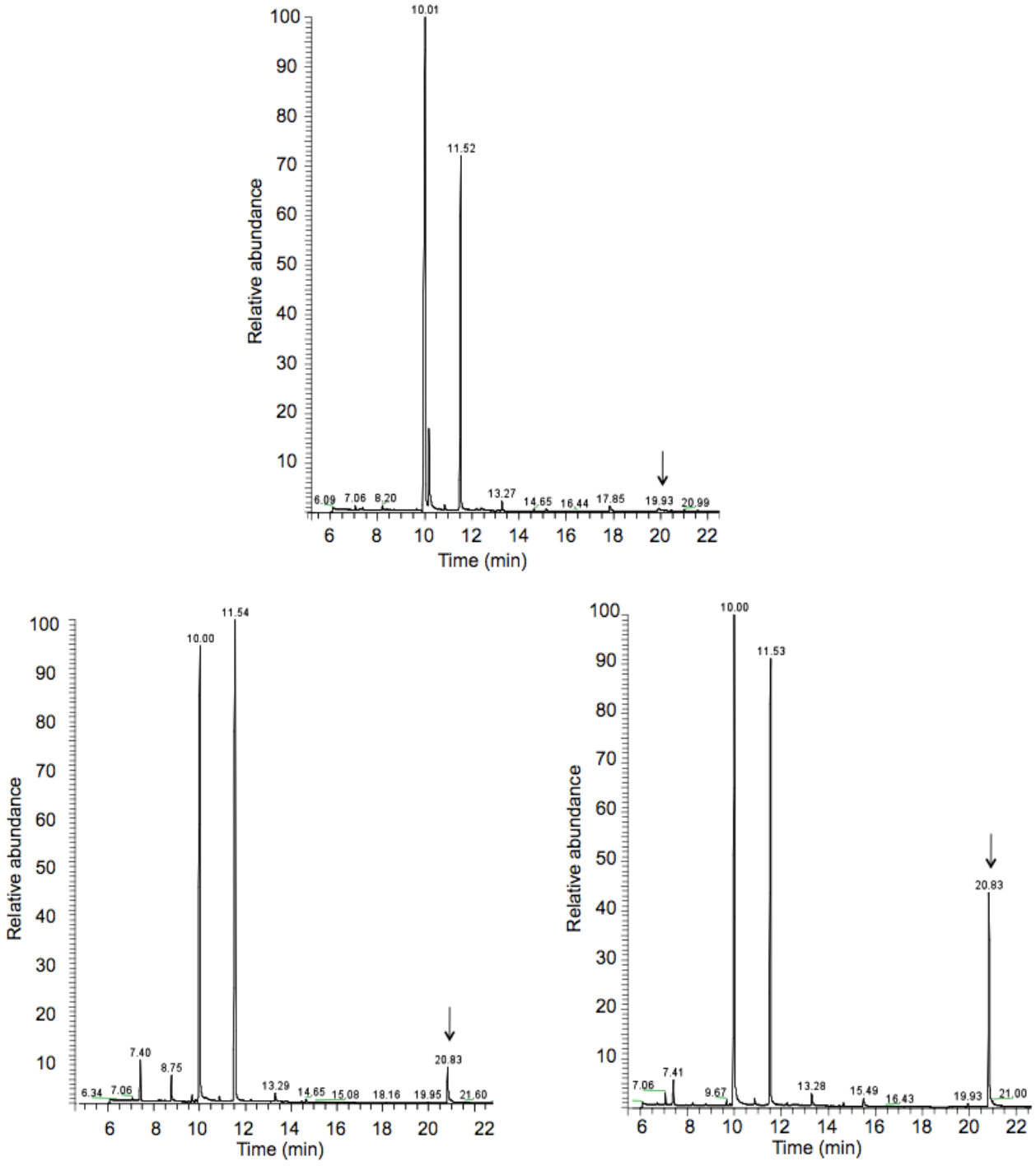

Figure 3.20 GC-MS traces of lipids extracted from minimal media M9 containing heptadecanoic acid (C_{17}). 20 ml of M9 minimal media was spiked with 0, 15 and 45 μg of C_{17}, corresponding peak detected at RT 20.83, indicated by arrow. Two peaks at RT 10.00 min and 11.5 min correspond to trigrlyceride peaks present in the media.

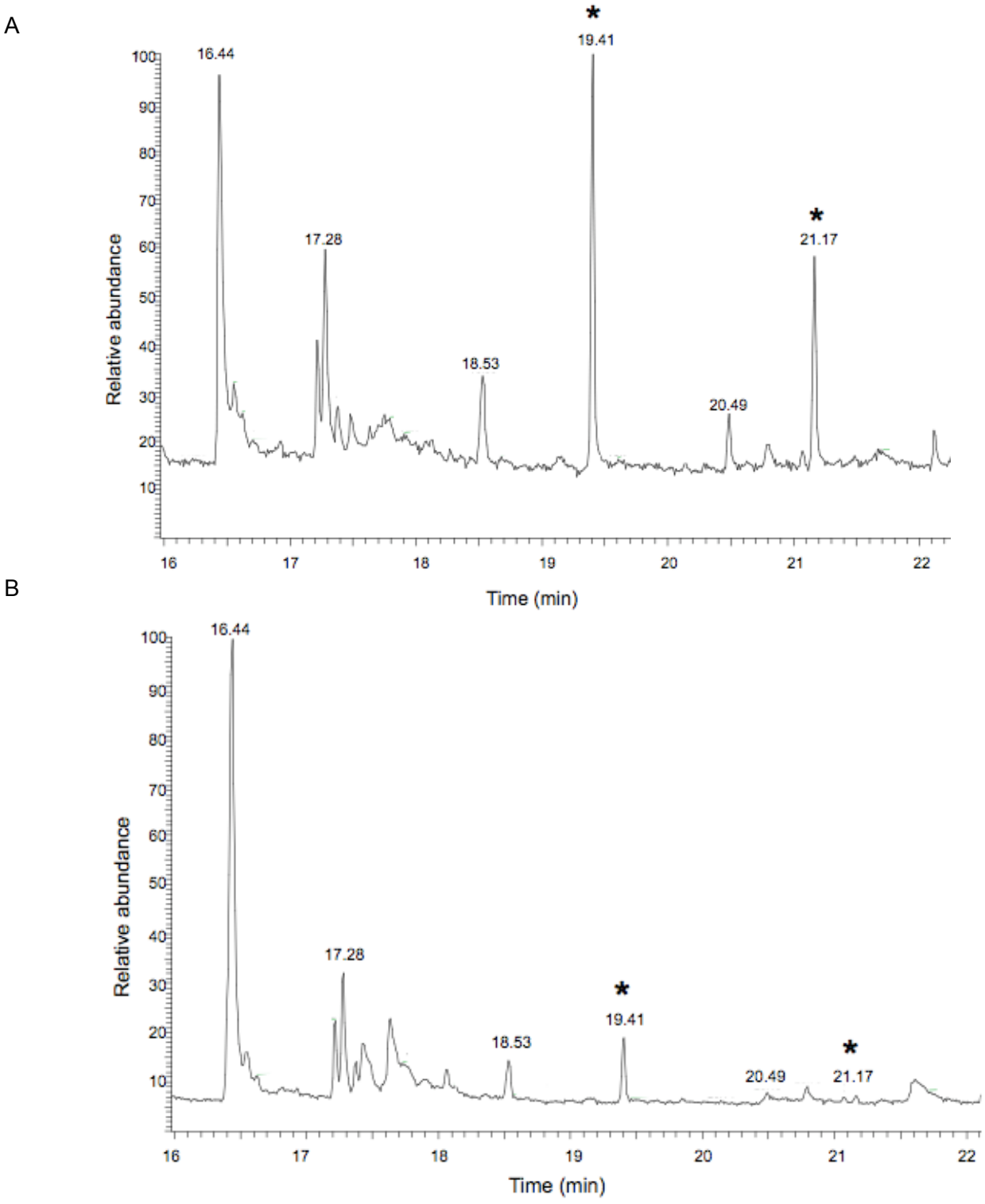

Figure 3.21. FFAs present in wild type (A) and *tolC*$^{-}$ mutant (B) supernatants determined by GC-MS

Trace displays typical result from stationary phase samples. Two peaks corresponding to fatty acids present indicated by (*) at RT 19.41 min and 21.17 min, both in greater abundance within the wild type.

Mass spectra	Compound structure

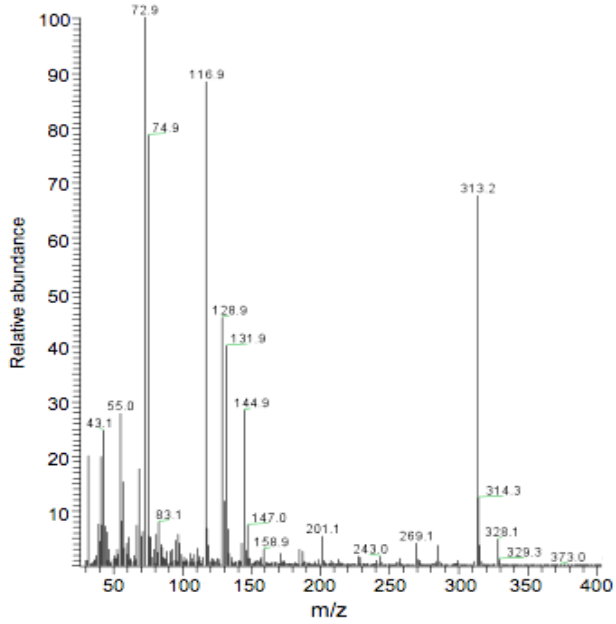

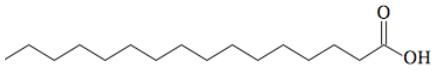

RT	Name	RSI	Probability
19.41	Hexadecanoic acid	898	92.21

Mass spectra	Compound structure

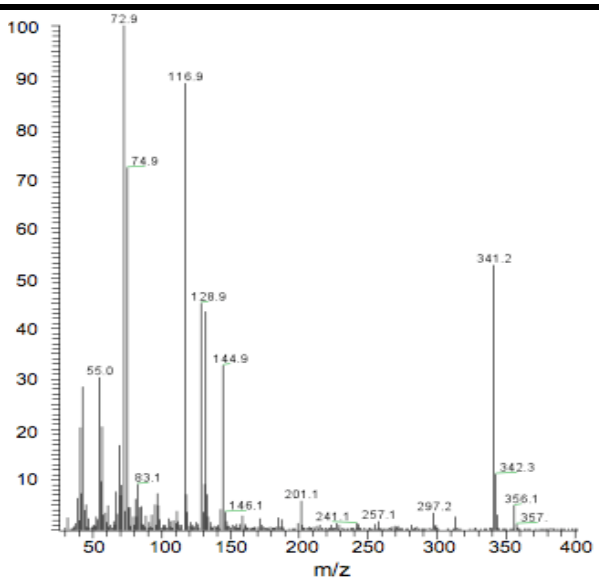

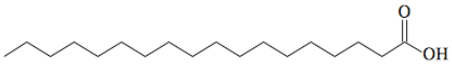

RT	Name	RSI	Probability
21.17	Octadecanoic acid	936	91.13

Figure 3.22. Mass spectrometry data of FFAs detected in *V. furnissii* supernatants.

C_{16} and C_{18} FFAs detected at RT 19.41 and 21.17 min respectively. RSI and probability values are indicated.

nutrient defined media however, the background detection levels made identification of specific fatty acids very difficult. Bacteria were therefore cultured in M9 minimal media for subsequent supernatant analysis. Initially, media containing 0, 15, and 45 μg of C_{17} mixed with chloroform and methanol and lipids were extracted using the adapted method from (Bligh and Dyer, 1959). Samples analysed on the GC-MS show a peak corresponding to heptadecanoic acid, of increasing abundance as concentration increases (Fig. 3.20), confirming that this method is effective at quantifying extracellular FFAs.

3.2.18. Investigating the secretion of free fatty acids

To determine the levels of FFAs secreted by the wild type and *tolC*$^-$ mutant, supernatants were filtered following centrifugation of wild type and mutant cultures at mid exponential, late exponential and stationary phase. Following the adapted protocol from Bligh and Dyer (1959), the lipids were extracted into the organic phase (20 ml) which was evaporated and re-suspended in 300 μl DCM containing 10 μg/ml of d8-napthalene for quantification. Extracts were collected from wild type and mutant supernatants (3 biological replicates and 3 technical replicates for both the wild type and mutant were obtained). Levels of secreted fatty acids were too low for detection in early and mid-exponential phase, however, during late exponential phase and stationary phase compounds could be accurately identified. It can be observed that there are two fatty acids eluting at RT 19.42 and 21.17 in wild type *V. furnissii* (Fig. 3.21A and Fig. 3.22). Parameters applied were the same as those for cell pellet compound analysis: RSI > 800 and probability > 90. Mass spectrometry determined the compounds as hexadecanoic acid and octadecanoic acid (Fig. 3.22). Hexadecanoic acid is present in both wild type and mutant supernatants, but significantly less appears to be secreted by the knockout mutant (Fig. 3.21A and 3.21B). Octadecanoic acid is present in the wild type supernatant and not detectable in the supernatant of the *tolC*$^-$ mutant suggesting it has not been secreted. Previous data show that more hexadecanoic acid accumulates within the *tolC*$^-$ mutant cell pellet (Fig. 3.17 and 3.18). Secreted octadecanoic acid however, is saturated, in contrast to the (9Z)-octadecenoic acid compound detected intracellularly (Fig. 3.22). The other peaks visible were not identifiable within the parameters (probability values <25), these peaks are also present within the control blank media samples. Analysis of extracellular quantities of FFAs show that less C_{16} and C_{18} FFAs are present in the *V. furnissii tolC*$^-$ mutant media suggesting a reduced quantity of FFAs is exported by the mutant.

3.2.19. Quantification of secreted C_{16} and C_{18} free fatty acids.

Concentrations of secreted hexadecanoic and octadecanoic acid were calculated from GC-MS traces using the internal standard d8-naphthalene, as for cellular fatty acid quantification (methods

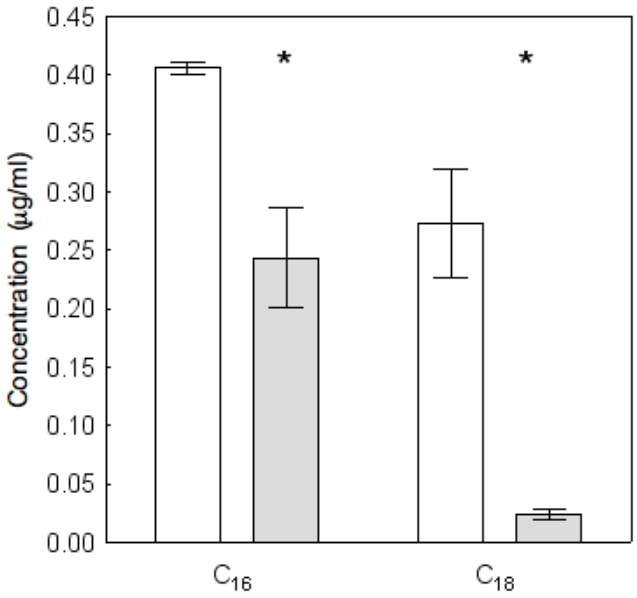

Figure 3.23. Concentration of compounds present in wild type and *tolC*⁻ mutant supernatants

Data obtained during stationary phase. C_{16}: hexadecanoic acid and C_{18}: octadecenoic acid fatty acids quantified from GC-MS results. Significant increase of FFAs in wild type supernatant, indicated by (*) (two tailed t-test, $p<0.05$). Wild type ▭, *tolC*⁻ mutant ▭

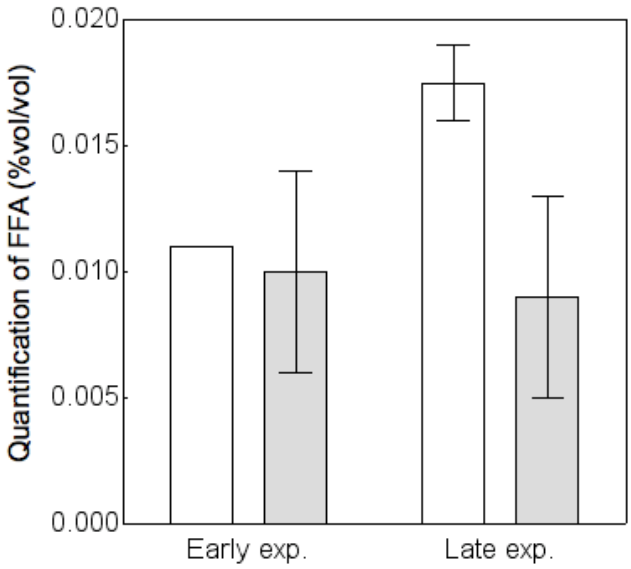

Figure 3.24. Quantification of total free fatty acids in wild type and *tolC*⁻ mutant supernatants.

Samples analysed at Shell Global Solutions using GC-MS. Decrease in the knockout mutant is not statistically significant, n=2, one tailed t-test $p<0.05$, late exp: $p = 0.09$.
Wild type ▭, *tolC*⁻ mutant ▭

2.22). There was a significant decrease in the presence of these two fatty acids in the knockout mutant supernatant compared to the wild type ($p<0.05$). Particularly octadecanoic acid, which was not detectable at all in two of the three knockout samples analysed (Fig. 3.23). To confirm levels of fatty acids and analyse total lipid secreted by the wild type and *tolC*$^-$ mutant, additional supernatant extracts were obtained and analysed by Shell Global Solutions (methods 2.21). Total secreted fats were quantified, including FFAs, mono acylgycerides (MAGs), diacylglycerides (DAGs), triacylglycerides (TAGs) and sterols however all detectable fats in the supernatant were solely identified as FFAs (Fig. 3.24). Levels of these FFAs are greater in the wild type supernatant, compared to the mutant during late exponential phase (Fig. 3.24), corresponding to previous supernatant analyses (Fig. 3.23). However, the difference is only statistically significant in original supernatant data obtained which can be explained by the fact that results from Shell Global Solution measure all FFAs and not those individually identified; hexadecanoic acid and octadecenoic acid. These data support the hypothesis that the difference in cellular FFA levels in the *tolC*$^-$ mutant is due to retention of these compounds as less are secreted by the mutant.

3.3. DISCUSSION

Data presented in this chapter exhibit evidence that an accumulation of FFAs occur in *V. furnissii* due to a lack of functioning TolC and has identified C_{16} and C_{18} fatty acids as previously unrecognised substrates of TolC in *Vibrio* species. Furthermore the role of RND efflux systems in antimicrobial resistance has been established in *V. furnissii.* RT-qPCR and the Nile Red fluorescence assay were used to confirm the lack of expression of TolC in the knockout mutant and the significant increase in expression within the overexpressor (Fig. 3.7 and 3.8). Data show that the complementation of the *tolC*$^-$ mutant with *tolC* resulted in phenotypic differences similar to that of the overexpressor as determined by Nile Red fluorescence. Both the complementation and overexpressor strains were unable to grow in defined nutrient or M9 minimal media and grew significantly slower than wild type in L.B. medium (appendices Fig. 8.3). Overexpression of efflux pumps has previously proven to have detrimental effects on bacterial cells (Ma *et al.*, 1995) and may explain why growth was inhibited in these strains. Unexpected phenotypes of TolC overexpressors were shown by antibiotic resistance analysis. Over expressing TolC alone did not confer antibiotic resistance, potentially due to the stress imposed on the cell as discussed by Piddock, 2006. Overexpression of a membrane protein in *E. coli,* maltoporin LamB, caused in a loss of membrane integrity altering the outer membrane composition and resulted in cell death (Reimann and Wolfe, 2011). Membrane stress imposed by TolC mutations has been a recent focus of the literature and is to be considered carefully when assessing phenotypic effects of manipulating TolC expression levels (Zgurskaya *et al.*, 2011).

The TolC overexpressor strain displayed a significant increase in resistance to all of the aminoglycosides (kanamycin, gentamicin, streptomycin and paromomycin) determined by IC_{50} data (Fig. 3.10B). Resistance to the aminoglycosides in this strain was not confirmed by MIC data (Table 3.1.) however, as previously discussed the overexpression of TolC leads to cellular stress and limited growth, which was observed during experimentation. Determining MIC involves culture growth in a 96 well plate with limited aeration and is the likely reason for the unexpected MIC results obtained. A significant increase in antimicrobial sensitivity was observed in the *tolC* knockout mutant to eight of the antibiotics investigated; presenting previously unknown antibiotic resistance data in an emerging pathogen and supporting the hypothesis that TolC confers antibiotic resistance (Table 3.1). In the *tolC* mutant reduced resistance to gentamicin, streptomycin, ampicillin, novobiocin, tetracycline, chloramphenicol, erythromycin and norfloxacin was observed, showing resistance is not restricted to any one group of antibiotics and confirming the broad range of TolC substrates. Notably wild type *V. furnissii* is particularly resistant to ampicillin, a result

observed in other *Vibrio* species (Sakazaki, 1992) (Fig. 3.10A). Increased resistance to all aminoglycosides in the overexpressor is an interesting result, as these compounds are more hydrophilic than other classes of antibiotics and are not as likely to cross the membrane. Resistance to aminoglycosides has not previously been associated with AcrAB-TolC, however they have been confirmed as AcrD substrates (a homologue of AcrB) (Magnet *et al.*, 2001, Elkins and Nikaido, 2002). These data imply that TolC interacts with an antiporter in *V. furnissii* other than the currently annotated AcrB (Lux *et al.*, 2011) and that this is possibly AcrD. Identifying antiporters interacting with TolC should be confirmed in order to fully understand the substrate export via TolC.

The Nile Red assay was used to determine random transposon mutants with increased cellular lipid content for use in this study. A significant difference in Nile Red fluorescence between the wild type and *tolC* mutant was confirmed by the Nile Red assay and confocal microscopy images however the nature of the fluorescence in individual cells was not expected (Fig. 3.12). Nile Red accumulation in *tolC*$^{-}$ mutants determined by fluorescence microscopy has not been previously described in bacteria, however recently in *E. coli*, mutations resulting in a lack of function of the outer membrane porin, LamB, displayed an increased in Nile Red fluorescence (Reimann and Wolfe, 2011). Within the *lamB* mutant, fluorescence microscopy showed nearly 100% of cells were fluorescing, similar results are observed in *tolC*$^{-}$ mutants within *V. furnissii* during stationery phase (Fig. 3.12). During the course of this project Nile Red was independently established as a substrate for TolC (Bohnert *et al.*, 2010). When analysing the wild type bacteria, expression of TolC would theoretically be indicated by efflux of Nile Red and therefore determined by a lack of fluorescence intensity. This does not explain the increase in the number of fluorescencing cells throughout wild type *V. furnissii* growth as expression of TolC, confirmed by RT-qPCR, does not correlate with the changes in fluorescence (i.e. TolC is more highly expressed during late exponential phase when Nile Red fluorescence is greater) (Fig 3.12 and Fig. 3.15). Furthermore, when analysing the mutant, lacking in TolC function, fluorescing and non-fluorescing cells can still be observed. This indicates that uptake of the Nile Red dye is growth phase dependent. Dividing wild type *V. furnissii* cells into fluorescing and non-fluorescing populations and re-culturing them resulted in bacteria returning to a mixed population (Fig. 3.14), supporting evidence that Nile Red uptake and consequential fluorescence is growth phase dependent.

Nile Red fluoresces in the presence of intracellular lipids which are detected in both the wild type and *tolC*$^{-}$ mutant. The increase in Nile Red fluorescence observed in the *tolC*$^{-}$ mutant correlates to an increase in fatty acid production, as determined by GC-MS (Fig. 3.18). However, the nature of Nile Red uptake and export has to be considered when using this assay to quantify lipids in the wild

type and *tolC*$^-$ mutant cells. The uptake of Nile Red is growth phase dependent and wild type *V. furnissii* cells export the fluorescent dye via TolC throughout cell growth. Notably, TolC expression in wild type *V. furnissii* peaks during late expoenential phase which is when the difference in Nile Red fluorescence between wild type and *tolC*$^-$ mutant is the greatest (Fig 3.11). Comparing lipid content in the wild type and *tolC*$^-$ mutant using this assay alone can therefore not be exact. These data support the hypothesis that Nile Red is a substrate of TolC and give an in depth analysis of how and when Nile Red export occurs. Given these findings, Nile Red fluorescence could not solely be attributed to differences in cellular lipid content in wild type and *tolC*$^-$ mutant cells. Further experimentation was therefore required to give conclusive evidence of lipid accumulation in mutant cells.

Analysis obtained from Shell Global Solutions shows that the composition of intracellular lipids within *V. furnissii* is largely composed of DAGs (>85%) (appendices Table 8.2) and an increase in intracellular FFAs acids was observed in the *tolC*$^-$ mutant. GC-MS analysis carried out within this study showed these compounds to be octadecenoic acid (18:1), hexadecenoic acid (16:1) and hexadecanoic acid (16:0) (Fig. 3.18). Notably unsaturated fatty acids (octadecenoic acid (18:1), and hexadecenoic acid (16:1)) are also reported to give rise to high levels of Nile Red fluorescence (Greenspan and Fowler, 1985). Previous reports have shown that in *V. furnissii* M1, up to 60% of cell biomass corresponds to straight chain alkanes (Park *et al.*, 2005). However, there is no evidence of genes required for the production of alkanes in the recently published genome of *V. furnissii* NCTC 11218 (Lux *et al.*, 2011), supporting our data that have experimentally determined a lack of such compounds (Fig. 3.16). However, within *V. furnissii,* FFAs are produced in large quantities compared to *E. coli* (Fig. 3.19). Overall the lipid content (MAGS, DAGS, TAGS, sterols and FFAs) in wild type *V. furnissii* is approximately 5 fold greater than *E. coli*, and up to 10 fold greater than *E. coli* in the *V. furnissii tolC*$^-$ mutant (Fig. 3.19). The ratios of octadecenoic acid (18:1), hexadecenoic acid (16:1) and hexadecanoic acid (16:0) in the wild type and *tolC*$^-$ mutant remained consistent. Furthermore, FFA composition in *V. furnissii* is similar to that in *E. coli* (Keweloh *et al.*, 1991) and other *Vibrio* species (Oliver and Colwell, 1973), confirming the consistency of the data.

The octadecenoic acid (18:1), hexadecenoic acid (16:1) and hexadecanoic acid (16:0) compounds produced by *V. furnissii* are relevant to the study of bio-fuels and engineering cells to increase production of these compounds has been carried out in *E. coli* (Lu *et al.*, 2008). It is worth considering that although *V. furnissii* does not appear to produce hydrocarbons*,* this study shows that this bacterium produces considerably more FFAs than does *E. coli* and could ultimately be engineered in the same way to potentially produce significantly greater quantities. Furthermore,

TolC should be recognized as a potential target for overexpression to increase export of these compounds, however, results here have supported previous data that overexpression of this protein has consuqeuntial effects on cellular growth.

A significant advantage of investigating *V. furnissii* for FFA production is the capacity for wild type *V. furnissii* to export these compounds. GC-MS analysis (undertaken at Shell Global Solutions) shows that FFAs comprise 100% of exported fats. Investigation into the export of FFAs by GC-MS shows that wild type supernatants contain significantly more saturated fatty acids in contrast to the *tolC*$^{-}$ mutant; hexadecanoic (C_{16}) and octadecanoic acid (C_{18}) (Fig. 3.21 and 3.22). These are among the most abundant FFAs, comprising 70% of total FFAs produced (Keweloh *et al.*, 1991). It should be noted that the extracellular C_{16} and C_{18} fatty acids are saturated and the unsaturated C_{16} and C_{18} compounds are only present intracellularly. The reason why only saturated fatty acids are traceable in the supernatant is unknown, but this adaptation may be due to the steric hindrance when exporting saturated fatty acids. Efflux of fatty acids and other long carbon chain compounds has been shown in *D. desulfuricans* and *C. pasteurianum* (Davis, 1968, Bagaeva and Zinurova, 2004) and C_{16} compounds have recently been observed in the supernatants of *Alcanivorax* species (Manilla-Pérez *et al.*, 2010). The ability for trimeric membrane pumps to export hydrophobic agents such as fatty acids and solvents has also been shown (Ramos *et al.*, 2002). These data support evidence presented in this study that C_{16} and C_{18} FFAs are exported by bacterial cells and that this occurs via TolC. The reason for bacteria to export energetically expensive compounds such as FFAs is unknown. Reports have suggested that *P. fluorescens* secretes fatty acids for cell adhesion to surfaces (Nikolaev *et al.*, 2001) and compounds such as isoprene have been suggested to work as secondary metabolites in cell to cell signalling (Hastings and Greenberg, 1999).

Free fatty acids are biologically significant and synthesis of these compounds is comprehensively studied, particularly hexadecanoic acid biosnthesis (O'Leary, 1962). Unsaturated fatty acids (UFAs) octadecenoic and hexadecenoic acids produced by *V. furnissii,* are linked to membrane fluidity and transmembrane signalling (Aguilar and De Mendoza, 2006). Data show that when membranes become more rigid, bacteria adapt causing an increase in UFAs returning membrane fluidity (Mansilla and de Mendoza, 2005). It is worth considering that disruption to the membrane by removing the function of TolC could potentially be linked to the bacteria producing larger amounts of fatty acids. However, data presented here support the hypothesis that the difference in cellular concentration is due to secretion via TolC. Experimental results show that the overall increase in total lipids and FFAs in the *tolC*$^{-}$ mutant is only significant during late exponential phase. This corresponds with the increase of relative TolC expression during this growth phase determined by

RT-qPCR (Fig. 3.15). This confirms that during late exponential phase, the wild type is able to export FFAs via TolC, resulting in a relatively constant level within the cell. Within the mutant this is not possible resulting in internal FFA accumulation.

CHAPTER 4 - MUTATION IN *TOLC* DISRUPTS QUORUM SENSING REGULATION.

4.1 INTRODUCTION

Quorum sensing is a process by which bacteria secrete signalling compounds in order to communicate, coordinate gene expression and synchronise cellular activity. Membrane diffusion has been the accepted method of signalling compound export (Kaplan and Greenberg, 1985), however the additional requirement of active efflux, particularly via RND export systems has been suggested (Evans *et al.*, 1998, Pearson *et al.*, 1999). Furthermore, this connection between efflux proteins and quorum sensing is thought to be due to shared regulatory pathways associated with virulence factor expression e.g. *toxT* (Higgins and DiRita, 1994, Evans *et al.*, 1998, Bina *et al.*, 2008). Data presented in the previous chapter showed that TolC has the potential to export naturally synthesised fatty acids and that this is altered throughout growth phase. Quorum signalling is a growth dependant process which involves the secretion of biosynthetic molecules. RND efflux and quorum sensing are systems widely studied in *Vibrio* species (Kelly *et al.*, 2009, Bina *et al.*, 2008) but not yet in *V. furnissii.* The *tolC*$^{-}$ mutants in *V. furnissii* will be used in this study to determine if TolC is involved in quorum sensing, either as an exporter of signalling compounds or via a connection to regulatory pathways controlling signalling molecule synthesis and detection.

Homoserine lactones (HSLs) are the most common quorum sensing compounds utilised by bacteria, however the genes required for HSL production are not present in *V. cholerae* (Heidelberg *et al.*, 2000). More recent literature shows that *Vibrio* species more commonly produce autoinducer molecules, such as AI-2 ((2*S*,4*S*)-2-methyl-2,3,3,4 tetrahydroxytetrahydrofuran borate) (Chen *et al.*, 2002) and a number of structural variances on CAI-1 ((*S*)-3-hydroxytridecan-4-one) (Higgins *et al.*, 2007, Ng *et al.*, 2011) (Table 4.1). *V, harveyi* has been shown to produce three types of autoinducer: HAI-1, AI-2 and CAI-1, however the number of autoinducer molecules used by *Vibrio* species varies. Of 25 *Vibrio* species, 20 have shown AI-2 activiy, 11 show AHL activity but only 6 show CAI-1 activiy (Yang *et al.,* 2011). *V. furnissii* is among the six strains that appear able to produce all three types of autoinducers. CAI-1 is the least commonly produced and research has recently shown that there are a number of structural variances on this C_{13} compound (Ng *et al.*, 2011). The synthesis and detection of CAI-1 type structures has been analysed in *V. cholerae* and *V. harveyi* and the latter is more selective in the signalling structures it uses for cell-cell communication (Ng *et al.*, 2011). The reason for chemically distinct signalling molecules is thought to restrict interspecies communication but there are some compounds which are detected by multiple species, primarily AI-2. AI-2 is synthesised and detected by a large number of Gram-

positive and Gram-negative bacteria and is thought to be a "universal signalling molecule" (Schauder *et al.*, 2001, Xavier and Bassler, 2003). The concept of varying autoinducer (AI) specificity needs to be investigated in order to correlate species with virulence factors regulated by quorum sensing, in particular, the ability to form biofilms, toxin secretion and motility. Although there is evidence that *V. furnissii* can produce three types of autoinducers (Yang *et al.,* 2011), the structure of signalling compounds utilised by this bacteria have not been determined. Investigating these compound structures and the genes involved in their synthesis and detection will add to the expanding knowledge of how bacteria distinguish between these molecules.

Autoinducers are detected by neighbouring cells and a regulatory pathway is consequently triggered. The detection of HAI-1 by a receptor regulates the Lux pathway and ultimately bioluminescence in *V. harveyi.* Expression of the luciferase operon occurs at high cell densities when LuxR is expressed (Lilley and Bassler, 2000). However, in *V. cholerae* the LuxR homologue (HapR) (Jobling and Holmes, 1997) is a negative regulator of virulence factors (Miller *et al.*, 2002) (Fig 4.1). Therefore it is during low cell densities that virulence factors are expressed; this negative regulation of virulence factors by LuxR homologues has also been identified in *V. vulnificus* (Shao *et al.*, 2011). The reasons for increased expression of virulence factors during lower cell densities are unclear but a speculated model in *V. cholerae* presented by Zhu *et al* (2002) suggests that during initial colonization of hosts, when cell density is lower, LuxO represses HapR and allows expression of virulence factors.

There are three autoinducer detection pathways studied in *Vibrio* species (Bassler, 2002). CAI-1 (and other CAI type compounds) are produced by one of the systems, in which CqsS is the synthase and CqsA is the sensor (Kelly *et al.*, 2009) (Fig 4.1). The variances in CAI-1 structures have not been widely researched although it has been determined recently that *V. cholerae* and *V. harveyi* have different affinities for each of the CAI-1 structures based on structural differences in CqsS and CqsA (Ng *et al.*, 2011). In addition, amino-CAI-1 structures have recently been determined as CAI-1 precursors (Table 4.1) (Ng *et al.*, 2011). It is via a second system that AI-2 is produced, in which LuxS is the synthase and LuxP and LuxQ work together as sensors (Surette *et al.*, 1999, Chen *et al.*, 2002) (Fig 4.1). In addition the *V. harveyi* autoinducer, only produced by *V. harveyi* and close relative *V. parahaemolyticus* (Waters and Bassler, 2006), is synthesised by LuxL and LuxM and detected by LuxN (Bassler *et al.*, 1993).

Signalling mechanisms and signalling molecule production within *V. furnissii* has not yet been investigated, however Ng *et al* (2011) suggest CAI-1 type compounds could be produced by this

bacterium. LuxR was not annotated within the *V. furnissii* NCTC 11218 genome (Lux *et al.*, 2011), however preliminary investigation confirms the presence of a LuxR homologue; OpaR. OpaR shows 81% identity to its closest associated protein SmcR which is the LuxR homolgue in *V. vulnificus* (Kim *et al.*, 2003). Confirmation of CAI-1 type compound synthesis by this bacterium and its regulation by the CqsS/CqsA and Lux pathway is to be determined particularly the consequential affect of the *tolC* mutation on CAI-1 secretion.

Research suggests the need for a transport system for export of autoinducers although little has been established. Taking into account the emerging structural variances, it should not be assumed that all signalling compounds diffuse freely across the cellular membrane as shown in *V. harveyi* (Kaplan and Greenberg, 1985). There is evidence to support the hypothesis that efflux systems are required to export signalling compounds, particularly more polar autoinducers e.g. AI-2 secretion within *S.* Typhimurium, (Kamaraju *et al.*, 2011), Furthermore, The MexAB-OprM RND efflux system is associated with signalling molecule secretion in *P. aeruginosa* (Poole and Srikumar, 2001). Piddock (2006) discusses the connection between overexpression of efflux pump MexAB-OprM and an increase in signalling molecule concentration, which ultimately reduces virulence factor expression. Hypothetically the connection between TolC and virulence gene expression is linked by quorum sensing and directly affects or is affected by the efflux of signalling compounds. This study investigates the potential role for TolC in secretion of these naturally produced compounds within *V. furnissii*. Given the relevance of quorum sensing within *Vibrio* species, the *V. furnissii tolC*$^{-}$ mutants are a paradigm for the investigation of quorum derived compound synthesis and secretion via TolC.

Name	Structure	Chemical name
CAI-1	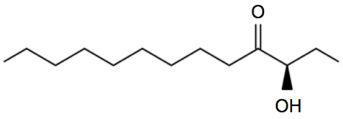	(*S*)-3-hydroxytridecan-4-one
Am-CAI-1	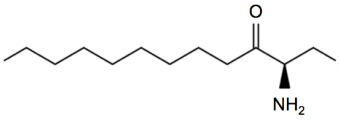	(*S*)-3-aminotridecan-4-one
Ea-CAI-1	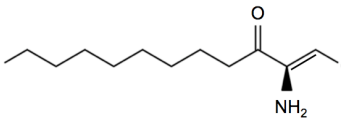	3-aminotridec-2-en-4-one
C8-CAI-1	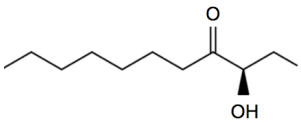	(*S*)-3-hydroxydecan-4-one
Am-C8-CAI-1	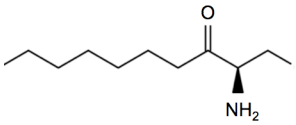	(*S*)-3-aminoundecan-4-one
Ea-C8-CAI-1	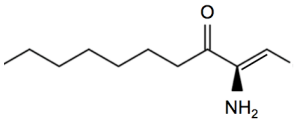	(*Z*)-3-aminoundec-2-en-4-one

Table 4.1 Structural variants on the CAI-1 autoinducer compound.

Strutures obtained from (Ng *et al.*, 2011).

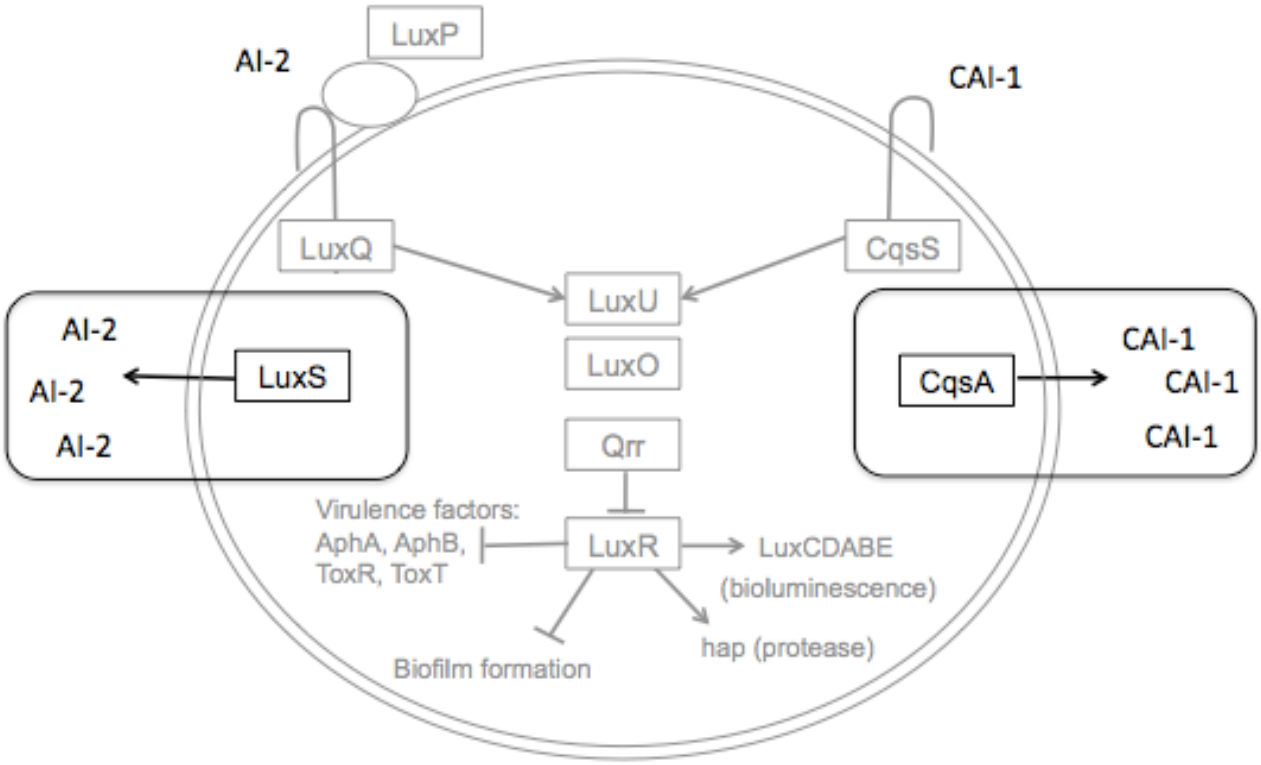

Figure 4.1. Diagram displaying autoinducer synthesis and detection in *V. cholerae*.

CAI-1 and AI-2 synthesis (CqsA and LuxS respectively) and detection (LuxPQ and CqsS respectively) with LuxU and response regulator LuxO. When autoinducer concentration is high, LuxR is expressed, positively and negatively regulating a wide range of factors in various organisms. At low cell densities LuxO activates expression of quorum regulatory RNA (Qrr), repressing LuxR expression. AI-2 and CAI-1 export across the double membrane is highlighted displaying currently understood method of diffusion.

4.2. RESULTS

4.2.1 Identifying the Lux pathway regulatory systems within V. furnissii*.*

To establish the presence of a quorum sensing pathway in *V. furnissii*, the amino acid sequences of proteins in the Lux pathway in *V. harveyi* were aligned to *V. furnissii* using the basic local alignment search tool (BLASTp). The quorum sensing response regulator (LuxO) is present within *V. furnissii* as well as LuxU and LuxR (Table 4.2). The LuxU amino acid sequence in *V. furnissii* has a low identity to the LuxU protein in *V. harveyi* (51%) compared to the other Lux proteins. However, like *V. harveyi* the *luxU* gene (vfu_A02580) is adjacent to *luxO* within the genome (vfu_A02581) suggesting that despite a low amino acid sequence identity, this protein is part of the Lux system in *V. furnissii.* CqsA and LuxS, required for CAI-1 synthesis and AI-2 synthesis respectively, are conserved in *V. furnissii,* however proteins required for HAI-1 signalling (Lux LMN) or bioluminescence (LuxCDABE) are absent. CqsS and LuxP/Q, required for CAI-1 and AI-2 detection respectively, are also conserved however identity to *V. harveyi* detector proteins is also relatively low (53%, 65% and 48%). Notably, the *V. furnissii* quorum sensing genes are located on both chromosomes; the regulator gene is present on chromosome 1 and genes involved in the CAI-1 pathway on chromosome 2 (Table 4.2). These data show that genes for AI-2 and CAI-1 synthesis and detection are present in *V. furnissii* and that the synthesis genes in *V. furnissii* and *V. harveyi* show an identity of 60% (CqsA) and 84% (LuxS).

4.2.2 Comparing similarity of the V. furnissii *CAI-1 regulatory system to other* Vibrio *species.*

The genes encoding CAI-1 synthase protein (CqsA) and sensory kinase (CqsS) are present in *V. furnissii.* A number of CAI-1 type compounds are synthesised by CqsA in *Vibrio* species and CAI-1 selectivity varies between *Vibrio* species. CAI-1 synthesis and detection within *V. harveyi* is more selective compared to *V. cholerae.* To investigate CAI-1 selectivity in *V. furnissii,* phylogenetic analysis was used to compare the amino acid sequences of CAI-1 synthase and sensory kinase in *V. cholerae* or *V. harveyi.* Amino acid sequences of CqsA and CqsS in *Vibrio* species were aligned using BLASTp and *Vibrio* species showing similarity >50% were analysed using the multiple alignment tool MUSCLE. Results were curated using G Blocks to eliminate poorly aligned positions. Phylogentic trees were created using PhyML and branch lengths displayed. CqsA, (CAI-1 synthase) in *V. furnissii* shows greatest similarity to *V. anguillarum*, *V. cholerae* and *V. mimicus* (>70% identity) and shows least similarity to *V. harveyi* (60% identitiy) (Fig 4.2A). CqsS shows greatest similarity to *V. anguilarum*, *V. ordalii* and *V. metchnikovi*, however in *V. anguillarum* and *V. ordailii* CqsS shows sequence similarity to the detector protein, LuxN (Fig 4.2B). *V. furnissii* CqsA and CqsS sequences show least similarity to *V. harveyi* proteins (60% and 53% identity respectively). Compared to *V. harveyi* both CqsA and CqsS in *V. furnissii* show greater similarity to

	Protein	Gene		Amino acid	
		V. harveyi	*V. furnissii*	Coverage	identity
	LuxU	har_02958	vfu_A02580	92%	51%
	LuxR	har_00157	vfu_A00883	99%	78%
Regulator	LuxO	har_02959	vfu_A02581	97%	87%
AI-2 detection	LuxP	har_05351	vfu_B00359	99%	65%
	LuxQ	har_05352	vfu_B00358	99%	48%
AI-2 synthesis	LuxS	har_03484	vfu_A02965	99%	84%
CAI-1 detection	CqsS	har_06089	vfu_B00270	100%	53%
CAI-1 synthesis	CqsA	har_06088	vfu_B00269	99%	60%
HAI-1 detection	LuxN	har_02766	N/A	N/A	N/A
HAI-1 synthesis	LuxLM	har_02765	N/A	N/A	N/A
Luciferase operon	LuxCDABE	har_06244 - 06240	N/A	N/A	N/A

Table 4.2. Amino acid sequence coverage and identity (%) of quorum sensing related gene products in *V. furnissii* and *V. harveyi* (ATCC BAA-1116).

HAI-1 synthase, HAI-1 sensory kinase and the luciferase operon are not present in *V. furnissii.* Gene ID numbers starting “A” indicates gene location on chromosome 1,and “B” indicates location on chromosome 2. N/A displays no sequence similarity between amino acid sequences.

A

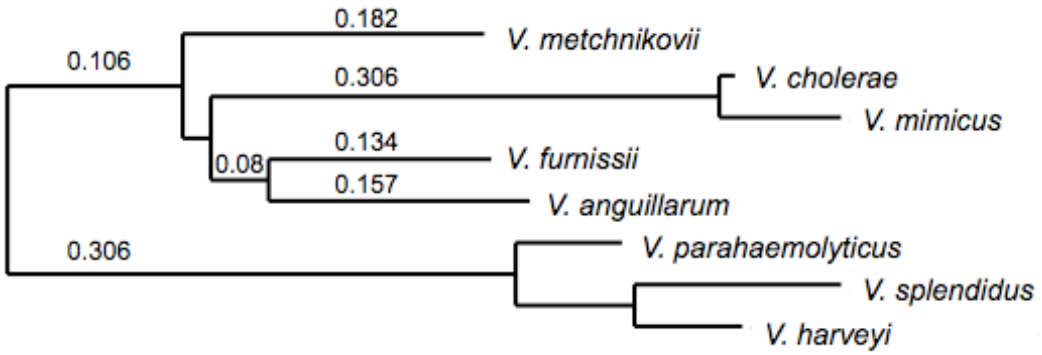

B

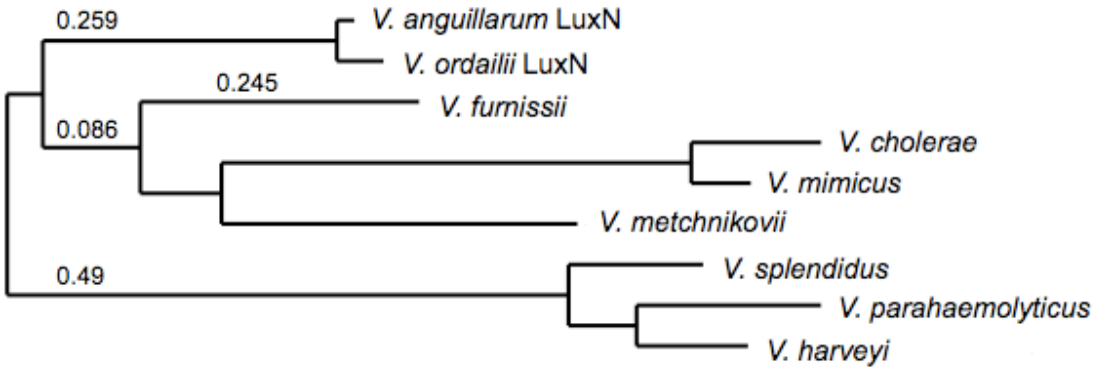

Figure 4.2. Phylogeny trees based on the protein alignment of the CqsA and CqsS members of *Vibrio* species.

A: CqsA, CAI-1 synthesiser shows greatest identity to *V. anguillarum* (77%) *and V. cholerae* (75%), least similar to *V. harevyi* (60% identity), determined by BLASTp.

B: CqsS, CAI-1 detector shows greatest identity to *V. anguillarum* (LuxN) (65%). Identity to *V. cholerae* (58%). least similar to *V. harveyi* (53%), determined by BLASTp.

V. cholerae (75% and 58% identity respectively). This suggests CAI-1 synthesis and detection has broader specificity, similar to that of *V. cholerae.*

4.2.3. Investigating the relationship between bacterial growth and quorum sensing

In order to investigate an association between TolC and cell-cell signalling, the stationary phase $O.D._{600nm}$ in wild type and *tolC*$^-$ mutant were compared. To determine when wild type and *tolC*$^-$ mutant enter stationary phase, bacteria were cultured in M9 minimal media and the $O.D._{600nm}$ was measured ar regular time intervals. Glucose (20 mM) was used as a carbon source which has been shown to optimise autoinducer production in *S.* Typhimurium and *P. aeruginosa* (Surette *et al.*, 1999, Ortori *et al.*, 2011). The *tolC*$^-$ mutant grows to a lower optical density compared to the wild type; wild type $O.D._{600nm}$ reached 2.4, and the *tolC*$^-$ only reached 2.0. Wild type entered stationary phase at approximately 9 h compared to the mutant which entered stationary phase at approximately 6 h (Fig 4.3). The growth rates, determined by the hill slope values (following sigmoidal dose-response analysis on linear data using Prism) showed no significant difference. To investigate how the wild type and *tolC*$^-$ mutant interact, wild type and knockout mutant were both grown on an L.B. agar plate, inoculated with 2 μl of over night cultures in stationary phase.

4.2.4. Establishing expression changes in the Lux pathway within the tolC$^-$ *mutant.*

To determine the impact of the *tolC* mutation on quorum sensing, differential expression of proteins in the Lux pathway was analysed. Microarray data were obtained for wild type *V. furnissii* and *tolC*$^-$ mutant following RNA extraction from late exponential phase cultures (n=3) and cDNA was synthesised and sent to Nottingham Arabidopsis Stock Centre (NASC) for chip hybridisation. The wild type and *tolC*$^-$ mutant transcriptomes were analysed using GeneSpring GX v11.5 software to allow comparison of individual gene expression (methods 2.26). Full analysis of the transcriptome is discussed in the following chapter, however expression data regarding the Lux operon has been analysed here in detail to support related experimental data. Within the *tolC*$^-$ mutant, significant increases in expression were noted in LuxU and response regulator LuxO and a decrease in LuxR expression (negatively regulated by LuxO) confirming that the *tolC*$^-$ mutation has a consequential affect on this quorum regulatory pathway (Table 4.3). LuxP and LuxQ, specifically involved in AI-2 detection do not show statistical differential expression. Notably, expression of the CAI-1 detector (CqsS) is significantly increased in the mutant (1.42 fold) and CAI-1 synthesiser (CqsA) is decreased in the mutant (2.9 fold). The decreased expression of CqsA is a comparatively large fold change although it is not statistically significant ($p<0.05$).

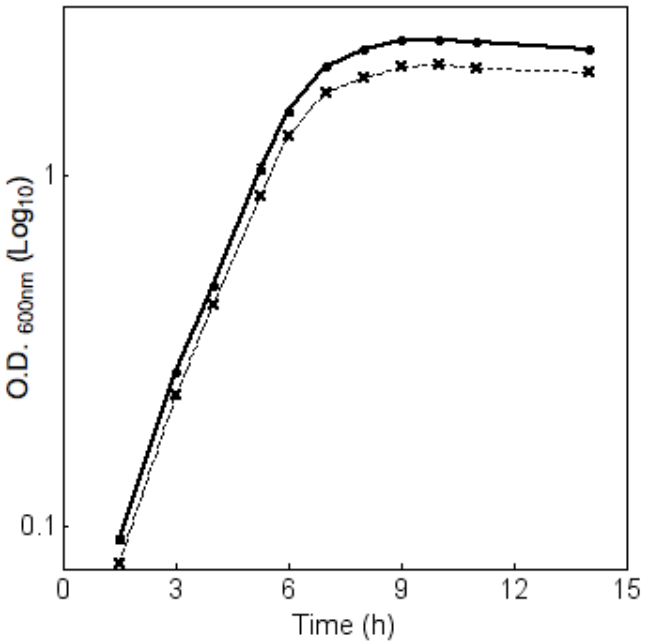

Figure 4.3. Growth curves of wild type and *tolC*$^{-}$ mutant bacteria.

Growth curves of bacteria cultured in M9 minmal media (Log_{10}). Growth rates do not differ between wild type and *tolC*$^{-}$ mutant however stationary phase optical density is lower in the mutant. Statistical analysis of 5 stationary phase growth points show this difference is significant (two tailed t-test $p<0.05$) n=3. Wild type ——, tolC- mutant ------

Protein	Gene in *V. furnissii*	Change in expression in *tolC*$^{-}$		p value
CqsA	vfu_B00269	2.9	down	0.09
CqsS	vfu_B00270	1.42	up	0.010
LuxP	vfu_B00359	1.01	down	0.92
LuxQ	vfu_B00358	1.40	up	0.15
LuxS	vfu_A02965	1.48	up	0.001
LuxU	vfu_A02580	1.34	up	0.011
LuxO	vfu_A02581	1.37	up	0.006
LuxR	vfu_A00883	1.47	down	0.001

Table 4.3. Differential expression of proteins involved in the Lux pathway in wild type and *tolC*$^{-}$ mutant

Data determined by analysis of microarray data. Those entities with significant differential expression (two tailed t-test, $p<0.05$) are highlighted in grey.

4.2.5. Detecting secreted signalling compounds by GC-MS.

There is bioinformatic and experimental evidence supporting the hypothesis that quorum sensing molecules are secreted by *V. furnissii* and that TolC is associated with this process. During analysis of hydrocarbon production in chapter 1, GC-MS data identified compounds containing long hydrocarbon chains (Fig 3.22). Some autoinducer compounds are comprised of hydrocarbon chains (e.g. CAI-1 has a C_{13} chain) and may therefore be detected by GC-MS. Wild type and *tolC*$^-$ mutant were cultured on M9 minimal media containing 20 mM glucose to late exponential phase (O.D. $_{600nm}$ 2.1). Supernatants were prepared and extraction of hydrocarbons was performed. Following sample derivitisation, GC-MS analysis was carried out on supernatant extracts in triplicate (methods 2.21). Results did not show any compounds resembling signalling compounds, however an indole stucture was detected within wild type supernatants but not in *tolC*$^-$ mutant supernatants (Fig 4.4). The indole derivative may be a genuine secreted product however, it's presence was not consistent and the concentration varied significantly between wild type samples making identification of the structure difficult. This could be due to its secretion at very specific growth points or it could be a contaminant.

Samples were subsequently sent for analysis at Shell Global Solutions, where derivitised and non-derivitised samples were tested to eliminate any products resulting from this process. The indole product was not detected and no HSLs or AIs were identified. Given the expected low concentrations of AI compounds, it is likely GC-MS is not a sensitive enough method. A peak at RT 23.78 mins was detected in wild type supernatant extracts but was absent in *tolC*$^-$ mutant supernatants (Fig. 4.5) and sample derivitisation did not make a difference to the presence of this peak. Chemical ionisation using methane was carried out to obtain molecular weight and structural information for all peaks present in Fig. 4.5. Two of these were shown to be products of derivitisation (RT 10.7 and 13.6) (Table 4.4.). A number of pyrrole structures were present but these were present in equal amounts in the wild type and *tolC*$^-$ mutant. The peak present at RT 23.78 was identified as dioctyl phthalate, a plasticiser with no structural similarities to signalling molecules and a probable contaminant.

4.2.6. Detection of quorum derived compounds by Liquid Chromatography-Mass Spectrometry

Liquid Chromatography-Mass Spectrometry (LC-MS) was performed to detect lower concentrations of potential signalling compounds. LC-MS sorts compounds based on the mass to charge ratio of the compounds ion. Separation is determined by polarity and molecular features as opposed to boiling point in GC-MS, thus making it a more suitable method for detecting autoinducers. Phylogenetic analysis showed that the CqsS/CqsA system in *V. furnissii* shows greater similarity to

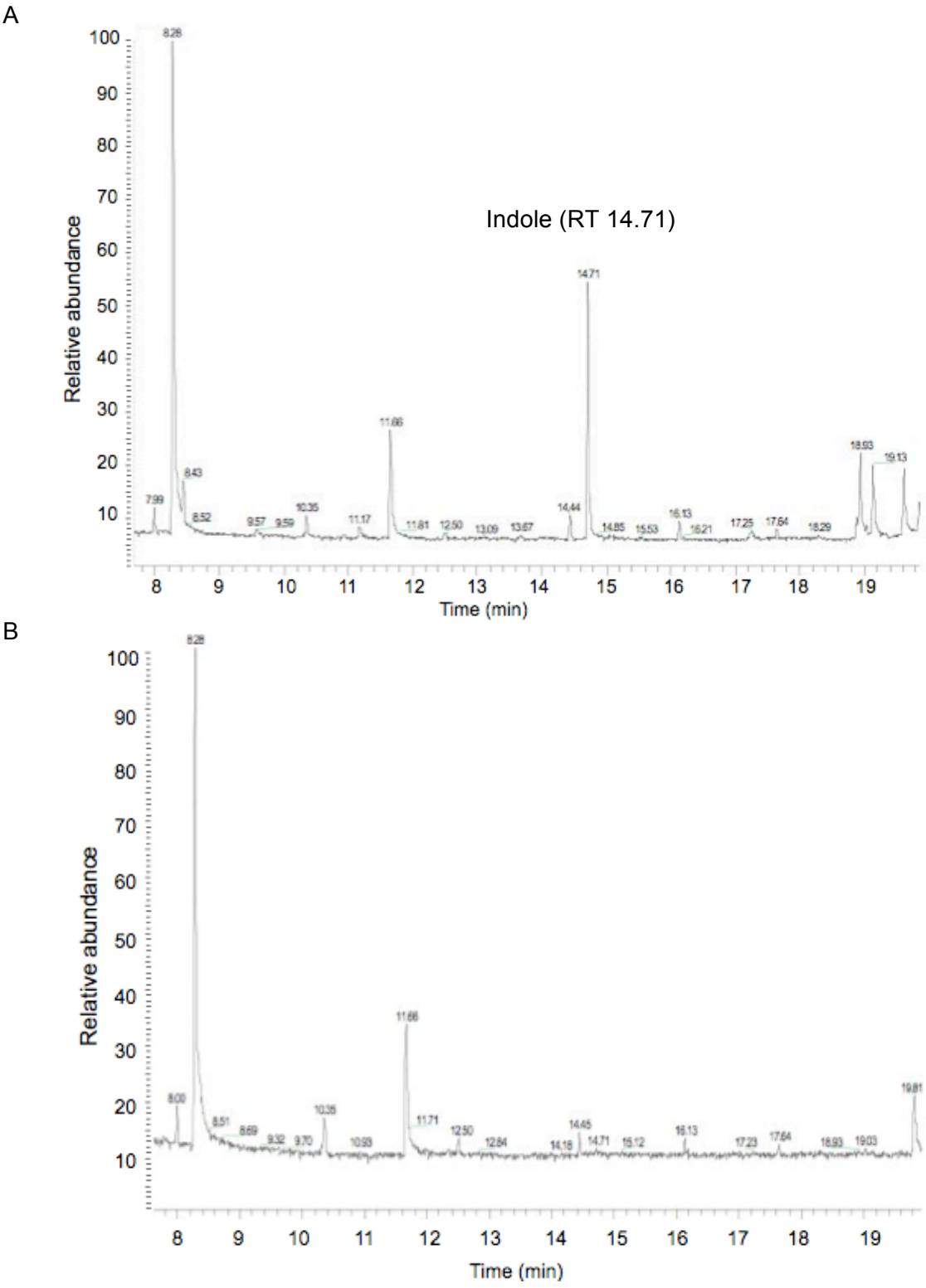

Figure 4.4. GC-MS traces of wild type and *tolC*⁻ mutant supernatants.

Traces display secreted indole (RT 14.71) in wild type supernatants (A) and an absence in *tolC*⁻ mutant supernatant extracts (B).

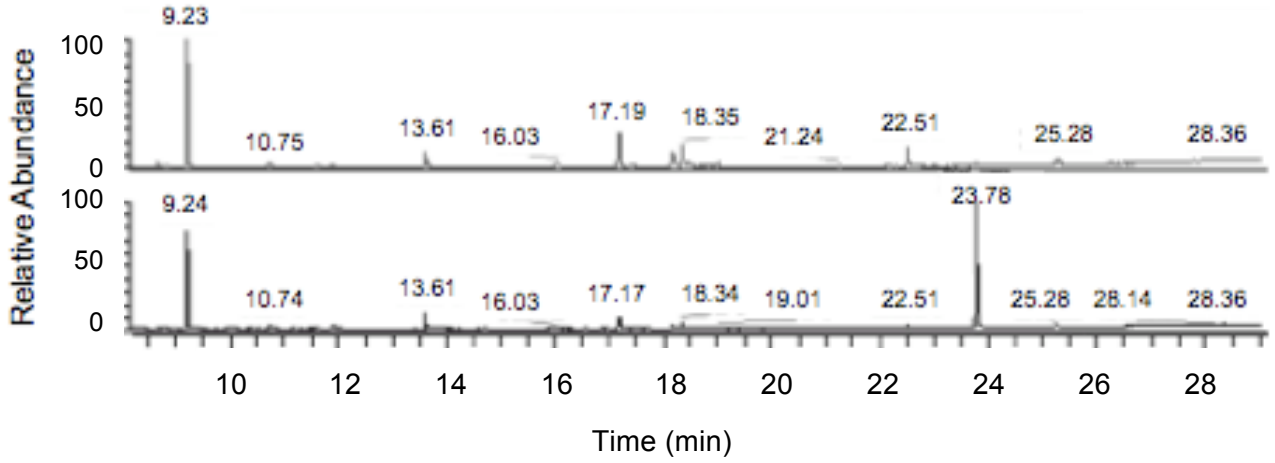

Figure 4.5. Cold on column GC-MS traces of wild type and *tolC*⁻ mutant supernatants.

GC-MS data acquisition and analysis carried out at Shell Global Solutions. Peak at 23.78 present in wild type (bottom) and absent in *tolC*⁻ mutant (top).

R.T	Identity	Conclusions
9.2	Deuteronaphthalene	Internal standard
10.7	Butyl phenol	Product of derivitisation
13.6	Dibutyl phenol	Product of derivitisation
17.2, 18.4, 22.5	Pyrroles	Levels in wild type and mutant not significantly different
23.7	Dioctyl phthalate plastisiser MW 390 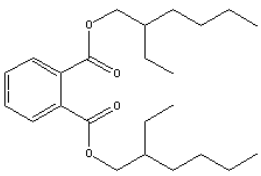	Probable contaminant, no properties of a signalling molecule

Table 4.4. Compounds identified by GC-MS on supernatant extracts.

Analysis carried out on wild type and *tolC*⁻ supernatants, results obtained from Shell Global Solutions, no potential signalling molecules for further investigation observed.

V. cholerae compared to *V. harveyi* suggesting that, similarly to *V. cholerae, V. furnissii* can detect and/or synthesise a broader range of CAI-1 type structures. Initially all positive ion $(M+H)^+$ and negative ion $(M-H)^-$ masses were calculated for all known CAI-1 type compounds to be scanned using the Quadrouple Time of Flight method (Q-TOF) (Table 4.5). This is a nonspecific method where, after passing through a nebuliser, ions are accelerated in an electric field with either a positive or negative charge. Compounds elute in positive or negative mode depending on the tendency to gain or lose a proton. It is favourable for compounds with an OH group to lose a proton (therefore elute in negative mode), and those with an NH_2 group to gain a proton (elute in positive mode) (Table 4.5).

4.2.7. LC-MS Q-TOF based detection of CAI-1 compounds

To determine which CAI-1 type compounds are produced by wild type *V. furnissii,* supernatants of wild type bacteria (cultured in triplicate to O.D. $_{600nm}$ 2.1) were prepared and extraction of signalling compounds carried out using acidified ethyl acetate following a protocol adapted from Fletcher *et al* (2007) (methods 2.27). Samples were initially analysed for presence of CAI-1 type compounds using Q-TOF giving total ion chromatograms (TICs) in positive and negative mode (methods 2.28). All CAI-1 compounds were scanned using ion masses in Table 4.5 giving an extracted ion chromatogram (EIC). The EIC displays analytes detected with corresponding mass values (m/z). A peak was detected in positive mode with mass corresponding to Am-C8-CAI-1 (expected ion mass: 186.1852, detected ion mass: 186.1845) eluting at 5.744 min (Fig 4.6A). However, fragmentation of this peak did not correspond with the structure of Am-C8-CAI-1 suggesting the biological compound detected was not Am-C8-CAI-1. In negative mode a compound with mass corresponding to CAI-1 (expected ion mass: 213.1860, detected ion mass: 213.1493) eluting at 4.065 min was detected (Fig. 4.6B). Fragmentation of this ion shows masses of 59.012, 92.925 and 153.132 corresponding to the structure of CAI-1 (Fig. 4.7). The product ion of mass 59.012 is significant as it indicates the presence of the C_3H_7O group. Notably no mass corresponding to AI-2 was detected by Q-TOF.

4.2.8. Establishing decreased CAI-1 secretion in the tolC$^-$ *mutant.*

Q-TOF LC-MS was used to directly compare levels of the detected CAI-1 compound with an expected negative ion mass 213.1860 in wild type and *tolC*$^-$ mutant supernatants. Extractions using acidified ethyl acetate were carried out on wild type and *tolC*$^-$ mutant supernatants, obtained from cultures grown to late exponential phase (wild type: O.D. $_{600nm}$ 2.1, mutant: O.D. $_{600nm}$ 1.8). All compounds listed in Table 4.5 were scanned again in the mutant but no others were detected. Within the mutant the presence of the target compound with expected mass 213.1860 was investigated. A peak was detected in the extracted ion chromatogram at the expected elution time

Name	Structure	Mass	(M+H)+	(M-H)-
CAI-1 $C_{13}H_{26}O_2$	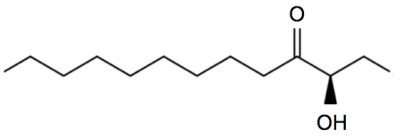	214.1933	215.2006	**213.1860**
C8-CAI-1 $C_{11}H_{22}O_2$	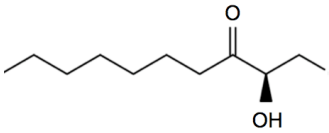	186.182	187.1693	**185.1547**
Am-CAI-1 $C_{13}H_{27}NO$	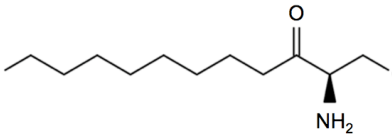	213.2093	**214.2165**	212.2014
Ea-CAI-1 $C_{13}H_{26}NO$	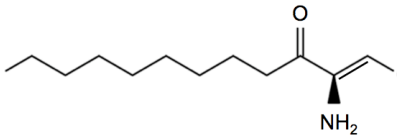	212.2014	**213.2087**	211.1942
Am-C8-CAI-1 $C_{11}H_{23}NO$	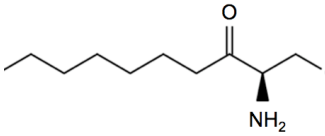	185.178	**186.1852**	184.1707
Ea-C8-CAI-1 $C_{11}H_{22}NO$	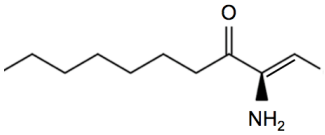	184.1701	**185.1774**	183.1629
AI-2 $C_5H_{10}BO_7$	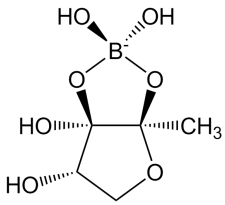	193.052	194.0592	**192.0447**

Table 4.5. CAI-1 type compounds analysed by LC-MS Q-TOF.

Positive (M+H)+ and negative (M-H)- precursor ions listed. Compounds with NH_2 groups, run in positive mode and those with OH groups run in negative mode. Ions to be detected highlighted in bold.

A

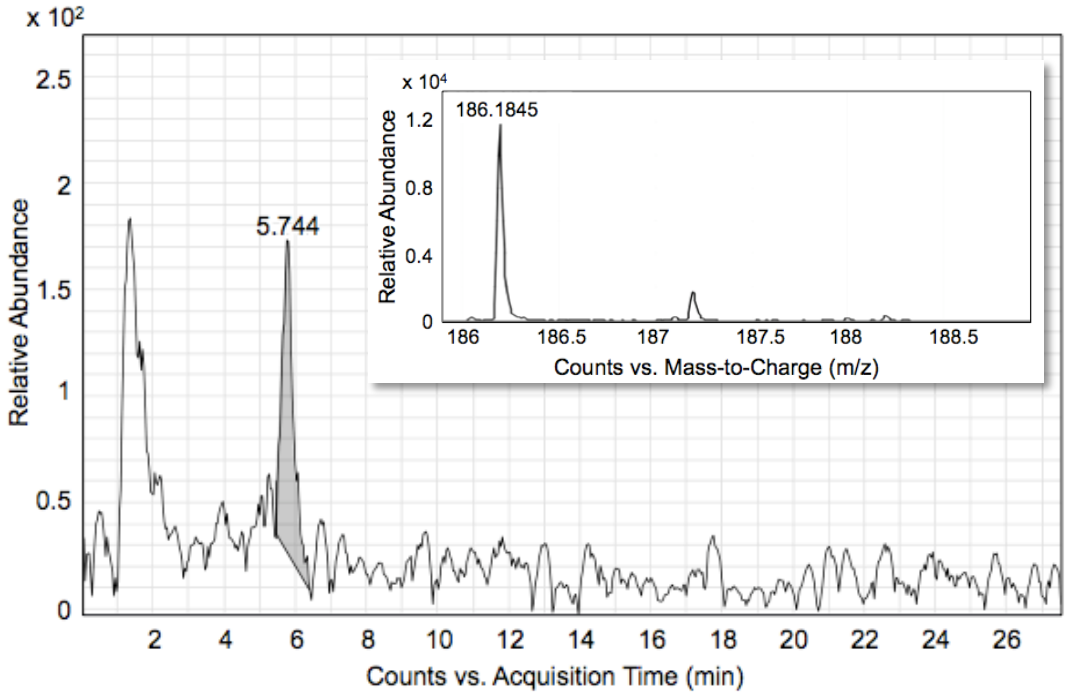

B

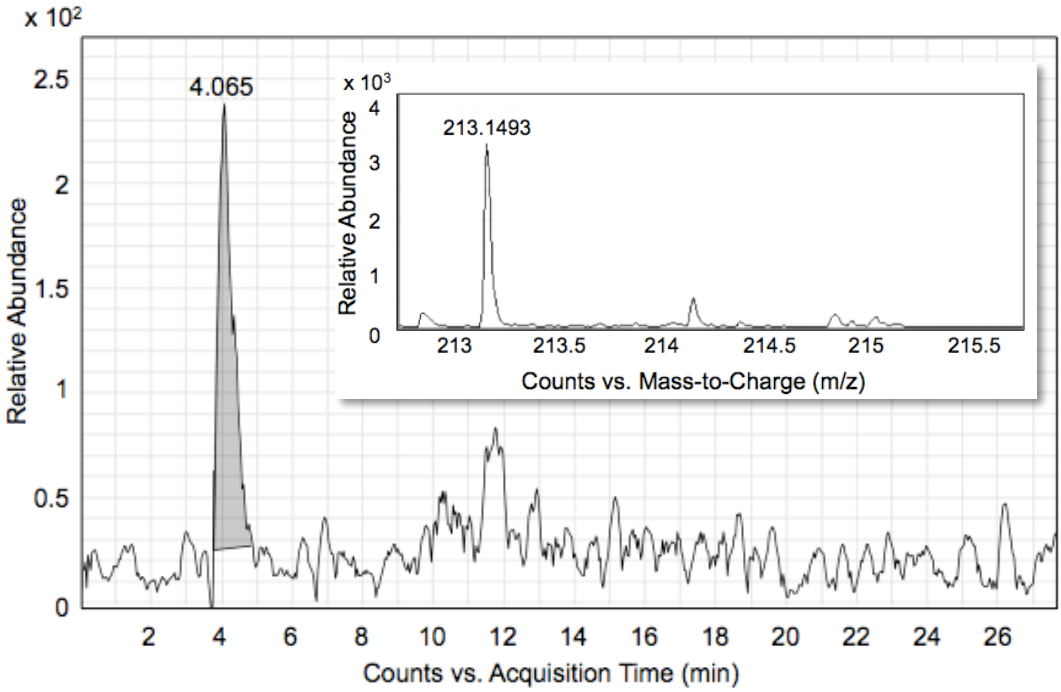

Figure 4.6. Extracted Ion Chromatograms (EICs) of ions detected by Q-TOF.

Insets display the m/z of the detected ion. For the compounds analysed the mass specificity was ~2-3 ppm. Data is representative of n=4 replicates. A: EIC of 186.1852 ion in positive mode (Am-C8-CAI-1), eluting at 5.744 min, m/z of extracted ion: 186.1845. B: EIC of 213.1860 ion in negative mode (CAI-1), eluting at 4.065 min, m/z of extracted ion: 213.1493

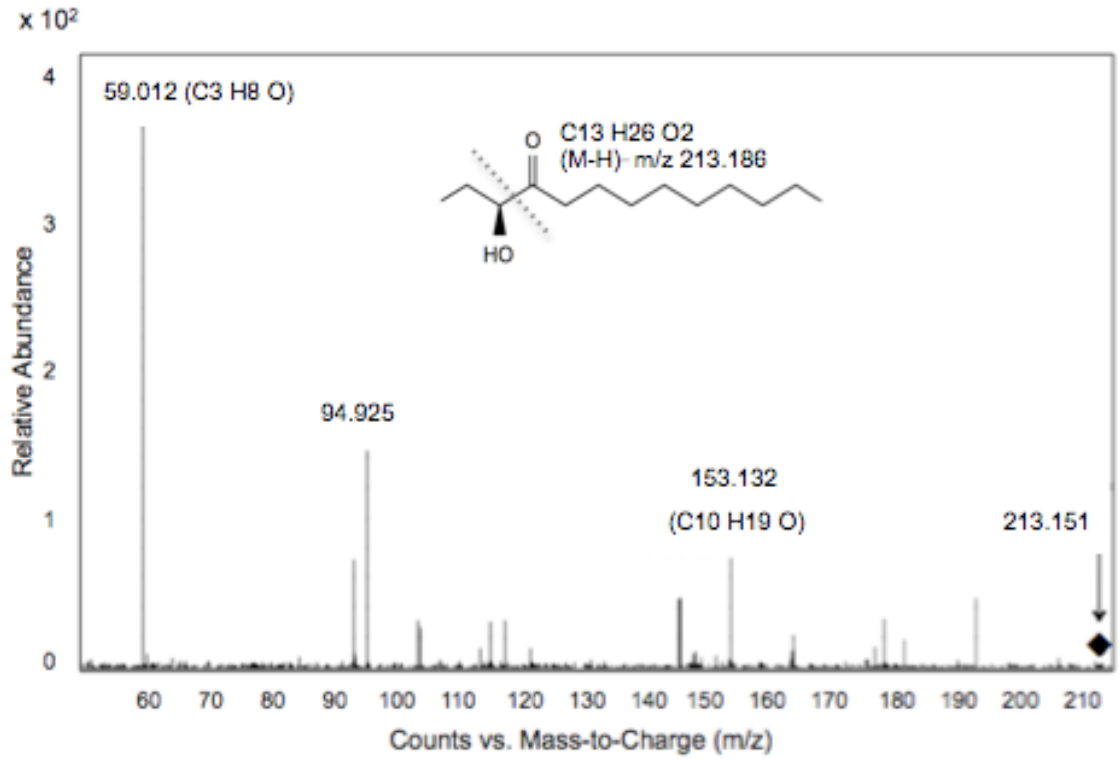

Figure 4.7. Fragmentation spectra of extracted ion detected by Q-TOF within wild type *V. furnissii.*

Spectrum shows strong similarities to CAI-1 structure (expected mass - 213.186, target compound mass – 213.151) and similar fragmentation (parent ion indicated by ◆). The dominant mass peaks are labeled with the m/z values and mass peaks 59.012 and 153.132 are labeled with the predicted elemental composition. The major peaks correspond to predicted fragmentation products particularly the 59.012 peak corresponding to the C_3H_7O fragment. The original ion (m/z 213.151) peak is small indicating complete fragmentation.

(3.958 mins), however its abundance was comparatively low as indicated by the peak size (Fig. 4.8). This difference was observed in all replicates (n=3).

4.2.9. Confirming the presence of a CAI-1 type compound in V. furnissii *supernatants*

For more accurate analysis of the CAI-1 structure synthesised by *V. furnissii* and for quantification of the compound within bacterial supernatants, samples were analysed by triple quadrupole (QQQ) LC-MS (methods 2.28). This method targets a specific ion and fragments it. The first quadropole selects ion of specific mass (Q1), the second quadropole (Q2) fragments it, third (Q3) scans all the ions (m/z) for the correct product ion. In this case, the CAI-1 precursor ion (m/z 213.2) and the product ion (m/z 59.1) were scanned. As both precursor and product ion are being scanned, both are rounded to one decimal place. For QQQ analysis, wild type and *tolC*$^{-}$ mutant bacteria were cultured on minimal M9 media with glucose to late exponential phase (O.D. $_{600nm}$ 2.1). Cultures were centrifuged and extraction of autoinducer compounds was performed on bacterial supernatants using the acidified ethyl acetate method. The target compound was detected in the extracts using the QQQ multiple reaction monitoring (MRM) method, a sensitive method only allowing detection of the pre determined precursor ion and product ion. This confirms the presence of the CAI-1 compound and allows for more accurate relative quantification in wild type and mutant (Fig. 4.9A). The peak area of the extracted CAI-1 ion is greater in wild type samples in contrast to *tolC*$^{-}$ mutant consolidating results obtained from Q-TOF analysis (Fig. 4.9A). The ion eluted quickly off the column (0.6 mins) establishing it as a particularly hydrophilic compound.

4.2.10. Quantification of secreted CAI-1 in wild type and tolC^{-} *mutant supernatants*

Signalling compounds are secreted during late exponential phase. Following the hypothesis that the CAI-1 compound is an autoinducer secreted by TolC, the secreted levels of CAI-1 would be expected to be lower during earlier stages of bacterial growth and secreted levels of CAI-1 would only show a difference between wild type and tolC^{-} *mutant during late exponential phase. To compare the presence of the target CAI-1 compound at different growth stages in wild type and* tolC^{-} *mutant, extractions were carried out on supernatants from mid and late exponential phase cultures (O.D.* $_{600nm}$ *1.6 and 2.1 respectively). Samples were analysed by QQQ LC-MS as previously described and peak areas were determined for all samples. During late exponential phase, significantly less CAI-1 is present in the* tolC^{-} *mutant supernatant (Fig. 4.9B). Within the mutant, the levels of CAI-1 secreted are the same throughout growth and is significantly less than wild type levels (p<0.05).*

4.2.11. Analysis of homoserine lactone (HSL) secretion

To compare levels of CAI-1 relative to any other homoserine lactones (HSLs) potentially produced,

all HSLs in Table 4.6 were analysed using LC-MS QQQ. Conditions for HSL detection by LC-MS

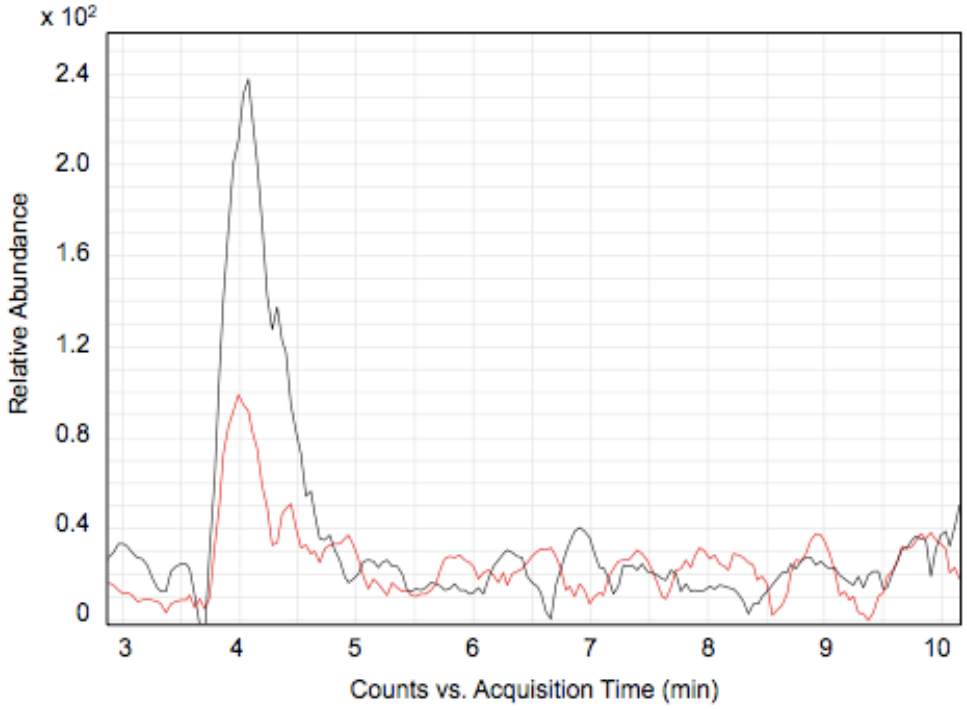

Figure 4.8. Comparing quantities of 213.186 ion corresponding to CAI-1 compound determined by extracted ion chromatograms (EICs).

Wild type (black) and *tolC*$^{-}$ mutant (red) late exponential supernatant extracts run on the Q-TOF in negative mode.

A

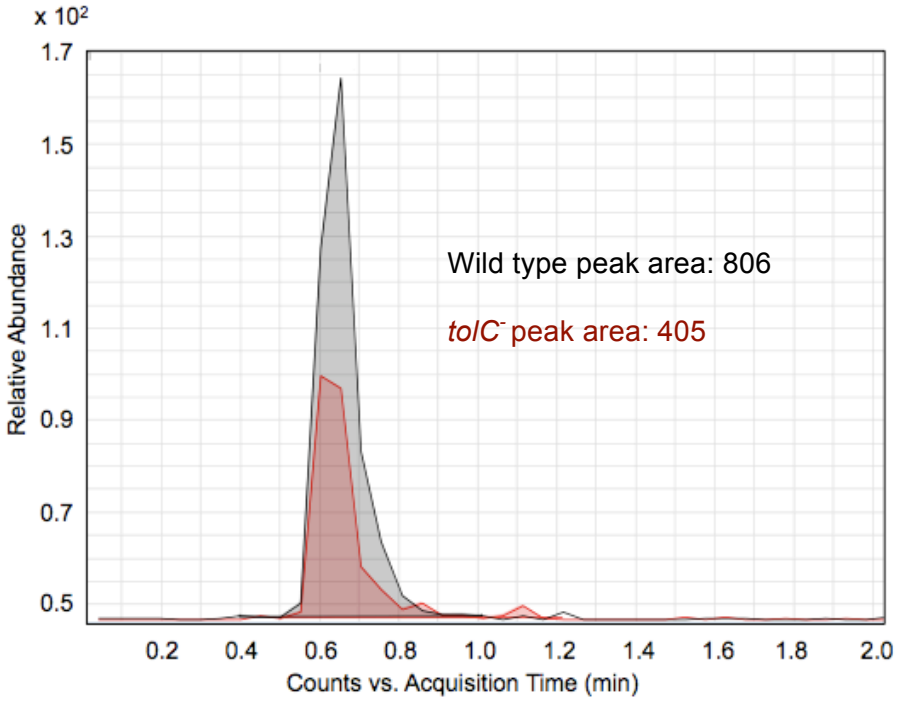

B

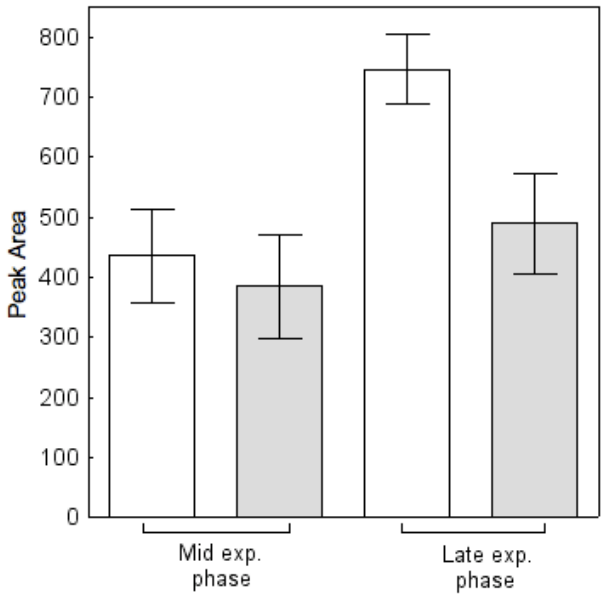

Figure 4.9. Quantification of 213.186 ion corresponding to CAI-1 compound determined by LC-MS QQQ Multiple Reaction Monitoring (MRM) data.

A: scan of selected precursor ion (m/z 213.2) and product ion (m/z 59.1) in wild type (black) and *tolC*⁻ mutant (red) late exponential supernatant extracts. Relative peak area determined in wild type (806) and *tolC*⁻ mutant (405) indicates approximately half the quantity of CAI-1 within the mutant.
B. Quantification of peak areas. Wild type ☐ knockout mutant ▭. Significant increase of detected compound in wild type during late exponential phase (n=2) (two tailed t-test, $p<0.05$).

have been established so the product ion and precursor ion masses were obtained from (Ortori *et al.*, 2011) (methods 2.28, Table 2.4). Wild type and *tolC*$^{-}$ mutant supernatants were collected during late exponential phase (O.D. $_{600nm}$ 2.1) in triplicate. Extraction of HSLs from the bacterial supernatants was performed, additional extractions were carried out on M9 minimal media as a control. All HSLs were scanned by QQQ (in positive mode) and CAI-1 (in negative mode) in wild type, *tolC*$^{-}$ mutant and M9 media (Fig. 4.10). Results show three ions with mass corresponding to HSLs; 3-OH-C12-HSL, C10-HSL and C12-HSL eluting at 3.30, 7.22 and 9.42 min respectively. However, these can be detected within the media controls and therefore cannot be determined as secreted compounds. The peak corresponding to the target CAI-1 compound (A) is clear within the wild type and, as previously determined, markedly reduced within the *tolC*$^{-}$ mutant supernatant. There is also no trace of the target compound within media controls placing it as the only truly secreted compound.

4.2.12. Synthesis of CAI-1 to enable comparison to biosynthetic compound.

The target compound detected by LC-MS has the correct precursor ion and product ion masses, with a fragmentation profile expected for CAI-1 (Fig. 4.7). For confirmation of the structure and to establish compound concentration, CAI-1 was synthesised and compared to the biological sample using LC-MS QQQ. The compound was synthesised as described by Kelly *et al.,* (2009), (methods 2.29) by Dr. Mark Wood at Exeter University and 100 µM run on LC-MS QQQ. Both the sample containing the biological target compound (wild type *V. furnissii*) and the sample containing synthesised CAI-1 were scanned for the product ion (213.2 m/z) using selected ion monitoring (SIM). A peak is present in both samples but there is a significant difference in the elution time and therefore the polarity of the biological and synthesised compounds (Fig 4.11). Synthesised CAI-1 elutes at 8 min in contrast to the biological compound at 1.7 min, this difference shows that the target compound is significantly more hydrophilic than synthesised CAI-1. Kelly *et al* (2009) detected synthesised CAI-1 in positive mode, so both the wild type *V. furnissii* sample containing the biological CAI-1 type compound and the synthesised CAI-1 sample were run again in positive and negative mode on the QQQ. The biosynthetic compound ran in both positive and negative mode however the synthesised compound only eluted in positive mode. To analyse the fragmentation profile of CAI-1 eluting in positive mode, the synthesised CAI-1 compound obtained from Dr. Mark Wood was compared to the fragmentation spectra of synthesised CAI-1 by (Kelly *et al.*, 2009). The spectra of the two synthetic CAI-1 structres show strong similarites, with peaks in synthesised for this study is CAI-1 (Fig 4.12A and 4.12B). The fragmentation spectrum of the biosynthetic compound shows a number similarities to that of the synthesised CAI-1 spectra, similar ratios of approximate masses; 57, 71, 81 and 95 m/z confirming that the compound including

QSSM	Mass	Precursor ion	Product ion
HSLs		$(M+H)^+$	
C4-HSL	171.1	172.1	102.1
C6-HSL	199.1	200.1	102.1
C8-HSL	227.1	228.1	102.1
C10-HSL	255.1	256.1	102.1
C12-HSL	283.1	284.1	102.1
C14-HSL	311.1	312.1	102.1
3-oxo-C4-HSL	185.1	186.1	102.1
3-oxo-C6-HSL	213.1	214.1	102.1
3-oxo-C8-HSL	241.1	242.1	102.1
3-oxo-C10-HSL	269.1	270.1	102.1
3-oxo-C12-HSL	297.1	298.1	102.1
3-oxo-C14-HSL	325.1	326.1	102.1
3-OH-C4-HSL	187.1	188.1	102.1
3-OH-C6-HSL	215.1	216.1	102.1
3-OH-C8-HSL	243.1	244.1	102.1
3-OH-C10-HSL	271.1	272.1	102.1
3-OH-C12-HSL	299.1	300.1	102.1
3-OH-C14-HSL	327.2	328.2	102.1
		$(M-H)^-$	
CAI-1	214.2	213.2	59.1

Table 4.6. Homoserine lactones (HSLs) and CAI-1 compound to be analysed by QQQ.

Mass values obtained from (Ortori *et al.*, 2011)

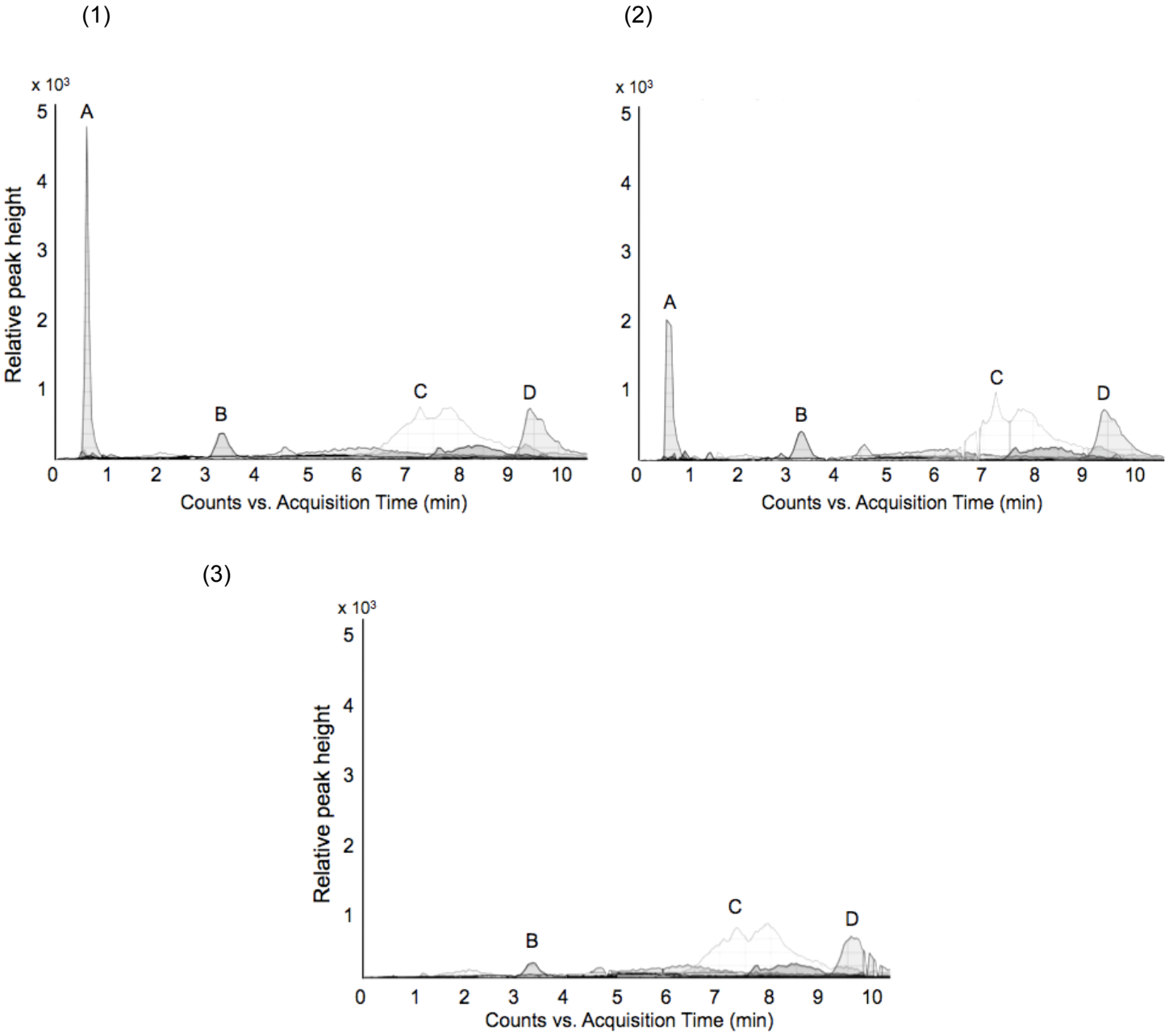

Figure 4.10. Determining presence of HSLs and CAI-1 compounds in supernatants.

All HSLs and CAI-1 scanned by LC-MS QQQ, multiple reaction monitoring (MRM) using precursor and product ions (Table 4.6) within wild type (1) *tolC*$^{-}$ mutant (2) and blank M9 media (3) extracts.

A – $(M\text{-}H)^{-}$ m/z: 213.2, product ion: 59.1 (CAI-1)

B - $(M+H)^{+}$ m/z: 300.1, product ion: 102.1

C - $(M+H)^{+}$ m/z: 256.1, product ion: 102.1

D - $(M+H)^{+}$ m/z: 284.1, product ion: 102.1

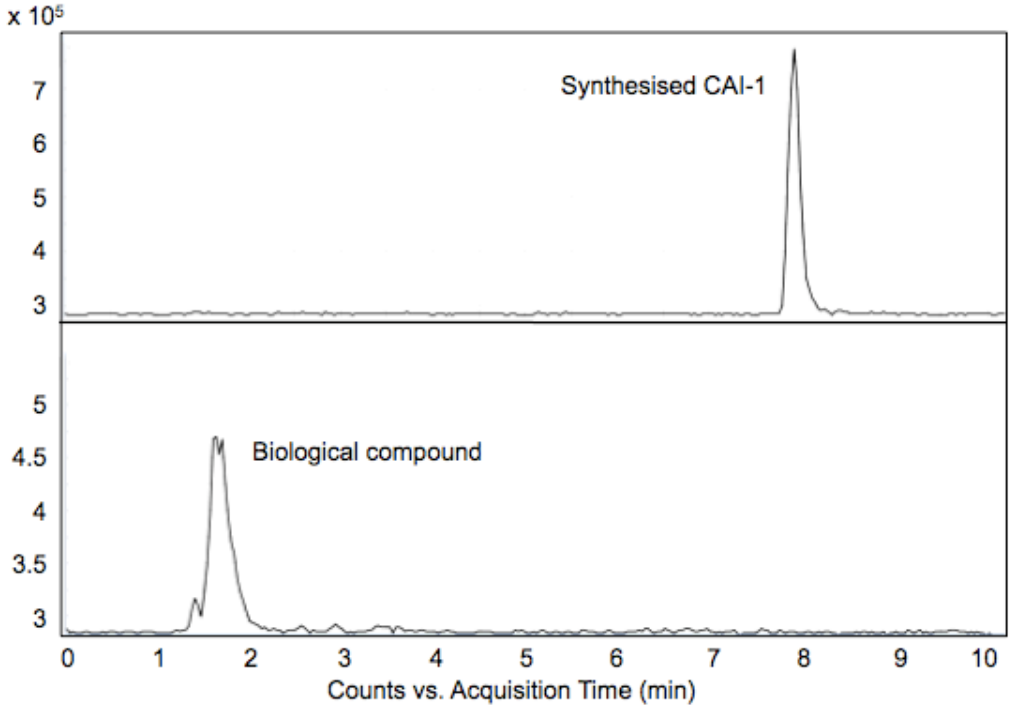

Figure 4.11. LC-MS traces of synthetic CAI-1 and biological compound.

Selected Ion Monitoring (SIM) scan of synthesised CAI-1 compound and biosynthetic compound. Elution times differ (8 min and 1.7 min) determining difference in polarity.

A

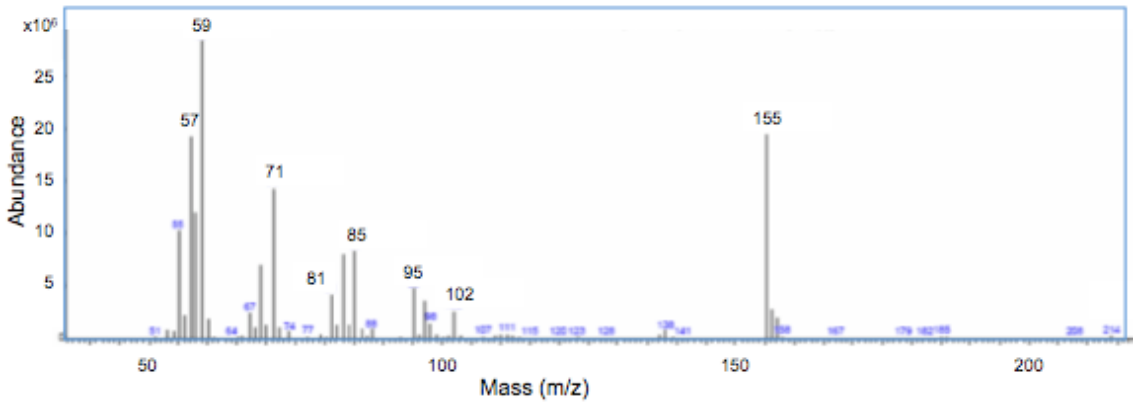

B

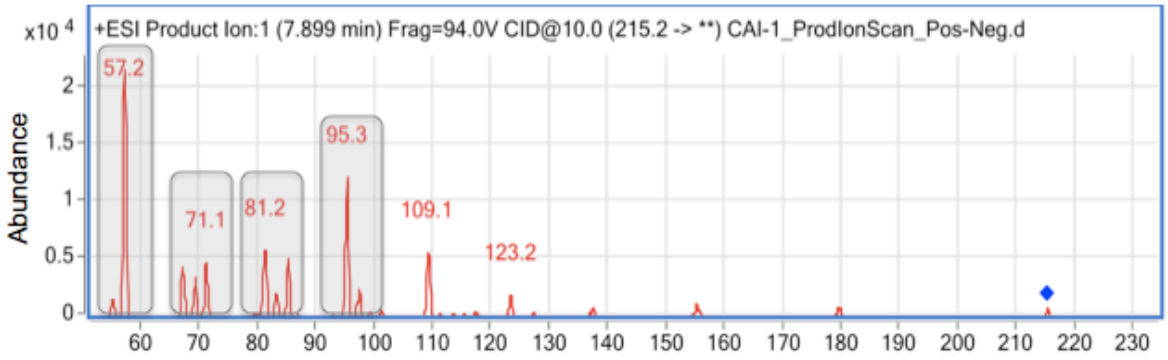

C

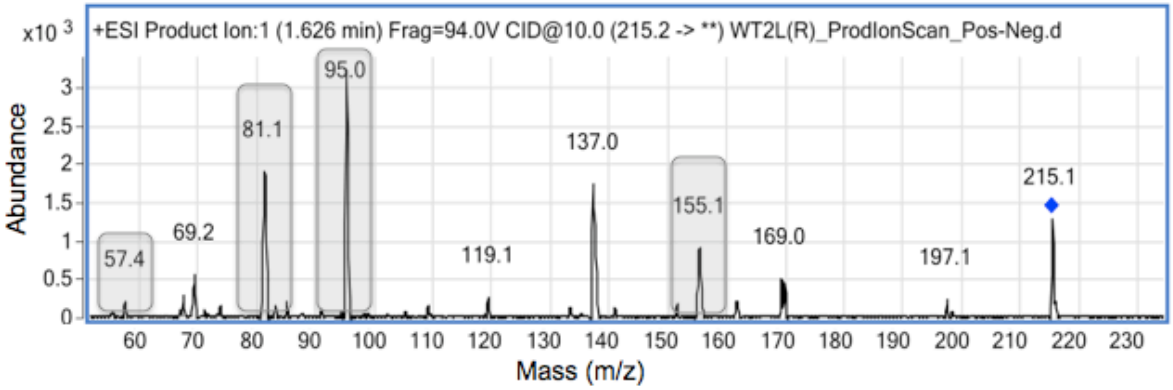

Figure 4.12. Fragmentation spectra of synthesised CAI-1 and biological sample.

A: Synthesised CAI-1 figure obtained from (Kelly *et al.*, 2009)

B: Synthesised CAI-1 from this study, parent ion indicated by ◆, fragmentation pattern similar to data obtained by (Kelly *et al.*, 2009) (peaks present in A and B are highlighted in grey)

C: Biosynthetic compound, parent ion indicated by ◆, also containing similar peaks with masses ~57, 81, 95, and 155 m/z, however in different proportions to both synthesised compounds. All fragmentation spectra obtained from ion detected in positive mode.

fragment masses of 155.1 m/z, 95.0 m/z, 81.1 m/z and 57.4 m/z (Fig 4.12C). The mass peak of 155.1 m/z corresponds to the C10-acyl group as determined by Kelly *et al* 2009. Notably, there are differences between the biological CAI-1 spectrum and synthesised CAI-1 spectra, particularly the difference in the fragment mass ratios. The 57.4 m/z peak is markedly smaller compared to the fragmentation spectra of the other two spectra (Fig 4.12). However, the elemental composition of the fragments in the biosynthetic compound shows that some properties of this compound are similar to that of synthesised CAI-1.

4.2.13. Determining the affect CAI-1 on bacterial growth

The target compound secreted by wild type V. furnissii, shows some structural similarities to CAI-1 but given significant differences in polarity, the structure of the compound synthesised by the bacteria is not identical to CAI-1. Although the compounds are not the same, synthesised CAI-1 was re-introduced into *tolC*$^{-}$ mutant cultures at mid exponential phase ($O.D._{600nm}$ 1.5) to determine if the presence of CAI-1 increased stationary phase cell density to that of the wild type. This was to ascertain if CAI-1 was a signalling molecule lacking in the tolC- mutant cultures and if the reduced stationary phase optical density is due to the absence of this compound. Synthesised CAI-1 was suspended in MeOH and re-introduced (at final concentrations of 100 nm, 10 nm, 1μM, 10 μM and 20 μM) into growing wild type and tolC- mutant cultures entering stationary phase (methods 2.30). The optical density during stationary phase is not altered by the addition of CAI-1 at any of the tested concentrations (Fig. 4.13).

4.2.14. The affect of secreted compounds on bacterial growth

To ascertain if any compounds secreted by wild type play a role in quorum sensing, supernatants of wild type and *tolC*$^{-}$ mutant were freeze dried, concentrated and re-introduced into growing *tolC*$^{-}$ mutant cultures (methods 2.30). Growth of the bacterial cultures was monitored to determine if the *tolC*$^{-}$ mutant stationary phase $O.D._{600nm}$ returned to that of the wild type. When wild type supernatant concentrate was added to knockout mutant cultures, the stationary phase $O.D._{600nm}$ increased to that of the wild type, entering stationary phase at the same time point (9 h) and at the same optical density ($O.D._{600nm}$ 2.1) (Fig. 4.14A). This increase in optical density (from $O.D._{600nm}$ 1.8 to 2.1) can also be observed when growth curves are plotted on a Log_{10} scale (Fig 4.14B). However, addition of supernatant concentrate obtained from mutant cultures and the concentrated M9 minimal media control also resulted in an increase to $O.D._{600nm}$ 2.1, suggesting that the alteration to growth is not due to secreted compounds but due to an addition of nutrients remaining in spent media.

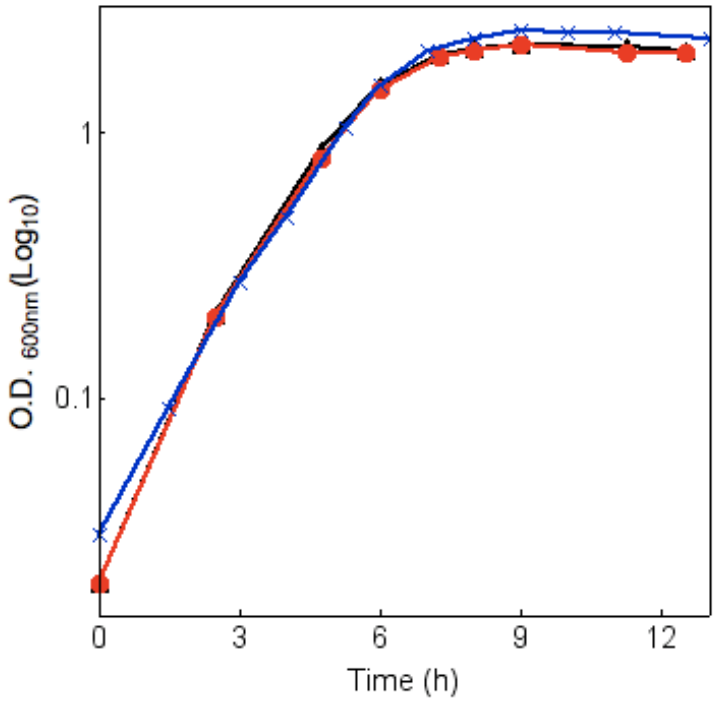

Figure 4.13. Reintroduction of sythesised CAI-1 into growing cultures.

Growth curves (Log_{10}) following addition of synthesised CAI-1 (20 μM), wild type control, *tolC*⁻ mutant control, *tolC*⁻ mutant within introduction of CAI-1. Addition of 20 μM CAI-1 displayed as a representative. Growth curves following addition of CAI-1 at 100 nm, 10 nm, 1μM and 10 μM were also obtained but all data sets are the same showing no change to growth.

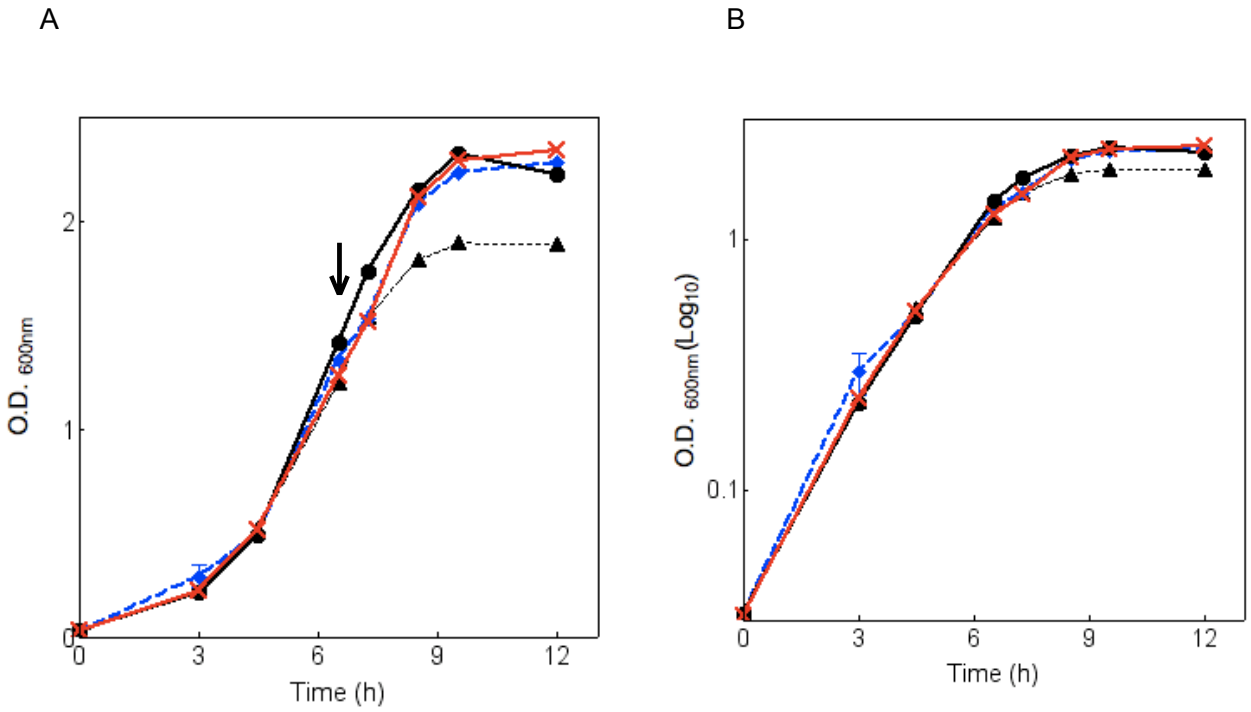

Figure 4.14. Re-introduction of freeze dried supernatant concentrate into *tolC*⁻ mutant cultures.

Growth curves following addition of freeze dried supernatant concentrate (from wild type and mutant) added to *tolC*⁻ mutant cultures at O.D. $_{600nm}$1.5 (indicated by arrow). Wild type control ——, *tolC*⁻ mutant control - - - - - - *tolC*⁻ mutant with introduction of wild type supernatant concentrate at O.D.$_{600nm}$ 1.5 —×— *tolC*⁻ mutant with introduction of *tolC*⁻ mutant supernatant concentrate at O.D.$_{600nm}$ 1.5 - -◆- -. Introduction of both supernatant extracts and minimal media concentrate result in an increased stationary phase optical density. A – Linear scale, B – Log_{10} scale.

4.3. DISCUSSION

Our understanding of how bacteria detect quorum sensing signalling compounds and how this process regulates metabolic processes is still expanding. Results presented in this study give a comprehensive analysis of the quorum sensing system in *V. furnissii*. Data correspond with previous findings that *V.furnissii* is capable of produing CAI-1, a signalling molecule only produced by 6 or 25 *Vibrio* species (Yang *et al.,* 2011). Variances on the CAI-1 structure have been presented in the literature (Ng *et al.,* 2011) and data here show that *V. furnissii* potentially produces an additional signalling structure. The amino acid structure of CqsA, required for CAI-1 synthesis, shows greatest identity to the CAI-1 synthesis protein in *V. cholerae* (75%) suggesting the structure of the compound produced by *V. furnissii* may be similar. A compound with correct mass and predicted structural fragmentation of CAI-1 was detected by LC-MS in wild type supernatants in significantly greater quantities compared to any other signalling compounds scanned (Fig 4.7 and 4.10). Comparing the CAI-1 type compound present in *V. furnissii* to synthesised CAI-1 showed significant differences in polarity between the two structures. Synthetic CAI-1 eluted at 8 min compared to the biological compound which eluted at 1.7 min, establishing that the biosynthetic compound is significantly more hydrophilic (Fig 4.11). Comparison of biosynthetic and synthetic compound fragmentation shows that there are strong structural similarities, with the functional C10-acyl group detected in both fragmentation spectra (Fig 4.12. Unexpectedly, the biosynthetic compound eluted in both positive and negative mode. It is possible that within biological extracts there is a combination of Am-CAI-1 (the amino precursor to CAI-1 containing an NH_2 group, Table 4.1) and CAI-1, which would account for two compounds with similar mass and structure but with different polarity. Synthesis of Am-CAI-1 by CqsA has been evidenced by Kelly *et al.*, (2009) supporting this hypothesis. CqsA sequence similarities vary between *Vibrio* species, possibly giving rise to structural variances on CAI-1 type compounds. *V. furnissii* CqsA shows greater sequence similarity to *V. cholerae* CqsA (able to produce CAI-1. Ea-CAI-1 and Ea-C8-CAI-1), compared to CqsA in *V. harveyi* which synthesises C8-CoA (Ng *et al.*, 2011) (Fig 4.2). This suggests that *V. furnissii* utilises a wider range of CAI-1 type compounds for quorum sensing.

Within wild type supernatants the concentration of the target CAI-1 compound increased from mid exponential phase to stationary phase, but in the *tolC*$^-$ mutant supernatants, the levels stay the same (Fig. 4.9). This supports the hypothesis that this CAI-1 type compound is involved in signalling and the *tolC* mutation affects the amount secreted. A significant decrease in stationary phase $O.D._{600nm}$ was observed in the *tolC*$^-$ mutant compared to *V. furnissii* wild type (Fig 4.3). Previous literature suggests a connection between this observation and disruption in quorum sensing genes in *E. coli* (Yang *et al.*, 2006). During lower cell densites there is a reduced

concentration of autoinducer molecules (Bassler, 1999a; Freeman and Bassler, 1999a, b; Freeman *et al*., 2000) so in contrast to the wild type, there would hypothetically be fewer autoinducers present within the media. LC-MS results support the theory that quorum sensing is affected by the *tolC* mutation by demonstrating a lower concentration of a suspected signalling compound with strong structural similarities to CAI-1 within the *tolC*$^-$ mutant supernatant (Fig 4.12).

Re-introduction of the synthesised CAI-1 into growing cultures did not alter the $O.D._{600nm}$ of the *tolC*$^-$ mutant in stationary phase (Fig 4.13) suggesting that, if quorum sensing does effect cell density in *V. furnissii*, this bacterium does not detect the *V. cholerae* CAI-1 compound. Given the precise threshold concentrations required to initiate transcriptional changes, re-introduction of synthetic autoinducers and monitoring alterations to growth may not be a sensitive enough method. Furthermore, additional signalling compounds may be synthesised by *V. furnissii* which have not been detected. Although non-targeted GC-MS analysis did not identify any autoinducer compounds within bacterial supernatants, indole was detected as a potential substrate of TolC, secreted only by wild type (Fig 4.4). Indole derivatives have been shown to act as signalling compounds (Di Martino *et al.*, 2003, Lee *et al.*, 2007). Furthermore they are associated with the Lux pathway (Yao *et al.*, 2006) and RND efflux components AcrEF and AcrD (Hirakawa *et al.*, 2005). However, the presence of this compound was not consistent throughout all replicates, detection of indole derivatives by more sensitive methods such as LC-MS should be undertaken.

Further evidence is provided for a reduced level of signalling molecule secretion or production in the *tolC*$^-$ mutant as the gene responsible for CAI-1 synthesis (*cqsA*) is down regulated (2.9 fold) in the mutant (Table 4.3). Despite the relatively large fold change, the decreased expression of CqsA does not alone comply with significance parameters (p=0.09). However, considering the expression of the Lux pathway as a whole, there is strong evidence that the CqsA/CqsS pathway is feeding back to regulate the expression of genes in the Lux pathway. The *tolC*$^-$ mutant ultimately reaches a lower cell density compared to the wild type (Fig 4.3), at lower cell densities, phosphate is transferred from the receptor (CqsS) to LuxU then to LuxO. Phospho-LuxO activates a repressor that represses the expression of LuxR leading to expression of virulence factors (Zhu *et al.*, 2002) (Fig. 4.14.). The sequence of expression changes expected when autoinducer concentrations are low is apparent within the *tolC*$^-$ mutant; significant increased expression of LuxO and LuxU (1.37 and 1.34 respectively) followed by subsequent decrease in LuxR expression (1.47) (Table 4.3, Fig. 4.14). The 1.42 increase in expression of autoinducer detector, CqsS, within the mutant is less easily explained, however, it is possible that this protein is expressed at low cell densities and is repressed at a threshold concentration of autoinducer. Notably, although the AI-2 synthesiser

protein LuxS shows increased expression in the *tolC*$^{-}$ mutant the detector proteins which feedback to the shared regulator operon show no significant differential expression (Table 4.3). Research has shown that bacteria discriminate between different autoinducer signalling pathways (Waters and Bassler, 2006), data presented in this study show that in *V. furnissii,* the CAI-1 pathway is dominant. Considering the role of AI-2 as a universal signalling molecule required for interspecies communication, its expression may not be required in a *V. furnissii* culture where no other bacteria are present.

The combination of data showing phenotypic differences between wild type and *tolC*$^{-}$ mutant and the consequential expression changes in the quorum sensing pathway furthers our understanding of how cell-cell signalling works and how TolC is involved. It could be hypothesised that the *tolC* mutation affects the regulation of quorum sensing pathway genes, linking TolC to the decreased expression of CqsA. This would initiate the expression changes in the quorum sensing pathway and consequentially reduce secretion of the CAI-1 compound, observed in lower quantities in the mutant supernatants. Alternatively, it could be suggested that a lack of functioning TolC results in reduced CAI-1 secretion in *V. furnissii* which leads to the observed expression changes within the Lux pathway. It is also possible that an accumulation or inefficient secretion of this CAI-1 signalling molecule occurs in the *tolC*$^{-}$ mutant cells. This may give a false indication of higher cell densities leading the *tolC*$^{-}$ mutant cultures to enter stationary phase sooner. It is worth noting the nature of the compound detected in this study, its strong hydrophilic nature further suggests an export system such as AcrAB-TolC is required to remove it from the cell. However, it is still detected within the *tolC*$^{-}$ mutant supernatants suggesting that if a TolC efflux system does aid secretion, some of the compound may still diffuse through the membrane (Fig 4.15A). Another explanation for less effective secretion of the signalling compound is the disruption to the membrane caused by the *tolC* mutation, limiting diffusion (Fig 4.15B). It is clear that the mutation in *tolC* results in changes to the quorum sensing mechanism and likely impedes release of a CAI-1 type compound. Whether the secretion of the CAI-1 type compound occurs directly via TolC in *V. furnissii* or its production is indirectly reduced, expression of genes in the *lux* pathway are altered in the *tolC*$^{-}$ mutant. Expression changes in LuxR results in a number of transcriptional changes effecting virulence factor production, cell motility and cellular growth (Fig 4.14 and 4.15). A range of phenotypes arise from *tolC*$^{-}$ mutations (Zgurskaya *et al.*, 2011) and given the clinical relevance of this export protein it is important to understand how these phenotypic changes occur. Data presented here show that the connection between OMPs such as TolC and associated phenotypic changes could be connected by the quorum sensing regulatory pathway.

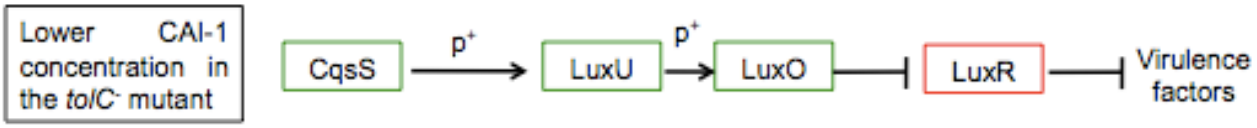

Figure 4.14. Differential expression of proteins in the Lux pathway within wild type *V. furnissii* and *tolC*⁻ mutant.

Green indicates increased expression (CAI-1 detector: CqsS 1.42 fold change, LuxU 1.34 fold change and LuxO 1.37 fold change), red indicates decreased expression: LuxR 1.47 fold change. All expression changes significant (two tailed t-test, $p<0.05$).

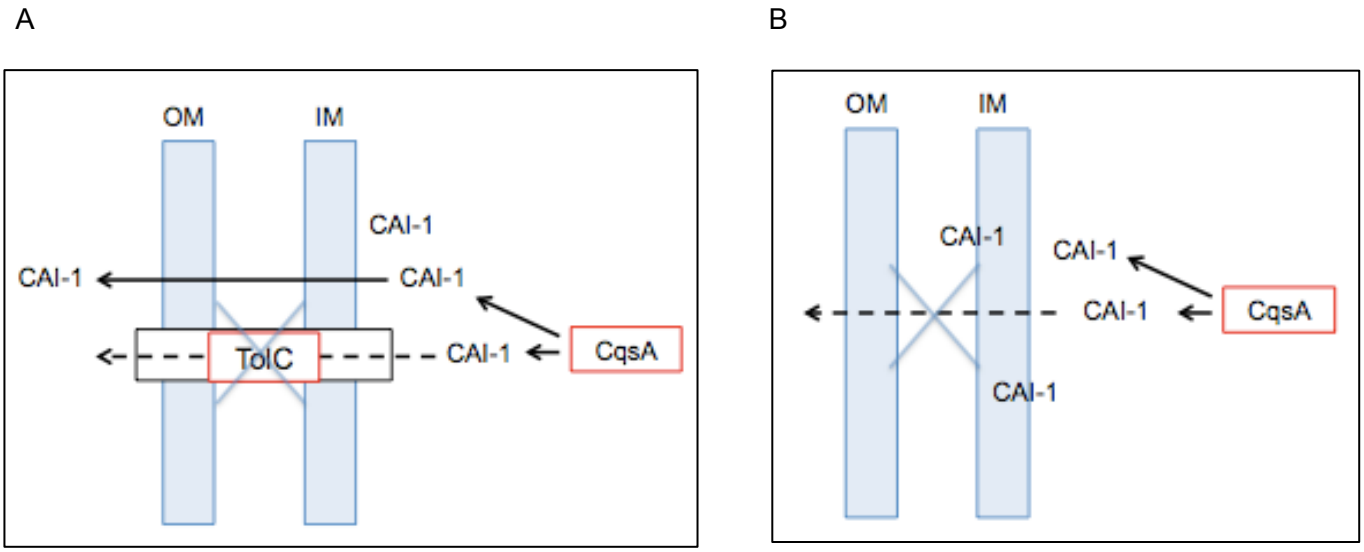

Figure 4.15. Diagram to illustrate suggested implications of the *tolC* mutation.

Impeding export of CAI-1 type compound in *V. furnissii* via the inner membrane (IM) and outer membrane (OM). Either due to removal of TolC as a direct exporter (A), or as a result of membrane disruption affecting diffusion across the membrane (B). CqsA outlined in red to illustrate decreased expression in the *tolC*⁻ mutant (2.9 fold).

CHAPTER 5 - INVESTIGATING GLOBAL GENE EXPRESSION CHANGES WITHIN A *TOLC*⁻ MUTANT

5.1 INTRODUCTION

Mutations in *tolC* result in pleiotropic phenotypes likely due to the interaction of TolC with extensive functional and regulatory pathways that promote resistance to antimicrobials and survival in varying conditions (Zgurskaya *et al.*, 2011). In order to determine if phenotypic differences reported in this study are directly related to transport via TolC or due to associated changes in gene expression, the transcriptomes of both the wild type and the *tolC*⁻ mutant will be investigated. Previous chapters have shown that TolC plays an important role in a number of bacterial processes in *V. furnissii,* some are well established; decreased antibiotic resistance for example corresponds with numerous reports of mutations in RND efflux systems. Data presented in chapter 4 show that cell-cell signalling is associated with TolC but that differences in exported compound levels may be due to expression changes and not direct export. An additional difference determined in the *tolC*⁻ mutant is decreased fatty acid secretion, this phenotypic change is not well documented in other species and further investigation into the role TolC plays in this process is required. Efflux systems are of great clinical interest and understanding the connection between the fundamental component; TolC and other bacterial pathways is of interest.

A number of points have been raised during experimentation, in particular the membrane proteins associated with TolC comprising the trimeric efflux pump. The recently published *V. furnissii* genome (Lux *et al.*, 2011) shows the presence of only one membrane associated RND; annotated as AcrB showing greatest amino acid sequence similarity to AcrB in *Aeromonas veronii* (69% identity). It has therefore been assumed that TolC is part of an AcrAB-TolC efflux system in *V. furnissii*; an RND efflux system also found in *V. cholerae*. However, antibiotic resistance analysis shows that an efflux system in this bacterium is responsible for secreting aminoglycosides (chapter 3). Due to their hydrophilic nature, aminoglycosides are reported substrates of AcrD but not AcrB (Rosenberg *et al.*, 2000), however, in the *tolC*⁻ mutant reduced resistance to a number of antimicrobials which are specifically AcrB substrates was observed (e.g. chloramphenicol, erythromycin and tetracycline), (Elkins and Nikaido, 2002). This suggests that TolC is interacting with both AcrB and AcrD or AcrB in *V. furnissii* is capable of binding and exporting aminoglycosides. Determining potential AcrB homologues in *V. furnissii* and analysing the expression of these in the wild type and *tolC*⁻ mutant will give an indication of those interacting with TolC.

Previous work shows increased cellular levels of hexadecanoic, hexadecenoic and octadecenoic acids within the *tolC*$^-$ mutant. Data show that there are lower quantities of fatty acids secreted in the absence of TolC and that this increase is due to cellular accumulation (chapter 3). A comprehensive study of the highly conserved fatty acid biosynthesis pathway (fab) (Campbell and Cronan Jr, 2001) and unsaturated fatty acid synthesis proteins (TesAB) will be carried out to establish any corresponding changes in fatty acid enzyme expression which occur within the *tolC*$^-$ mutant. Given the increased focus on the pleiotropic expression changes that occur in *tolC*$^-$ mutants it is important to establish if the phenotypic change is directly due to TolC or decreased expression of the fatty acid pathway. The null hypothesis, following previous results, is that the expression of the fatty acid pathway is not significantly altered in the mutant.

Efflux pumps are associated with virulence in bacteria and results in previous chapters suggest this association between TolC and virulence is connected by quorum sensing. A comprehensive study of the Lux pathway in *V. furnissii* confirmed significant differential expression of quorum regulatory proteins compared to the *tolC*$^-$ mutant. Ultimately, the regulatory factor LuxR shows decreased expression in the *tolC*$^-$ mutant which is a starting point of further study in this chapter. LuxR negatively regulates a number of virulence factors in other bacteria (Miller *et al.*, 2002). ToxT regulates a virulence cascade and its expression is regulated by LuxR in *V. cholerae* (Higgins and DiRita, 1994, Zhu and Mekalanos, 2003) (Fig 5.1). Increased expression of *toxT* was observed in *V. cholerae tolC*$^-$ mutants when cultured in M9 media (Minato *et al.*, 2011). Global gene expression changes will be investigated in wild type *V. furnissii* and *tolC*$^-$ mutant with a focus on those virulence factors outlined in Fig. 5.1; AphAB, ToxRS, ToxT, TcpHP, HapA and additional virulence factors.

V. furnissii has been acknowledged as a potential pathogen (Dalsgaard *et al.*, 1997, Derber *et al.*, 2011). Determining proteins associated with virulence and analysing the expression of these in wild type and *tolC*$^-$ mutant will allow an understanding of this strains pathogenicity and the involvement of TolC in expression of virulence factors. Transcriptome analysis of *tolC*$^-$ mutants in *S.* Typhimurium have shown significant differential expression of a number of pathways significant to virulence and host invasion however the regulatory network connecting these is not currently documented (Webber *et al.*, 2009). Within this chapter an overview of protein expression in the wild type and *tolC*$^-$ mutant, including those highlighted in Fig 5.1 will be determined. The express aim of this study is to establish further connections between the *tolC*$^-$ mutant, the quorum sensing regulatory pathway and expression of virulence factors.

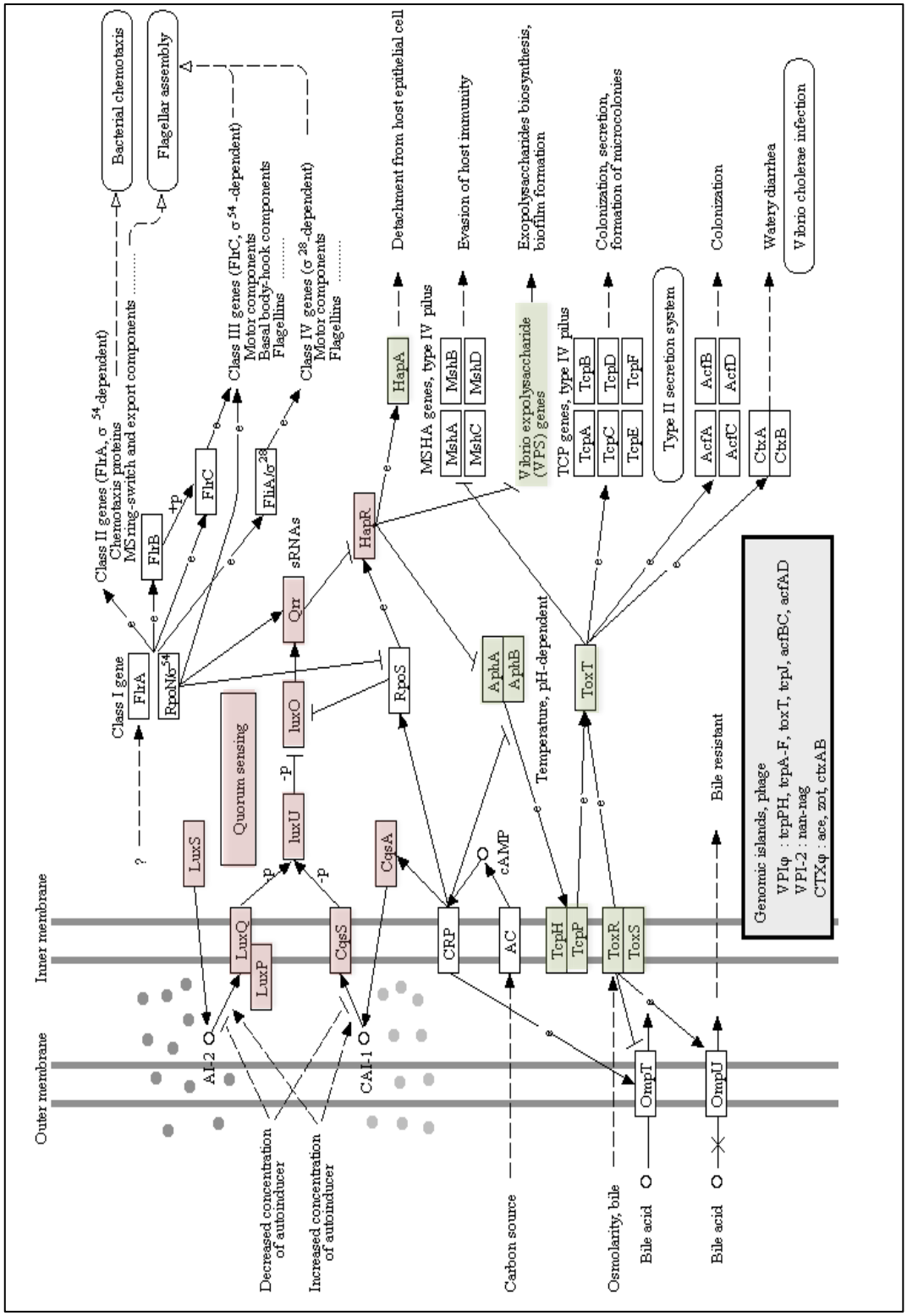

Figure 5.1. *V. cholerae* pathogenic cycle taken from Kyoto Encyclopedia of Genes and Genomes (KEGG) pathway database.

Quorum sensing proteins highlighted in red, previously analysed in *V. furnissii* (chapter 2). Expression of virulence factors, regulated by HapR, to be analysed in *V. furnissii* wild type and *tolC*⁻ mutant are highlighted in green.

5.2. RESULTS

5.2.1. Global differential expression in wild type and tolC⁻ mutant

In order to establish the global affect of the *tolC* mutation, a direct comparison of the expression of all genes in the wild type control group and *tolC*⁻ mutant group was carried out. In order to analyse the transcriptomes, wild type and *tolC*⁻ mutant bacteria were cultured in L.B. media until late exponential phase. RNA was extracted and cDNA synthesised and transcriptomes subsequently analysed following microarray chip hybridisation, performed at The Nottingham Arabidopsis Stock Centre (NASC) (methods 2.26). The microarray expression visualisation and analysis was carried out using GeneSpring GX software by initially grouping of the six microarray chip samples into the control group (3 x wild type samples) and the mutant group (3 x *tolC*⁻ mutant samples) (methods 2.26). The absolute ratio of normalised expression between the average intensities of the 3 samples in each group was performed by GeneSpring GX software, ultimately giving the difference in expression (or fold change) of each gene between wild type and *tolC*⁻ mutant. All 8974 entities in *V. furnissii* were filtered on a volcano plot using the Benjamini-Hochberg FDR multiple testing correction, p value multiple testing correction is necessary when analysing a large number of entities in order to reduce errors that occur by chance. Gene products showing significant expression differentiation were determined by applying a filter (corrected p value < 0.05), showing 123 genes with significant differential expression between the wild type and mutant. 38 out of the 123 genes express hypothetical proteins, intergenic regions or unknown products. The remaining 85 are listed in Table 5.1. The 38 unknown entities were checked for homology to other organisms by nucleotide sequence alignment using BLAST, none showed sequence similarity to genes in other species (identity >60%). The majority of the remaining 85 gene products show increased expression in the *tolC*⁻ mutant (83%). The list is ordered by the gene number, displaying those closely associated within the genome, those with the annotation “A” are on chromosome 1 and those beginning “B” located on choromosome 2.

Results confirm that expression of TolC in the mutant is significantly decreased by a fold change of 33.38, satisfying statistical parameters (unpaired t-test, $p<0.05$). The normalised expression of TolC is presented in Fig 5.2. Notably, of the 123 genes showing differential expression in the mutant, 13 are associated with cell motility, 12 of which show increased expression within the mutant. This will be further analysed in chapter 6 along with those entities involved in oxidative stress, also highlighted in Table 5.1.

Gene	Description	FC
vfu_A00008	peptidyl-prolyl cis-trans isomerase, FKBP-type	1.23
vfu_A00059	**thiol-disulfide isomerase and thioredoxin**	**3.83**
vfu_A00113	ISSod6, transposase	6.87
vfu_A00119	glycosyltransferase	7.66
vfu_A00122	O-antigen flippase	8.03
vfu_A00182	transposase, IS3 family	2.01
vfu_A00391	universal stress protein A	1.90
vfu_A00479	LexA repressor	1.57
vfu_A00482	soluble pyridine nucleotide transhydrogenase	1.43
vfu_A00506	phosphoenolpyruvate carboxykinase	1.63
vfu_A00732	sigma-54 modulation protein, putative	2.02
vfu_A00817	ribose-5-phosphate isomerase A	2.13
vfu_A00819	ribose-5-phosphate isomerase A	2.88
vfu_A00821	2-octaprenyl-6-methoxyphenyl hydroxylase	1.68
vfu_A00830	RNA polymerase sigma factor RpoE	3.79
vfu_A00832	sigma-E factor regulatory protein RseB	2.16
vfu_A00833	sigma-E factor regulatory protein RseC	2.83
vfu_A00859	**outer membrane protein TolC**	**33.38**
vfu_A00921	HesB family protein	2.90
vfu_A00930	transcription elongation factor GreA	1.90
vfu_A00933	cell division protein FtsH	1.41
vfu_A00945	lipoprotein NlpI	1.43
vfu_A00946	**transcriptional regulator, MarR family**	**2.36**
vfu_A01007	23S rRNA pseudouridine synthase D/large subunit	2.15
vfu_A01113	lipoprotein	3.47
vfu_A01121	flagella basal-body rod protein B	3.50
vfu_A01122	flagella basal-body rod protein FlgC	3.75
vfu_A01123	flagella basal body rod modification protein D	2.93
vfu_A01124	flagella hook protein FlgE	3.07
vfu_A01125	flagella basal body rod protein FlgF	3.38
vfu_A01126	flagella basal body rod protein FlgG	3.37
vfu_A01127	flagella L-ring protein FlgH	2.93
vfu_A01132	flagellin	3.36
vfu_A01180	polar flagellin	5.56
vfu_A01182	flagella protein FlaG	3.25
vfu_A01189	flagella hook-basal body complex protein FliE	1.62
vfu_A01196	flagella basal body-associated protein FliL	1.59
vfu_A01239	zinc ABC transporter, ATP-binding protein	1.60
vfu_A01361	flagella basal-body rod protein FlgG	2.06
vfu_A01591	ATP phosphoribosyltransferase	1.35
vfu_A01690	Cold shock protein	2.21
vfu_A01744	GTP cyclohydrolase II	2.05
vfu_A02051	formate hydrogen-lyase transcriptional activator for fdhF, hyc and hyp operons	1.66
vfu_A02068	sensor kinase citA, putative	1.82
vfu_A02346	short chain acyl-CoA thioesterase	3.39
vfu_A02351	Holliday junction DNA helicase B	2.15
vfu_A02369	ABC-type histidine transport system, ATPase component	2.02
vfu_A02478	Inactive homolog of metal-dependent protease	1.53
vfu_A02487	methionine sulfoxide reductase B	1.52

vfu_A02533	bacteriophage CI repressor protein	2.34
vfu_A02543	Recombinational DNA repair protein	1.53
vfu_A02550	AphB/LysR family protein	1.26
vfu_A02628	membrane protein	1.55
vfu_A02636	phosphocarrier protein HPr	4.43
vfu_A02736	SsrA-binding protein	1.90
vfu_A02744	fimbrial protein	1.99
vfu_A02772	outer membrane protein assembly complex subunit	1.58
vfu_A02785	HesB family protein	2.02
vfu_A02877	purine nucleoside phosphorylase	1.59
vfu_A02890	hemerythrin HHE cation binding domain subfamily, putative	1.80
vfu_A02930	cell division protein FtsQ	2.71
vfu_A02931	UDP-N-acetylmuramate--alanine ligase	1.19
vfu_A02975	carbon storage regulator	1.91
vfu_A02979	recombinase A	1.51
vfu_A03109	MSHA pilin protein MshB	1.70
vfu_A03118	MSHA biogenesis protein MshI	1.52
vfu_B00060	putative acetyltransferase	1.79
vfu_B00081	acetyltransferase	1.40
vfu_B00095	transketolase 1	1.49
vfu_B00133	**glutathione S-transferase**	**2.88**
vfu_B00140	two component transcriptional regulator	2.81
vfu_B00180	amidase, hydantoinase/carbamoylase family protein	1.59
vfu_B00243	putataive membrane protein	1.81
vfu_B00338	helicase IV	1.75
vfu_B00471	hypothetical dipeptidase	2.35
vfu_B00511	nicotinic acid mononucleotide adenylyltransferase	2.64
vfu_B00561	cold-shock DNA-binding domain protein	4.10
vfu_B00570	soluble cytochrome b562	1.71
vfu_B00722	Protein chain release factor B	1.40
vfu_B01064	transcriptional regulator, MerR family	2.70
vfu_B01065	deoxyribodipyrimidine photolyase, cyclobutane pyrimidine dimer-specific	2.94
vfu_B01076	putative membrane protein	1.54
vfu_B01099	putative phosphomannomutase	1.33
vfu_B01125	hemolysin	1.71
vfu_B01152	cyclic diguanylate phosphodiesterase (EAL) domain protein	1.72

Table 5.1. List of entities showing significant differential expression in *tolC*⁻ mutant.

Data presented following unpaired t-test and multiple testing correction ($p<0.05$). 38 of 123 genes are described as hypothetical or unknown products and have not been listed. 69 out of 85 gene products show increase expression in the mutant (highlighted in green), those showing decreased expression are highlighted in red. Gene ontology analysis of genes involved in cell movement and motility listed 13 genes showing significant differential expression ($p<0.05$), highlighted in grey. TolC is highlighted in bold type as well as three genes involved in cellular detoxification; glutathione-s-transferase, a Mar family transcriptional regulator and a thioredoxin, relevant to studies in chapter 7.

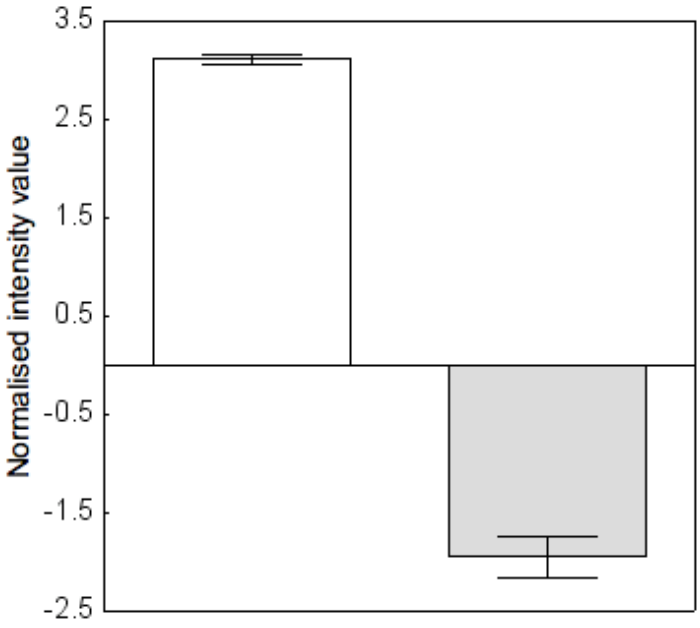

Figure 5.2. Expression of TolC, normalised to all other genes.

In wild type ☐ and *tolC*⁻ mutant. ▭. The normalised intensity values displaying TolC expression were obtained following microarray fold change analysis performed by GeneSpring GX software. TolC is significantly down regulated in the *tolC*⁻ mutant (fold change 33.38 X, two tailed t-test, $p<0.05$, $n=3$).

5.2.2. Summary of gene expression changes in the tolC⁻ mutant

To analyse global expression changes in wild type and *tolC*⁻ mutant, the expression changes determined by significance parameters are summarised in Table 5.2. 178 gene products show differential expression of 5 times fold change of more, but only 8 satisfy the parameters imposed by the unpaired t-test and multiple testing correction ($p<0.05$). Of these 8, one gene shows significant differential expression with a fold change greater than 10, this gene expresses TolC. The remaining 7 entities show a significant fold change greater than 5, all of which are increased (two intergenic regions and 1 hypothetical protein) (Table 5.3). Two proteins within this list are membrane associated O-antigen flippase and glycosyltransferase. The remaining protein with a less direct connection to TolC is the polar flagellin protein which has an increased expression of 5.6 within the *tolC*⁻ mutant.

5.2.3. Determining the effect of antibiotic selection on the tolC⁻ mutant transcriptome.

For accurate comparison of the wild type and *tolC*⁻ mutant transcriptomes only one variable (the strain) was changed. Antibiotic selection could not be used for the knockout mutant when drawing comparison to the wild type, particularly due to the nature of TolC as an antibiotic exporter. However, in order to determine the effect antibiotic selection has on global gene expression, RNA was extracted from the knockout mutant cultured with kanamycin (50 μg/ml) selection for subsequent microarray analysis. Fold change analysis was carried out between the two groups (3 x *tolC*⁻ mutant samples with antibiotic selection and 3 x *tolC*⁻ mutant samples without antibiotic selection). Of the total 8794, 1076 gene products show significant differential expression ($p<0.05$), with 16 displaying a fold change greater than 10 ($p<0.05$) (Table 5.4). The majority of these 16 gene products are involved in antibiotic resistance including arginine transporters. Despite a high number of expression changes between the *tolC*⁻ mutant cultured with kanamycin and without it, TolC does not show differential expression.

5.2.4 Identification of AcrB/D/F family antiporters in V. furnissii

Analysis was performed on wild type and *tolC*⁻ mutant transcriptomes to determine the presence of all AcrB/D/F type proteins interacting with TolC. A list of all potential proteins belonging to this family in *V. furnissii* was obtained from the Pfam database. This multiple sequence alignment enables identification of conserved domains giving functional regions of proteins with potentially similar functions. Nine proteins were identified by this procedure, the expression of which were investigated in the wild type and *tolC*⁻ mutant transcriptomes (Table 5.5.). A two tailed t-test was performed on the data but no statistical filters were applied to to enable visualistion of the fold change and p value of the nine gene products. Three of the nine proteins obtained from the Pfam

	Corrected p value		
	All	<0.05	<0.02
FC All	8974	**123**	11
FC >1.1	7612	123	11
FC >1.5	3328	110	10
FC >2.0	1505	68	6
FC >3.0	634	26	3
FC >5.0	178	8	1
FC >10.0	15	1	1

Table 5.2. Results summary of differential expression analysis between wild type and *tolC*⁻ mutant.

Determined by unpaired two tailed t-test asymptotic p-value computation and Benjamini-Hochberg multiple testing correction. 123 statistically significant entities filtered highlighted in bold.

Gene	Annotation	Reg. in *tolC*⁻	FC
vfu_A00859	outer membrane protein TolC	down	33.38
vfu_AI024	intergenic region	up	5.41
vfu_A01180	polar flagellin	up	5.56
vfu_AI012	intergenic region	up	5.80
vfu_A00113	ISSod6, transposase	up	6.87
vfu_A00119	glycosyltransferase	up	7.66
vfu_A00122	O-antigen flippase	up	8.03
vfu_A00123	hypothetical protein	up	9.24

Table 5.3. Genes showing significant differential expression with fold change (FC) greater than 5.

Of the 5 entities, 2 are intergenic regions and one hypothetical protein. All proteins, apart from TolC, show an increased expression in mutant.

	Corrected p value				
	All	<0.05	<0.02	<0.01	<0.005
FC All	8974	1076	399	140	29
FC >2	727	456	252	105	24
FC >5	46	43	35	23	10
FC >10	17	16	13	11	5

Table 5.4. The global effect of antibiotic selection on *V. furnissii tolC*⁻ mutant protein expression

Comparison if two sample groups: *tolC*⁻ mutant samples without antibiotic selection (kanamycin) and *tolC*⁻ mutant samples with antibiotic selection. All entities filtered on a volcano plot following statistical analysis (two tailed t-test), establishing those with a fold change (FC) over certain p value thresholds. P-values displayed are those following the Benjamini-Hochberg multiple testing correction.

Gene	Annotation	Reg. in *tolC*⁻	FC	p value
vfu_A00237	AcrB protein	up	1.04	0.77
vfu_B00431	Acriflavin resistance plasma membrane protein	down	1.6	0.057
vfu_A02663	Multidrug resistance protein, putative	up	1.06	0.47
vfu_A00253	Cation/multidrug efflux protein	down	1.12	0.3
vfu_A00178	Cation efflux system transmembrane protein	up	1.04	0.88
vfu_A00923	Cation/multidrug efflux pump	up	1.33	0.23
vfu_A01433	Putative cation efflux system transmembrane protein	down	3.2	0.01
vfu_A01666	Transporter, AcrB/D/F family	down	2.5	0.04
vfu_B00283	Transporter, AcrB/D/F family	down	2.36	0.04

Table 5.5. Proteins obtained from Pfam analysis of all AcrB/D/F type proteins present in *V. furnissii*.

Regulation in the *tolC*⁻ mutant and the fold change (FC) displayed with corresponding p value. Three genes show significant change in expression (two tailed t-test, $p<0.05$). All those significantly down regulated are highlighted in grey.

database showed significant decrease in the *tolC*⁻ mutant ($p<0.05$) (vfu_A01433, vfu_A01666 and vfu_B00283). The vfu_A00237 gene product shows greatest similarity to AcrB/D/F family proteins in other species (66% identity to *S.* Typhimurium AcrB and 62% to *E. coli* AcrB), however the expression of this gene is not altered in the *tolC*⁻ mutant. Decreased expression of antiporter proteins encoded by vfu_A01433, vfu_A01666 and vfu_B00283 in the *tolC*⁻ mutant suggests interaction of these proteins with TolC.

5.2.5 Identification and location of associated membrane fusion proteins

The gene encoding the membrane fusion protein (MFP) *acrA* is found within the same operon as *acrB* however *acrD* is located separately within the genome (Okusu *et al.*, 1996). Identifying potential MFPs within the same operon as the antiporter will help distinguish the proteins as either AcrB or AcrD. Flanking regions of the genes were analysed using Artemis. Vfu_A01666 and vfu_ B00283 (both of which show >90% similarity to the *V. cholerae* AcrB/D/F family) are adjacent to genes vfu_A01665 and vfu_B00284 respectively. These genes code for a HlyD family secretion protein (vfu_A01665) and an RND efflux family transporter, MFP subunit (vfu_B00284) showing >70% amino acid sequence similarity to MFPs in *V. cholerae* (Table 5.6). The HlyD family secretion protein and the RND efflux MFP subunit in *V. furnissii* display significantly decreased expression in the *tolC*⁻ mutant. This suggests vfu_A01666 is an AcrB transporter interacting with the HlyD family secretion protein (vfu_A01665) and similarly, vfu_ B00283 codes for an AcrB transporter interacting with RND efflux MFP subunit (vfu_B00284). Both AcrAB systems also appear to be interacting with TolC. The gene vfu_A01433, however, is contained within a copper/silver efflux coding operon containing 5 genes (vfu_A01432 to vfu_A01435) with an associated outer membrane spanning channel protein (vfu_A01435). Considering the expression change of vfu_01433 in the *tolC*⁻ mutant, the protein this gene codes for can be determined as an antiporter interacting with TolC. Given that the gene encoding this antiporter is not on the same operon as AcrA, suggests that this sequence encodes for an AcrD.

5.2.6. Sequence similarity of antiporters in V. furnissii

Within the *tolC*⁻ mutant, significant differential expression is observed in vfu_A01433, vfu_A0166 and vfu_B00283 gene products. To analyse if the amino acid sequences of these transporter proteins showed greater similarity to AcrB or close homologue AcrD in other bacteria, the amino acid sequences were aligned with AcrB and AcrD from *E. coli* and *S.* Typhimurium. Transporter proteins encoded by vfu_A01433, vfu_A0166 and vfu_B00283 in *V. furnissii,* and AcrB and AcrD amino acid sequences obtained from *E. coli* and *S.* Typhimurium*,* were aligned using BLAST and a phyologeny tree compiled (Fig 5.3A). The protein encoded by vfu_A01433 appears more closely

Gene	Annotation in *V. furnissii*	Similarity to *V. cholerae* HlyD secretion protein	Reg. in *tolC*⁻	FC	p value
vfu_A01665	HlyD family secretion protein	72%	down	5.05	0.01
vfu_B00284	RND efflux family transporter, MFP subunit	74%	down	1.56	0.045

Table 5.6. Determining potential membrane fusion proteins associated with transporter proteins.

Genes vfu_A01665 and vfu_B00284, adjacent to transporter protein encoding genes; vfu_A01666 and vfu_B00283, code for MFP proteins in *V. furnissii*. Amino acid sequences of the two MFPs show >70% identity to MFPs in *V. cholerae* (HlyD secretion proteins). Both the HlyD secretion protein and the RND efflux MFP subunit in *V. furnissii* are significantly down regulated in the *tolC*⁻ mutant, (two tailed t-test ($p<0.05$).

A

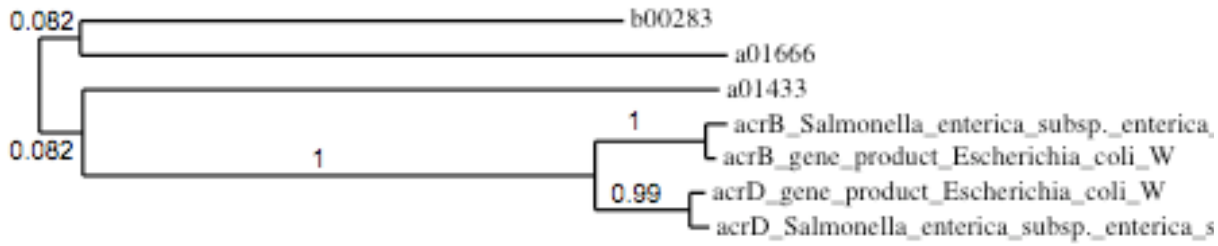

B

```
Vfu_01433 FHMRSSLVIALSLPVGILSAFIVMHWQGINANIMSLGGIAIAIGAMVDG 406
Vfu_01666 MGLRSGLLIGLILLLTVLGTFIFMQYFKIDLQRISLGALVIALGMLVDN 402
Vfu_00283 MGWREAIVVGLAVMVTLMITLFASWAWGFTLNRVSLFALIFSIGILVDD 376
Eco_AcrB  QNFRATLIPTIAVPVVLLGTFAVLAAFGFSINTLTMFGMVLAIGLLVDD 408
             *                                          *  **

Vfu_01433 VAVEIGVIMLVYLNQAWHYTKLKAQERQTNLTRQDLNDAIREGAGLRVR 977
Vfu_01666 MLLKNGIVLLDQIEIEMHS-------------GKDPYLAVVDASLSRVR 959
Vfu_00283 IIVRNSILLVDFIHQQVEQ-------------GVAFSEAVIQSAAVRAK 954
Eco_AcrB  LSAKNAILIVEFAKDLMDKE------------GKGLIEATLDAVRMRLR 973
                                           *       *
```

Figure 5.3. Determining RND transporter proteins present in *V. furnissii*

A. Phylogeny tree of three AcrB/D/F type proteins that show significant differential expression between the *V. furnissii* wild type and *tolC*⁻ mutant, aligned with AcrB and AcrD from *S.* Typhimurium and *E. coli*. vfu_A01433, isolated on separate branch with vfu_A01666, vfu_B00283 gene products showing greater similarity to AcrD in *E. coli* and *S.* Typhimurium.

B. Sequence alignment between the *V. furnissii* antiporters; vfu_01433, vfu_01666, vfu_00283 and AcrB from *E. coli.* Sections displayed containing functional Asp 407, Asp 408 and Lys 940 residues in *E. coli* AcrB are highlighted. Asp 407 conserved throughout all sequences, vfu_01433, only one residue conserved: Lys 940. Residues conserved in all four sequences (*).

related to AcrB and AcrD in *E. coli* and *S.* Typhimurium implied by the shorter branch length compared to vfu_A0166 and vfu_B00283, which are grouped together on a separate branch. This supports evidence that vfu_A0166 and vfu_B00283 genes encode for the same protein, AcrB and that vfu_01433 encodes for AcrD. Alignment of amino acid sequences encoded by vfu_A01666, vfu_B00283 and vfu_01433 and the *E. coli* AcrB sequence was performed to determine the presence of functional residues determined within *E. coli* AcrB (Asp 407, Asp 408 and Lys 940) established be site directed mutagenesis (Guan and Nakae, 2001, Murakami *et al.*, 2006). Two of the three residues are conserved in vfu_A01666 and vfu_B00283, however vfu_A01433 only shows one conserved residue (Asp 207) (Fig 5.3B). This further supports evidence that vfu_A01666 and vfu_B00283 are more closely related to AcrB and the remaining antiporter interacting with TolC is more likely to be an AcrD.

5.2.7. Expression of fatty acid synthesis genes is not altered within the tolC⁻ *mutant.*

This investigation has shown a higher level of fatty acids within *tolC*⁻ mutant cells compared to the wild type, that appeared to be caused by an accumulation of fatty acids within the mutant cells. To establish whether the detection of increased fatty acid levels within the mutant is due to a cellular build up or an increase in production, expression of fatty acid biosynthetic pathway genes in the wild type and the *tolC*⁻ mutant will be determined. Following the hypothesis that the FFAs detected are secreted by TolC, the regulation of the Fab pathway would not differ between the wild type and mutant. Proteins involved in the Fab pathway in *V. furnissii* were determined using the KEGG database (methods 2.23) (Fig. 5.4.). The overall expression of these genes in wild type and *tolC*⁻ mutant is displayed in a box-whisker plot showing no significant change in the regulation of this pathway ($p<0.05$) (Fig 5.4). Expression of TesAB and YciA, specifically involved in synthesis of hexadecanoic and octadecenoic acid, were also analysed for significant differential expression between the wild type and mutant however no changes were observed.

5.2.8 Determining the affect of the tolC mutation on virulence factor expression

For an overview of virulence factor expression in wild type *V. furnissii* and in the *tolC*⁻ mutant, known virulence gene sequences in *V. cholerae* (identified from Chun *et al* (2009)) were aligned against the non-redundant nucleotide database using BLAST to identify homologous sequences in *V. furnissii* (data acquisition carried out by Dr. Thomas Lux). Out of 439 virulent factors identified in *V. cholerae*, 162 displayed significant similarity (>60%) to proteins in *V. furnissii*. When analysing the whole transcriptome, 123 genes exhibit significant differential expression between the wild type and *tolC*⁻ (Table 5.1). The list of 162 virulence genes was compared to the group of 123 gene products showing differential expression between the wild type and mutant. 6 of the 162 virulence

Protein	Gene in *V. furnissii*
FabH	vfu_A00110, vfu_A01306, vfu_B00433
FabD	vfu_A01307
FabB	vfu_A01515, vfu_A01213
FabF	vfu_A01512, vfu_A01310
FabG	vfu_A01513, vfu_A00106, vfu_A01308, vfu_B00263, vfu_B01434, vfu_B01436
FabZ	vfu_A01080

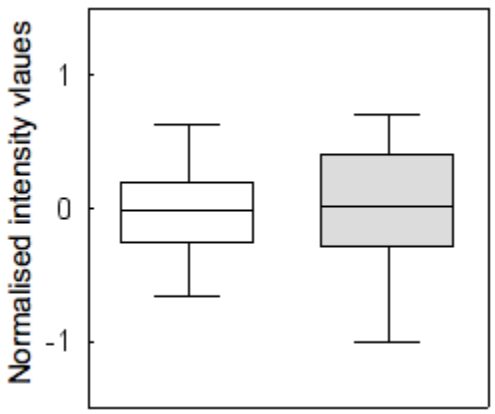

Figure 5.4. Fatty acid (FA) biosynthesis pathway genes present in *V. furnissii.*

FA proteins determined by the KEGG database and overall normalised expression established in wild type ☐ and *tolC*⁻ mutant ▭. Statistical analysis shows no significant difference in the expression of genes in the FA synthesis pathway between wild type and mutant (t-test, two tailed, p = 0.8898).

factors were present in the list, all of which show increased expression in the knockout mutant (Table 5.1 and Table 5.7.). Those increased by the greatest fold change (5.56 and 3.36) within the mutant, are associated with flagella assembly. The affect the *tolC* mutation has on motility and flagella assembly will be studied in detail in the following chapter. Notably, the expression of AphB, a virulence factor negatively regulated by HapR and closely associated with quorum sensing (Fig 5.1) is significantly increased in the *tolC*⁻ mutant (Table 5.7 and Table 5.1).

Following analysis of individual virulence associated gene expression, overall expression changes of these virulence factors between the wild type and *tolC*⁻ mutant was investigated. 62 of the 162 virulence factors showed significant differential expression between wild type and mutant fulfilling statistical parameters (uncorrected p value<0.05). Despite some fundamental virulence factors displaying significant differential expression in the mutant, statistical analysis shows that overall this difference is not significant (two tailed, paired t-test p<0.05) (Fig 5.5).

5.2.9 Virulence factor regulation by LuxR

It was observed that AphB is among the 123 significantly differentially expressed sequences in *V. furnissii* wild type and mutant. AphB is a significant virulence factor, negatively regulated by LuxR (Fig. 5.1.) and notably, the increased expression of AphB in the *tolC*⁻ mutant correlates with the decreased expression of LuxR. This finding supports evidence that the association between TolC and virulence factors such as biofilm formation and motility is connected by quorum sensing regulations. To investigate the expression of additional virulence factors regulated by quorum sensing in *V. furnissii*, those proteins displayed in Fig 5.1, obtained from the KEGG database, were analysed for differential expression in wild type and *tolC*⁻ mutant. ToxT, TcpHP are not conserved in *V. furnissii* (established by BLAST analysis of amino acid sequences). Expression of ToxRS is not altered significantly in the mutant but AphA and AphB both show similar increases in expression within the mutant (1.27 and 1.26 fold change respectively) (Table 5.8). Increase in expression of AphA and AphB in the mutant is only significant in AphB (unpaired t-test, p<0.05). HapA, another significant virulence factor, displays the highest fold change increase in the mutant (1.49) but this does not satisfy the significance parameters (p<0.05).

Gene	Annotation	Change in regulation in *tolC*⁻	
vfu_B01043	conserved hypothetical protein	1.7	UP
vfu_A02550	AphB/LysR family protein	1.26	UP
vfu_A02736	SsrA-binding protein	1.9	UP
vfu_A01897	hypothetical protein	1.79	UP
vfu_A01180	polar flagellin	5.56	UP
vfu_A01132	flagellin	3.36	UP

Table 5.7. Differential expression of virulence factors.

Differential expression of the 162 virulence factors was determined between wild type and *tolC*⁻ mutant showing 6 genes with a significant difference in regulation (two tailed t-test, corrected p value<0.05 taken from Table 5.4). All of the 6 virulence associated genes show a significant increase in expression in the *tolC*⁻ mutant.

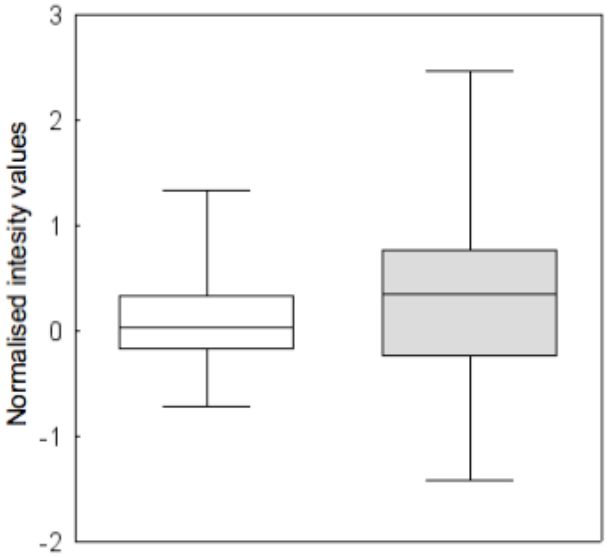

Figure 5.5. Normalised expression of 62 virulence factors

Expression of virulence factors, normalised to all other genes, determined in *V. furnissii* wild type ▭ and *tolC*⁻ mutant ▭ and presented as a box whisker plot. Lowest and highest normalised intensity values are indicated by the end of the whiskers. Results show that despite individual genes displaying siginificant differential expression between the wild type and mutant (indicated by whiskers) statistical analysis shows overall the expression of virulence factors in mutant is not altered significantly, p=0.11 (two tailed, t-test, p<0.05).

Protein	Gene in *V. furnissii*	Change in regulation in *tolC*⁻ mutant		p value
ToxR	vfu_A02616	1.06	down	0.8
ToxS	vfu_A02617	1.19	up	0.7
AphA	vfu_A00617	1.27	up	0.11
AphB	vfu_A02550	1.26	up	$8x10^{-7}$
HapA	vfu_B00520	1.49	up	0.07

Table 5.8. Differential expression of virulence factors regulated by LuxR

Fundamental virulence factors AphA and AphB show increased differential expression in *tolC*⁻ mutant, statistically significant in the AphB (two tailed t-test, $p<0.05$), highlighted in grey. ToxRS and HapA expression is not significantly altered in the mutant.

5.3. DISCUSSION

Data in this chapter were obtained from investigation of differential expression between wild type *V. furnissii* and the *tolC*⁻ mutant. As expected the expression of TolC is significantly decreased in the mutant (by a reduction factor of 33.38) resulting in significant changes in the expression of 123 other genes (Table 5.1). This is similar to *S.* Typhimurium *tolC*⁻ mutants, where 171 genes showed differential expression, in contrast expression of over 1500 genes in *S. meliloti tolC*⁻ mutants were altered, the majority of which showed increased expression (Webber *et al.*, 2009, Santos *et al.*, 2010). When comparing the *tolC*⁻ mutant transcriptomes cultured with and without antibiotic selection, the number showing significant differential expression was higher, at 1076 ($p<0.05$) (Table 5.4), confirming that there kanamycin has a significant effect on global gene expression within the mutant. Comparison of gene expression in wild type and *tolC*⁻ mutant shows that O-antigen flippase and glycosyltransferase exhibit a large differential expression (fold change>5) (Table 5.3). Flippase proteins are involved in membrane formation and glycosyltransferases are involved in glycosidic bond formation, found in membrane bound proteins such as TolC. The reason for increased expression of these proteins in the *tolC*⁻ mutant could be attributed to changes to the membrane structure caused by the mutation, leading to increased expression of membrane forming proteins as a compensatory mechanism. Among the list of entities with a fold change greater than 5 was another hypothetical protein, the gene coding for this (vfu_A00123) is adjacent to the O-antigen flippase gene (vfu_A00122) and closely associated the glycosyltransferase and transposase gene (vfu_A00119 and vfu_A00113 respectively) (Table 5.3) suggesting expression changes in these genes are also a direct result of changes to the struture of the membrane caused by the mutation. Similar protein disruptions have been observed in *S.* Typhimurium *tolC*⁻ mutants (Webber *et al.*, 2009).

AcrB and AcrD proteins from *E. coli* have a sequence similarity of 66% and both act as membrane bound transporters interacting with OMPs, however, it is important to define these proteins within bacteria as substrate specificity varies (Rosenberg *et al.*, 2000, Elkins and Nikaido, 2002). Difference in substrate specificities is significant when confronting increasing antimicrobial resistance achieved by MDR efflux systems. Products of three *acrB/D/F* homologues showed decreased expression in the mutant; vfu_01433, vfu_A01666 and vfu_B00283 (Fig 5.3A). Two of these genes (one on each chromosome) appear to be in independent operons with genes encoding MFPs (vfu_01666 and vfu_B00283), suggesting these may function as AcrB proteins. This possibility is supported by amino acid sequence alignment confirming conservation of two of three functional domains in AcrB (Fig. 5.3B) (Guan and Nakae, 2001, Murakami *et al.*, 2006). Although not as widely researched as AcrB, AcrD behaves in a similar way, interacting with AcrA and

obtaining substrates from the periplasm, evidenced in *E. coli* (C. A. Elkins and H. Nikaido, 2002) and *S.* Typhimurium (Yamasaki *et al.,* 2011).

Analysis of the suspected *V. furnissii* transporters expressed by vfu_A01433, vfu_A01666 and vfu_B00283 helped to identify the nature of these proteins as AcrB or AcrD. The vfu_A01666 and vfu_B00283 genes are both in operons with a MFP (vfu_A01665; an HlyD family secretion protein and vfu_B00284; an RND efflux MFP subunit respectively) (Table 5.6), suggesting these are AcrB type proteins. The vfu_A01433 gene product however, is not associated with an MFP protein within the genome and is therefore more likely to an AcrD. Phylogenetic analysis and sequence alignment confirm that vfu_A01666 and vfu_B00283 gene products are more closely associated than the protein expressed by vfu_A01433. Furthermore, of the three functional amino acid resisdues conserved in AcrB from *E. coli* (Asp 407, Asp 408 and Lys 940) (Guan and Nakae, 2001, Murakami *et al.*, 2006), vfu_A01666 and vfu_B00283 gene products display two conserved residues and vfu_A01433 only shows one (Fig 5.3B). These data support evidence in chapter 3 that resistance to different antibiotics is conferred by both AcrB and AcrD in *V. furnissii* and that vfu_A01666 and vfu_B00283 code for AcrB and vfu_A01433 codes for AcrD.

Data presented in this chapter confirm FFAs are substrates of AcrAB-TolC and/or AcrAD-TolC. The presence of fatty acid biosynthesis genes required for synthesis of C_{16} and C_{18} fatty acids as well as unsaturated fats were determined in *V. furnissii*. Analysing differential expression of these proteins in wild type and the *tolC*⁻ mutant showed that there are no significant changes within this pathway (Fig 5.4). This finding supports our previous observation that there is not an increase in production of fatty acids in the mutant but that the fatty acids are retained due to lack of functioning TolC.

TolC has been recently shown to alter virulence gene expression in *V. cholerae* (Minato *et al.*, 2011). Out of 123 gene products showing significant differential expression, 6 show significant similarity to virulence factors in *V. cholerae* and all of these display increased expression in the *tolC*⁻ mutant (Table 5.6). The increased regulation of virulence factors is a possible compensatory mechanism as literature strongly suggests that *tolC*⁻ mutants result in less virulent phenotypes e.g. AcrAB-TolC disruptions in *S.* Typhimurium reduces host colonization (Buckley *et al.*, 2006). Data associated with quorum sensing also show that overexpression of efflux systems results in reduced virulence in *P. aeruginosa* (Sánchez 2002). Overall, expression of virulence factors are not significantly altered in *V. furnissii* (Fig 5.5), however, the *tolC* mutation does subsequently alter

expression of some significant virulence regulators, in particular AphB associated with quorum sensing (Table 5.8).

ToxT, TcpP and TcpH are not conserved within *V. furnissii*, but ToxR, AphA and AphB all showed increased expression within the *tolC*$^{-}$ mutant (Table 5.8). AphB is a fundamental protein in a virulence cascade in *V. cholerae* (Xu *et al.,* 2010) (Fig 5.1) which shows a significant increase in expression in the *tolC*$^{-}$ mutant. Although AphA expression is not significantly altered, similarities in the fold change in gene product expression between AphA and AphB (1.27 and 1.26 respectively) and the close interaction of these proteins, makes this result relevant. AphB is a virulence factor negatively regulated by LuxR and the increase in AphB expression in the mutant corresponds with the decrease in LuxR expression (1.46 fold decrease in the mutant). These expression changes support the hypothesis that phenotypic differences associated with virulence, observed in *tolC*$^{-}$ mutants, are related by the quorum regulatory pathway. Hypothetically, in *tolC*$^{-}$ mutant cultures there are fewer autoinducer molecules being released resulting in the repression of LuxR and the triggering of virulence gene expression. Furthermore, the flagella assembly pathway appears to be down regulated in the mutant (Table 5.1). Investigation into expression of genes involved in flagella assembly and differences in wild type and *tolC*$^{-}$ mutant cell motility will be carried out in the following chapter.

The global expression changes observed in the mutant support evidence that TolC is intrinsicly linked to a number of pathways (Zgurskaya *et al.*, 2011), however how these pathways are linked is not clear. It is possible that virulence factors controlled by quorum sensing (e.g. ToxT, AphB) are directly affected by TolC expression, leading to changes in the Lux pathway and ultimately signalling compound synthesis and/or secretion. Alternatively, TolC due to its function as a membrane bound export protein, is more closely linked to signalling molecule expression or direct export (as previously discussed in chapter 4) and this in turn alters the regulation of virulence factors. Quorum sensing regulates biofilm formation and colonization of host cells which are phenotypes previously observed in *S.* Typhimurium *tolC*$^{-}$ mutants (Buckley *et al.*, 2006). These data show that it is the disruption to the quorum sensing pathway in *V. furnissii tolC*$^{-}$ mutants that connects mutations in *tolC* and reduced expression of virulence factors. The same connection to quorum sensing could explain reduced biofilm formation and impaired adhesion to host cells in *tolC*$^{-}$ mutants in clinically relevant bacteria such as *S.* Typhimurium and *V. cholerae.*

It has been recently suggested that phenotypic changes arising from mutations in *tolC* are a direct result of membrane damage (Santos *et al.*, 2010). Subsequent oxidative stress is a potential

explanation for compensatory mechanisms, making a direct connection between *tolC* and subsequent gene expression changes difficult. There are changes in expression of genes relating to membrane stress; thioredoxin and glutathione–s-transferase are enzymes which assist bacteria in coping with oxidative stress and both show increased expression in the *tolC*$^-$ mutant (Table 5.1). In addition a MarR family protein is up regulated in the mutant, the Mar family are associated with *tolC* and cellular detoxification (Rosner and Martin, 2009). Given the considerable regulatory changes which occur in the *tolC*$^-$ mutant, investigating the impact of membrane stress should be considered as a reason for some of the phenotypic changes observed and will be studied further in chapter 7.

Despite evidence that a number of phenotypic changes may be directly due to expression changes and not a direct link to the function of TolC as an exporter, the accumulation of C_{16} and C_{18} FFAs appears to be a genuine phenotype. Data here support recent evidence that analysis of subsequent expression changes in *tolC*$^-$ mutants is necessary when analysing experimental evidence (Webber *et al.*, 2009, Santos *et al.*, 2010, Zgurskaya *et al.*, 2011).

CHAPTER 6 – TOLC⁻ MUTATION RESULTS IN REDUCED MOTILITY

6.1. INTRODUCTION

Differential expression analysis of *V. furnissii* wild type and *tolC*⁻ mutant transcriptomes displayed significant changes in flagella gene expression. Flagella protrude from cells into the extracellular environment, primarily enabling cell motility and responding to environmental stimuli. Similarly to TolC, regulation of flagella protein expression leads to transcriptional regulation of other virulence associated factors (Syed *et al.*, 2009). The pathogenicity of monotrichous *V. cholerae* is attributed to its singular flagellum and subsequently motile nature (Richardson, 1991). In Gram-negative bacteria flagella are anchored to a basal body via a series of rings, integrated in both the inner and outer membranes (Fig. 6.1). Assembly of the flagella proteins requires export through the inner membrane which is achieved by the type III secretion system (Macnab, 2004).

The connection between TolC and motility has been recently recognised however the relation between them is unclear. Within *Sinorhizobium meliloti tolC*⁻ mutants, increased expression of flagella proteins encoding the basal body, L and P rings, hook filament and motor switch was determined (Santos *et al.*, 2010). Increased swarming was also shown in the *S. meliloti tolC*⁻ mutant although swimming motility was not altered. By contrast, transcriptome analysis of *S.* Typhimurium *tolC*⁻ and *acrB*⁻ mutants compared to the parent strain, showed significant *decreased* expression of proteins involved in motility, including the *flgLMK* operon. Within the *acrB*⁻ mutants, fewer flagella were displayed on electron micrographs and decreased motility on minimal agar was observed (Webber *et al.*, 2009). Of 123 proteins showing differential expression between the wild type and *tolC*⁻ mutant in *V. furnissii,* 13 were associated with flagella assembly and 12 showed increased expression within the mutant (Table 5.1). Experimental evidence is required to determine if the changes in flagella expression results in a phenotypic change.

Although determining the genes with the most significantly altered expression is a suitable method for direct comparison of the two transcriptomes, further analysis into flagella protein expression is required. Flagella assembly is a complex process, comprising nearly 50 genes in *S.* Typhimurium and *E. coli* and many loci consist of several genes (Iino *et al.*, 1988, Jones and Macnab, 1990, Kubori *et al.*, 1992). Changes in expression of individual proteins may not appear significant but considering these differences in the context of an entire system will give a better idea of overall expression changes in motility associated proteins. This study aims to look in detail at changes in flagella protein expression as a result of the *tolC* mutation.

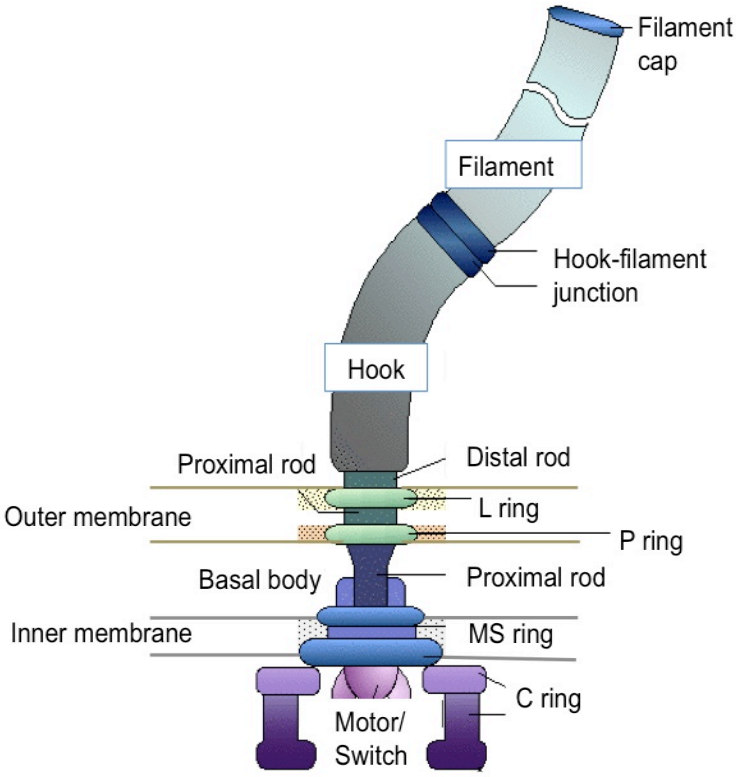

Figure 6.1. Representation of flagella assembly in Gram-negative bacteria.

Diagram adapted from the KEGG pathway database shows flagella spanning both the inner and outer membranes.

6.2. RESULTS

6.2.1 Identifying functions of flagella proteins showing differential expression

In order to confirm the function to the 13 flagella proteins showing differential expression between wild type and *tolC*- mutant, the amino acid sequences were compared directly with the GenBank non-redundant protein database using BLASTp. The gene and protein name are summarised in Table 6.1 with the expression change in the mutant. Notably, the one flagella gene showing decreased expression in the *tolC*- mutant is a co-expresser of a protein also showing increased expression (FlgG). Motility is fundamental in bacterial virulence and the flagella protein showing the greatest increase in expression (FliC; 5.36 fold change increase in the mutant) is also expressed in *V. cholerae* and is classed as a virulent determinant within this bacterium (Chun *et al.*, 2009) (Table 6.1).

6.2.2 Mapping the flagella proteins showing differential expression

The flagella proteins in Table 6.1 were mapped using the flagella assembly pathway on the KEGG database (vfu_02040) (methods 2.23) in order to determine the location of the proteins encoded by those genes showing increased differential expression in the *tolC*- mutant. Notably, FliC which showed the greatest fold change, can be identified as an extracellular filament (Table 6.1, Fig 6.2). The majority of proteins with increased expression are involved in the extracellular assembly of the flagella or are associated with the cell membrane, FlgBCFG proteins are specifically required for assembly of the membrane integrated basal body which all show increased expression in the *tolC*- mutant (Fig 6.1 and 6.2). To identify all flagella proteins in *V. furnissii,* a list of assembly genes were obtained from the KEGG pathway “vfu_02040” (methods 2.23) and were subsequently identified and located within the genome using Artemis. The 68 flagella encoding genes can be separated into four clusters adjacent within the genome, the intracellular, extracellular or membrane bound nature of the proteins was ascertained from the KEGG database (appendices, Table 8.3). This confirmed that the genes showing significant differential expression in the *tolC*- mutant code for extracellular or membrane bound proteins, furthermore is showed that these genes are in one of four clusters.

6.2.3 Visualisation of flagella by transmision electron microscopy (TEM).

To identify if increased expression of the 12 flagella proteins in the *tolC*- mutant results in increased motility, wild type and mutant cells were analysed by transmission electron microscopy (TEM).

Bacteria were cultured to exponential phase and fixed for microscope visualisation (methods 2.33). Images representative of microscope obervations show wild type cells with in tact flagella and *tolC*$^{-}$

Gene	Description	Protein	FC	Regulation in *tolC*$^{-}$ mutant
vfu_A01121	flagella basal-body rod protein	FlgB	3.50	up
vfu_A01122	flagella basal-body rod protein	FlgC	3.75	up
vfu_A01123	flagella basal body rod modification protein D	FlgD	2.93	up
vfu_A01124	flagella hook protein	FlgE	3.07	up
vfu_A01125	flagella basal body rod protein	FlgF	3.38	up
vfu_A01126	flagella basal body rod protein	FlgG	3.37	up
vfu_A01127	flagella L-ring protein	FlgH	2.93	up
vfu_A01132	**flagellin**	**FliC**	**3.36**	**up**
vfu_A01180	**polar flagellin**	**FliC**	**5.56**	**up**
vfu_A01182	flagella protein	FlaG	3.25	up
vfu_A01189	flagella hook-basal body complex protein	FliE	1.62	up
vfu_A01196	flagella basal body-associated protein	FliL	1.59	up
vfu_A01361	flagella basal-body rod protein	FlgG	2.06	down

Table 6.1. List of flagella proteins showing significant differential expression between wild type and *tolC*$^{-}$ mutant.

Gene annotations vfu_A01132 and vfu_A01180 (highlighted in bold) show >60% similarity to virulence associated proteins in *V. cholerae* (Table 5.7.).

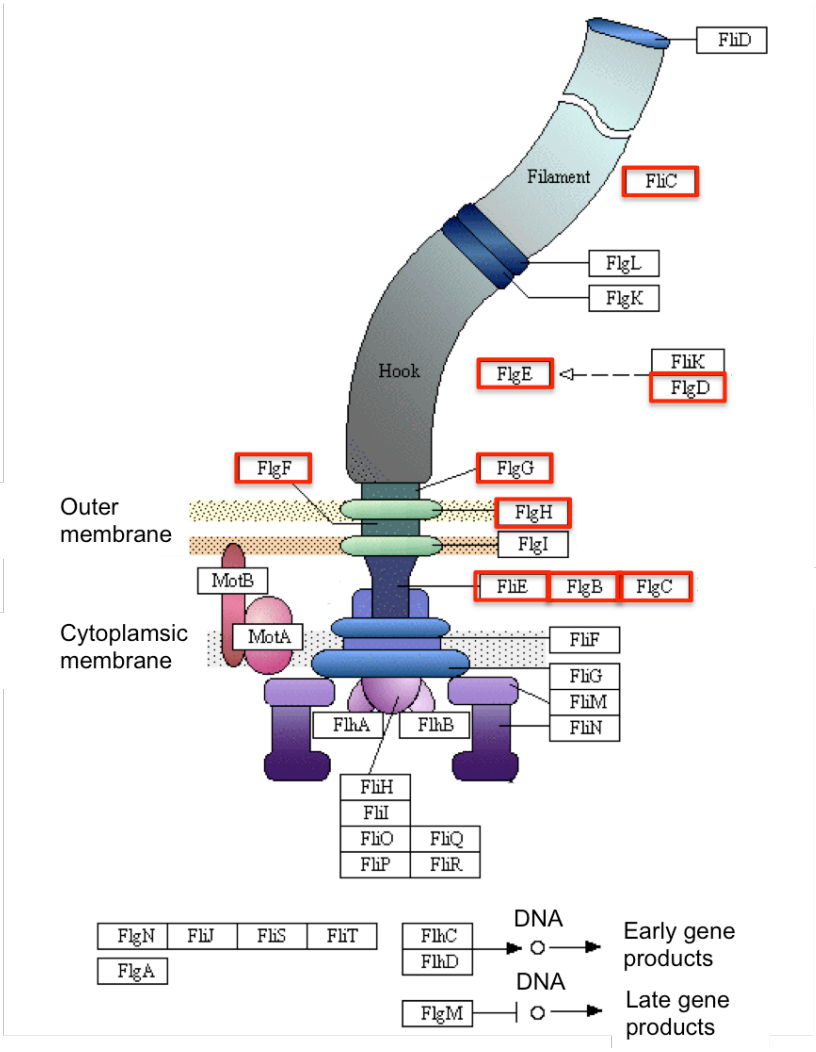

Figure 6.2. Adapted KEGG diagram of flagella assembly proteins.

All proteins are expressed in *V. furnissii,* those with increased expression in *tolC*⁻ mutant highlighted in red.

mutant cells with missing flagella (Fig 6.3A and B). Accurate numerical analysis could not be obtained from the images due to the fragility of the flagella, the breaking of which may have occurred during sample preparation. However, more cells appeared to contain in tact flagella in the wild type cultures and the images presented were a typical representation of the sample (Fig 6.3A). In addition images confirm that *V. furnissii* is a monotrichous bacterium; producing only one flagellum. These experimental data show that despite the significant increased expression of 12 flagella genes in the *tolC*$^{-}$ mutant, flagella assembly is not as successful as in the wild type.

6.2.4. Cell motility in wild type and tolC^{-} *mutant*

Experimental investigation into wild type and *tolC*$^{-}$ mutant motility was subsequently undertaken by analysing the ability for cells to migrate across semi solid agar. L.B. agar plates were made containing two difference concentrations of agar (0.25% and 0.5%) and inoculated and incubated for 24 h. The *tolC*$^{-}$ mutant colony size is markedly smaller implying decreased motility (Fig 6.4A). Colony size was measured on multiple plates and summarised (Fig 6.4B) showing the difference to be significantly greater on both 0.25% and 0.5% agar (two tailed t-test $p<0.05$). The experiment was also carried out using a sterile loop for inoculation and bacteria straight from glycerol stocks, this yielded the same results although an additional 12 h incubation was required. This result is consistent with the TEM imaging showing decreased flagella expression in the *tolC*$^{-}$ mutant and shows that despite significant increased expression of 12 flagella genes in the mutant, overall, motility is decreased.

A B

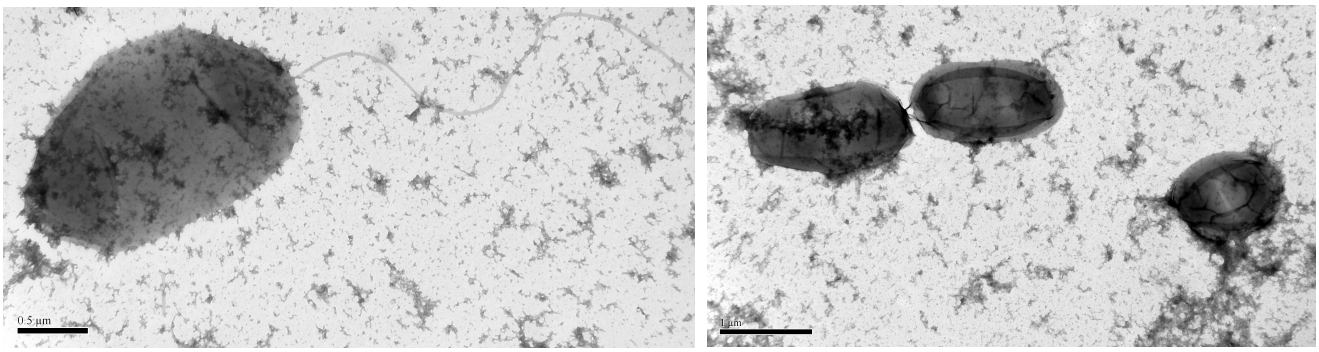

Figure 6.3. Transmission electroscopy microscope images of flagella

A: wild type and B: *tolC*⁻ mutant exponential phase cultures. Images display in tact flagellum in wild type and absent in *tolC*⁻ mutant.

A B

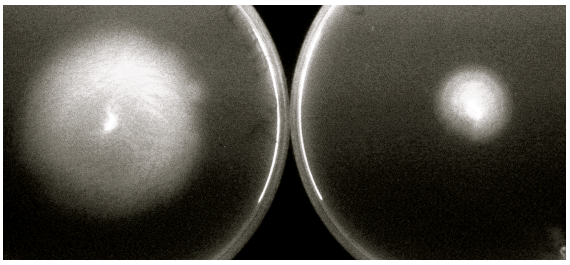

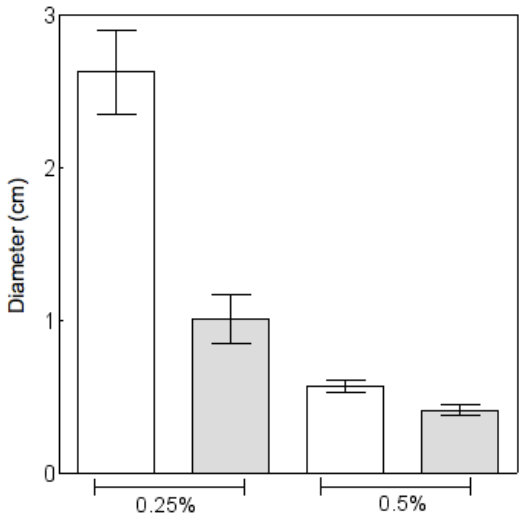

Figure 6.4. Cell motility assay.

A: Wild type (left) and *tolC*⁻ mutant (right) grown on L.B. plates (0.25% agar). Wild type colony size is notably larger than the mutant colony.

B: Colony size measurements after 24 h in 0.25% and 0.5% L.B. agar. *V. furnissii* wild type ▭ and *tolC*⁻ mutant ▭ (n=6). Difference between wild type and *tolC*⁻ mutant is significant on both 0.25% and 0.5% agar (two tailed t-test, $p<0.05$).

6.3. DISCUSSION

Experimental data obtained from *V. furnissii* wild type and *tolC*⁻ show that the mutation in *tolC* results in decreased motility, consistent with data obtained in *S.* Typhimurium (Webber *et al.*, 2009). Twelve flagella assembly genes showed a significant increase in expression in the *tolC*⁻ mutant compared wild type during initial global transcriptome fold change analysis. However, results in this chapter show that this does not result in increased motility (Fig 6.4). TEM displayed fewer intact flagella in *tolC*⁻ mutant cells within *V. furnissii* (Fig 6.3) and the distance the mutant migrated over semisolid agar was found to be at least 50% less than the wild type (Fig 6.4). Further analysis by light microscopy could also be used to identify the motility of the cells. It should also be considered that growth conditions for TEM visualization differed to the growth conditions for RNA extraction. For TEM imaging, the bacteria were cultured in M9 minimal media (as opposed to L.B. for RNA extractions) as it was not possible to visualise the flagella when bacteria were cultured on L.B. media. This variable should be noted, however, the motility assay on L.B. agar is consistent with the data. For clarity of individual cells, the images shown in Fig 6.3 are from exponential phase cultures, however, the bacteria were also observed at late exponential phase and flagella assembly still appeared unsuccessful in the *tolC*⁻ mutant.

Flagella assembly is a complex process, and in *V. furnissii,* there are 68 flagella genes arranged into four clusters on chromosome 1 (appendices, Table 8.3)*,* similarly, *S.* Typhimurium is reported to have at least 50 flagella genes also separated into four clusters (Kutsukake *et al.*, 1990). The flagella genes showing significant increase in expression in the *V. furnissii tolC*⁻ mutant express proteins closely associated with the membrane or are located extracellularly (appendices, Table 8.3, Fig. 6.2). Given the evidence that motility is decreased, the increase in extracellular protein expression may be compensation due to mis-assembly of flagella. Within *Sinorhizobium meliloti tolC*⁻ mutants, motility gene expression was increased (Santos *et al.*, 2010), however, within *S. meliloti* the factor increase of flagella expression in the *tolC*⁻ mutant was considerably greater than the 12 flagella proteins showing increased expression in the *V. furnissii tolC*⁻ mutant. Membrane bound FlgF and FlgG genes displayed an increased expression of 15.64 and 11.03 fold consecutively in *S. meliloti tolC*⁻ mutants (compared to a 3.38 and 3.37 fold increase in *V. furnissii)* (Table 6.1) however, increased swimming motility in the *S. meliloti tolC*⁻ mutants was not observed (Santos *et al.*, 2010).

As implied by recent studies, multiple transcriptional regulatory elements are affected by *tolC*⁻ mutants and it is now thought that most of these are due to membrane damage and oxidative stress caused by the mutation (Santos *et al.*, 2010, Zgurskaya *et al.*, 2011). Findings in this study

support evidence that this particular phenotypic change is a likely outcome of structural changes to the membrane possibly caused by the mutation. In *V. furnissii,* those proteins being up regulated are largely membrane bound (expression of FlgBCFG in particular are among those with the greatest increased fold change in the *tolC*$^{-}$ mutant) (Table 6.1), suggesting a stress-induced reaction to loss of membrane integrity. This is also discussed in relation to motility gene expression changes in *S. meliloti,* notably those genes with the greatest increase in expression in *tolC*$^{-}$ mutants code for MotA, FlgF, FlgC, FlgG and FlgB (Santos *et al*., 2010). FlgBCFG are intrinsicly linked to the cell membrane and are integral to the stability of the complex as determined in *S.* Typhimurium (Jones and Macnab, 1990) (Fig 6.2). These proteins are transported across the inner membrane and co-assemble to form the basal rod, although until assembled this structure is not particularly stable (Jones and Macnab, 1990, Kubori *et al.*, 1992). This further supports the hypothesis that loss of membrane integrity in the *tolC*$^{-}$ mutant would primarily lead to a dysfunctional basal rod assembly. The increased expression of these specific proteins observed in both *V. furnissii* and *S. meliloti tolC*$^{-}$ mutants can therefore be explained as a compensatory response for the mutation. Ultimately, in *V. furnissii tolC*$^{-}$ mutants this response mechanism is unsuccessful and flagella assembly is impaired, resulting in decreased motility. Compromised flagella assembly in *tolC*$^{-}$ mutants would provide one explanation for reduced pathogenicity in *tolC*$^{-}$ mutants. These data suggest that targeting TolC as part of the RND efflux system for antimicrobial drug development is not only supported by its role in antibiotic export but also reduced cellular motility which occurs following disruption of the TolC function.

CHAPTER 7 - THE ROLE OF TOLC IN CELLULAR DETOXIFICATION IN *VIBRIO FURNISSII*

7.1. INTRODUCTION

Multiple factors lead to observed changes in pathogenicity, motility and quorum sensing in *tolC*$^-$ mutants and it has been postulated that these phenotypes are all a consequence of oxidative damage to the cell membrane (Santos *et al.*, 2010, Zgurskaya *et al.*, 2011). Mutations in *tolC* within *E. coli* and *S.* Typhimurium result in increased expression of the *marA/soxSR*/*rob* regulon which is responsible for combating superoxides (Tsaneva and Weiss, 1990, Rosner and Martin, 2009, Webber *et al.*, 2009). Superoxides, capable of inflicting huge amounts of cellular damage, are toxic by-products resulting from a number of metabolic processes, including those induced by oxidative stress. Enzymes such as glutathione reductase, glutathione-S-transferase, superoxide dismutase and thioredoxins are involved in cell detoxification (Imlay, 2008) and expression of glutathione reductase and superoxide dismutase in particular is associated with OMP TolC. Within *Sinorhizobium meliloti* regulation of these detoxifying enzymes is increased in *tolC*$^-$ mutants and it is thought that this is a response to oxidative stress caused by the mutation (Santos *et al.*, 2010). Furthermore, within *E. coli,* depleted glutathione occurs due to growth defects following the disruption of TolC (Dhamdhere and Zgurskaya, 2010). Transcriptome analysis of the wild type *V. furnissii* and *tolC*$^-$ mutant supports evidence of a connection between TolC expression and regulation of detoxifying enzymes. Within the *tolC*$^-$ mutant a 2.8 fold increase in expression of fundamental detoxification enzyme glutathione-s-transferase is observed, as well as a 3.83 fold increase in expression of a thioredoxin and 2.36 fold increase in expression of a transcriptional regulator (Mar family protein) (Table 5.4). How the expression of TolC and the regulation of *soxRS* and detoxification enzymes are connected is not clear. Given the role of TolC as an exporter of toxic substrates, it is possible that *tolC*$^-$ mutant cells preempt a build up of toxins and employ detoxification mechanisms. However, the increase in MarA/SoxRS expression and superoxide combating enzymes may also be a compensatory mechanism resulting from oxidative stress caused by the *tolC*$^-$ mutation (Zgurskaya *et al.*, 2011). This work aims to test the *tolC*$^-$ mutants capability to deal with increased superoxide levels in order to determine how detrimental the mutation is to cell survival under increased oxidative stress.

Selenate and selenite are toxic anions reduced by some bacteria to produced red elemental selenium and this process results in superoxide production (Kessi *et al.*, 1999, Kessi and Hanselmann, 2004) (Fig 7.1). Introducing selenite into cultures induces superoxide production and tests the cells ability to cope with increased oxidative stress. Glutathione-s-transferase is up

regulated in the *V. furnissii tolC*$^-$ mutant and is a major cellular detoxification enzyme, responsible for dispelling endogenous and exogenous toxins (Fig 7.2) (Wilce and Parker, 1994, Leiers *et al.*, 2003). Members of the *soxSR* regulon are also upregulated in the presence of selenite, increasing the cells tolerance to the toxic anion (Bébien *et al.*, 2002). Culturing bacteria in the presence of selenite and monitoring selenium production provides a quantitative and colourmetric assay for comparing superoxide resistance in the wild type and *tolC*$^-$ mutant.

There is extensive evidence for the process by which bacteria reduce selenium anions. For example, in the well characterised selenate respirer *Thauera selenatis* (Macy *et al.*, 1993) selenate is used as an electron acceptor. This process initially involves the reduction of selenate to the more toxic selenite anion which is ultimately metabolised to form selenium (Fig. 7.1). Non-selenate respiring bacteria such as *Desulfovibrio desulfuricans* reduce selenium anions by way of detoxifying the cell, although less is known about this process (Tomei *et al.*, 1995). Characterisation of selenate and selenite reducing bacteria show that gamma proteobacteria rich in glutathione are typical of such species capable of reducing selenium anions. Glutathione plays an important role in selenium oxyanion detoxification which was determined in *Rhodospirilliem rubrum* by showing that the rate of selenite reduction was decreased when bacteria synthesised lower than normal levels of glutathione (Kessi *et al.*, 1999). A series of reactions have been proposed for the reaction between selenite and glutathione (Painter, 1941, Ganther, 1970, Kessi and Hanselmann, 2004) and investigation into selenite reduction in *R. rubrum* led to the proposal that the initial step results in the production of superoxide anions (Fig 7.1) (reaction 1). Degradation of superoxides is catalysed by enzymes that are upregulated when bacteria experience oxidative stress (Bébien *et al.*, 2002). In addition, glutathione reductase and thioredoxin reductases are required for reduction of the intermediatry selenium glutathione complex (Fig 7.1). The ability for *Vibrio* species to reduce selenite has not been investigated. Glutamate–cysteine ligase and glutathione synthetase genes are present within the *V. furnissii* genome which infers that this bacterium is capable of glutathione production. Furthermore, *V. furnissii* is a gamma proteobacterium, generally present in oxic marine conditions and is therefore likely to be capable of selenite reduction to selenium. Selenite resistance varies between bacteria (Burton Jr *et al.*, 1987) but the reason for this variance is not established. Determining selenite resistance in *V. furnissii* may therefore help to explain what links bacteria that possess high and low resistance to the toxic anion.

The process by which the insoluble elemental selenium products are exported from bacterial cells is not fully understood and given the nature of TolC it is worth considering that direct transport may occur. Intracellular and extracellular selenium have been discovered in a number of species and

transmission electron microscopy has identified cytoplasmic selenium in *R. rubrum* (Kessi and Hanselmann, 2004) and *D. desulfuricans* (Tomei *et al.*, 1995). Within some selenate respiring bacteria, selenium particles are observed intracellularly and extracellularly, for example, *E. cloacae* SLD1a-1 (Losi and Frankenberger Jr, 1997) and *T. selenatis* (Debieux *et al.*, 2011). RND efflux pumps have been attributed to export of other inorganic compounds, however export of insoluble inorganic products like selenium via the AcrAB-TolC efflux pump has not yet been investigated. Losi and Frankenberger (1997) suggest that selenium is expelled by a membrane efflux pump although little has been discovered about the ability for TolC to accommodate such large inorganic molecules. It has also been suggested that selenium particles are released via cell lysis (Tomei *et al.*, 1995) and that associated proteins are required for the export of the nanoparticles (Debieux *et al.*, 2011). Given the toxic nature of selenium oxyanion, selenite (SeO_3^{2-}), it is possible bacterial cells will remove it from the cell via an OMP such as TolC. Export of this anion may be a favoured mechanism for non-selenate respiring bacteria as a detoxification process.

Mutations in *tolC* result in pleiotropic phenotypes and a connection between the expression of TolC and proteins that promote cell survival, such as superoxide combating enzymes, has been identified. This study aims to investigate the connection between TolC and detoxification of selenite, primarily the *tolC*$^-$ mutants ability to cope with oxidative stress but also the potential export of an additional toxic substrate via TolC.

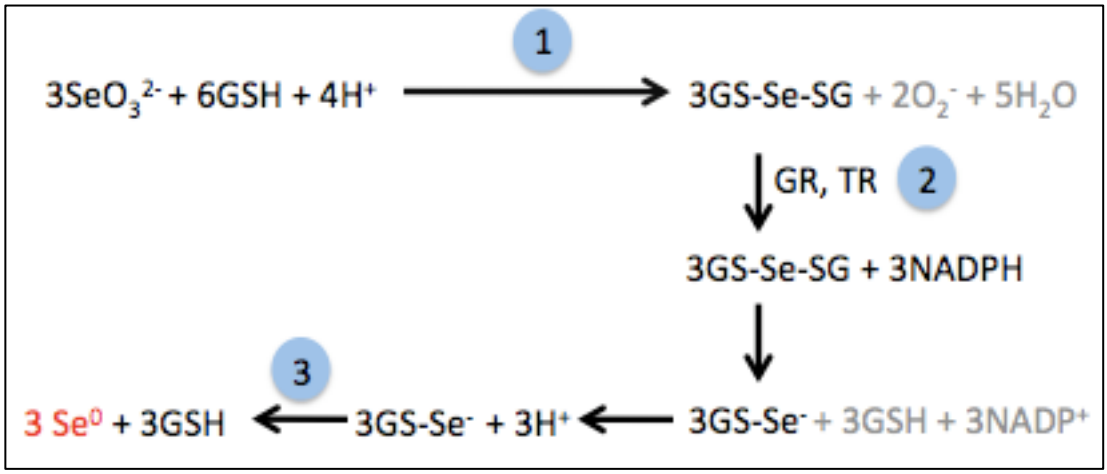

Figure 7.1. Biological reduction of selenite to elemental selenium.

Diagram adapted from Kessi and Hanselmann, (2004). Glutathione (GSH) and selenite (SeO_3^{2-}) form a selenodiglutathione complex (GS-Se-SG), releasing superoxide O_2^- (reaction 1). GS-Se-SG is then reduced by either glutathione reductase (GR) or thioredoxin reductase (TR) (reaction 2), leading to the formation of the selenopersulfide of glutathione (GS-Se). This dismutates into reduced glutathione (GSH) and elemental selenium (Se^0) (reaction 3).

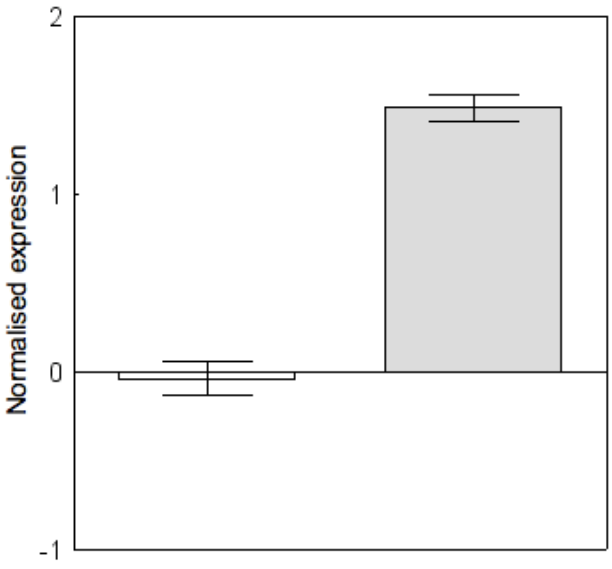

Figure 7.2. Expression of glutathione S-transferase, normalised to expression of all other genes.

Wild type and *tolC*$^-$ mutant. Data show significant increase in expression within the mutant.

7.2. RESULTS

7.2.1. Determining selenite resistance in wild type V. furnissii

In order to determine selenite resistance in *V. furnissii,* the bacteria were cultured in 50 ml L.B. medium containing selenite at concentrations of 0, 2, 5, 10, 20 and100 mM. The O.D. $_{600nm}$ was recorded after 18 h to establish the ability for the bacteria to grow in the presence of increasing concentrations of selenite (Fig 7.3A). At all concentrations of selenite, bacterial growth is markedly reduced and at concentrations of 20 mM and 100 mM, the O.D. $_{600nm}$ less than 0.5 after 18 h growth time. However, in the presence of 2 mM selenite, the bacteria are able to grow to an O.D. $_{600nm}$ of 1.0 and reduce selenite to elemental selenium (Fig. 7.3B). These data establish *V. furnissii* as a selenite reducing bacterium.

7.2.2. Quantification of selenium produced by wild type V. furnissii

To confirm the presence of and quantify the selenium within the cultures, an assay was adapted from Biswas *et al.*, (2011). Cell pellets, washed in NaCl (1 M), were-re suspended in 1M Na_2S to dissolve the elemental selenium and absorption of the red-brown solution was measured at 500 nm to quantify the selenium present. Wild type bacteria were cultured in L.B. medium containing 2 mM and 10 mM selenite and the selenium levels were measured after 12, 18 and 24 h of growth (Fig 7.3C). It should be noted that the absorbance of selenium at 500 nm may interfere with the O.D. $_{600nm}$ reading, particularly when the selenium concentration is high. Therefore, for this experiment, selenium quantification is carried out at set time periods as opposed to defined growth stages defined by O.D.$_{600nm}$ readings. These data confirm that selenium is produced by the bacterium and that there is an approximate 400% increase in selenium production between 12h and 24 h. However, cultures grown on 2 mM, 5 mM, 10 mM and 20 mM selenite for 18 h display slight variances in orange colouring, indicating a difference in the amount of selenium produced (Fig 7.3D). As the selenite concentration increases, a decrease in the selenium produced can be observed, implying that the bacteria are not growing successfully in the presence of higher concentrations of selenite. After 18 h growth the images show a slight decrease in selenium production between cultures containing 2 mM and 10 mM selenite however, the assay determines that statistically there is no difference in selenium levels produced. This confirms that although *V. furnissii* can grow on higher concentrations of selenite, culturing *V. furnissii* in 2 mM selenite is an optimal concentration for successful bacterial growth and selenium production over 24 h.

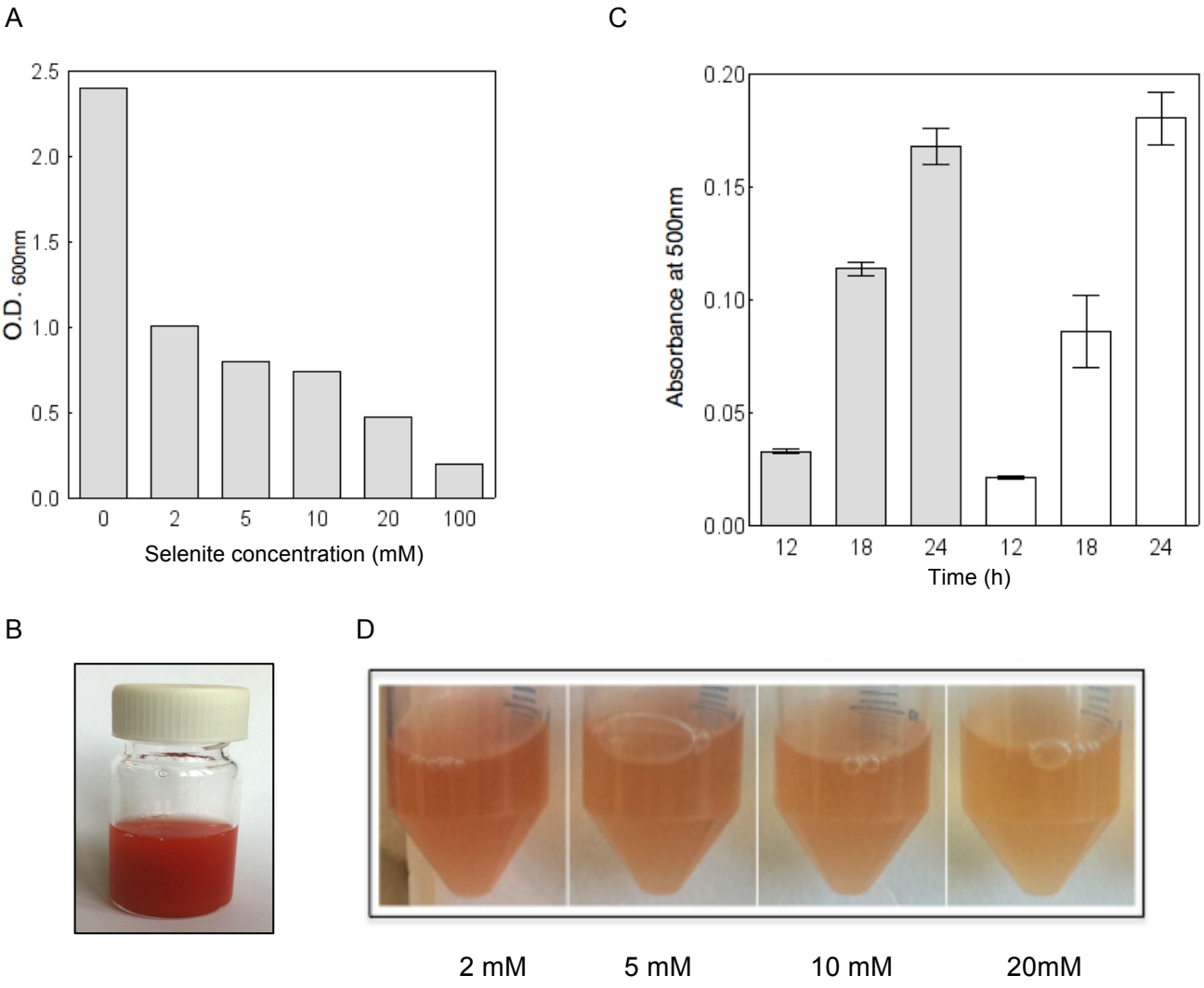

Figure 7.3. Selenite resistance in *V. furnissii.*

A. Wild type bacteria cultured in L.B. medium containing varying concentrations of selenite (2 mM – 100 mM). O.D. $_{600nm}$ readings observed after 18 h growth.

B. Wild type cultured in L.B. medium containing selenite (2mM), red selenium particles visible.

C. Selenium quantified by absorbance at 500 nm after extractions from wild type cultures, bacteria were grown on L.B. medium containing 2 mM and 10 mM selenite, assay completed at 12, 18 and 24 h, error bars represent n=3. Increase in selenium production over time is visible, however there is not a significant increase in selenium production between cultures containing different concentrations of selenite.

2 mM ▭ and 10 mM ▭ selenite.

D. Bacteria grown on L.B. medium with increasing concentrations of selenite (2 mM - 20mM), images acquired after 18 h growth.

7.2.3 Comparing resistance to oxidative stress using selenium production as a colourmetric assay

Selenium was quantified in both wild type *V. furnissii* and *tolC*$^-$ mutant to determine the ability for bacteria to reduce selenite and ultimately cope with increased superoxide production. Initially cultures were analysed visually for differences in the red colouring, indicative of selenium production. The *tolC*$^-$ mutant culture containing 2 mM selenite displays a darker red colouring in contrast to the wild type indicating more selenium is present (Fig 7.4A). However when bacteria are cultured with 20 mM and 40 mM selenite, the mutant is producing less selenium suggesting sensitivity is higher in the mutant. For quantification of selenium during during bacterial growth, an assay to measure the selenium was carried out at regular time intervals. When bacteria are cultured on 2 mM selenite, more selenium is consistently produced by the mutant (approximately 100% more than wild type at each time point) (Fig 7.4B). These data suggest that the mutant reduces selenite to selenium more efficiently than the wild type.

7.2.4. The role of TolC in selenium secretion.

Data show that more selenium is present in the *tolC*$^-$ mutant cultures when grown on 2 mM selenite, however the assay used does not determine if the particles are intracellular or extracellular. Given that the role of TolC is to remove a variety of compounds from the cell, the potential export of inorganic selenium via this OMP is to be investigated. This can be achieved by using transmission electron microscopy (TEM) to view wild type and *tolC*$^-$ mutant cells. Bacteria were grown on 10 ml L.B. medium to mid exponential phase and prepared for TEM. Images show that within wild type and mutant cells, darker areas can be seen indicating presence of selenium (Fig 7.5 1A). It can also be noted that the mutant cells have a larger proportion of cells containing this dark colouring (Fig 7.5 2A and 2B). A closer view of the selenium nanoparticles within the wild type and mutant cells displays that both have accumulated selenium (Fig 7.5 1B). Notably, in the wild type cells separate clusters of selenium particles can be observed (approximately 50 nm) whereas in the mutant they are grouped together. The TEM images do not give conclusive evidence of extracellular selenium in either wild type or *tolC*$^-$ mutant cultures, particulate can be observed extracellularly in all images but it is irregular in shape and size indicating it is not selenium. If selenium is present in the media it is in markedly small amounts and such low levels are likely to be due to cell lysis. Furthermore, when centrifuging wild type and mutant cultures, the supernatant remained clear and the red selenium pelleted with the cells strongly suggesting selenium isn't exported. When bacteria secrete selenium, a separate red layer can be seen in the pellet, for example in *T. selenatis* (Prof. Clive Butler, unpublished data), however within *V. furnissii* the bacterial pellet is entirely red.

A

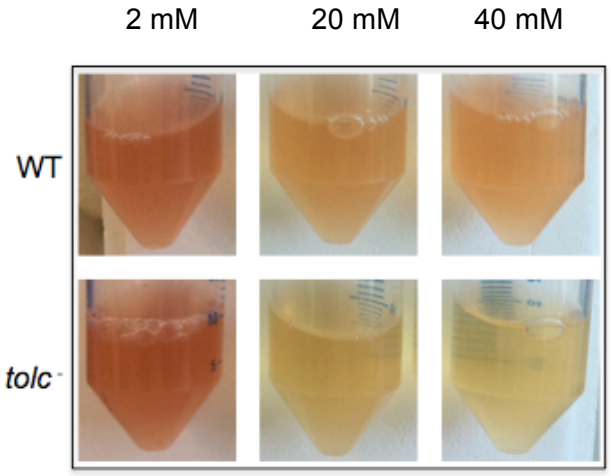

B

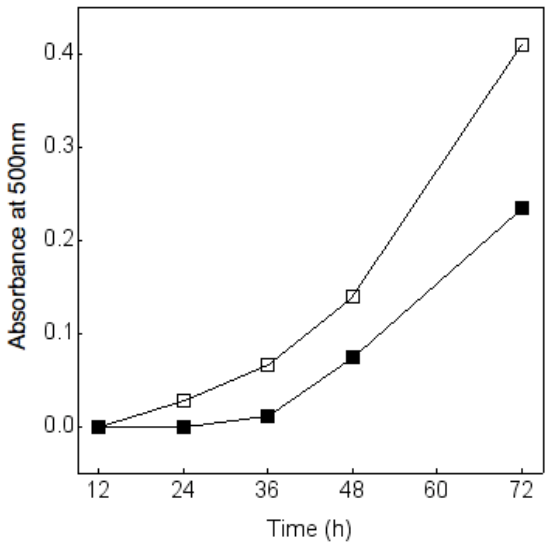

Figure 7.4. Selenite toxicity in wild type *V. furnissii* and *tolC*$^{-}$ mutant determined by selenium production.

A. Wild type and mutant bacteria grown on L.B. medium with increasing concentrations of selenite 2 mM, 20 mM and 40 mM, images acquired after 18 h growth. Wild type reduces more selenite to selenium at higher concentrations of 20 mM and 40 mM.

B. Selenium accumulation in wild type and mutant cultures grown in L.B. medium containing selenite (2 mM), over 72 h. Selenium extracted from cultures at regular time intervals and quantified. Wild type —■— and *tolC*$^{-}$ mutant —□—. More selenium is produced, throughout growth, by the *tolC*$^{-}$ mutant. Control: wild type culture containing no selenite, absorbance at 500nm = 0.021

1A

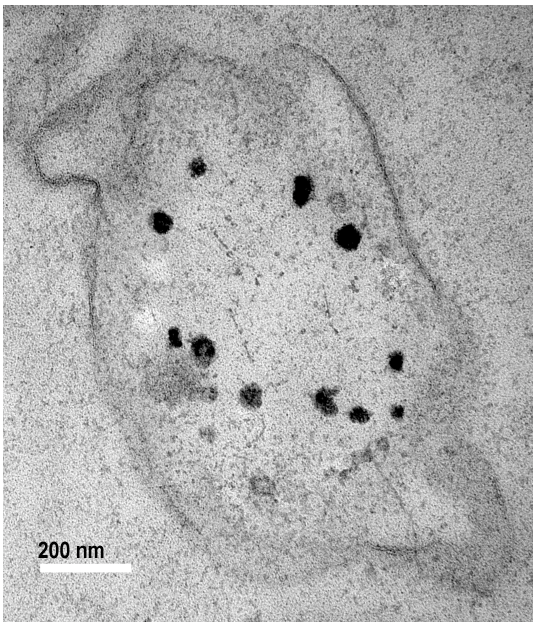

1B

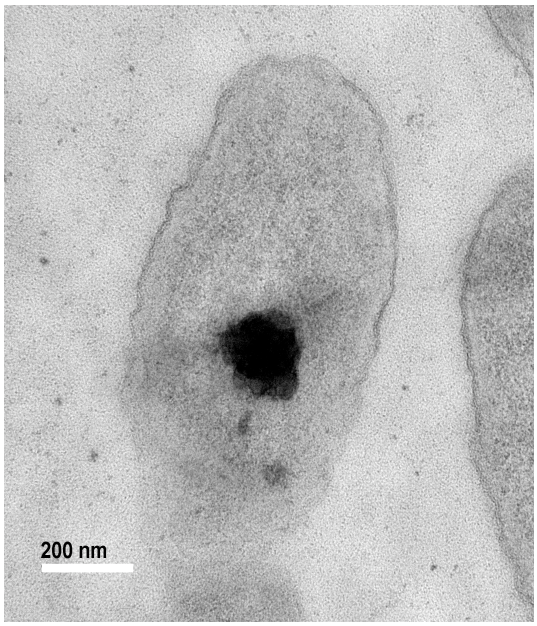

2A

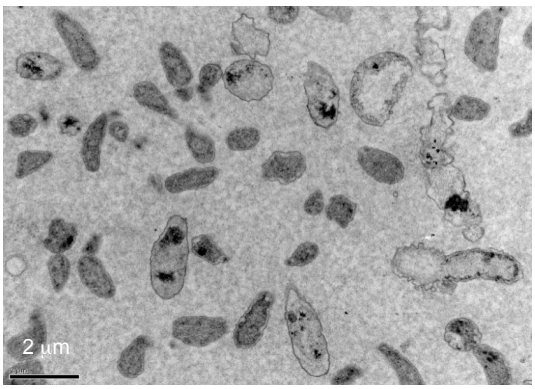

2B

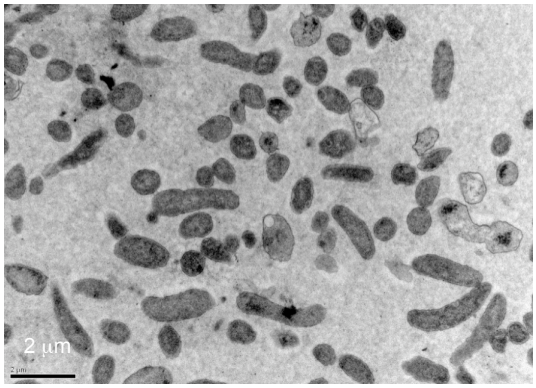

Figure 7.5. Transmission electron graphs of wild type *V. furnissii* and *tolC*$^{-}$ mutant

Bacteria cultured in L.B. medium, with 2 mM selenite until stationary phase. 10 ml of each culture was fixed for TEM. 1: Individual cells, 2: Cultures, Wild type (A) and *tolC*$^{-}$ mutant (B). Images are typical of 8 images taken of individual cells (4 wild type, 4 *tolC*$^{-}$ mutant) and 8 images of cultures (4 wild type, 4 *tolC*$^{-}$ mutant). Number of selenium clusters in wild type cells: average 10, n=4, standard deviation 1.42. Selenium clusters in *tolC*$^{-}$ mutant cells: average 1.5, n=4, standard deviation 0.58.

7.2.5. Export of selenite as a detoxification mechanism

The *tolC*$^-$ mutant produces more selenium at a faster rate when cultured on 2 mM selenite (Fig 7.4B). One hypothesis could be that this is due to cellular accumulation of the toxic anion in the absence of TolC, forcing the cell to metabolise it faster. To investigate the involvement of TolC in selenite export, an assay was carried out to quantify the amount of selenite remaining in both wild type and *tolC*$^-$ mutant cultures. The experiment, adapted from Kessi *et al.*, (1999) determines how much residual selenite remains intracellularly and extracellularly. Bacterial cultures were mixed with 0.1 M HCl, 0.1 M EDTA, 0.1 M NaF, 0.1 M disodium oxalate and 0.1 M 2,3-diaminonaphthalene to create a selenium-2,3-diaminonaphthalene complex. This complex was extracted with cyclohexane and the absorbance at 377 nm read to detect selenite present.

A standard curve was created by performing the assay on L.B. medium containing increasing concentrations of selenite between 0 and 2.0 mM (Fig 7.6A). Assays were also carried out on media containing selenite (2 mM) at 0, 24, 48 and 72 h to ensure depletion of selenite does not occur in the absence of bacteria. 100% of the selenite remained within the media throughout this time period (Absorbance at 377 nm 0.59).

7.2.5.1. Selenite depletion in cultures

To investigate the relationship between selenite reduction and selenium production, selenite concentration was measured and selenium levels quantified at regular time intervals throughout growth of wild type and mutant bacteria. Results show that in both cultures, as selenite is depleted, selenium is produced (Fig 7.6 B and C). Total selenite depletion occurs over 72 h in both cultures but initial rate of selenite depletion (between 0 and 36 h) is slower in the mutant. However, during this initial period more selenium is produced by the mutant compared to the wild type (Fig 7.4B). This suggests that initially more selenite is retained within the mutant cells and reduced to selenium. Differences in wild type and mutant growth rate when cultured in the presence needs to be considered when analysing these data.

7.2.6. Growth analysis to determine the affect of increased oxidative stress.

Following the hypothesis that *tolC*$^-$ mutant cells retain more selenite, it can be assumed that the mutant cells would be under greater oxidative stress leading to an adverse affect on the bacterial growth rate. 50 ml L.B. media containing 2 mM selenite was inoculated with wild type and *tolC*$^-$ mutant starter cultures (2% inoculum). A sigmoidal dose-response (variable slope) equation was applied to the growth curves and the Hill slope (indicating growth rate) was identified using Prism (Fig. 7.7, Table 7.1). In the presence of selenite, the exponential growth rate of the mutant is slower

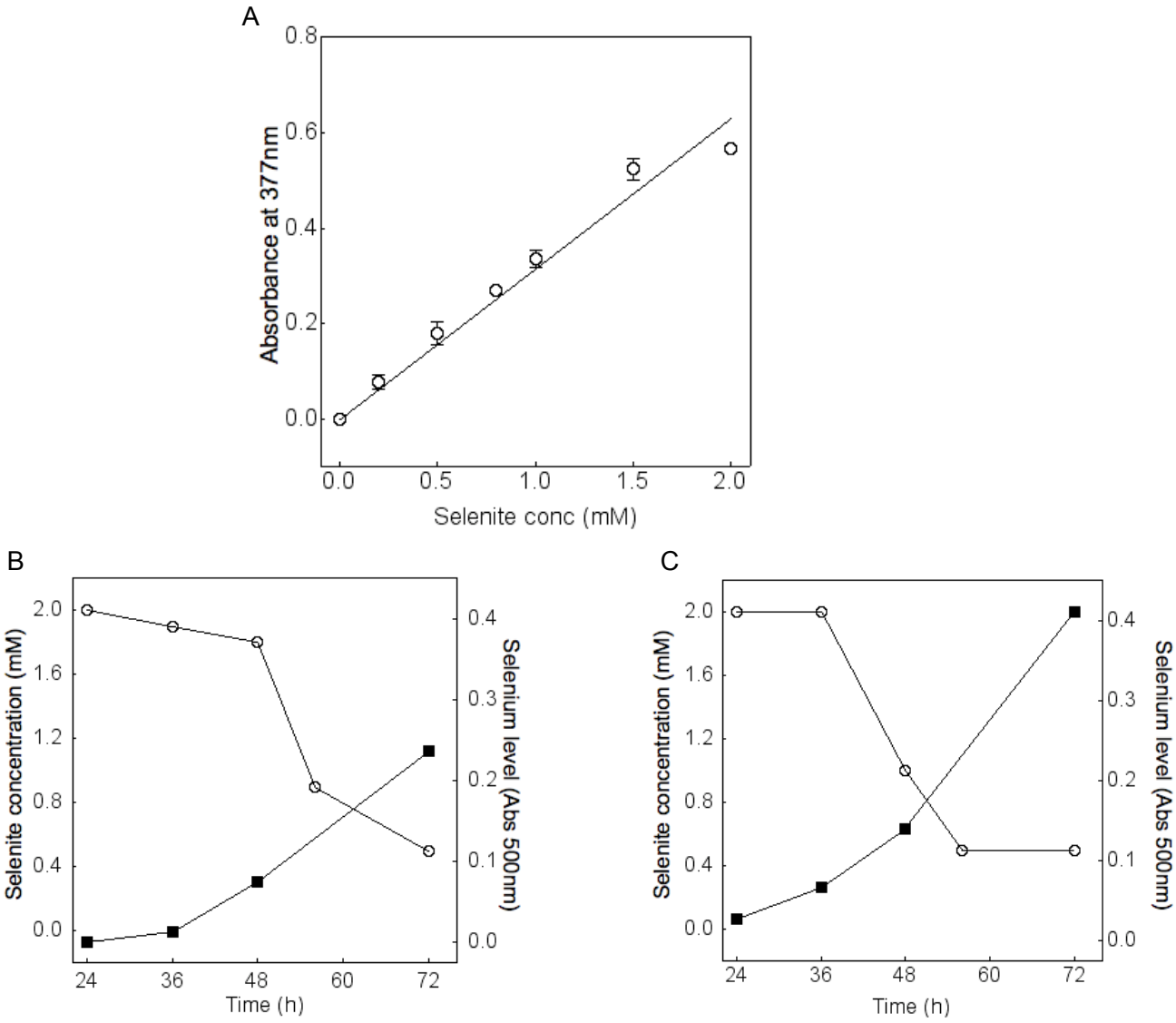

Figure 7.6. Selenite depletion and selenium production in *V. furnissii* wild type and *tolC*⁻ mutant.

A: Selenite standard curve showing linear relationship between selenite concentration (0, 0.2, 0.5, 0.8, 1.0, 1.5, 2.0 mM) abd absorbance at 377nm.

B and C. Selenite depletion and selenium accumulation in cultures grown on L.B. medium with selenite (2 mM). At regular time points, selenite levels were determined, initially as absorbance at 377 nm and concentration (mM) calculated from standard curve. Selenium extracted at same time points and quantified as absorbance at 500 nm. B: Wild type, C: *tolC*⁻ mutant. —○— Selenite depletion —■— Selenium production.

Controls: Wild type containing no selenite absorbance at 377 nm: 0, L.B. media containing selenite (2 mM) assayed at 0, 24, 48 and 72 h, absorbance at 377 nm remained constant (0.59).

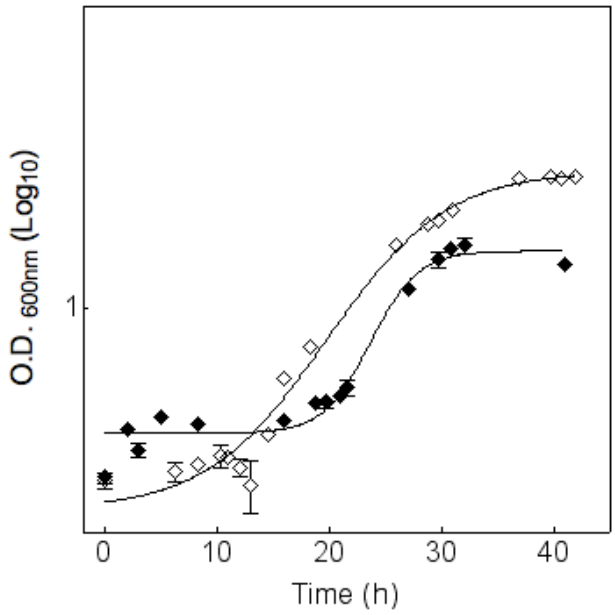

Figure 7.7. Selenite toxicity in wild type *V. furnissii* and *tolC*$^{-}$ mutant determined by growth analysis.

Wild type and *tolC*$^{-}$ mutant cultured in L.B. medium containing selenite (2 mM) and O.D. $_{600nm}$ obtained at regular time intervala. A sigmoidal dose-response (variable slope) equation was applied using Prism. Error bars represent triplicate samples. Wild type —◆—, *tolC*$^{-}$ mutant —◇—

	Wild type	*tolC*$^{-}$ mutant	Wild type + selenite (2 mM)	*tolC*$^{-}$ mutant + selenite (2 mM)
Exponential growth rate (μ)	0.426	0.487	0.157	0.081
Std. error	(+/-) 0.017	(+/-) 0.036	(+/-) 0.024	(+/-) 0.005
Optimum O.D. $_{600nm}$	2.18	2.12	1.36	2.08
Std. error	(+/-) 0.023	(+/-) 0.022	(+/-) 0.028	(+/-) 0.031

Table 6.1. Statistical analysis of wild type and *tolC*$^{-}$ mutant growth curves cultured with selenite.

Data obtained from growth curve analysed by Prism, non-linear regression fit applied, exponential growth rate and optimum stationary phase O.D.$_{600nm}$ of wild type and *tolC*$^{-}$ mutant with and without selenite displayed.

compared to the wild type (0.081μ compared to 0.157μ in the wild type), however it reaches a notably higher stationary phase $O.D._{600nm}$ (2.08μ compared to 1.36μ) (Fig 7.7, Table 7.1.). It shoud be considered that selenium production could affect the $O.D._{600nm}$ readings, particularly the stationary phase cell density readings. However, the optimum $O.D._{600nm}$ reached by the wild type is almost half in the presence of selenite compared to the control ($O.D._{600nm}$ 1.36 compared to $O.D._{600nm}$ 2.18 in the control) suggesting that the selenium particulate interference is not significant. In comparison, the stationary phase optical density of the mutant is not significantly altered ($O.D._{600nm}$ 2.08 compared to $O.D._{600nm}$ 2.12 in the control). Wild type and mutant bacteria were cultured on L.B. medium without selenite as controls and the growth rate was also calculated. Growth of wild type and mutant cultures containing selenite show a notable decrease in growth rate compared to bacterial growth rates without the toxic anion. If selenium particles were interfering with $O.D._{600nm}$ readings, an increased rate would be notable in those cultures containing selenite, however, this is not the case. The wild type replicates at a rate 2.7 times slower in the presence of selenite (0.157μ compared to 0.426μ), comparably, the mutant grows 6 times slower (0.081μ compared to 0.487μ) (Table 7.1). These data show that the *tolC*$^-$ mutant growth rate is significantly reduced in the presence of selenite and is comparatively more affected than the wild type growth rate suggesting that the mutant is more sensitive to the toxic selenium anion.

7.2.7. Reduction of selenite relative to growth.

The growth of wild type and *tolC*$^-$ mutant are affected in different ways by the presence of selenite, therefore the growth rate must be taken into account when analysing the selenite depletion. To analyse bacterial growth more accurately, a CFU count was obtained for each time point that the selenite assay was completed. The assay and CFU count were carried out a regular time intervals over a period of 72 h, until all of the selenite had depleted. L.B. medium containing 2 mM selenite was inoculated with wild type and *tolC*$^-$ mutant starter cultures (2% inoculation volume). The selenite concentration within the cultures reduces consistently over 72 h in both wild type and mutant and notably selenite is processed during lag phase (Fig 7.8). Bacteria begin to enter exponential phase (CFU = 5.00×10^8) when the selenite is reduced to a concentration of approximately 0.8 mM in both wild type and mutant (indicated by a dashed line). Within the *tolC*$^-$ mutant, the selenite is processed at a rate of 0.03 mM/h during lag phase, and growth begins at approximately 45 h (Fig 7.8B), whereas in the wild type, selenite is processed faster during lag phase (0.054 mM/h) and cultures enter exponential phase earlier at 24 h (Fig 7.8A). This evidence that wild type grows more successfully in the presence of selenite supports earlier data that the mutant is more sensitive to the toxic anion, a likely affect if mutant cells are unable to export

A

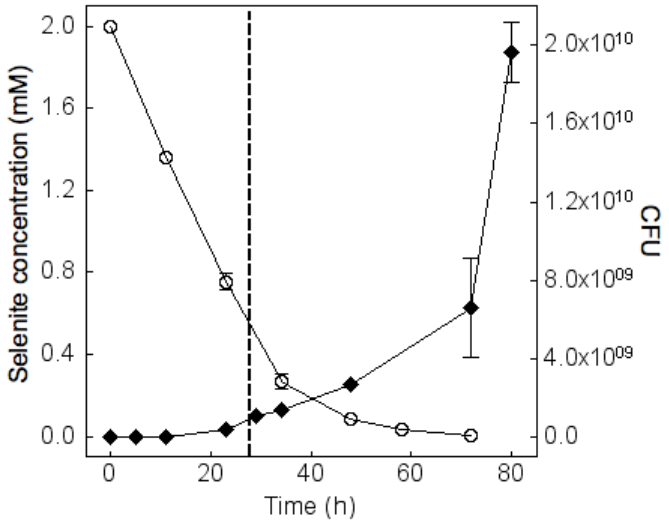

B

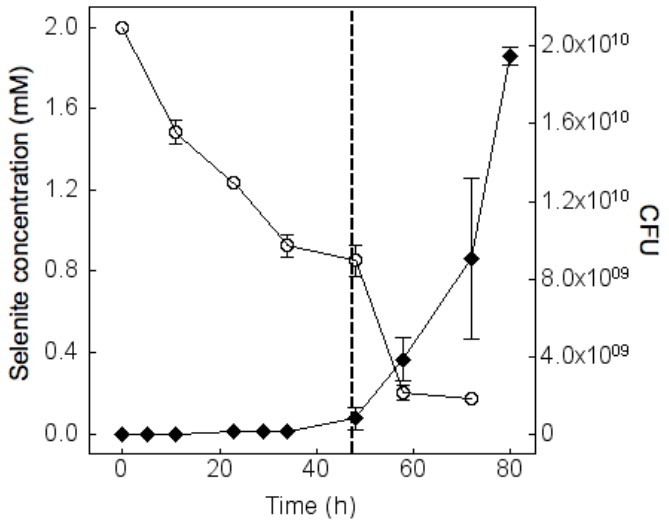

Figure 7.8. Selenite reduced by *V. furnissii* monitored during bacterial growth.

A and B: Growth of *V. furnissii* displayed as colony forming units (CFU) and selenite concentration in culture. Bacteria grown on L.B. medium with 2mM selenite. Selenite levels in culture determined as absorbance at 377 nm, concentration (mM) calculated from standard curve. Dashed line indicates cultures entering exponential phase, when the CFU count is above 5.00 x 10^8. A: wild type, B: *tolC*$^-$ mutant, —○— Selenite —◆— CFU

selenite. Notably, once all the selenite has been reduced to selenium in both wild type and mutant cultures, the bacterial growth rate increases dramatically, confirming the toxicity of selenite to the cells.

7.2.8. Wild type and tolC$^-$ *mutant detoxification calculated per CFU.*

The *tolC*$^-$ mutant, hypothesised to retain more selenite, displays greater sensitivity however it still continues to process the toxic anion and ultimately produces more selenium. To analyse when selenite is reduced and at what rate by both wild type and mutant, the amount processed in each culture (per CFU) was calculated. The concentration of selenite remaining in the culture was deducted from the initial 2 mM of selenite present in the media to determine the concentration metabolised by the bacteria. This concentration, calculated for each biological replicate, was subsequently divided by the CFU at the corresponding time point. The data displays that within mutant cultures more selenite is processed per CFU, significantly more between 34 and 48 h, corresponding to early exponential phase (Fig 7.9). These figures indicate that despite selenite reduction initially occurring at a slower rate in the mutant, there are fewer cells present and therefore each cell is processing more selenite.

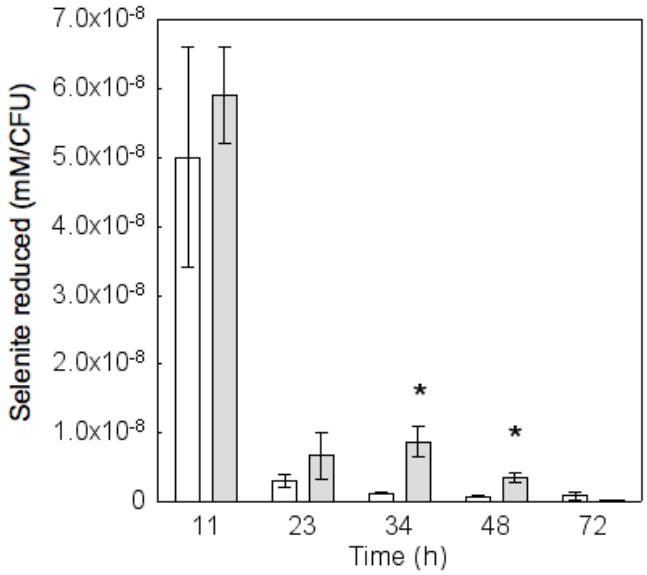

Figure 7.9. Selenite processed in relation to number of colony forming units.

Data obtained at 11h, 23 h (beginning of bacterial growth), 34 h, 48 h and 72 h (total depletion of selenite in culture). Significant increase in reduction of selenite/ CFU in *tolC*$^{-}$ mutant between 34 and 48 h (one tailed t-test, $p<0.05$). ☐ Wild type, ▭ *tolC*$^{-}$ mutant, error bars represent n=3.

7.3. DISCUSSION

This work set out to identify *V. furnissii* as a selenite reducing bacterium and to determine the effect of the *tolC*$^{-}$ mutation on the cells ability to cope with increased superoxide production. Results in this chapter confirm that *V. furnissii* is a selenite reducing bacterium resistant to concentrations of selenite up to 20 mM (Fig 7.3). Optimal selenite concentration for experimentation has been determined at 2 mM, however over longer periods of time, wild type *V. furnissii* was able to produce selenium when cultured on 20 mM and 40 mM selenite (Fig 7.4). A variety of Gram-negative bacteria isolated from selenium contaminated sites including *Aeromonas*, *Corynebacterium* and *Pseudomonas* species are resistant to levels of selenite up to 20 mM (Burton Jr *et al.*, 1987). This can be compared to selenite resistance in *R. rubrum*, *E. coli* and *D. desulfuricans* that are reported to grow in concentrations as low as 0.1 – 1 mM (Tomei *et al.*, 1995, Kessi *et al.*, 1999). Innate resistance to selenite in *V. furnissii* can therefore be considered to be relatively high.

There is evidence that selenate respiring bacteria export selenium to the extracellular environment (Debieux *et al.*, 2011), however TEM images in this study show this is not the case in *V. furnissii* (Fig 7.5). Furthermore, centrifugation of the *V. furnissii* cultures result in a clear supernatant where pelleted bacteria remained closely associated with the elemental selenium, implying that TolC is not involved in selenium secretion. It is possible that selenium is exported by the cells but that it remains closely associated with the outer cell membrane and is therefore not detected by TEM. Scanning electron microscopy (SEM) would be able to detect any selenium closely associated with the outer membrane but if this was the case, there is no evidence to suggest TolC is involved in the export of selenium. It appears that unlike selenate respiring bacteria (*T. selenatis* and *E. cloacae*), bacteria such as *V. furnissii*, *R. rubrum* and *D. desulfuricans* are capable of selenium anion reduction but incapable of selenium export (Tomei *et al.*, 1995, Kessi and Hanselmann, 2004). Similarly, bacteria also capable of respiring oxyanions of tellurium posses the mechanism to export tellurium ($Te^{(0)}$), confirmed by TEM and SEM in *B. selenitireducens* (Baesman *et al.*, 2007, Baesman *et al.*, 2009) and *Bacillus beveridgei* MLTeJB (Baesman *et al.*, 2009). During selenate respiration in *T. selenatis* evidence shows that a secreted protein SefA is associated with selenium nanoparticle assembly, however the full mechanism of export from the cell is unknown (Debieux *et al.*, 2011). Analysis of the *V. furnissii* genome revealed there are no homologues of *sefA* present, presenting additional evidence that *V. furnissii* cannot be categorised as a bacterium able to export selenium. It can be hypothesised that bacteria found in selenium rich environments capable of selenate or selenite respiration have developed a system for export of selenium deposits. However,

bacteria such as *V. furnissii and R. rubrum,* not adapted to this environment, do not contain a secretion mechanism.

Despite being able to reduce high concentrations of selenite, the amount of selenium produced by *V. furnissii* (on both 2 mM and 10 mM selenite) is not significantly different between 12 and 24 h (Fig 7.3C). This implies that there is a limit to the selenite that can be processed by the cell. It is likely that there is more than one mechanism employed by *V. furnissii* cells to cope with any excess selenite and results in this study show that TolC plays a role in the process of removing selenite from the cell. Analysis of cultures grown with selenite show that the growth rate, selenite resistance and selenium production vary between wild type and *tolC*$^{-}$ mutant cells indicating the significance of TolC in selenite resistance. The growth rate of the *tolC*$^{-}$ mutant is markedly reduced in the presence of selenite (Fig 7.7, Table 7.1), significantly more so than the wild type. Furthermore, the rate of selenite depletion is slower (Fig 7.8). One interpretation of this could be that the *tolC*$^{-}$ mutant simply cannot cope as well under the stress of increased levels of superoxides. However, further analysis shows that the mutant cells can maintain a consistent although slower detoxification process and ultimately process more selenite and produce more selenium per cellular unit (Fig 7.9). Results presented here support the hypothesis that wild type cells export selenite via TolC, ensuring that the intracellular concentration remains at a manageable level. Within the mutant, this export has seemingly been prevented, resulting in cellular accumulation of selenite, reducing growth rate but ultimately forcing the cells to process more selenite.

The differences in wild type and *tolC*$^{-}$ mutant growth supports evidence that selenite is a substrate of TolC. Reduced growth rate of the mutant in comparison to the parent strain is an established phenotypic change observed when *tolC*$^{-}$ mutants are cultured in the presence of toxic substrates, e.g. bile in *V. cholerae* (Bina and Mekalanos, 2001). The reduced growth rate of the *V. furnissii tolC*$^{-}$ mutant in the presence of selenite is determined by both $O.D._{600nm}$ and CFU results (Table 7.1, Fig 7.8). CFU counts are similar in wild type and *tolC*$^{-}$ mutant cultures at 80 h, however the stationary phase $O.D._{600nm}$ of the mutant was significantly higher than the wild type. The difference in these data can be reasonably explained by the increase in selenium particulate in the mutant cultures interfering with the absorbance readings.

Overall, the *tolC*$^{-}$ mutant displays increased sensitivity to selenite compared to the wild type, showing reduced selenium production at higher concentrations of selenite (20 mM) (Fig. 7.4) and a slower growth rate when cultured on 2 mM. This could be directly related to stress already imposed on the mutant due to membrane damage caused by the disruption of TolC. However, despite

reduced growth rate, the cells are more efficient at processing the selenite, producing 100% more selenium than the wild type throughout growth over 72 h (Fig 7.6). In addition, during lag phase and early exponential phase, when cell count is low, selenite is still being reduced by the mutant. This shows that a relatively small number of mutant cells are processing the toxic anion in comparison to the wild type. This is confirmed by further analysis showing that more selenite is reduced per CFU by the *tolC*$^{-}$ mutant cells, significantly more so entering exponential phase (between 34 h and 48 h ($p<0.05$)) (Fig 7.9). This supports the hypothesis that a greater amount of selenite being retained and metabolised within the mutant cells. Furthermore, the increased expression of detoxification enzymes, e.g. glutathione-s-transferase, observed within the mutant may also aid this process (Fig 7.2). Considering the number of toxic substrates exported via TolC, removing the function of this protein would likely result in increased expression of enzymes to aid detoxification of damaging species entering the cell from the natural marine environment (Rosner and Martin, 2009).

This work determines that *V. furnissii* is resistant to high levels of selenite and capable of reducing the selenium anion to produce elemental selenium. Like *R. rubrum* and *D. desulfuricans*, selenite metabolism in *V. furnissii* is a detoxification process and does not appear to result in the export of selenium nanoparticles. Determining organisms that are able to reduce high concentrations of selenite has implications in bioremediation of selenium contaminated environments. Large scale bioremediation in the treatment of a Pit Lake in Wyoming showed removal of dissolved selenium (selenate/selenite) by bacteria where levels were reduced from 460 μg/L to a concentration less than 10 ug/L. This was presumed to have occurred by reduction to elemental selenium (Martin *et al.,* 2009).

TolC plays a role in selenite resistance within *V. furnissii and* there is strong evidence to support that this toxic selenium anion is an additional substrate of TolC (Fig 7.10). The accumulation of selenite in *tolC*$^{-}$ mutant cells increases oxidative stress and requires detoxification enzymes to cope with increased production of superoxides (Santos *et al*., 2010). This provides an explanation as to why cells employ such compensatory mechanisms as a reponse to removing the TolC function. Increased expression of superoxide combating enzymes such as glutathione-s-transferase and thioredoxins detected in *V. furnissii tolC*$^{-}$ mutants may be due to oxidative stress caused by membrane disruption, however the mutant is still able to successfully process selenite. In fact, the compensatory regulatory mechanisms employed by the *tolC*$^{-}$ mutant appear to be sufficient to maintain survival and metabolise the exogenous toxic selenium anion at a faster rate than the wild type.

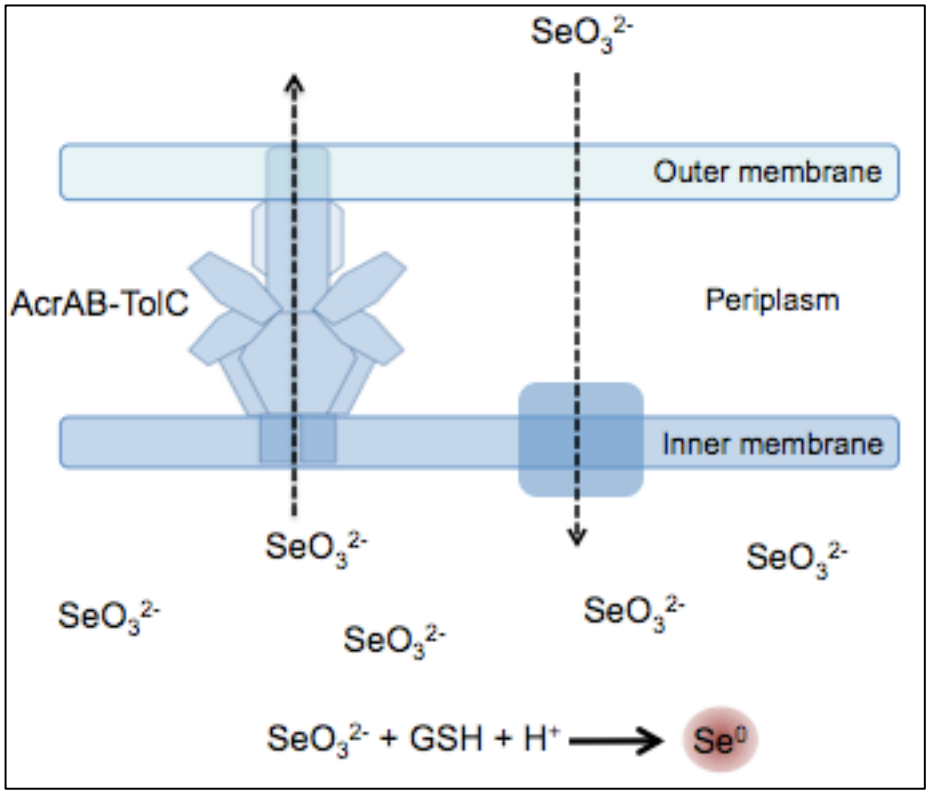

Figure 7.10. Representation of suggested path of selenite export via AcrAB-TolC in *V. furnissii*

CHAPTER 8 - CONCLUSIONS AND FUTURE WORK

8.1. CONCLUSIONS

Components of multidrug resistance pumps, particularly TolC, are targets for drug development (Blair and Piddock, 2009). When designing antimicrobials to inhibit the function of TolC, it is important to be aware of the consequence of disrupting the function of this integral membrane protein. This study has added to our knowledge of the clinically relevant outer membrane protein TolC, and provides a comprehensive analysis of the pleiotropic changes in the *tolC*$^-$ mutant. Data presented provide a broad view of the role of TolC within *V. furnissii;* an archetypal organism for the study of a number of processes relevant to this highly conserved membrane protein: antibiotic resistance, fatty acid secretion, quorum derived signalling, virulence, cell motility and cellular detoxification.

Free fatty acids, relevant to the bio-fuel industry, are exported by *V. furnissii* via TolC. Total lipid content of *V. furnissii* corresponds to approximately 2% of biomass in contrast to 0.5% of *E. coli* biomass. FFA content is also significantly greater in this marine bacterium and secretion into the extracellular environment is achieved by the wild type and significantly reduced within the *tolC*$^-$ mutant. Findings support data presented by (Wackett *et al.*, 2007) that *V. furnissii* 11218 is not able to synthesise significantly large quantities of alkanes. Due to the lower than previously reported amounts of hydrocarbons produced, this investigation does not focus on isolating and concentrating the secreted compounds but primarily gives greater insight into the role of TolC. It is worth considering that engineering bacteria to synthesise greater quantities of the fatty acids results in significant disruptions to cell growth. This thesis takes the approach of investigating the potential to alter secretion of relevant compounds and has identified TolC as an exporter of FFAs; hexadecanoic acid and octadecenoic acid. Although the *tolC* mutation has proven to affect a number of cellular processes including virulence and quorum regulatory pathways, the changes in these cellular processes do not alter growth rate or expression of the fatty acid synthesis pathway. This confirms that the observed increase in cellular FFAs in the *tolC*$^-$ mutant is due to retention of and not an increase in synthesis of the C_{16} and C_{18} compounds. This established that FFA accumulation in the mutant is a genuine phenotype directly related to export via TolC. Increasing both synthesis and secretion of fatty acids would avoid defects that occur due to cellular accumulation of fatty acids and may help to maintain continued production of these industrially relevant compounds.

This study also examines the membrane bound transporter proteins interacting with TolC in *V. furnissii.* TolC appears to interact with both an AcrD and AcrB and is therefore able to export aminoglycosides via the TolC efflux system.

The *V. furnissii tolC*$^{-}$ mutant provided a paradigm in which the role of TolC could be studied in relation to quorum-derived signalling commonly associated with *Vibrio* species. Results presented broaden our understanding of how TolC is connected to the fundamental process of cell-cell communication. In the *tolC*$^{-}$ mutant there is a reduced quantity of a predicted autoinducer showing strong structural similarites to the *V. cholerae* signalling compound CAI-1. Two scenarios have been discussed in this work; the direct export of this compound via TolC subsequently altering quorum gene expression, and the possibility that the *tolC* mutation indirectly results in decreased expression of the autoinducer synthase.

The microarray data provided a great deal of insight into co-incident gene expression changes in the *tolC*$^{-}$ mutant. Notably an increased expression of virulence factors associated with the quorum regulator LuxR protein (e.g. AphB) was observed in the *tolC*$^{-}$ mutant. The connection between TolC and pathogenicity has received a significant amount of attention and data here provide a better perception of this association. Given the network of genes altered within *tolC*$^{-}$ mutants, a direct connection between phenotypes is not easy to establish, however the microarray data suggest disruptions in quorum sensing pathways, flagella assembly and virulence factor expression are closely associated.

Decreased motility is observed in the *V. furnissii tolC*$^{-}$ mutant, supported by a global decrease in expression of flagella assembly proteins. Results in this study support evidence that *tolC*$^{-}$ mutants exhibit reduced motility, as shown in *S.* Typhimurium (Webber *et al.*, 2009), and establish that this is due to the disruption of flagella assembly. It can be suggested, due to the location of the flagella proteins, that assembly is compromised due to alterations in membrane structure resulting from the *tolC*$^{-}$ mutation. Mis-assembled flagella in *tolC*$^{-}$ mutants can be considered to be a contributory factor for less pathogenic phenotypes observed in the mutants and should be investigated in closely related clinically relevant bacteria such as *V. cholerae* and *S. Typhimuirum.*

It is reasonable to suggest this reduced motility has consequential effects on cell-cell communication. In *V. furnissii tolC*$^{-}$ mutants the optimum cell density reached is considerably lower than the wild type and expression of the quorum regulatory pathway is altered. Lower cell density within the mutant equates to lower concentration of autoinducers and altered expression of genes

in the Lux pathway. This ultimately results in reduced expression of LuxR which directly affects virulence factor expression (i.e. AphB, established in *V. furnissii*). LuxR regulates a number of virulence factors such as biofilm formation and host colonization, mechanisms which are compromised in *tolC*$^{-}$ mutants within clinically relevant bacteria such as *V. cholerae* and *S.* Typhimurium (Bina and Mekalanos, 2001, Buckley *et al.*, 2006). It should be considered that targeting TolC for antimicrobial drug development would not only decrease anitibiotic resistance but also reduce bacterial pathogenesis by consequential regulatory changes to the quorum sensing pathway.

The nature of TolC as an integrated membrane protein raises the question of the oxidative stress caused by disrupting the expression of this protein. Data presented here support evidence that observed alterations to the *tolC*$^{-}$ mutant physiology are a likely result of membrane stress, notably the disruption to flagella assembly. It is suggested that the mutations in *tolC* cause oxidative damage resulting in growth defects (Santos *et al.*, 2010), however results presented in this work support evidence that bacteria respond to the *tolC* mutation by employing a number of compensatory mechanisms.

Further insight has been gained into the ability for *tolC*$^{-}$ mutants to cope with metabolic pressures by exposing them to increased oxidative stress and raised levels of superoxides. This was achieved by growing *V. furnissii* in the presence of the selenium toxic anion, selenite. The *tolC* mutant cells efficiently reduced selenite to selenium and once the toxic anion was fully reduced, the mutant continued to grow successfully. During selenite detoxification, growth rate was reduced within the mutant but selenite processed per cellular unit was notably greater than within wild type. Data suggest this is due to a build up of selenite and that this toxic anion is a previously unknown TolC substrate. Ultimately the detoxification enzymes upregulated within *tolC*$^{-}$ mutants, such as thioredoxins, glutathione reductases and glutathione-s-transferase, observed in other organisms and within this study, appear to compensate for the increased oxidative stress. These mechanisms employed in *tolC*$^{-}$ mutants aid the cell during inevitable build up of toxins which occurs in the absence of a functioning TolC. The implications of the ability for bacteria to compensate for mutations in *tolC* suggest that the phenotypes observed in mutants should not be purely considered as a consequence of membrane damage.

RND efflux systems are targets for antimicrobial drug development. Studying *tolC*$^{-}$ mutants in *V. furnissii* has shown that removing TolC function results in decreased antibiotic resistance, reduced motility and changes to the quorum sensing pathway, which is established as a virulence factor

regulatory network in a number of bacteria. These data confirm that TolC, as an integral part of the RND efflux system, is a suitable target for drug development. Considering consequential expression changes resulting from the *tolC* knockout mutation alongside experimental data has helped identify some phenotypes directly associated with TolC as an export protein, notably the role of TolC in antibiotic and selenite resistance as well as the export of free fatty acids.

8.2. FUTURE WORK

There are a number of ways in which this work could be continued, firstly with regards to optimising the export of fatty acids for industrial applications. TolC is a target for further investigation into the export of FFAs and this function should be confirmed in other organisms. Although *V. furnissii* yields higher FFAs in contrast to *E. coli,* TolC should be investigated in hydrocarbon synthesising bacteria to investigate export of long chain alkanes via TolC. Determining the affects of engineering both synthesis and secretion of fatty acids simultaneously would establish a potential method for increasing production while maintaining bacterial viability. In order to do this, methods of successful overexpression of TolC need to be investigated. Identifying media able to support growth of the overexpressor and accurately quantify fatty acids requires further attention. To further analyse the industrial implications of exported fatty acids, methods for concentration and purification should be optimised.

To complete our study of autoinducer production in *V. furnissii* the exported compound needs to be identified. Analysis shows strong structural similarity between the CAI-1 type compound detected in *V. furnissii* and *V. cholerae* CAI-1, differences between autoinducers is consistent with the literature as structural differences are necessary to prevent inter species signalling. In order to determine the structure, synthesis of variances on the C_{13} chain should be carried out with the functional group present at varying positions along the carbon chain. Repositioning the functional group would not alter the mass but may alter the fragmentation to fit with the observed pattern in the biological sample. In addition the structure should be synthesised with an amino (NH_2) group in various positions along the carbon chain instead of the hydroxyl (OH) group. This would retain the same mass but change the polarity, another difference observed between CAI-1 and the biological product. These standards should be analysed by LC-MS alongside the biosynthetic compound. Furthermore, direct mutations in the CAI-1 synthase and subsequent LC-MS analysis would confirm that the detected autoinducer is synthesised by this pathway.

Continued investigation into the connection between the regulation of motility, quorum sensing and virulence will help to further expand our knowledge of these interactions. Targeted mutation in

genes identified in this study; *luxR, aphAB, cqsS* and flagella assembly genes, followed by subsequent comparison of the transcriptomes of these mutants will broaden understanding of the connection between these pathways and determine if TolC is integral to the differences observed in this work. In addition, analysis of the transcriptomes of the wild type *V. furnissii* and *tolC*$^{-}$ mutant transcriptomes when cultured on selenite would give further insights into how the *tolC*$^{-}$ mutant copes with oxidative stress.

CHAPTER 9 - APPENDICES

A

B

3'CTCTTAATTAATTTAAATCTAGAGTCGACCTGCAGGCATGCAAGCTTCAGGGTTGAGATGTGT
ATAAGAGACAGCTTCAAACGCTGCATCACGTTGTGCCGCTGCACTCAGCAGTTGAGGATCGTT
TTGTTTTGCTTGATCGTAAATTTGTGCAAGGTCATCTGCAGATGCTTGAGCACTTAGGCTGCCT
AGTGTTGCACTAATTAGTAGTGGAAGCAGTTTTTTCAT'5

Figure 8.1. Sequencing to confirm the location of the transposon within *tolC.*

A: Representation of primer design to determine the location of the insertion within the gene, primer "transposon rev" used (see methods Table 2.2).

B: Sequencing determining transposon is inserted 153 bp from the start of the gene. Blue indicates *tolC* sequence, grey highlighted section represents transposon sequence.

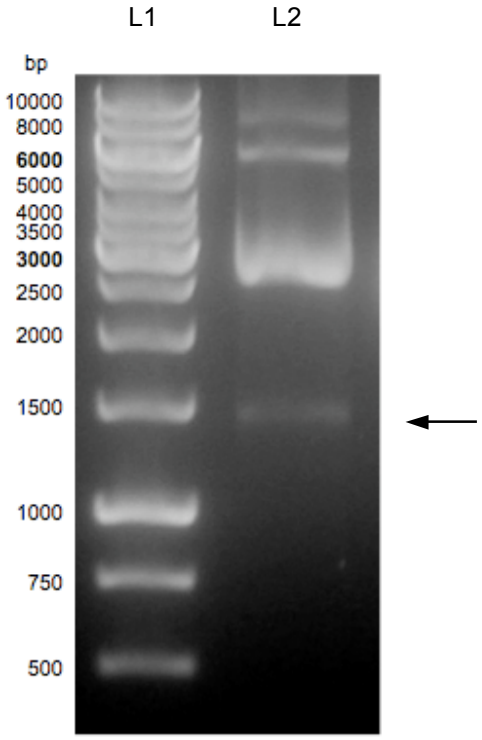

Figure 8.2. Digest of expression vector pSRKGmJAA-TolC.

Restriction digest performed with *Bam*H1 to confirm location of *tolC* within the expression vectior pSRKGmJAA following gateway cloning. Two *Bam*H1 restriction sites are present within the vector and a product of 1.5 kb corresponding to *tolC* is expected. L1 – Fermentas GeneRuler^{TM} ,1 kb. L2 - Digest with *Bam*H1, band at 1.5 kb indicated by arrow (corresponding to *tolC*), remaining bands corresponding to circular and super coiled DNA.

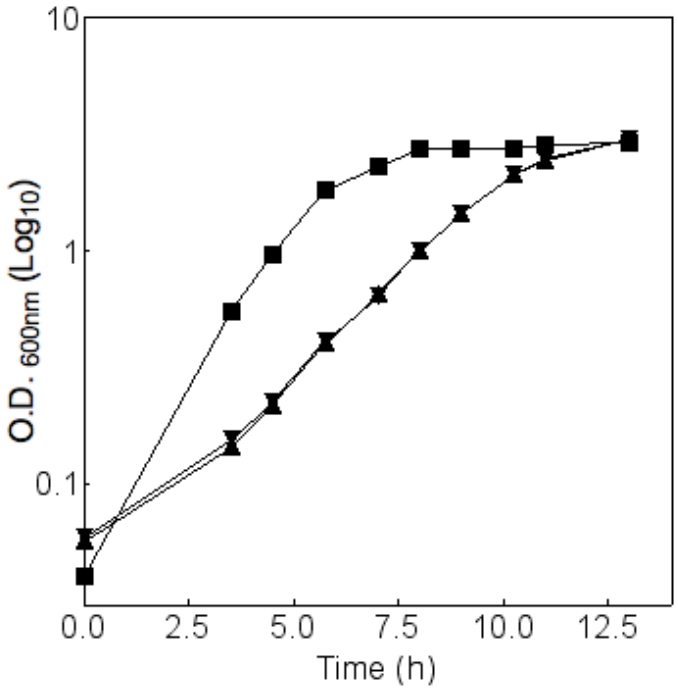

Figure 8.3. Growth curves of *V. furnissii* wild type and TolC overexpressor.

Wild type —■—, overexpressor cultured with IPTG (1 mM) —▼— and without IPTG —▲—. All strains cultured on L.B. medium Growth rate of overexpressor is slower and presence of IPTG does not alter the growth of this strain.

>vfu_A02488 vfu_A02488 glyceraldehyde-3-phosphate dehydrogenase 5'-3'

A

ATGACTATCAAAGTAGGTATTAACGGTTTTGGCCGTATCGGTCGTTTCGTATTCCGTGCA
GCGCAAGAGCGCAATGACATCGAAGTTGTAGGTATCAACGACCTGATCGACGTAGATTAC
ATGGCATACATGCTGAAATACGACTCAACTCACGGCCGTTTCAACGGTACTGTTGAAGTT
GAAGGCGGTCACCTGATCGTTAACGGCAAAACTGTACGTGTAACTGCAGAACGCAACCCA
GCGGACCTGAAATGGAACGAAATCGGTGTTGACGTTGTAGCAGAAGCAACTGGTCTATTC
CTGACTGACGAAACTGCTCGTAAACACATCGAAGCTGGCGCGAAAAAAGTTGTTCTGACT
GGTCCTTCAAAAGACAAAACTCCAATGTTCGTAATGGGTGTTAACCACACTACTTACGCA
GGTCAAGACATCGTTTCTAACGCTTCTTGCACTACTAACTGTCTGGCTCCTATCGCTAAA
GTTCTTAACGACAACTTCGGCATCGAGTCTGGTCTGATGACTACAGTTCACGCAACAACT
GCAACTCAAAAAACTGTTGACGGTCCTTCTGCGAAAGACTGGCGCGGTGGTCGTGGTGCT
GCTCAAAACATCATCCCATCTTCAACTGGT**GCAGCTAAAGCAGTAGGCGTTGTTC**TTCCA
GAACTAAACGGCAAACTGACTGGTATGGCTTTCCGCGTACCAACTGCAAACGTATCTGTA
GTTGACCTGACTGTTAACCTAGAAAAAGCAGCATCTTACGATGACATCAAAGCAGCAATG
AAAGCAGCTTCTGAAGGCGAACTTGCTGGCGTACTAGGCTACACTGAAGATGCAGTAGTA
TCTACTGACTTCAACGGCGACACTCGCACTTCAATCTTTGATGCTGCAGCAGGTATCGCA
CTGACTGACAAATTCGTTAAAGTTGTATCTTGGTACGACAACGAAATCGGTTACTCAAAC
AAAGTTCTAGACCTGATCGCTCACATCTCTAAATAA

>vfuA00859; outer membrane protein TolC - 2415844: 2417163 5'-3'

B

ATGAAAAAACTGCTTCCACTACTAATTAGTGCAACACTAGGCAGCCTAAGTGCTCAAGCA
TCTGCAGATGACCTTGCACAAATTTACGATCAAGCAAAACAAAACGATCCTCAACTGCTG
AGTGCAGCGGCACAACGTGATGCAGCGTTTGAAGCGATCAACTCAAGCCGCAGCTCTCTT
TTGCCACAAATCAATTTGACTGCGGGTTACAACATTAACCGTAGTGATGTTGATCTTCGC
GATAGCGACAAACTGAGCGCAGGCATCAACTTCTCGCAAGAATTGTATGACCGTTCAAGC
TGGGTTTCTCTGGATACATCTGAGAAACAAGCCCGTCAAGCTGACGCCCAATACGCCAAC
ACTCAGCAAAGCCTGATGTTGCGCGTGGCGCAAGCCTACTTTGACGTGTTGAGCGCGCAA
GATAACTTGGAATTTGTTCGTGCGGAAAAAGCCGCCGTTGGCCGCCAACTCGAGCAAACC
AAACAACGTTTTGAAGTGGGCTTGTCTGCCATCACTGACGTTCATGATGCACAAGCACAA
TACGATACCGTGCTGGCTGATGAAGTGCTGGCCGAAAACGCCCTGATCAACAGCTACGAG
TCATTGCGTGAAATCACTGGTCAAGAACACACCAACCTGAGTGTGCTCGACACCAACCGT
TTCTCCACCAGCCGCACCGCCGACTCCATGGAAGCGCTGATTGAGAAAGCACAAGAGAAA
AACTTGTCTCTGTTGTCTGCACGCATCTCGCAAGATGTTGCGAAAGACAACATCTCGCTG
GCAAGCTCGGGTCACTTACCTTCACTAACACTGGATGGTGGCTACAACTACGGTCGTGAA
TACAACGACAACTACAGCAGCTACAACACTTA**CCACGAAAATAACGACTTCAACATTGGT
CT**GAACCTAACCATTCCACTCTACAGCGGTGGTAATGTGTCGTCTCAAACCAAACAAGCG
GAATACGCGTACGTCGCAGCCAGCCAAGATCTGGAAGCGGCATACCGCAGCGTGGTGAAA
AATGTCCGTGCGTACAACAACAACATCAACGCGTCGATCGGTTCAGTGCGTGCGTATGAG
CAATCGGTGATTTCTGCGCAGTCTGCGTTGGATGCCACTGAAGCAGGTTTTGATGTGGGT
ACTCGTACCATCGTTGACGTTCTTGACGCAACGCGTACACTGTACAGCGTGAAGAAAAAC
CTGTCTGATGCACGTTACAACTACATCATCAGCGTGCTGCAACTGCGTCAAGCAGTGGGC
ACACTCAGCGAGCAAGACATCGTGGATGTCAACGCTGGCCTGAAAGCCATGAAGAAATAA

Table 7.1. RT-qPCR primer and probe design

Nucleotide sequences of *GAPDH* (A) and *tolC* (B) in *V. furnissii* displaying design of RT-qPCR primers (highlighted in grey) and probe (highlighted in bold), *GAPDH* product - 85 bp, *tolC* product - 100 bp.

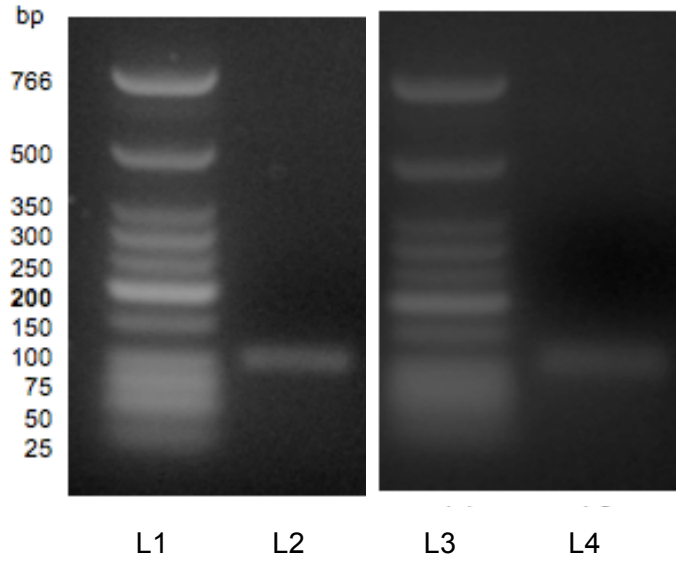

Figure 8.4. RT-qPCR primers optimised on cDNA

PCR products analysed by agarose gel following PCR amplification of wild type *V. furnissii* cDNA with *GAPDH* and *tolC* RT-qPCR primers (as laid out in Table 8.1), DNA fragments separated on 1.8% agarose gel. L1 and L3 - Biolabs Low MW ladder, L2 – amplification of *tolC*, expected product of 100 bp visible. L4 – amplification of *GAPDH*, expected product of 85 bp visible.

A

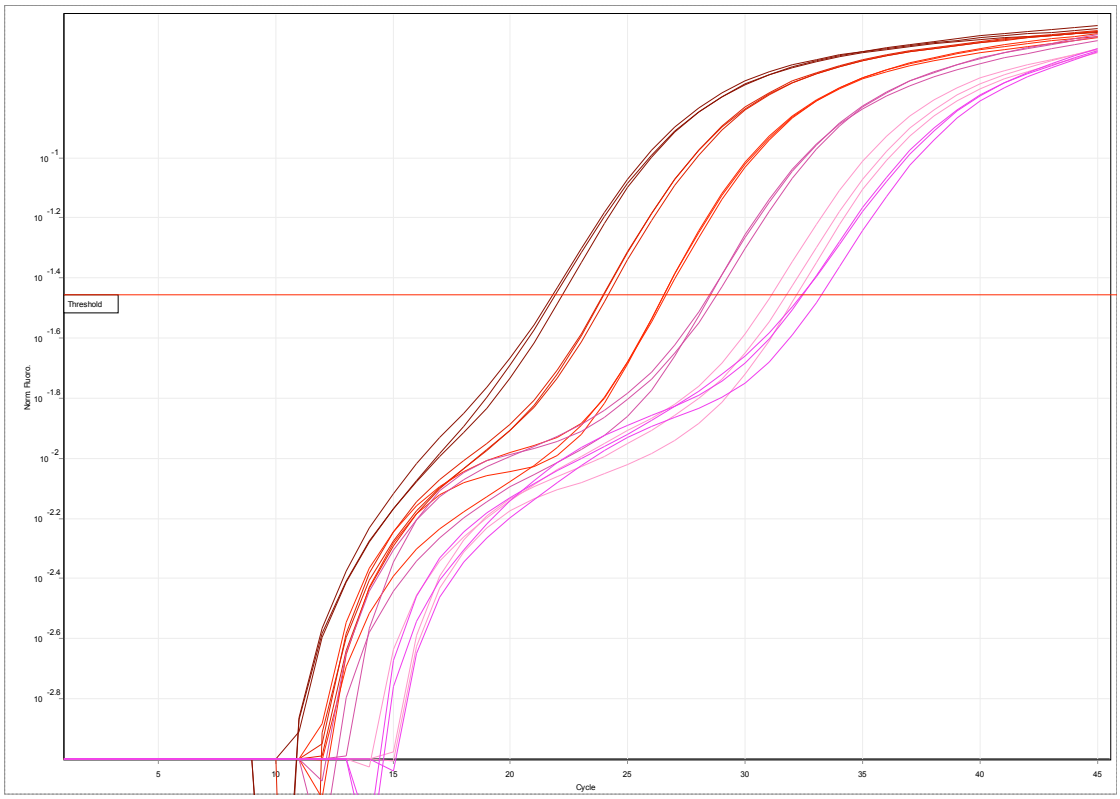

B

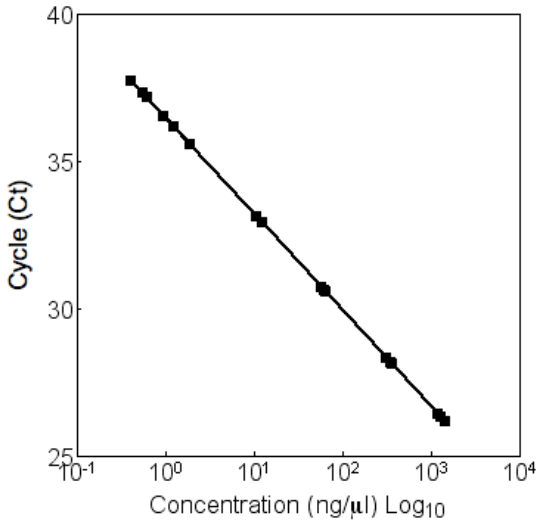

Figure 8.5. RT-qPCR *GAPDH* standard curve data.

A. Example of extension phase fluorescent emission data collected during the PCR amplification of *GAPDH*. Serial dilution concentrations (ng/µl): 1447, 285. 59.3, 10.8, 2, 0.4

B: Concentration (Log_{10}) plotted against threshold amplification cycle number (Ct), displaying linear regression. Each concentration was prepared in triplicate with six technical replicates

	Concentraion of antibiotic (µg/ml)											
	0.125	**0.25**	**0.5**	**1**	**2**	**4**	**8**	**16**	**32**	**64**	**128**	**256**
Chloramphenicol												
Wild type												
1	0.838	0.733	0.197	0.032	0.032	0.032	0.025	0.028	0.028	0.030	0.030	0.030
2	0.630	0.370	0.180	0.029	0.038	0.033	0.039	0.041	0.040	0.039	0.036	0.036
3	0.695	0.393	0.179	0.044	0.027	0.037	0.030	0.033	0.034	0.045	0.029	0.029
4	0.720	0.499	0.531	0.036	0.031	0.045	0.036	0.039	0.041	0.033	0.044	0.044
tolC⁻ mutant												
1	0.469	0.028	0.036	0.055	0.049	0.043	0.044	0.038	0.043	0.032	0.030	0.030
2	0.366	0.033	0.067	0.034	0.048	0.044	0.045	0.045	0.040	0.032	0.032	0.032
3	0.446	0.057	0.048	0.046	0.050	0.042	0.037	0.046	0.040	0.032	0.033	0.033
4	0.622	0.053	0.052	0.050	0.048	0.049	0.031	0.046	0.060	0.055	0.043	0.043
OE + IPTG												
1	0.235	0.242	0.035	0.032	0.219	0.044	0.033	0.031	0.032	0.031	0.037	0.037
2	0.237	0.228	0.041	0.069	0.215	0.043	0.040	0.038	0.033	0.033	0.036	0.036
3	0.228	0.265	0.041	0.038	0.241	0.040	0.041	0.036	0.036	0.036	0.036	0.036

Figure 8.6. Example of raw data obtained for minimal inhibitory concentration (MIC)

Determined for chloramphenicol in wild type (0.5 µg/ml), *tolC*⁻ mutant (0.125 µg/ml) and overexpressor with IPTG (0.25 µg/ml). Data is representative for tetracycline, ampilcillin, norfloxacin, novobiocin, gentamicin and streptomycin.

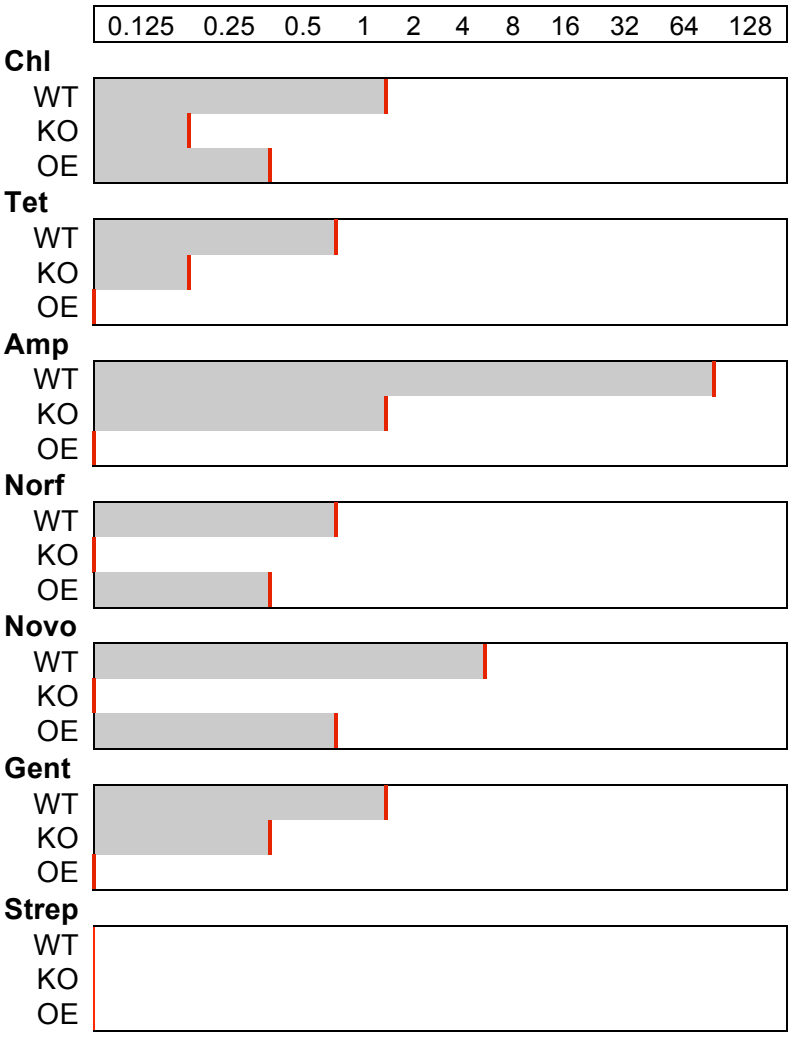

Figure 8.7. Summary of minimum inhibitory concentrations.

MICs determined for seven antibiotics; chloramphenicol, tetracycline, ampilcillin, norfloxacin, novobiocin, gentamicin and streptomycin determined for wild type (WT), *tolC*$^{-}$ mutant (KO) and overexpressor (OE). Knockout mutant displays decreased resistance to all antibiotics after 24 h of incubation, overexpressor shows no increase in resistance after 48 h. Data obtained n=4.

Sample	FFA	MAG	Sterols	DAG	TAG	Total (%vol/mass)
WT1	0.167	0.017	0.014	0.842	0.009	1.049
WT2	0.188	0.029	0.020	1.175	0.026	1.438
WT3	0.219	0.025	0.017	1.232	0.018	1.511
WT4	0.17	0.016	0.016	0.713	0.004	0.919
KO1	0.236	0.019	0.016	1.307	0.023	1.601
KO2	0.21	0.024	0.017	0.814	0.009	1.074
KO3	0.298	0.024	0.017	1.944	0.052	2.335
KO4	0.268	0.025	0.016	1.523	0.038	1.870
E-coli	0.118	0.019	0.012	0.012	<0.001	0.161
E-coli	0.174	0.016	0.02	0.109	0.004	0.323

Table 8.2. Composition of lipids in wild type *V. furnissii* and *tolC*$^{-}$ mutant.

Free fatty acids (FFA), monoacylglycerides (MAG), diacylglycerides (DAG), triacylglycerides (TAG) and sterols displayed as a percentage of cellular mass in wild type (WT) n=4, *tolC*$^{-}$ knockout mutant (KO) n=4 and *E. coli* n=2. Determined by GC-MS carried out at Shell Global. Combined mass of all lipids investigated (FFA, MAG, DAG, TAG and sterols) as a percentage of cellular mass also listed. Data show that of lipids investigated, *V. furnissii* cells comprise primarily of DAGs , in *E. coli,* total lipids are less than *V. furnissii*. Also notable is the FFA quantities are present in greater quantities within the *tolC*$^{-}$ mutant compared to wild type.

V. furnissii Genes			
Cluster 1 (vfu_A01178-vfu_A01203)	Cluster 2 (vfu_A01115-vfu_A01132)	Cluster 3 vfu_A01352-vfu_A01408)	Cluster 4 vfu_A02236-vfu_A02270)
Extracellular assembly proteins			
fliD	***fliC***	*fliC*	*fliC*
flgE	*flgL*	*flgL*	*fliC*
fliC	*flgK*	*flgE*	*flgK*
fliC	***flgE***	*flgK*	
flgK	***flgD***	*flgD*	
Proteins associated with outer membrane			
fliE	***flgF***	*flgF*	*flgF*
	flgG	***flgG***	*flgH*
	flgH	*flgH*	*fliE*
	flgI	*flgI*	*flgC*
	flgB	*fliE*	
	flgC	*flgB*	
		flgC	
Intracellular assembly proteins			
fliF	*flgN*	*fliF*	*fliN*
fliG	*flgA*	*fliG*	*fliQ*
fliM	*flgM*	*fliH*	*fliJ*
fliN		*fliI*	*flgA*
fliH		*fliR*	*flgM*
flhB		*fliQ*	
fliH		*fliP*	
fliI		*fliN*	
fliO		*flgN*	
fliP		*fliJ*	
fliQ		*flgA*	
fliR		*flgM*	
fliJ			
fliJ			

Table 8.3. List of flagellar genes in *V. furnissii*, obtained from KEGG database.

Separated into four clusters determined by location on genome and into 3 functional groups (extracellular assembly, membrane asscociated and intracellular assembly). Those with significant increased expression in the mutant are highlighted in bold. All genes in bold encode for proteins involved in extracullar and memrance bound assembly of flagella.

CHAPTER 10 - BIBLIOGRAPHY

AGUILAR, P. S. & DE MENDOZA, D. 2006. Control of fatty acid desaturation: a mechanism conserved from bacteria to humans. *Molecular microbiology,* 62**,** 1507-1514.

AKAMA, H., KANEMAKI, M., YOSHIMURA, M., TSUKIHARA, T., KASHIWAGI, T., YONEYAMA, H., NARITA, S., NAKAGAWA, A. & NAKAE, T. 2004. Crystal Structure of the Drug Discharge Outer Membrane Protein, OprM, of *Pseudomonas aeruginosa* Dual modes of membrane anchoring and occluded cavity end. *Journal of biological chemistry,* 279**,** 52816-52819.

ALBRO, P. W. & DITTMER, J. C. 1969. Biochemistry of long-chain, nonisoprenoid hydrocarbons. I. Characterization of the hydrocarbons of *Sarcina lutea* and the isolation of possible intermediates of biosynthesis. *Biochemistry,* 8**,** 394-405.

ALBRO, P. W. & DITTMER, J. C. 1969. Biochemistry of long-chain, nonisoprenoid hydrocarbons. II. Incorporation of acetate and the aliphatic chains of isoleucine and valine into fatty acids and hydrocarbons by *Sarcina lutea*. *Biochemistry,* 8**,** 953-959.

ALVAREZ, H. & STEINBÜCHEL, A. 2002. Triacylglycerols in prokaryotic microorganisms. *Applied microbiology and biotechnology,* 60**,** 367-376.

ALVAREZ, H. M., MAYER, F., FABRITIUS, D. & STEINBÜCHEL, A. 1996. Formation of intracytoplasmic lipid inclusions by *Rhodococcus opacus* strain PD630. *Archives of microbiology,* 165**,** 377-386.

ANDERSEN, C., HUGHES, C. & KORONAKIS, V. 2001. Protein export and drug efflux through bacterial channel-tunnels. *Current opinion in cell biology,* 13**,** 412-416.

AONO, R., TSUKAGOSHI, N. & YAMAMOTO, M. 1998. Involvement of outer membrane protein TolC, a possible member of the mar-sox regulon, in maintenance and improvement of organic solvent tolerance of *Escherichia coli* K-12. *Journal of bacteriology,* 180**,** 938-944.

BAESMAN, S. M., BULLEN, T. D., DEWALD, J., ZHANG, D., CURRAN, S., ISLAM, F. S., BEVERIDGE, T. J. & OREMLAND, R. S. 2007. Formation of tellurium nanocrystals during anaerobic growth of bacteria that use Te oxyanions as respiratory electron acceptors. *Applied and environmental microbiology,* 73**,** 2135-2143.

BAESMAN, S. M., STOLZ, J. F., KULP, T. R. & OREMLAND, R. S. 2009. Enrichment and isolation of *Bacillus beveridgei sp*. nov., a facultative anaerobic haloalkaliphile from Mono Lake, California, that respires oxyanions of tellurium, selenium, and arsenic. *Extremophiles,* 13**,** 695-705.

BAGAEVA, T. V. & ZINUROVA, E. E. 2004. Comparative characterization of extracellular and intracellular hydrocarbons of *Clostridium pasteurianum*. *Biochemistry (Moscow),* 69**,** 427-428.

BARKSDALE, L. & KIM, K. S. 1977. *Mycobacterium*. *Bacteriological reviews,* 41**,** 217.

BASSLER, B. L. 1999. How bacteria talk to each other: regulation of gene expression by quorum sensing. *Current opinion in microbiology,* 2**,** 582-587.

BASSLER, B. L. 2002. Small Talk:: Cell-to-Cell Communication in Bacteria. *Cell,* 109**,** 421-424.

BASSLER, B. L., WRIGHT, M., SHOWALTER, R. E. & SILVERMAN, M. R. 1993. Intercellular signalling in *Vibrio harveyi*: sequence and function of genes regulating expression of luminescence. *Molecular microbiology,* 9**,** 773-786.

BASSLER, B. L., WRIGHT, M. & SILVERMAN, M. R. 1994. Multiple signalling systems controlling expression of luminescence in *Vibrio harveyi*: sequence and function of genes encoding a second sensory pathway. *Molecular microbiology,* 13**,** 273-286.

BAUCHERON, S., TYLER, S., BOYD, D., MULVEY, M. R., CHASLUS-DANCLA, E. & CLOECKAERT, A. 2004. AcrAB-TolC directs efflux-mediated multidrug resistance in *Salmonella enterica serovar Typhimurium* DT104. *Antimicrobial agents and chemotherapy,* 48**,** 3729-3735.

BAVRO, V. N., PIETRAS, Z., FURNHAM, N., PEREZ-CANO, L., FERN√°NDEZ-RECIO, J., PEI, X. Y., MISRA, R. & LUISI, B. 2008. Assembly and channel opening in a bacterial drug efflux machine. *Molecular cell,* 30**,** 114-121.

BÉBIEN, M., LAGNIEL, G., GARIN, J., TOUATI, D., VERMÉGLIO, A. & LABARRE, J. 2002. Involvement of superoxide dismutases in the response of *Escherichia coli* to selenium oxides. *Journal of bacteriology,* 184**,** 1556-1564.

BHAKDI, S., MACKMAN, N., MENESTRINA, G., GRAY, L., HUGO, F., SEEGER, W. & HOLLAND, I. B. 1988. The hemolysin of Escherichia coli. *European journal of epidemiology,* 4**,** 135-143.

BINA, J. E. & MEKALANOS, J. J. 2001. *Vibrio cholerae tolC* is required for bile resistance and colonization. *Infection and immunity,* 69**,** 4681.

BINA, X. R., PROVENZANO, D., NGUYEN, N. & BINA, J. E. 2008. *Vibrio cholerae* RND family efflux systems are required for antimicrobial resistance, optimal virulence factor production, and colonization of the infant mouse small intestine. *Infection and immunity,* 76**,** 3595-3605.

BIRD, C. W. & LYNCH, J. M. 1974. Formation of hydrocarbons by micro-organisms. *Chemical society reviews,* 3**,** 309-328.

BISWAS, K., BARTON, L., TSUI, W., SHUMAN, K., GILLESPIE, J. & EZE, C. 2011. A novel method for the measurement of elemental selenium produced by bacterial reduction of selenite. *Journal of microbiological methods*.

BLAIR, J. & PIDDOCK, L. J. V. 2009. Structure, function and inhibition of RND efflux pumps in Gram-negative bacteria: an update. *Current opinion in microbiology,* 12**,** 512-519.

BLIGH, E. G. & DYER, W. J. 1959. A rapid method of total lipid extraction and purification. *Canadian journal of biochemistry and physiology,* 37**,** 911-917.

BOARDMAN, B. K. & SATCHELL, K. J. F. 2004. *Vibrio cholerae* strains with mutations in an atypical type I secretion system accumulate RTX toxin intracellularly. *Journal of bacteriology,* 186**,** 8137-8143.

BOHNERT, J. A., KARAMIAN, B. & NIKAIDO, H. 2010. Optimized Nile Red Efflux Assay of AcrAB-TolC Multidrug Efflux System Shows Competition between Substrates. *Antimicrobial agents and chemotherapy,* 54**,** 3770.

BRAWN, K. & FRIDOVICH, I. 1981. DNA strand scission by enzymically generated oxygen radicals. *Archives of biochemistry and biophysics,* 206**,** 414.

BREDEMEIER, R., HULSCH, R., METZGER, J. & BERTHE-CORTI, L. 2003. Submersed culture production of extracellular wax esters by the marine bacterium *Fundibacter jadensis*. *Marine biotechnology,* 5**,** 579-583.

BRENNER, D., HICKMAN-BRENNER, F., LEE, J., STEIGERWALT, A., FANNING, G., HOLLIS, D., FARMER, J., WEAVER, R., JOSEPH, S. & SEIDLER, R. 1983. *Vibrio furnissii* (formerly aerogenic biogroup of *Vibrio fluvialis*), a new species isolated from human feces and the environment. *Journal of clinical microbiology,* 18**,** 816-824.

BRENNER, D. J., HICKMAN-BRENNER, F. W., LEE, J. V., STEIGERWALT, A. G., FANNING, G. R., HOLLIS, D. G., FARMER 3RD, J. J., WEAVER, R. E., JOSEPH, S. W. & SEIDLER, R. J. 1983. *Vibrio furnissii* (formerly aerogenic biogroup of Vibrio fluvialis), a new species isolated from human feces and the environment. *Journal of clinical microbiology,* 18**,** 816.

BUCKLEY, A. M., WEBBER, M. A., COOLES, S., RANDALL, L. P., LA RAGIONE, R. M., WOODWARD, M. J. & PIDDOCK, L. J. V. 2006. The AcrAB-TolC efflux system of *Salmonella enterica serovar Typhimurium* plays a role in pathogenesis. *Cellular microbiology,* 8**,** 847-856.

BURTON JR, G. A., GIDDINGS, T., DEBRINE, P. & FALL, R. 1987. High incidence of selenite-resistant bacteria from a site polluted with selenium. *Applied and environmental microbiology,* 53**,** 185-188.

CAMPBELL, J. W. & CRONAN JR, J. E. 2001. Bacterial fatty acid biosynthesis: targets for antibacterial drug discovery. *Annual reviews in microbiology,* 55**,** 305-332.

CAO, J. G. & MEIGHEN, E. A. 1989. Purification and structural identification of an autoinducer for the luminescence system of *Vibrio harveyi. Journal of biological chemistry,* 264**,** 21670-21676.

CARLIOZ, A. & TOUATI, D. 1986. Isolation of superoxide dismutase mutants in *Escherichia coli:* is superoxide dismutase necessary for aerobic life? *The EMBO journal,* 5**,** 623.

CHEESBROUGH, T. M. & KOLATTUKUDY, P. E. 1984. Alkane biosynthesis by decarbonylation of aldehydes catalyzed by a particulate preparation from *Pisum sativum*. *Proceedings of the National Academy of Sciences,* 81**,** 6613-6617.

CHEESEMAN, K. & SLATER, T. 1993. An introduction to free radical biochemistry. *British medical bulletin,* 49**,** 481-493.

CHEN, X., SCHAUDER, S., POTIER, N., VAN DORSSELAER, A., PELCZER, I., BASSLER, B. L. & HUGHSON, F. M. 2002. Structural identification of a bacterial quorum-sensing signal containing boron. *Nature,* 415**,** 545-549.

CHUN, J., GRIM, C. J., HASAN, N. A., LEE, J. H., CHOI, S. Y., HALEY, B. J., TAVIANI, E., JEON, Y. S., KIM, D. W. & LEE, J. H. 2009. Comparative genomics reveals mechanism for short-term and long-term clonal transitions in pandemic *Vibrio cholerae*. *Proceedings of the National Academy of Sciences,* 106**,** 15442-15447.

CYBULSKI, L. E., ALBANESI, D., MANSILLA, M. C., ALTABE, S., AGUILAR, P. S. & DE MENDOZA, D. 2002. Mechanism of membrane fluidity optimization: isothermal control of the *Bacillus subtilis* acyl-lipid desaturase. *Molecular microbiology,* 45**,** 1379-1388.

DALSGAARD, A., GLERUP, P., HOYBYE, L., PAARUP, A., MEZA, R., BERNAL, M., SHIMADA, T. & TAYLOR, D. 1997. *Vibrio furnissii* isolated from humans in Peru: a possible human pathogen? *Epidemiology and infection,* 119**,** 143-149.

DANIELS, N. A., MACKINNON, L., BISHOP, R., ALTEKRUSE, S., RAY, B., HAMMOND, R. M., THOMPSON, S., WILSON, S., BEAN, N. H. & GRIFFIN, P. M. 2000. *Vibrio parahaemolyticus* infections in the United States, 1973–1998. *Journal of infectious diseases,* 181**,** 1661-1666.

DAVIES, D. G., PARSEK, M. R., PEARSON, J. P., IGLEWSKI, B. H., COSTERTON, J. & GREENBERG, E. 1998. The involvement of cell-to-cell signals in the development of a bacterial biofilm. *Science,* 280**,** 295.

DAVIS, J. B. 1968. Paraffinic hydrocarbons in the sulfate-reducing bacterium *Desulfovibrio desulfuricans. Chem. Geol,* 3**,** 155-160.

DAVIS, M. S., SOLBIATI, J. & CRONAN, J. E. 2000. Overproduction of acetyl-CoA carboxylase activity increases the rate of fatty acid biosynthesis in *Escherichia coli. Journal of biological chemistry,* 275**,** 28593.

DEBIEUX, C. M., DRIDGE, E. J., MUELLER, C. M., SPLATT, P., PASZKIEWICZ, K., KNIGHT, I., FLORANCE, H., LOVE, J., TITBALL, R. W. & LEWIS, R. J. 2011. A bacterial process for selenium nanosphere assembly. *Proceedings of the National Academy of Sciences,* 108**,** 13480-13485.

DENNIS, M. W. & KOLATTUKUDY, P. E. 1991. Alkane biosynthesis by decarbonylation of aldehyde catalyzed by a microsomal preparation from *Botryococcus braunii*. *Archives of biochemistry and biophysics (USA)*.

DERBER, C., COUDRON, P., TARR, C., GLADNEY, L., TURNSEK, M., SHANKARAN, S. & WONG, E. 2011. *Vibrio furnissii*: an Unusual Cause of Bacteremia and Skin Lesions after Ingestion of Seafood. *Journal of clinical microbiology,* 49**,** 2348-2349.

DHAMDHERE, G. & ZGURSKAYA, H. I. 2010. Metabolic shutdown in Escherichia coli cells lacking the outer membrane channel TolC. *Molecular microbiology,* 77**,** 743-754.

DI MARTINO, P., FURSY, R., BRET, L., SUNDARARAJU, B. & PHILLIPS, R. S. 2003. Indole can act as an extracellular signal to regulate biofilm formation of *Escherichia coli* and other indole-producing bacteria. *Canadian journal of microbiology,* 49**,** 443-449.

EBERHARD, A., BURLINGAME, A. L., EBERHARD, C., KENYON, G. L., NEALSON, K. H. & OPPENHEIMER, N. J. 1981. Structural identification of autoinducer of *Photobacterium fischeri* luciferase. *Biochemistry,* 20**,** 2444-2449.

ELKINS, C. A. & NIKAIDO, H. 2002. Substrate specificity of the RND-type multidrug efflux pumps AcrB and AcrD of *Escherichia coli* is determined predominately by two large periplasmic loops. *Journal of bacteriology,* 184**,** 6490-6498.

ELLIS, C. N., SCHUSTER, B. M., STRIPLIN, M. J., JONES, S. H., WHISTLER, C. A. & COOPER, V. S. 2012. Influence of Seasonality on the Genetic Diversity of V*ibrio parahaemolyticus* in New Hampshire Shellfish Waters as Determined by Multilocus Sequence Analysis. *Applied and environmental microbiology,* 7*8***,** 3778-3782.

ELSEY, D., JAMESON, D., RALEIGH, B. & COONEY, M. J. 2007. Fluorescent measurement of microalgal neutral lipids. *Journal of microbiological methods,* 68**,** 639-642.

ENGEBRECHT, J., NEALSON, K. & SILVERMAN, M. 1983. Bacterial bioluminescence: isolation and genetic analysis of functions from *Vibrio fischeri*. *Cell,* 32**,** 773-781.

ENGEBRECHT, J. A. & SILVERMAN, M. 1984. Identification of genes and gene products necessary for bacterial bioluminescence. *Proceedings of the National Academy of Sciences,* 81**,** 4154.

EVANS, K., PASSADOR, L., SRIKUMAR, R., TSANG, E., NEZEZON, J. & POOLE, K. 1998. Influence of the MexAB-OprM multidrug efflux system on quorum sensing in *Pseudomonas aeruginosa*. *Journal of bacteriology,* 180**,** 5443-5447.

FATH, M. J. & KOLTER, R. 1993. ABC transporters: bacterial exporters. *Microbiological reviews,* 57**,** 995-1017.

FEDERICI, L., DU, D., WALAS, F., MATSUMURA, H., FERNANDEZ-RECIO, J., MCKEEGAN, K. S., BORGES-WALMSLEY, M. I., LUISI, B. F. & WALMSLEY, A. R. 2005. The crystal structure of the outer membrane protein VceC from the bacterial pathogen *Vibrio cholerae* at 1.8A resolution. *Journal of biological chemistry,* 280**,** 15307-15314.

FLETCHER, M. P., DIGGLE, S. P., CAMARA, M. & WILLIAMS, P. 2007. Biosensor-based assays for PQS, HHQ and related 2-alkyl-4-quinolone quorum sensing signal molecules. *Nature protocols,* 2**,** 1254-1262.

FRALICK, J. A. 1996. Evidence that TolC is required for functioning of the Mar/AcrAB efflux pump of *Escherichia coli*. *Journal of bacteriology,* 178**,** 5803-5805.

FRIDOVICH, I. 1978. The biology of oxygen radicals. *Science,* 201**,** 875.

FRIDOVICH, I. 1983. Superoxide radical: an endogenous toxicant. *Annual review of pharmacology and toxicology,* 2*3***,** 239-257.

FUQUA, C., PARSEK, M. R. & GREENBERG, E. P. 2001. Regulation of gene expression by cell-to-cell communication: acyl-homoserine lactone quorum sensing. *Annual review of genetics,* 35**,** 439-468.

FUQUA, C., WINANS, S. C. & GREENBERG, E. P. 1996. Census and consensus in bacterial ecosystems: the LuxR-LuxI family of quorum-sensing transcriptional regulators. *Annual review of microbiology,* 50**,** 727.

GANTHER, H. E. Selenium: The biological effects of a highly active trace substance. 1970. 24-25.

GE, Q., YAMADA, Y. & ZGURSKAYA, H. 2009. The C-terminal domain of AcrA is essential for the assembly and function of the multidrug efflux pump AcrAB-TolC. *Journal of bacteriology,* 191**,** 4365-4371.

GERMAN, G. J. & MISRA, R. 2001. The TolC protein of *Escherichia coli* serves as a cell-surface receptor for the newly characterized TLS bacteriophage1. *Journal of molecular biology,* 308**,** 579-585.

GLESSNER, A., SMITH, R. S., IGLEWSKI, B. H. & ROBINSON, J. B. 1999. Roles of *Pseudomonas aeruginosa* las andrhl Quorum-Sensing Systems in Control of Twitching Motility. *Journal of bacteriology,* 181**,** 1623-1629.

GREENBERG, J. T., MONACH, P., CHOU, J. H., JOSEPHY, P. D. & DEMPLE, B. 1990. Positive control of a global antioxidant defense regulon activated by superoxide-generating agents in *Escherichia coli*. *Proceedings of the National Academy of Sciences,* 87**,** 6181.

GREENSPAN, P. & FOWLER, S. 1985. Spectrofluorometric studies of the lipid probe, nile red. *Journal of lipid research,* 26**,** 781-789.

GU, M. & IMLAY, J. A. 2011. The SoxRS response of *Escherichia coli* is directly activated by redox-cycling drugs rather than by superoxide. *Molecular microbiology,* 79**,** 1136-1150.

GUAN, L. & NAKAE, T. 2001. Identification of Essential Charged Residues in Transmembrane Segments of the Multidrug Transporter MexB of *Pseudomonas aeruginosa*. *Journal of bacteriology,* 183**,** 1734-1739.

HAMMER, B. K. & BASSLER, B. L. 2003. Quorum sensing controls biofilm formation in *Vibrio cholerae. Molecular microbiology,* 50**,** 101-104.

HAN, J. & CALVIN, M. 1969. Hydrocarbon distribution of algae and bacteria, and microbiological activity in sediments. *Proceedings of the National Academy of Sciences,* 64**,** 436-443.

HASTINGS, J. & GREENBERG, E. 1999. Quorum Sensing: the Explanation of a Curious Phenomenon Reveals a Common Characteristic of Bacteria. *Journal of bacteriology,* 181**,** 2667.

HEIDELBERG, J. F., EISEN, J. A., NELSON, W. C., CLAYTON, R. A., GWINN, M. L., DODSON, R. J., HAFT, D. H., HICKEY, E. K., PETERSON, J. D. & UMAYAM, L. 2000. DNA sequence of both chromosomes of the cholera pathogen *Vibrio cholerae*. *Nature,* 406**,** 477-483.

HENKE, J. M. & BASSLER, B. L. 2004. Quorum sensing regulates type III secretion in *Vibrio harveyi* and *Vibrio parahaemolyticus*. *Journal of bacteriology,* 186**,** 3794-3805.

HENKE, J. M. & BASSLER, B. L. 2004. Three parallel quorum-sensing systems regulate gene expression in *Vibrio harveyi*. *Journal of bacteriology,* 186**,** 6902-6914.

HICKMAN-BRENNER, F., BRENNER, D., STEIGERWALT, A., SCHREIBER, M., HOLMBERG, S., BALDY, L., LEWIS, C., PICKENS, N. & FARMER, J. 1984. *Vibrio fluvialis* and V*ibrio furnissii* isolated from a stool sample of one patient. *Journal of clinical microbiology,* 20**,** 125-127.

HIGGINS, D. A., POMIANEK, M. E., KRAML, C. M., TAYLOR, R. K., SEMMELHACK, M. F. & BASSLER, B. L. 2007. The major *Vibrio cholerae* autoinducer and its role in virulence factor production. *Nature,* 450**,** 883-886.

HIGGINS, D. E. & DIRITA, V. J. 1994. Transcriptional control of *toxT*, a regulatory gene in the ToxR regulon of *Vibrio cholerae*. *Molecular microbiology,* 14**,** 17-29.

HILLEN, L. W., POLLARD, G., WAKE, L. V. & WHITE, N. 1982. Hydrocracking of the oils of *Botryococcus braunii* to transport fuels. *Biotechnology and bioengineering,* 24.

HIRAKAWA, H., INAZUMI, Y., MASAKI, T., HIRATA, T. & YAMAGUCHI, A. 2005. Indole induces the expression of multidrug exporter genes in *Escherichia coli. Molecular microbiology,* 55**,** 1113-1126.

HOOVER, S. W., MARNER, W. D., BROWNSON, A. K., LENNEN, R. M., WITTKOPP, T. M., YOSHITANI, J., ZULKIFLY, S., GRAHAM, L. E., CHASTON, S. D. & MCMAHON, K. D. 2011. Bacterial production of free fatty acids from freshwater macroalgal cellulose. *Applied microbiology and biotechnology***,** 1-12.

HUECK, C. J. 1998. Type III protein secretion systems in bacterial pathogens of animals and plants. *Microbiology and molecular biology reviews,* 62**,** 379-433.

HUSAIN, F., HUMBARD, M. & MISRA, R. 2004. Interaction between the TolC and AcrA proteins of a multidrug efflux system of *Escherichia coli. Journal of bacteriology,* 186**,** 8533-8536.

IGBINOSA, E. O. & OKOH, A. I. 2008. Emerging *Vibrio* species: an unending threat to public health in developing countries. *Research in microbiology,* 159**,** 495-506.

IINO, T., KOMEDA, Y., KUTSUKAKE, K., MACNAB, R., MATSUMURA, P., PARKINSON, J., SIMON, M. & YAMAGUCHI, S. 1988. New unified nomenclature for the flagella genes of *Escherichia coli* and *Salmonella typhimurium*. *Microbiological reviews,* 52**,** 533-535.

IMLAY, J. A. 2008. Cellular defenses against superoxide and hydrogen peroxide. *Annual review of biochemistry,* 77**,** 755.

ISHIGE, T., TANI, A., SAKAI, Y. & KATO, N. 2003. Wax ester production by bacteria. *Current opinion in microbiology,* 6**,** 244-250.

ISHIGE, T., TANI, A., TAKABE, K., KAWASAKI, K., SAKAI, Y. & KATO, N. 2002. Wax ester production from n-alkanes by *Acinetobacter sp*. strain M-1: ultrastructure of cellular inclusions and role of acyl coenzyme A reductase. *Applied and environmental microbiology,* 68**,** 1192-1195.

JOBLING, M. G. & HOLMES, R. K. 1997. Characterization of *hapR*, a positive regulator of the *Vibrio cholerae* HA/protease gene *hap*, and its identification as a functional homologue of the *Vibrio harveyi* l*uxR* gene. *Molecular microbiology,* 26**,** 1023-1034.

JONES, C. J. & MACNAB, R. M. 1990. Flagella assembly in *Salmonella typhimurium*: analysis with temperature-sensitive mutants. *Journal of bacteriology,* 172**,** 1327-1339.

JONES, J. G. 1972. Studies on freshwater bacteria: association with algae and alkaline phosphatase activity. *The Journal of ecology***,** 59-75.

JONES, M. K. & OLIVER, J. D. 2009. *Vibrio vulnificus*: disease and pathogenesis. *Infection and immunity,* 77**,** 1723-1733.

JUDSON, N. & MEKALANOS, J. J. 2000. TnAraOut, a transposon-based approach to identify and characterize essential bacterial genes. *Nature biotechnology,* 18**,** 740-745.

KALSCHEUER, R., STÖVEKEN, T., MALKUS, U., REICHELT, R., GOLYSHIN, P. N., SABIROVA, J. S., FERRER, M., TIMMIS, K. N. & STEINBÜCHEL, A. 2007. Analysis of storage lipid accumulation in *Alcanivorax borkumensis:* evidence for alternative triacylglycerol biosynthesis routes in bacteria. *Journal of bacteriology,* 189**,** 918-928.

KAMARAJU, K., SMITH, J., WANG, J., ROY, V., SINTIM, H., BENTLEY, W. & SUKHAREV, S. 2011. Effects on membrane lateral pressure suggest permeation mechanisms for bacterial quorum signaling molecules. *Biochemistry*.

KANEHISA, M., GOTO, S., KAWASHIMA, S. & NAKAYA, A. 2002. The KEGG databases at GenomeNet. *Nucleic acids research,* 30**,** 42-46.

KAPLAN, H. B. & GREENBERG, E. P. 1985. Diffusion of autoinducer is involved in regulation of the Vibrio fischeri luminescence system. *Journal of Bacteriology,* 163**,** 1210-1214.

KELLY, R. C., BOLITHO, M. E., HIGGINS, D. A., LU, W., NG, W. L., JEFFREY, P. D., RABINOWITZ, J. D., SEMMELHACK, M. F., HUGHSON, F. M. & BASSLER, B. L. 2009. The *Vibrio cholerae* quorum-sensing autoinducer CAI-1: analysis of the biosynthetic enzyme CqsA. *Nature chemical biology,* 5**,** 891-895.

KESSI, J. & HANSELMANN, K. W. 2004. Similarities between the abiotic reduction of selenite with glutathione and the dissimilatory reaction mediated by *Rhodospirillum rubrum* and *Escherichia coli*. *Journal of Biological Chemistry,* 279**,** 50662.

KESSI, J., RAMUZ, M., WEHRLI, E., SPYCHER, M. & BACHOFEN, R. 1999. Reduction of selenite and detoxification of elemental selenium by the phototrophic bacterium *Rhodospirillum rubrum. Applied and environmental microbiology,* 65**,** 4734.

KEWELOH, H., DIEFENBACH, R. & REHM, H. J. 1991. Increase of phenol tolerance of *Escherichia coli* by alterations of the fatty acid composition of the membrane lipids. *Archives of microbiology,* 157**,** 49-53.

KHAN, S. R., GAINES, J., ROOP II, R. M. & FARRAND, S. K. 2008. Broad-host-range expression vectors with tightly regulated promoters and their use to examine the influence of TraR and TraM expression on Ti plasmid quorum sensing. *Applied and environmental microbiology,* 74**,** 5053-5062.

KIM, S. Y., LEE, S. E., KIM, Y. R., KIM, C. M., RYU, P. Y., CHOY, H. E., CHUNG, S. S. & RHEE, J. H. 2003. Regulation of Vibrio vulnificus virulence by the LuxS quorum sensing system. *Molecular microbiology,* 48**,** 1647-1664.

KITAOKA, M., MIYATA, S., UNTERWEGER, D. & PUKATZKI, S. 2011. Antibiotic resistance mechanisms of *Vibrio cholerae*. *Journal of medical microbiology,* 60**,** 397.

KLASS, D. 1998. Biomass for renewable energy, fuels, and chemicals. *Biomass for renewable energy, fuels, and chemicals.*

KÖHLER, T., KOK, M., MICHEA-HAMZEHPOUR, M., PLESIAT, P., GOTOH, N., NISHINO, T., CURTY, L. K. & PECHERE, J. C. 1996. Multidrug efflux in intrinsic resistance to trimethoprim and sulfamethoxazole in *Pseudomonas aeruginosa*. *Antimicrobial agents and chemotherapy,* 40**,** 2288-2290.

KÖHLER, T., MICHEA-HAMZEHPOUR, M., PLESIAT, P., KAHR, A. L. & PECHERE, J. C. 1997. Differential selection of multidrug efflux systems by quinolones in *Pseudomonas aeruginosa. Antimicrobial agents and chemotherapy,* 41**,** 2540-2543.

KORONAKIS, V. 2003. TolC–the bacterial exit duct for proteins and drugs. *FEBS letters,* 555**,** 66-71.

KORONAKIS, V., ESWARAN, J. & HUGHES, C. 2004. Structure and function of TolC: The Bacterial Exit Duct for Proteins and Drugs. *Annual review of biochemistry,* 73**,** 467-489.

KORONAKIS, V., SHARFF, A., KORONAKIS, E., LUISI, B. & HUGHES, C. 2000. Crystal structure of the bacterial membrane protein TolC central to multidrug efflux and protein export. *Nature,* 405**,** 914-919.

KUBORI, T., SHIMAMOTO, N., YAMAGUCHI, S., NAMBA, K. & AIZAWA, S. I. 1992. Morphological pathway of flagella assembly in *Salmonella typhimurium. Journal of molecular biology,* 226**,** 433-446.

KUTSUKAKE, K., OHYA, Y. & IINO, T. 1990. Transcriptional analysis of the flagella regulon of *Salmonella typhimurium*. *Journal of bacteriology,* 172**,** 741-747.

LADYGINA, N., DEDYUKHINA, E. G. & VAINSHTEIN, M. B. 2006. A review on microbial synthesis of hydrocarbons. *Process Biochemistry,* 41**,** 1001-1014.

LAM, S. Y. S. & GOI, L. 1985. Isolations of" Group F *Vibrios*" from human stools. *Singapore Med. J,* 26**,** 300-302.

LEE, J., JAYARAMAN, A. & WOOD, T. K. 2007. Indole is an inter-species biofilm signal mediated by SdiA. *BMC microbiology,* 7**,** 42.

LEIERS, B., KAMPKÖTTER, A., GREVELDING, C. G., LINK, C. D., JOHNSON, T. E. & HENKLE-DÜHRSEN, K. 2003. A stress-responsive glutathione S-transferase confers resistance to oxidative stress in *Caenorhabditis elegans*. *Free Radical Biology and Medicine,* 34**,** 1405-1415.

LENZ, D. H., MOK, K. C., LILLEY, B. N., KULKARNI, R. V., WINGREEN, N. S. & BASSLER, B. L. 2004. The small RNA chaperone Hfq and multiple small RNAs control quorum sensing in *Vibrio harveyi* and *Vibrio cholerae*. *Cell,* 118**,** 69-82.

LI, M., ZHANG, X., AGRAWAL, A. & SAN, K. Y. 2012. Effect of acetate formation pathway and long chain fatty acid CoA-ligase on the free fatty acid production in *E. coli* expressing acy-ACP thioesterase from *Ricinus communis*. *Metabolic engineering*.

LILLEY, B. N. & BASSLER, B. L. 2000. Regulation of quorum sensing in *Vibrio harveyi* by LuxO and Sigma‚Äê54. *Molecular microbiology,* 36**,** 940-954.

LIN, J., SAHIN, O., MICHEL, L. O. & ZHANG, Q. 2003. Critical role of multidrug efflux pump CmeABC in bile resistance and in vivo colonization of *Campylobacter jejuni*. *Infection and immunity,* 71**,** 4250-4259.

LOMOVSKAYA, O., WARREN, M. S., LEE, A., GALAZZO, J., FRONKO, R., LEE, M., BLAIS, J., CHO, D., CHAMBERLAND, S. & RENAU, T. 2001. Identification and characterization of inhibitors of multidrug resistance efflux pumps in *Pseudomonas aeruginosa*: novel agents for combination therapy. *Antimicrobial agents and chemotherapy,* 45**,** 105-116.

LOSI, M. E. & FRANKENBERGER JR, W. T. 1997. Reduction of selenium oxyanions by *Enterobacter cloacae* SLD1a-1: isolation and growth of the bacterium and its expulsion of selenium particles. *Applied and environmental microbiology,* 63**,** 3079.

LU, X., VORA, H. & KHOSLA, C. 2008. Overproduction of free fatty acids in *E. coli:* implications for biodiesel production. *Metabolic engineering,* 10**,** 333-339.

LUX, T. M., LEE, R. & LOVE, J. 2011. Complete Genome Sequence of a Free-Living *Vibrio furnissii sp*. nov. Strain (NCTC 11218). *Journal of bacteriology,* 193**,** 1487.

MA, D., COOK, D. N., ALBERTI, M., PON, N. G., NIKAIDO, H. & HEARST, J. E. 1995. Genes *acrA* and *acrB* encode a stress induced efflux system of *Escherichia coli*. *Molecular microbiology,* 16**,** 45-55.

MACNAB, R. M. 2004. Type III flagella protein export and flagella assembly. *Biochimica et Biophysica Acta (BBA)-Molecular Cell Research,* 1694**,** 207-217.

MACY, J., RECH, S., AULING, G., DORSCH, M., STACKEBRANDT, E. & SLY, L. 1993. T*hauera selenatis gen. nov., sp*. nov., a member of the beta subclass of Proteobacteria with a novel type of anaerobic respiration. *International journal of systematic bacteriology,* 43**,** 135-142.

MAGALHÃES, V., CASTELLO FILHO, A., MAGALHÃES, M. & GOMES, T. T. 1993. Laboratory evaluation on pathogenic potentialities of *Vibrio furnissii*. *Memórias do Instituto Oswaldo Cruz,* 88**,** 593-597.

MAGNET, S., COURVALIN, P. & LAMBERT, T. 2001. Resistance-nodulation-cell division-type efflux pump involved in aminoglycoside resistance in *Acinetobacter baumannii* strain BM4454. *Antimicrobial agents and chemotherapy,* 45**,** 3375-3380.

MAGNUSON, K., JACKOWSKI, S., ROCK, C. & CRONAN JR, J. 1993. Regulation of fatty acid biosynthesis in *Escherichia coli*. *Microbiological reviews,* 57**,** 522-542.

MAKULA, R., LOCKWOOD, P. & FINNERTY, W. 1975. Comparative analysis of the lipids of *Acinetobacter species* grown on hexadecane. *Journal of bacteriology,* 121**,** 250-258.

MANILLA-PÉREZ, E., REERS, C., BAUMGART, M., HETZLER, S., REICHELT, R., MALKUS, U., KALSCHEUER, R., WÄLTERMANN, M. & STEINBÜCHEL, A. 2010. Analysis of Lipid Export in Hydrocarbonoclastic Bacteria of the Genus *Alcanivorax*: Identification of Lipid Export-Negative Mutants of *Alcanivorax borkumensis* SK2 and *Alcanivorax jadensis* T9. *Journal of bacteriology,* 192**,** 643.

MANSILLA, M. C. & DE MENDOZA, D. 2005. The *Bacillus subtilis* desaturase: a model to understand phospholipid modification and temperature sensing. *Archives of microbiology,* 183**,** 229-235.

MARTIN, A. J., JONES, R. & BUCKWALTER-DAVIS, M. 2009. Passive and semi-passive treatment alternatives for the bioremediation of selenium from mine waters.

MASI, M., DURET, G., DELCOUR, A. H. & MISRA, R. 2009. Folding and trimerization of signal sequence-less mature TolC in the cytoplasm of *Escherichia coli*. *Microbiology,* 155**,** 1847-1857.

MATA, T. M., MARTINS, A. A. & CAETANO, N. S. 2010. Microalgae for biodiesel production and other applications: A review. *Renewable and Sustainable Energy Reviews,* 14**,** 217-232.

MCCARTER, L. L. 1998. OpaR, a homolog of *Vibrio harveyi* LuxR, controls opacity of *Vibrio parahaemolyticus. Journal of bacteriology,* 180**,** 3166-3173.

MCDOUGALD, D., RICE, S. A. & KJELLEBERG, S. 2000. The marine pathogen *Vibrio vulnificus* encodes a putative homologue of the *Vibrio harveyi* regulatory gene, *luxR*: a genetic and phylogenetic comparison. *Gene,* 248**,** 213-221.

MERDINGER, E. & FRYE, R. H. 1966. Distribution of C14 from Glucose-1-C 14 in the Lipid Fractions of *Debaryomyces hansenii*. *Journal of bacteriology,* 91**,** 1831-1833.

METZGER, P. & LARGEAU, C. 2005. *Botryococcus braunii*: a rich source for hydrocarbons and related ether lipids. *Applied microbiology and biotechnology,* 66**,** 486-496.

MICHAEL, B., SMITH, J. N., SWIFT, S., HEFFRON, F. & AHMER, B. M. M. 2001. SdiA of *Salmonella enterica* is a LuxR homolog that detects mixed microbial communities. *Journal of bacteriology,* 183**,** 5733-5742.

MILLER, M. B. & BASSLER, B. L. 2001. Quorum sensing in bacteria. *Annual Reviews in Microbiology,* 55**,** 165-199.

MILLER, M. B., SKORUPSKI, K., LENZ, D. H., TAYLOR, R. K. & BASSLER, B. L. 2002. Parallel Quorum Sensing Systems Converge to Regulate Virulence in *Vibrio cholerae Cell,* 110**,** 303-314.

MILTON, D. L., HARDMAN, A., CAMARA, M., CHHABRA, S. R., BYCROFT, B. W., STEWART, G. & WILLIAMS, P. 1997. Quorum sensing in *Vibrio anguillarum*: characterization of the *vanI/vanR* locus and identification of the autoinducer N-(3-oxodecanoyl)-L-homoserine lactone. *Journal of bacteriology,* 179**,** 3004-3012.

MINATO, Y., SIEFKEN, R. L. & HÄSE, C. C. 2011. TolC affects virulence gene expression in *Vibrio cholerae*. *Journal of bacteriology,* 193**,** 5850-5852.

MODALI, S. & ZGURSKAYA, H. 2011. The periplasmic membrane proximal domain of MacA acts as a switch in stimulation of ATP hydrolysis by MacB transporter. *Molecular microbiology*.

MODALI, S. D. & ZGURSKAYA, H. I. The periplasmic membrane proximal domain of MacA acts as a switch in stimulation of ATP hydrolysis by MacB transporter. *Molecular microbiology*.

MURAKAMI, S., NAKASHIMA, R., YAMASHITA, E., MATSUMOTO, T. & YAMAGUCHI, A. 2006. Crystal structures of a multidrug transporter reveal a functionally rotating mechanism. *Nature,* 443**,** 173-179.

MURAKAMI, S., NAKASHIMA, R., YAMASHITA, E. & YAMAGUCHI, A. 2002. Crystal structure of bacterial multidrug efflux transporter AcrB. *Nature,* 419**,** 587-593.

MURAKAMI, S., TAMURA, N., SAITO, A., HIRATA, T. & YAMAGUCHI, A. 2004. Extramembrane central pore of multidrug exporter AcrB in *Escherichia coli* plays an important role in drug transport. *Journal of biological chemistry,* 279**,** 3743-3748.

NACCARATO, W. F., GILBERTSON, J. R. & GELMAN, R. A. 1974. Effects of different culture media and oxygen upon lipids of *Escherichia coli K-12*. *Lipids,* 9**,** 322-327.

NAWABI, P., BAUER, S., KYRPIDES, N. & LYKIDIS, A. 2011. Engineering *Escherichia coli* for Biodiesel Production Utilizing a Bacterial Fatty Acid Methyltransferase. *Applied and environmental microbiology,* 77**,** 8052-8061.

NG, W. L., PEREZ, L. J., WEI, Y., KRAML, C., SEMMELHACK, M. F. & BASSLER, B. L. 2011. Signal production and detection specificity in *Vibrio* CqsA/CqsS quorum-sensing systems. *Molecular microbiology,* 79**,** 1407-1417.

NIKOLAEV, Y. A., PANIKOV, N. S., LUKIN, S. M. & OSIPOV, G. A. 2001. Saturated C sub (21)-C sub (33) hydrocarbons are involved in the self-regulation of *Pseudomonas fluorescens* adhesion to a glass surface. *Microbiology/Mikrobiologiya,* 70**,** 138-144.

O'LEARY, W. M. 1962. The fatty acids of bacteria. *Microbiology and molecular biology reviews,* 26**,** 421.

OH, W. S., IM, Y. S., YEON, K. Y., YOON, Y. & KIM, J. 2007. Phosphate and carbon source regulation of alkaline phosphatase and phospholipase in *Vibrio vulnificus*. *Journal of Microbiology,* 45**,** 311-317.

OKUSU, H., MA, D. & NIKAIDO, H. 1996. AcrAB efflux pump plays a major role in the antibiotic resistance phenotype of *Escherichia coli* multiple-antibiotic-resistance (Mar) mutants. *Journal of bacteriology,* 178**,** 306.

OLIVER, J. D. & COLWELL, R. R. 1973. Extractable lipids of gram-negative marine bacteria: fatty-acid composition. *International journal of systematic bacteriology,* 23**,** 442-458.

OPPENHEIMER, C. H. 1965. Bacterial production of hydrocarbon-like materials. *Zeitschrift fur allgemeine Mikrobiologie,* 5.

ORO, J., TORNABENE, T. G., NOONER, D. W. & GELPI, E. 1967. Aliphatic hydrocarbons and fatty acids of some marine and freshwater microorganisms. *Journal of bacteriology,* 93**,** 1811-1818.

ORTORI, C. A., DUBERN, J. F., CHHABRA, S. R., CÁMARA, M., HARDIE, K., WILLIAMS, P. & BARRETT, D. A. 2011. Simultaneous quantitative profiling of N-acyl-l-homoserine lactone and 2-alkyl-4 (1H)-quinolone families of quorum-sensing signaling molecules using LC-MS/MS. *Analytical and bioanalytical chemistry,* 399**,** 839-850.

PAINTER, E. P. 1941. The Chemistry and Toxicity of Selenium Compounds, with Special Reference to the Selenium Problem. *Chemical reviews,* 28**,** 179-213.

PALLEN, M. J., CHAUDHURI, R. R. & HENDERSON, I. R. 2003. Genomic analysis of secretion systems. *Current opinion in microbiology,* 6**,** 519-527.

PARK, M. O. 2005. New pathway for long-chain n-alkane synthesis via 1-alcohol in *Vibrio furnissii* M1. *Journal of bacteriology,* 187**,** 1426-1429.

PARK, M. O., HEGURI, K., HIRATA, K. & MIYAMOTO, K. 2005. Production of alternatives to fuel oil from organic waste by the alkane-producing bacterium, *Vibrio furnissii M1*. *Journal of applied microbiology,* 98**,** 324-331.

PARK, M. O., TANABE, M., HIRATA, K. & MIYAMOTO, K. 2001. Isolation and characterization of a bacterium that produces hydrocarbons extracellularly which are equivalent to light oil. *Applied microbiology and biotechnology,* 56**,** 448-452.

PAULSEN, I. T., BROWN, M. H. & SKURRAY, R. A. 1996. Proton-dependent multidrug efflux systems. *Microbiological reviews,* 60**,** 575-608.

PEARSON, J. P., GRAY, K. M., PASSADOR, L., TUCKER, K. D., EBERHARD, A., IGLEWSKI, B. H. & GREENBERG, E. 1994. Structure of the autoinducer required for expression of *Pseudomonas aeruginosa* virulence genes. *Proceedings of the National Academy of Sciences,* 91**,** 197.

PEARSON, J. P., VAN DELDEN, C. & IGLEWSKI, B. H. 1999. Active efflux and diffusion are involved in transport of *Pseudomonas aeruginosa* cell-to-cell signals. *Journal of bacteriology,* 181**,** 1203-1210.

PIDDOCK, L. J. V. 2006. Multidrug-resistance efflux pumps? not just for resistance. *Nature reviews microbiology,* 4**,** 629-636.

PIDDOCK, L. J. V., WHITE, D. G., GENSBERG, K., PUMBWE, L. & GRIGGS, D. J. 2000. Evidence for an efflux pump mediating multiple antibiotic resistance in *Salmonella enterica serovar Typhimurium. Antimicrobial agents and chemotherapy,* 44**,** 3118.

POOLE, K. 2000. Efflux-mediated resistance to fluoroquinolones in Gram-negative bacteria. *Antimicrobial agents and chemotherapy,* 44**,** 2233-2241.

POOLE, K. 2001. Multidrug efflux pumps and antimicrobial resistance in *Pseudomonas aeruginosa* and related organisms. *Journal of molecular microbiology and biotechnology,* 3**,** 255-264.

POOLE, K. & SRIKUMAR, R. 2001. Multidrug Efflux in *Pseudomonas aeruginosa* Components, Mechanisms and Clinical Significance. *Current topics in medicinal chemistry,* 1**,** 59-71.

RAMOS, J. L., DUQUE, E., GALLEGOS, M. T., GODOY, P., RAMOS-GONZLEZ, M. I., ROJAS, A., TERAN, W. & SEGURA, A. 2002. Mechanisms of solvent tolerance in Gram-negative bacteria. *Annual reviews in microbiology,* 56**,** 743-768.

REIMANN, S. A. & WOLFE, A. J. 2011. Constitutive Expression of the Maltoporin LamB in the Absence of OmpR Damages the Cell Envelope. *Journal of bacteriology,* 193**,** 842.

RICHARDSON, K. 1991. Roles of motility and flagella structure in pathogenicity of *Vibrio cholerae*: analysis of motility mutants in three animal models. *Infection and immunity,* 59**,** 2727-2736.

ROCK, C. O., JACKOWSKI, S. & CRONAN, J. E. 1996. Lipid metabolism in prokaryotes. *New comprehensive biochemistry,* 31**,** 35-74.

ROSENBERG, E. Y., BERTENTHAL, D., NILLES, M. L., BERTRAND, K. P. & NIKAIDO, H. 2003. Bile salts and fatty acids induce the expression of *Escherichia coli* AcrAB multidrug efflux pump through their interaction with Rob regulatory protein. *Molecular microbiology,* 48**,** 1609-1619.

ROSENBERG, E. Y., MA, D. & NIKAIDO, H. 2000. AcrD of *Escherichia coli* is an aminoglycoside efflux pump. *Journal of bacteriology,* 182**,** 1754-1756.

ROSNER, J. L. & MARTIN, R. G. 2009. An excretory function for the *Escherichia coli* outer membrane pore TolC: upregulation of *marA* and *soxS* transcription and Rob activity due to metabolites accumulated in *tolC* mutants. *Journal of bacteriology,* 191**,** 5283.

ROSS, D. 1988. Glutathione, free radicals and chemotherapeutic agents: Mechanisms of free-radical induced toxicity and glutathione-dependent protection. *Pharmacology & therapeutics,* 37**,** 231-249.

RUMBAUGH, K. P., GRISWOLD, J. A., IGLEWSKI, B. H. & HAMOOD, A. N. 1999. Contribution of Quorum Sensing to the Virulence of *Pseudomonas aeruginosa* in Burn Wound Infections. *Infection and immunity,* 67**,** 5854-5862.

SAKAZAKI, R. 1992. Bacteriology of Vibrio and related organisms. *Cholera. Plenum Medical Book Company, New York, NY*, 37-55.

SANDKVIST, M. 2001. Biology of type II secretion. *Molecular Microbiology,* 40, 271-283.

SANDKVIST, M. 2001. Type II secretion and pathogenesis. *Infection and immunity,* 69, 3523-3535.

SANTOS, M., COSME, A., BECKER, J., MEDEIROS, J., MATA, M. & MOREIRA, L. 2010. Absence of functional TolC protein causes increased stress response gene expression in *Sinorhizobium meliloti*. *BMC microbiology,* 10, 180.

SAWAYAMA, S., MINOWA, T. & YOKOYAMA, S. Y. 1999. Possibility of renewable energy production and CO_2 mitigation by thermochemical liquefaction of microalgae. *Biomass and Bioenergy,* 17, 33-39.

SCHAUDER, S., SHOKAT, K., SURETTE, M. G. & BASSLER, B. L. 2001. The LuxS family of bacterial autoinducers: biosynthesis of a novel quorum sensing signal molecule. *Molecular microbiology,* 41, 463-476.

SCHIRMER, A., RUDE, M., LI, X., POPOVA, E. & DEL CARDAYRE, S. 2010. Microbial biosynthesis of alkanes. *Science (New York, NY),* 329, 559.

SHAO, C. P., LO, H. R., LIN, J. H. & HOR, L. I. 2011. Regulation of Cytotoxicity by Quorum-Sensing Signaling in *Vibrio vulnificus* Is Mediated by SmcR, a Repressor of *hlyU*. *Journal of bacteriology,* 193, 2557.

SOLOMAKOS, N., PEXARA, A. & GOVARIS, A. 2012. *Vibrio parahaemolyticus* in seafood associated outbreaks (in English). *Journal of the hellenic veterinary medical society,* 63, 54-62.

SRIKUMAR, R., LI, X. Z. & POOLE, K. 1997. Inner membrane efflux components are responsible for beta-lactam specificity of multidrug efflux pumps in *Pseudomonas aeruginosa*. *Journal of bacteriology,* 179, 7875-7881.

STEEN, E. J., KANG, Y., BOKINSKY, G., HU, Z., SCHIRMER, A., MCCLURE, A., DEL CARDAYRE, S. B. & KEASLING, J. D. 2010. Microbial production of fatty-acid-derived fuels and chemicals from plant biomass. *Nature,* 463, 559-562.

STONE, R. W. & ZOBELL, C. E. 1952. Bacterial aspects of the origin of petroleum. *Industrial & engineering chemistry,* 44, 2564-2567.

STOREY, D. G., UJACK, E. E., RABIN, H. R. & MITCHELL, I. 1998. *Pseudomonas aeruginosa lasR* Transcription Correlates with the Transcription of *lasA, lasB, and toxA* in Chronic Lung Infections Associated with Cystic Fibrosis. *Infection and immunity,* 66, 2521-2528.

STUKEY, J. E., MCDONOUGH, V. M. & MARTIN, C. E. 1990. The OLE1 gene of *Saccharomyces cerevisiae* encodes the delta 9 fatty acid desaturase and can be functionally replaced by the rat stearoyl-CoA desaturase gene. *Journal of Biological Chemistry,* 265, 20144.

SURETTE, M. G., MILLER, M. B. & BASSLER, B. L. 1999. Quorum sensing in *Escherichia coli, Salmonella typhimurium,* and *Vibrio harveyi:* a new family of genes responsible for autoinducer production. *Proceedings of the National Academy of Sciences of the United States of America,* 96, 1639.

SYED, K. A., BEYHAN, S., CORREA, N., QUEEN, J., LIU, J., PENG, F., SATCHELL, K. J. F., YILDIZ, F. & KLOSE, K. E. 2009. The *Vibrio cholerae* flagella regulatory hierarchy controls expression of virulence factors. *Journal of bacteriology,* 191, 6555-6570.

SYMMONS, M. F., BOKMA, E., KORONAKIS, E., HUGHES, C. & KORONAKIS, V. 2009. The assembled structure of a complete tripartite bacterial multidrug efflux pump. *Proceedings of the National Academy of Sciences,* 106, 7173.

TACKET, C. O., HICKMAN, F., PIERCE, G. V. & MENDOZA, L. F. 1982. Diarrhea associated with *Vibrio fluvialis* in the United States. *Journal of clinical microbiology,* 16, 991-992.

TAKATSUKA, Y., CHEN, C. & NIKAIDO, H. 2010. Mechanism of recognition of compounds of diverse structures by the multidrug efflux pump AcrB of *Escherichia coli*. *Proceedings of the National Academy of Sciences,* 107, 6559.

TIKHONOVA, E., YAMADA, Y. & ZGURSKAYA, H. 2011. Sequential Mechanism of Assembly of Multidrug Efflux Pump AcrAB-TolC. *Chemistry & biology,* 18, 454.

TOMEI, F. A., BARTON, L. L., LEMANSKI, C. L., ZOCCO, T. G., FINK, N. H. & SILLERUD, L. O. 1995. Transformation of selenate and selenite to elemental selenium by *Desulfovibrio desulfuricans. Journal of industrial microbiology & biotechnology,* 14**,** 329-336.

TORNABENE, T. G., GELPI, E. & ORÓ, J. 1967. Identification of fatty acids and aliphatic hydrocarbons in *Sarcina lutea* by gas chromatography and combined gas chromatography-mass spectrometry. *Journal of bacteriology,* 94**,** 333-343.

TORNABENE, T. G., MORRISON, S. J. & KLOOS, W. E. 1970. Aliphatic hydrocarbon contents of various members of the family *Micrococcaceae*. *Lipids,* 5**,** 929-937.

TOUZÉ, T., ESWARAN, J., BOKMA, E., KORONAKIS, E., HUGHES, C. & KORONAKIS, V. 2004. Interactions underlying assembly of the *Escherichia coli* AcrAB–TolC multidrug efflux system. *Molecular microbiology,* 53**,** 697-706.

TSANEVA, I. R. & WEISS, B. 1990. *soxR,* a locus governing a superoxide response regulon in *Escherichia coli* K-12. *Journal of bacteriology,* 172**,** 4197-4205.

VIOQUE, J. & KOLATTUKUDY, P. E. 1997. Resolution and Purification of an Aldehyde-Generating and an Alcohol-Generating Fatty Acyl-CoA Reductase from Pea Leaves (*Pisum sativum*.). *Archives of biochemistry and biophysics,* 340**,** 64-72.

VITOLO, S. & GHETTI, P. 1994. Physical and combustion characterization of pyrolytic oils derived from biomass material upgraded by catalytic hydrogenation. *Fuel,* 73**,** 1810-1812.

WACKETT, L. P., FRIAS, J. A., SEFFERNICK, J. L., SUKOVICH, D. J. & CAMERON, S. 2007. *Vibrio furnissii* M1: genomic and biochemical studies demonstrating the absence of an alkane-producing phenotype. *Applied and environmental microbiology*.

WANDERSMAN, C. & DELEPELAIRE, P. 1990. TolC, an *Escherichia coli* outer membrane protein required for hemolysin secretion. *Proceedings of the National Academy of Sciences,* 87**,** 4776.

WANG, X. & KOLATTUKUDY, P. E. 1995. Solubilization and purification of aldehyde-generating fatty acyl-CoA reductase from green alga *Botryococcus braunii*. *FEBS letters,* 370**,** 15-18.

WATERS, C. M. & BASSLER, B. L. 2005. Quorum sensing: cell-to-cell communication in bacteria. *Annu. Rev. Cell dev. Biol.,* 21**,** 319-346.

WATERS, C. M. & BASSLER, B. L. 2006. The *Vibrio harveyi* quorum-sensing system uses shared regulatory components to discriminate between multiple autoinducers. *Genes & development,* 20**,** 2754.

WEBBER, M. A., BAILEY, A. M., BLAIR, J., MORGAN, E., STEVENS, M. P., HINTON, J. C. D., IVENS, A., WAIN, J. & PIDDOCK, L. J. V. 2009. The global consequence of disruption of the AcrAB-TolC efflux pump in *Salmonella enterica* includes reduced expression of SPI-1 and other attributes required to infect the host. *Journal of bacteriology,* 191**,** 4276.

WEI, Y., PEREZ, L. J., NG, W. L., SEMMELHACK, M. & BASSLER, B. L. 2011. Mechanism of *Vibrio cholerae* autoinducer-1 biosynthesis. *ACS chemical biology*.

WERNER, J., AUGUSTUS, A. M. & MISRA, R. 2003. Assembly of TolC, a structurally unique and multifunctional outer membrane protein of *Escherichia coli* K-12. *Journal of bacteriology,* 185**,** 6540-6547.

WILCE, M. & PARKER, M. W. 1994. Structure and function of glutathione-S-transferases. *Biochimica et biophysica acta,* 1205**,** 1.

WILLIAMS, P. & CÁMARA, M. 2009. Quorum sensing and environmental adaptation in Pseudomonas aeruginosa: a tale of regulatory networks and multifunctional signal molecules. *Current opinion in microbiology,* 12**,** 182-191.

XAVIER, K. B. & BASSLER, B. L. 2003. LuxS quorum sensing: more than just a numbers game. *Current opinion in microbiology,* 6**,** 191-197.

XU, X., STERN, A. M., LIU, Z., KAN, B. & ZHU, J. 2010. Virulence regulator AphB enhances *toxR* transcription in *Vibrio cholerae*. *BMC microbiology,* 10**,** 3.

YAMASAKI, S., NAGASAWA, S., HAYASHI-NISHINO, M., YAMAGUCHI, A. & NISHINO, K. 2011. AcrA dependency of the AcrD efflux pump in *Salmonella enterica serovar Typhimurium*. *The journal of antibiotics*.

YANG, S., LOPEZ, C. R. & ZECHIEDRICH, E. L. 2006. Quorum sensing and multidrug transporters in *Escherichia coli*. *Proceedings of the National Academy of Sciences of the United States of America,* 103**,** 2386.

YANG, Q., HAN, Y. & ZHANG, X. H. 2011. Detection of quorum sensing signal molecules in the family *Vibrionaceae*. *Journal of applied microbiology,* 110**,** 1438-1448.

YAO, Y., MARTINEZ-YAMOUT, M. A., DICKERSON, T. J., BROGAN, A. P., WRIGHT, P. E. & DYSON, H. J. 2006. Structure of the *Escherichia coli* quorum sensing protein SdiA: activation of the folding switch by acyl homoserine lactones. *Journal of molecular biology,* 355**,** 262-273.

ZALDIVAR, J., NIELSEN, J. & OLSSON, L. 2001. Fuel ethanol production from lignocellulose: a challenge for metabolic engineering and process integration. *Applied microbiology and biotechnology,* 56**,** 17-34.

ZGURSKAYA, H. I., KRISHNAMOORTHY, G., NTREH, A. & LU, S. 2011. Frontiers: Mechanism and Function of the Outer Membrane Channel TolC in Multidrug Resistance and Physiology of *Enterobacteria*. *Frontiers in antimicrobials, resistance and chemotherapy,* 2.

ZGURSKAYA, H. I. & NIKAIDO, H. 1999. Bypassing the periplasm: reconstitution of the AcrAB multidrug efflux pump of *Escherichia coli*. *Proceedings of the National Academy of Sciences,* 96**,** 7190.

ZGURSKAYA, H. I. & NIKAIDO, H. 2000. Multidrug resistance mechanisms: drug efflux across two membranes. *Molecular microbiology,* 37**,** 219-225.

ZHENG, C. J., YOO, J. S., LEE, T. G., CHO, H. Y., KIM, Y. H. & KIM, W. G. 2005. Fatty acid synthesis is a target for antibacterial activity of unsaturated fatty acids. *FEBS letters,* 579**,** 5157-5162.

ZHU, J. & MEKALANOS, J. J. 2003. Quorum sensing-dependent biofilms enhance colonization in *Vibrio cholerae*. *Developmental cell,* 5**,** 647-656.

ZHU, J., MILLER, M. B., VANCE, R. E., DZIEJMAN, M., BASSLER, B. L. & MEKALANOS, J. J. 2002. Quorum-sensing regulators control virulence gene expression in *Vibrio cholerae*. *PNAS,* 99**,** 3129-3134.